The Challenge of Selectivity in Ethylene Oligomerization: Ligand Design and Metal Valence States

Indira Thapa

Thesis submitted to the
Faculty of Graduate and Postdoctoral Studies
in partial fulfillment of the requirements
for the degree of

Doctorate in Philosophy
in
Chemistry

Ottawa-Carleton Chemistry Institute
University of Ottawa

Candidate
Indira Thapa

Supervisor
Professor Sandro Gambarotta

Abstract

Catalytic ethylene oligomerization is a well understood industrially viable process. The large majority of scientific literature and patents concerning this process has been developed with the use of chromium catalysts. Commercial systems producing selective tri/tetramerization, non-selective oligomerization and polymerization are all based on this metal with the exception of a few systems based on other transition metals (Zr, Ti, Ni etc.). This versatility raises interesting questions about chromium's unique behaviour. Essentially, selective or non-selective oligomerization and polymerization processes could be regarded as belonging to the same category of C-C bond forming reactions, though different mechanisms are involved.

The first part of this thesis explores a variety of chromium complexes for ethylene oligomerization purposes. In order to gather further information about the unique behaviour of chromium, we have explored a variety of nitrogen and phosphorus containing ligands. We started with a simple bi-dentate anionic amidophosphine (NP) ligand and assessed the role of the ligand's negative charge and number of donor atoms in determining the type of catalytic behaviour in relation to the metal oxidation state. This ligand proved capable of generating a series of chromium dimeric, tetrameric or polymeric and even heterobimetallic chromium-aluminate complexes in different valence states. This allowed us to isolate a "single component" self activating Cr(II) complex as well as a rare example of mixed valence Cr(I)/Cr(II) species. Additionally, each of these species acted as switchable catalyst depending on the type of co-catalyst and solvent used (Chapter 2).

To systematize out comprehension of the NP ligand, we have replaced the acidic proton in an (NP) anionic ligand with an alky group. An impressive selectivity switch from trimerization to tetramerization (>90%) was observed (Chapter 3). One of the important achievements during the study of this thesis work was the finding of a first ever selective tetramerization catalyst reaching >99% selectivity for 1-octene with Cr-amino-bispyridine ligand systems (Chapter 4). In search of a clue to introduce the selectivity in the catalytic cycle we have uncovered the ability of simple dicyclohexyl amido ligand to stabilize the monovalent state of chromium (Chapter 5). Extending this concept, a variety of bi-dentate and tri-dentate amidinate (NCN) and amidate (NCO) ligands were also assessed for highly active and non-selective polymer free oligomerization behaviours as they have shown enough ability to stabilize the divalent oxidation state of chromium (Chapter 6).

The second part of this thesis explores a few nickel based complexes. Aiming of our study at low valent nickel complexes and their catalytic performances towards ethylene oligomerization, we have chosen different well established ligands in this field. To this end, we were able to isolate a novel nickel dinitrogen complex Ni(0), a nickel hydride complex Ni(II) and even the first example of a nickel alky bis(imino)pyridine complex Ni(I). The “non-innocent” nature of the ligand and its involvement in the organometallic chemistry of the metal centre has been studied. All of these complexes were assessed for their ethylene oligomerization behaviour (Chapter 7). Even in this case, we were looking for highly reactive monovalent species and have isolated a rare example of heterobimetallic Ni(I) species with a dianionic tripyrrolide ligand (Chapter 8). Characteristics C-C bond forming and C-C bond cleavage properties of nickel were

revealed by isolating corresponding dimethyl pyrrolid-nickel complexes (Chapter 9). All of these complexes were tested for their unique ethylene dimerization behaviour.

This work is dedicated to my father Padma Bahadur Thapa and my mother Hira Kumari Thapa whose love for family, compassion for others, honesty in life and thirst for knowledge has always inspired me and kept me moving in every chaos in my life.

"TO DREAM ANYTHING THAT YOU WANT TO DREAM. THAT IS THE BEAUTY OF HUMAN MIND.
TO DO ANYTHING THAT YOU WANT TO DO. THAT IS THE STRENGTH OF HUMAN WILL.
TO TRUST YOURSELF TO TEST YOUR LIMITS. THAT IS THE COURAGE TO SUCCEED."

-Bernard Edmonds

Acknowledgments

At this point of thesis completion, I shall be eternally indebted to my research supervisor Professor Sandro Gambarotta for his highly inspiring and invaluable guidance, continuous encouragement, advice and most importantly kindness of giving freedom during this research work. There is no need to mention how much Sandro has had impact in organometallic chemistry, but very few have this fortunate opportunity to know him, how an extraordinary human being he is. His simplicity, kindness, politeness and honesty despite being rich in unimaginable wealth of knowledge, has always inspired me and make me to consider one of the fortunate person to share these valuable assets with him. His passion to research and life is unexplainable. Sandro recognized my hungry, dedicated and passionate researcher inside me. When I was ready to giving up Sandro told me " I truly believe in you, if you ever think of it, you will lose my respect", and those words echo in my head as life saver that kept me going up to this point where I am today.

My deepest gratitude goes to Professor Robert Duchateau for his insightful suggestions and warm hospitality during my both visits to Eindhoven University, The Netherlands. I greatly appreciate his collaborative effort with Gambarotta group and consider myself fortunate to have an opportunity to work with him. I am grateful for those moments when I met a supportive friend Khalid in the lab. It is my pleasure working with Shaneesh, Sebastiano, Yacoob, Saba, Ahmed and Indu. Christopher and Joanna deserve special thanks for taking time to proof read the first chapter of my thesis. I had an opportunity to mentor two very talented and dedicated Master's student from France, Virginie and Aude-claire, thank you both of you. Supervising a very enthusiastic

and hard working undergraduate students Christopher, Dannya and Yan was equally exciting experience.

I am grateful to Dr. Ilia Korobkov not only as a qualified crystallographer but also as a helpful scientist and colleague. I am also thankful to Dr. Glenn Yap, Dr. Tara Burchell for X-ray crystallography; Dr. Clem Kazakoff for Mass Spectrometry and Dr. Glenn facey for NMR facility. Many thanks go to a great help provided by Professor Muralee Murugesu for SQUID measurement and Professor Peter Budzelaar for DFT calculations. I would like to take this opportunity to thank my research proposal committee: Professor Darrain Richeson, Professor Tom Woo and Professor Muralee Murugesu for their invaluable suggestions and encouragement.

Most of all, my heartfelt appreciation goes to my family. My sweet little son Arpeace, your innocent smile always fills me with incredible amount of energy and makes me to believe that *there is always a silver lining in every cloud*. My dear daughter Avipsha, you inspire me to be strong to survive. My husband Shail, if you were not there for those very difficult moments, I would probably be not able to write this thesis today; I owe my Ph.D to you. My mom Hira, who travelled all the way from Nepal to here and provided me all the support, unconditional love throughout my life and my brothers (Bhoj, Laxman, Narayan) for all your love and supports, I will be grateful forever. Above all, I am missing you too much dad, yet I am proud, I fulfilled your dream; I can feel, you are blessing me as usual from the sky.

Finally, University of Ottawa and financial agencies are acknowledged.

Publications and Patent based on this thesis work

Publications:

[1] **Thapa, I.**; Gambarotta, S.; Duchateau, R.; Kulangara, S. V; Chevalier, R. *Organometallics***2010**, *29*(18), 4080-4089.

[2] Licciulli, S.; **Thapa, I.;** Albahily, K.; Korobkov, I.; Gambarotta, S.; Duchateau, R.; Chevalier, R.; Schuhen, K. *Angew. Chem. Int. Ed*. **2010,** *49*(48), 9225-9228.

[3] Zhu, D.; **Thapa, I**.; Korobkov, I.; Gambarotta, S.; Budzelaar, P.H.M. *Inorg. Chem*. **2011,** *50*(20), 9879-9887.

[4] **Thapa, I**.; Gambarotta, S.; Korobkov, I.; Murugesu, M.; Budzelaar, P. .H.M *Organometallics* **2012**, *31*(1), 486 – 494.

[5] **Thapa, I**.; Gambarotta, S.; Korobkov, I. *Organometallics* (Submitted).

[6] **Thapa, I**.; Gambarotta, S.; Descour, C.; Duchateau, R. *Organometallics* (Manuscript ready to submit).

[7] **Thapa, I**.; Doiseau, A. C.; Gambarotta, S.; Korobkov, I. *Organometallics* (Submitted).

[8] **Thapa, I**.; Peneau, V.; Noel, C.W; Gambarotta, S.; Korobkov, I. *Organometallics* (Submitted).

[9] **Thapa, I**.; Gambarotta, S.; Korobkov, I. *Inorg. Chem* (Submission in process).

[10] **Thapa, I**.; Gambarotta, S.; Korobkov, I. *Inorg. Chem* (Submission in process).

[11] **Thapa, I**.; Gambarotta, S.; Korobkov, I. *Inorg. Chem* (Submission in process).

[12] Kulangara, S. V.; Mason, C.; Juba, M.; **Thapa, I**.; Gambarotta, S.; Korobkov, I.; Duchateau, R. *Organometallics* (Submitted).

Patent:

[13] Schuhen, K; Chevalier, R; Gambarotta, S; Licciulli, S; **Thapa, I**; Duchateau, R. PCT Int. Appl. (**2011**), WO 2011085951 A1 20110721.

Presentations:

- **Oral Presentation:** **2010 International Chemical Congress of Pacific Basin Societies**, December 15-20, **2010** Honolulu, Hawaii, USA.
- **Oral Presentation:** **93rd Canadian Chemistry Conference and Exhibition, (CSC)** Toronto, ON, Canada May 29-June 2, **2010**.
- **Oral Presentation:** **Ottawa-Carleton Day (OCCI)**, University of Ottawa, **2009**.
- **Research Poster :** **Ottawa-Carleton Day (OCCI)**, University of Ottawa, **2008.**
- **Research Poster :** **Inorganic Development Week Conference (IDW),** Toronto Nov 2-4, **2007.**

Table of Contents

List of Figures

List of Schemes

List of Tables

List of Abbreviations

Ar	aromatic group
BIPY	bipyridine
Bz	benzoyl
calcd	calculated
Cy	cyclohexyl
DEAC	diethylaluminum chloride
DFT	Density Functional Theory
DIM	diiminetetramethyl
DIMPY	diiminemethylpyridine
DMP	2,5-dimethylpyrrole
ESI	Electro Spray Ionization (Mass Spectrometry)
Et	ethyl
Et_2O	diethyl ether
GC-MS	Gas Chromatography-Mass Spectroscopy
i-Bu	iso-butyl
i-Pr	iso-propyl
IR	Infrared
IMPY	iminemethylpyridine

MAO	methylaluminoxane
Me	methyl
MMAO	modified- methylaluminoxane
Mw	weight-average molecular weight
m/z	mass to charge ratio
NMR	Nuclear Magnetic Resonance
PDI	polydispersity Index
PE	polyethylene
Ph	phenyl
PVC	polyvinyl chloride
S.F	Schulz-Flory distribution (statistical distribution)
t-Bu	tert-Butyl
TEAl	triethylaluminum
TERPY	terpyridine
TIBA	tri-isobutylaluminum
TIBAO	tetraisobutyldialuminoxane
THF	tetrahydrofurane
TMA	trimethylaluminum
SQUID	Superconducting Quantum Interference Device

CHAPTER ONE

1. General Introduction

1.1 Polyolefin: Historical Development

In their natural forms polymers have revealed their existence as tar, shellac, tortoise shell, silk, wool and tree saps producing amber and latex. During World War II, when natural sources of latex, wool, silk and other material became scarce, the need of synthetic polymers became more urgent. Since then, the polymer industry has continued to grow. In over 50 years it has evolved into one of the fastest growing industries in the world. Its production increased from 1.5 million tones in 1950 to 230 million tones in 2009. There is hardly any aspect of life that is not affected by synthetic polymers today, from simple household commodities, to even highly specialized applications such as artificial knee and hip implants are just a few of the many of synthetic polymers, contributing to the trillion dollar industry.[1]

As the Greek philosopher Democritus has quoted: "Everything existing in this Universe is the fruit of chance and necessity". Louis Pasteur also stated that "Chance favours the prepared mind". The invention of polyolefin is no exception with this respect. Polyethylene was first discovered at the end of the 18th century in the lab of the German chemist Hans von Pechmann as a *polymethylene* when diazomethane thermally decomposed in an experiment.[2] The second observation was due to Eric Fawcett and Reginald Gibson at Imperial Chemical Industries (ICI) at the beginning of 1930. While exploring high pressure and temperature reactions projected for the dyestuffs industry, radical polymerization of ethylene was serendipitously obtained.[3] The polymer produced in this process utilizes the free radical pathway, resulting in a highly branched

low-density polyethylene (LDPE). This was in fact the birth of LDPE. The polymer production required very harsh conditions, (300 ^{o}C, and 3000 bar of ethylene pressure) and low melting (~ 110 ^{o}C), semi-crystalline elastomers of poor mechanical properties were obtained. This in fact turned out to be advantageous for usage of LDPE as insulating material for wires and packaging.[3]

Another accidental discovery at the beginning of the 1950's marked a milestone with the finding of high-density polyethylene (HDPE). Since these polymers were not produced from free-radical mechanism they were linear, resulting in high melting temperature (130-137 ^{o}C). In addition, a higher degree of crystallinity was obtained and which eventually gave stiffer, stronger, and heat resistant plastics, thus enabling to expand the number of applications. In 1951, Hogan and Banks at Phillips Petroleum invented the first low-pressure method for the linear polymerization of ethylene over a Cr-oxide supported catalyst.[4] Followed by this discovery Karl Ziegler in 1953 published the formation of HDPE by using for the first time transition metals, with a low-pressure catalytic system based on titanium-halides and aluminum alkyls. This was a major discovery that was honored with the Nobel Prize in Chemistry in 1963, shared with Giulio Natta for his equally remarkable discovery of isotactic polypropylene.[5]

Both of these inventions marked the beginning of a new industrial era in the world of polyolefin. Today more than 100 million metric tons of plastics, elastomers, and rubber producing olefins are produced using these catalyst systems.[6] Not only has the industrial world benefited from this invention, but the field of organometallic chemistry has also been blooming under the pressure of discovering more performing catalysts. These inventions lead to the development of ultra-high molecular weight polyethylene (UHMWPE), a class of high-density

polyethylene with molecular weight above 10^6 g/mol and with a lesser degree of branching. The materials produced from this invention have a high degree of resistance and tensile strength and are used to produce heavy duty cables, fibers, artificial knees, hip implants, and other various applications. However, these new plastics were still susceptible from the problems of stiffness and cracking. The shortcomings of these polymers challenged scientists to do further research and eventually led to the invention of a more flexible, thin and transparent polyethylene with high tensile strength and puncture resistance value known as linear-low density polyethylene (LLDPE).[7]

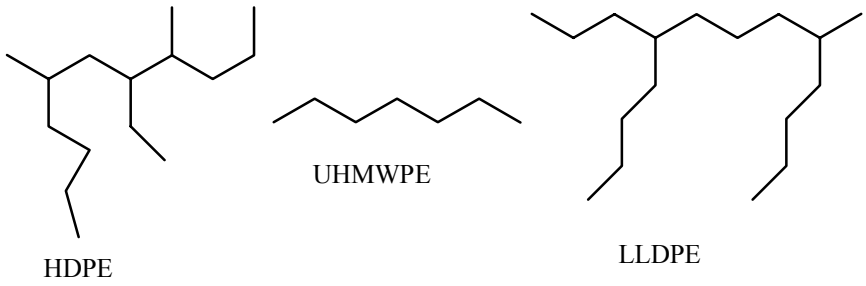

Figure 1.1 Microstructure of HDPE, UHMWPE, LLDPE

LLDPE is the highest demanded PE with 8.3% annual increase worldwide, this is followed by polypropylene (6.1%) and then HDPE (3.8%).[8] In order to satisfy the ever-growing demand for LLDPE, the use of linear α-olefins (LAO) is a viable alternatives and made these species the most important additives for polyolefin and polymer industry. LAO's are produced by the carbon-carbon bond forming processes referred to as oligomerization. This has resulted in products that range from four to twenty-four carbon chain units, contrary to the products in the category of polymerization which retain a carbon chains ranging from thousands to millions.

As mentioned earlier, the beginning of today's industrialized polyethylene business started in 1964 with the Ziegler-Natta discovery of the titanium-halide based catalyst in presence of aluminum alkyls. This invention opened up a whole new area of research in the field of organometallic chemistry and encouraged the exploration of aluminum alkyl compounds in catalysis and polymerization research. Nonetheless, the heterogeneous nature of the catalytic system poses a great obstacle to understanding mechanistic details of the polymerization. The major breakthrough in its understanding was achieved by Cossee and Arlman. According to their proposal, the $TiCl_4$ becomes reduced to $TiCl_3$ upon combining with the aluminum alkyl (Scheme 1.1). $TiCl_3$ and aluminum alkyls react on the surface of the particles to generate metal-carbon (Ti-C) bonds. An ethylene molecule is then π-coordinated to the Ti center, followed by insertion into the Ti-alkyl bond via a four-member cyclic transition state. Repeated coordination and insertion of ethylene into the growing polymer chain constitutes the chain propagation steps as shown in Scheme 1.1.[9]

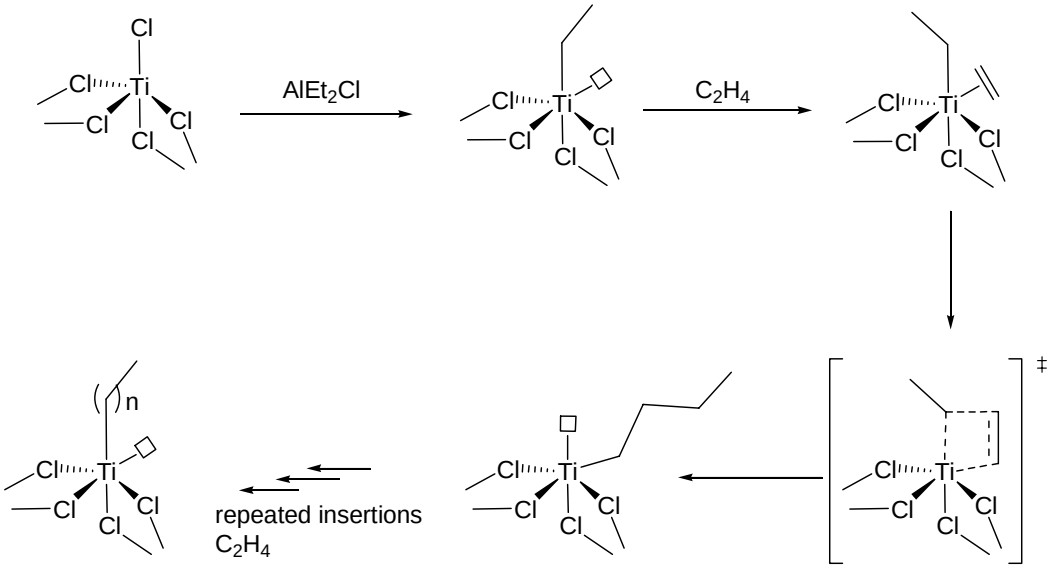

Scheme 1.1: Cossee-Arlman mechanism for polymerization.[9]

The transition state as shown in Scheme 1.1 is the result of 2+2 cycloaddition. Even though, this process is usually symmetry-forbidden, it is made possible by the polarity of the bonds and the contribution of the metal d-orbitals. The termination step is usually caused by *β*-hydrogen elimination. The nature of the products formed is determined by the relative rates of propagation versus termination. A relatively fast termination compared to propagation results in the formation of oligomers while a relatively slow termination rate leads to polymerization products.

Another disadvantage of the heterogeneous nature of the Ziegler catalytic system is the production of broad molecular weight distribution polymers, presumably due to the multi-facet catalytic species formed during the polymerization. A solution came in the form of homogeneous, single-site catalysts. In 1957, Breslow, Newburg and Natta discovered the first titanocene Cp_2TiCl_2/AlR_2Cl system. The homogeneous nature of the system provided an opportunity to re-evaluate the polymerization process. Evidence shows that the initial activation step creates a cationic metal alkyl species which remains as a solvent separated ion-pair in equilibrium with the alkyl-bound contact ion-pair, as shown in Scheme 1.2.[10] Nucleophilic attack to the electron deficient metal center by the weakly basic ethylene molecule facilitates the typical Cossee–type mechanism. The chain termination step occurs either by 1) *β*-hydrogen transfer (or elimination) from the polymer chain to either the coordinated monomer or the metal center, or 2) chain transfer to aluminum (Scheme 1.2).[11]

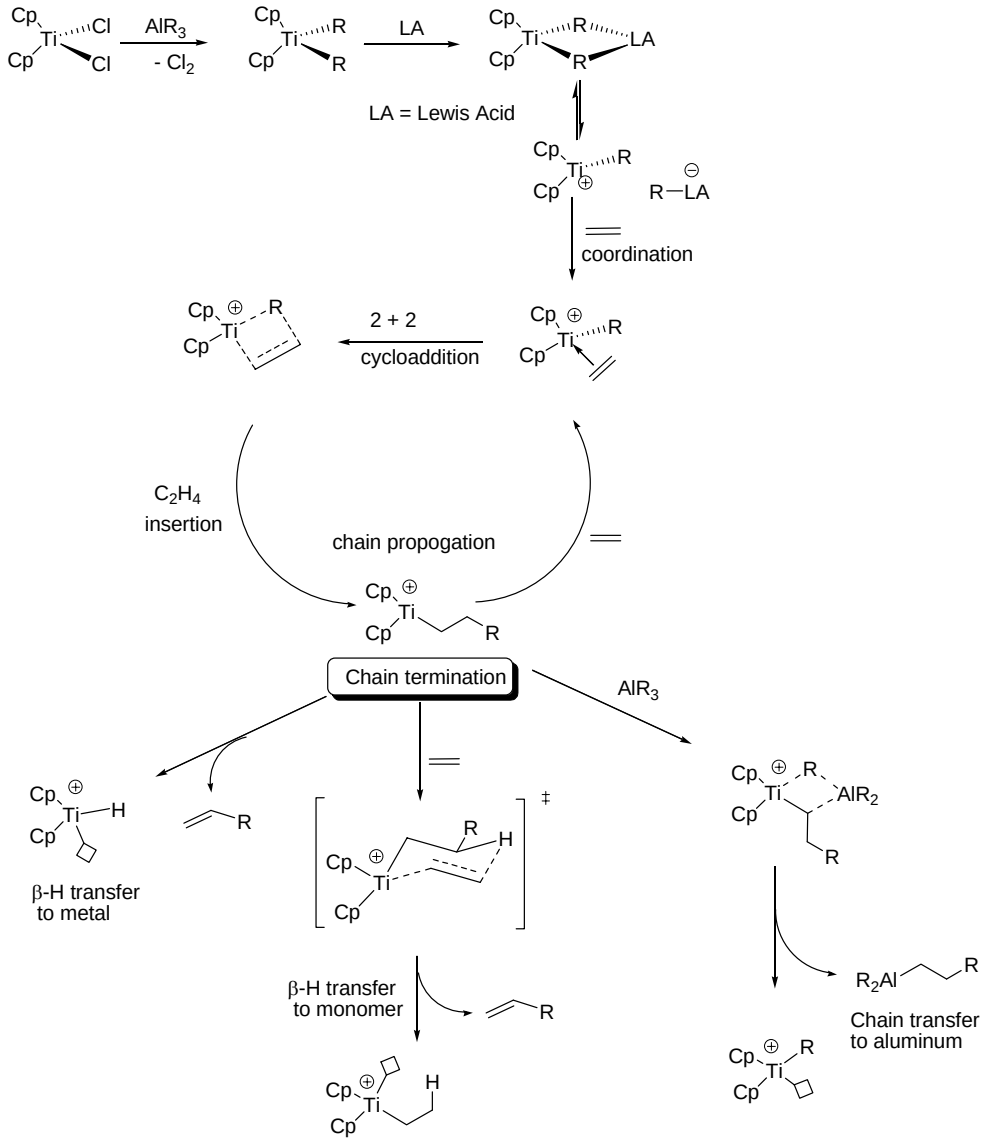

Scheme 1.2: Proposed polymerization mechanism for homogeneous system.[10]

The mechanistic understanding led to the development of a very large variety group-IV metallocene catalysts which are successfully used for the olefin polymerization industry.[11]

1.2 Post-Metallocene Catalysts:

With the monumental success in metallocene research, the next generation of catalysts which have slightly or completely different structures were synthesized and used.[12a] Depending on the type of ligand and metal used, these post-metallocene catalysts show different reactivity and selectivity towards the comonomer incorporation. A detailed discussion of this topic is not within the scope of this thesis although an overview of these post-metallocenes is schematically highlighted below (Figure 1.2).[12 b]

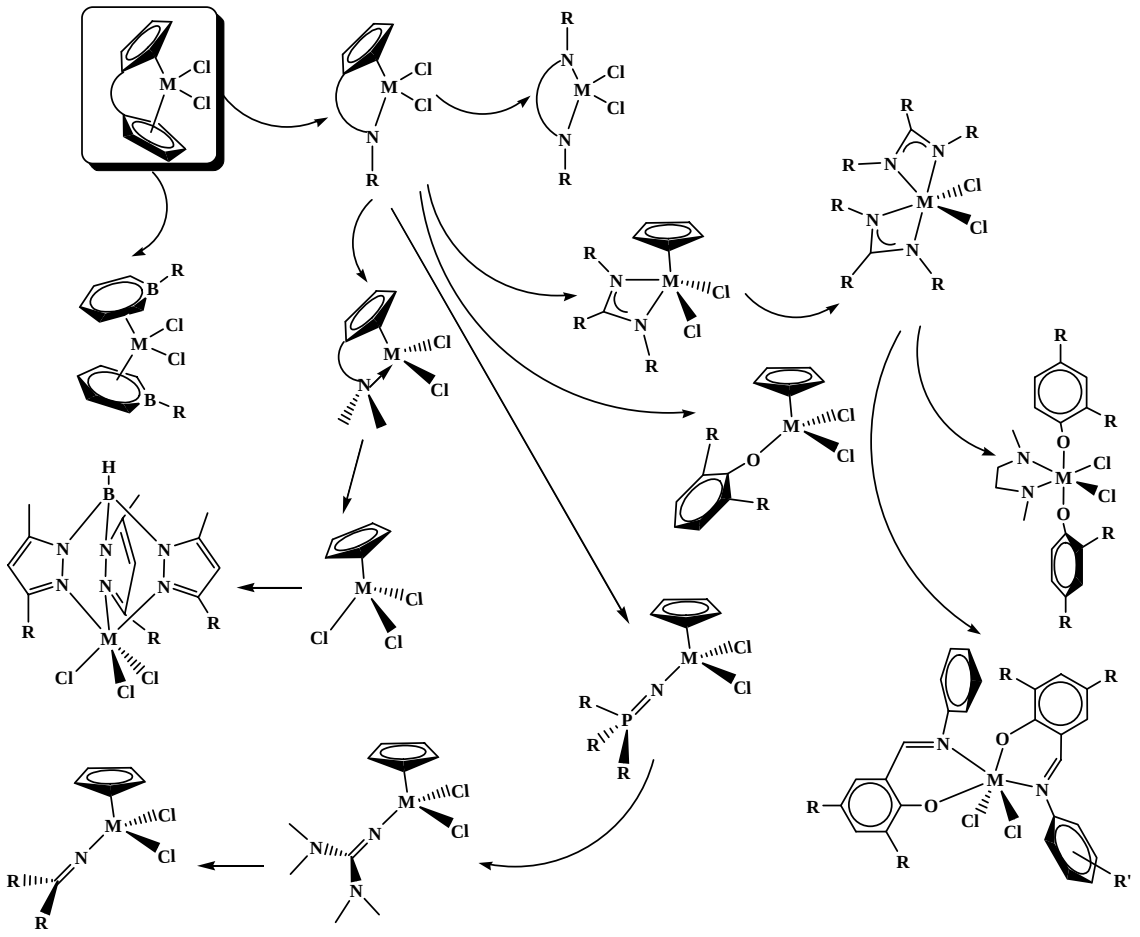

Figure 1.2: Development of early transition metal post-metallocene catalysts.[12b]

1.3 Ethylene Oligomerization

With this wealth of knowledge and the demand for the development of improved quality polyethylene (PE) products, the main focus of research today is on the development of a new type of polymer that incorporates different monomer in a controlled fashion conveying desired properties to the polymer. As a result, the number of carbon units on the co-monomers will have a direct effect on the nature of the polymer produced (Table 1.1).

Table 1.1: *Applications of Linear Alpha Olefins (LAO)*[13]

LAO Fractions	Main applications
$C_4 – C_8$	Polyolefin co-monomer (LLDPE, HDPE), poly-butene-1, plasticizer alcohol, intermediate in the production of oxo alcohols, hexyl mercaptans, octyl mercaptans, amines, organo-aluminum compounds and synthetic fatty acids.
C_{10}-C_{12}	An intermediate in the production of epoxides, amines, oxo alcohols, synthetic lubricants, synthetic fatty acids, alkylated aromatics and synthetic lubricants, plasticizer alcohol, Production of linear alkylbenzene, detergent alcohols (oxo alcohols), amines and amine oxides, mercaptans, epoxides.
C_{16+}	Alpha olefin sulfonate, detergent alcohols (oxo alcohols), lubricant additives, wax lubricants.

The market demand of these LAO's according to their specific applications is depicted in (Figure 1.3).[14] The data provided has shown that the fractions C_4 - C_8 are in high demanded as a co-monomer for the production of LLDPE. LLDPE incorporates 10-20% of 1-hexene or 1-octene in the structure which results in its characteristic clear and thin film with high tensile strength and puncture resistance value. Consequently, a vast majority of industrial and academic research has been continuously focusing on developing the catalytic systems responsible for selective tri- and tetramerization of ethylene hoping for eventually gaining the mechanistic

understanding and the knowledge of the parameters responsible for generating such high purity products required in the polymer industry.[15]

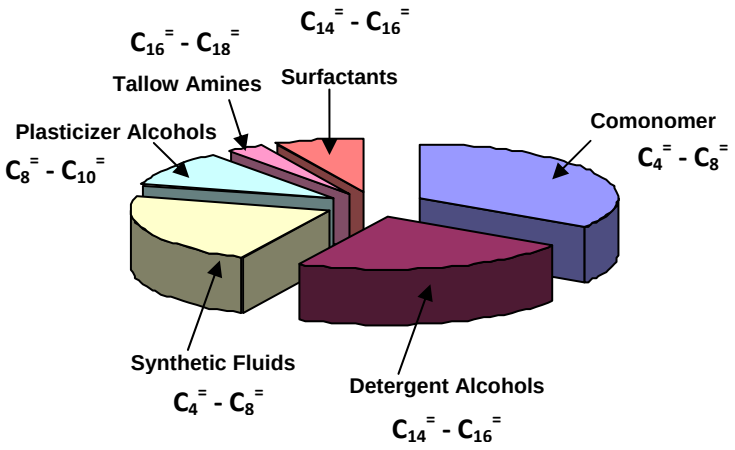

Figure 1.3: Market distribution of α-olefins.[14]

1.3.1 Mechanism for Ethylene Oligomerization

Mechanistic understanding is the key for rationally designing and fine tuning the improved catalyst systems. Due to the versatile behavior of producing selective and non-selective oligomerization products as well as polymerization products, over 90% of patents and scientific literature for ethylene oligomerization processes are based on chromium catalysts. This versatile behavior is believed to be due to the redox dynamisms that exist between the different oxidation states of organo-chromium species (Figure 1.4). Consequently, the majority of the mechanistic studies and proposals have been carried out on chromium-based catalytic systems.

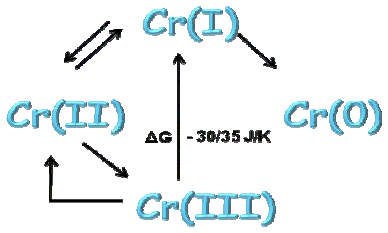

Figure 1.4: Redox dynamism between the different oxidation states of Chromium.

A brief highlight of the accepted mechanisms for tri-/tetramerization and non-selective and selective oligomerization, as well as an alternative mechanism for the selective tetramerization of ethylene based on chromium systems is given in the following section.

1.3.1.1 Linear Chain Growth Mechanism (Non-Redox):

The main feature of the linear chain growth mechanism proposed by Cossee-Arlman (Scheme 1.3) is that the metal oxidation state remains constant through out the catalytic cycle, the driving force being the Lewis acidity of the metal centre that initiates the coordination of the ethylene molecule.[16] Following this event is the insertion between metal-carbon bonds. The product is released via *β*-hydrogen elimination and the cycle continues until the catalyst is deactivated. The nature of the product formed is based on the rate of elimination versus the rate of insertion. If the rate of elimination is faster than the rate of insertion, shorter carbon chains containing oligomeric products are formed. In contrast, faster rates of insertion compared to the elimination of the products result in longer chain products. This mechanism is able to explain the general oligomerization pathways as shown in Scheme 1.3.

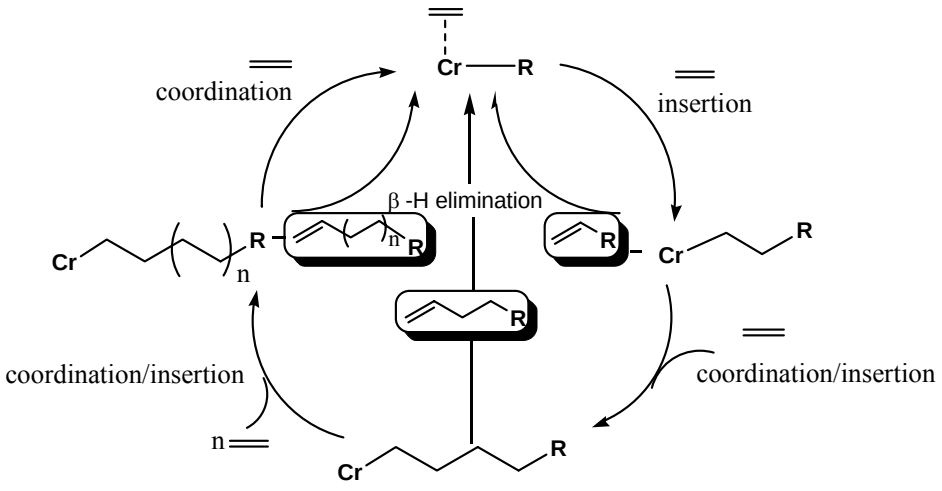

Scheme 1.3: Cossee – Arlman Linear Chain Growth Mechanism (non-redox).

1.3.1.2 Ring Expansion or Metallacycle Mechanisms (2-electron redox process):

In 1964, Manyik was the first to propose metallacycle mechanisms for selective trimerization of ethylene.[17] In contrast with the linear chain growth mechanisms, ring expansion mechanisms follow the 2-electron redox process as the oxidation state of the metal centre changes throughout the catalytic cycle (Scheme 1.4).

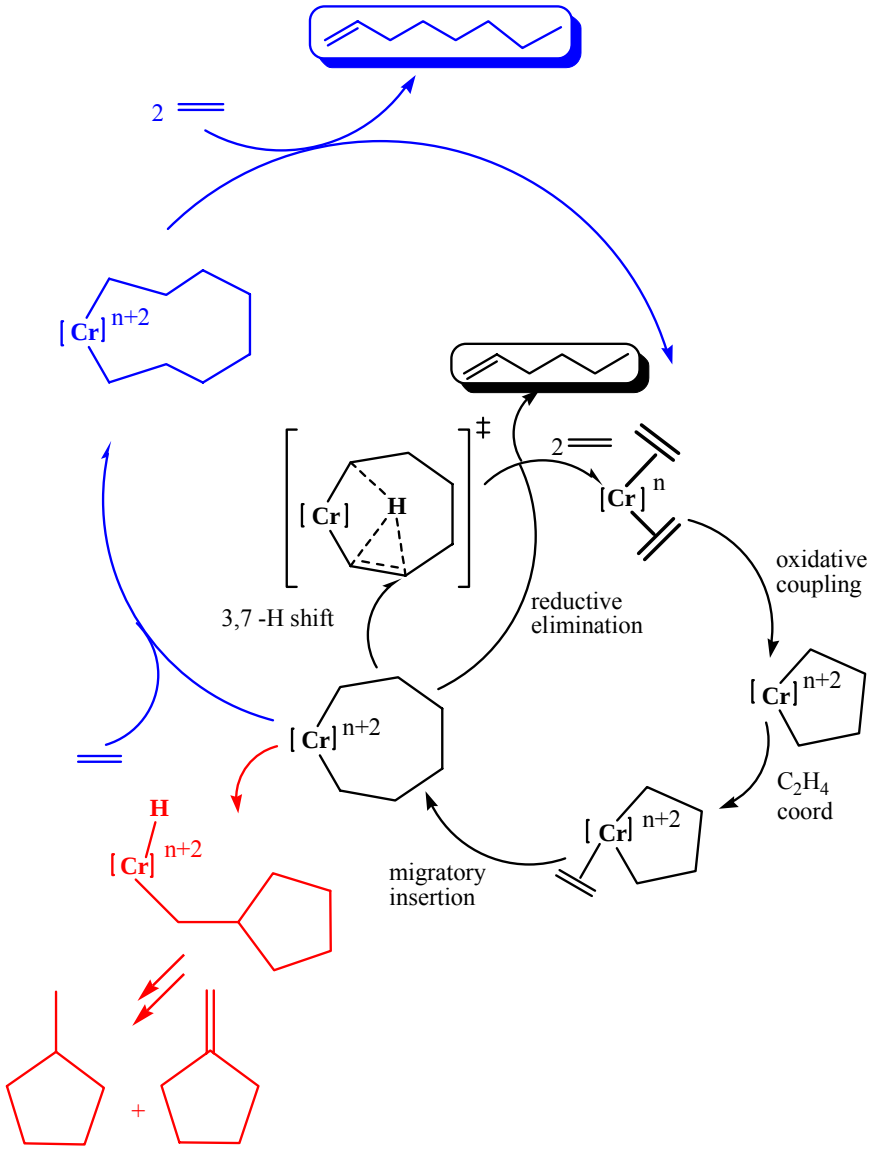

Scheme 1.4: Metallacycle mechanism for selective tri-/tetramerizatiom.

The key step in this cycle is the formation of metallacyclopentane intermediate via the oxidative coupling of two molecules of coordinated ethylene to the low valent metal centre. This is followed by the insertion of a third molecule of ethylene to generate a 7-membered metallacycle. If the ring is stable enough, and the rate of elimination is faster than the rate of insertion of ethylene, selective formation of 1-hexene is obtained via β-hydrogen transfer followed by reductive elimination. The computational studies reveal that the two steps β-hydrogen transfer and reductive elimination, to yield 1-hexene, is in fact one step concerted 3,7-H transfer as shown in Scheme 1.4.[18] However, if the rate of insertion is faster than the rate of decomposition, metallacycle growth continues via subsequent insertions of ethylene as long as ring geometry permits. The metallacycle may undergoes reductive elimination of α-olefin, restoring the original oxidation state of the metal, thus being ready to restart the next catalytic cycle.[18] The generation of 9-membered rings and eventually reductive elimination to 1-octene in a selective fashion is therefore highly unlikely. On the other hand, experimental evidence from studied of Sasol's Cr(PNP) tetramerization systems suggests the involvement of metal-hydride intermediate, contrary to the computational studies.[18] The observed formation of the cyclic by-products via metal-hydride intermediate such as methyl- and methylene-cyclopentane in a 1:1 ratio is rationalized in Scheme 1.4.

This is today a well-accepted mechanism for selective trimerization of ethylene. The experimental evidence for the formation of metallacycle intermediates was shown by Jolly in 1997 by isolating and crystallographically characterizing both chromacyclopentane and chromacycloheptane while the latter undergoing decomposition at 56 ^{o}C to 1-hexene (Figure 1.5).[19]

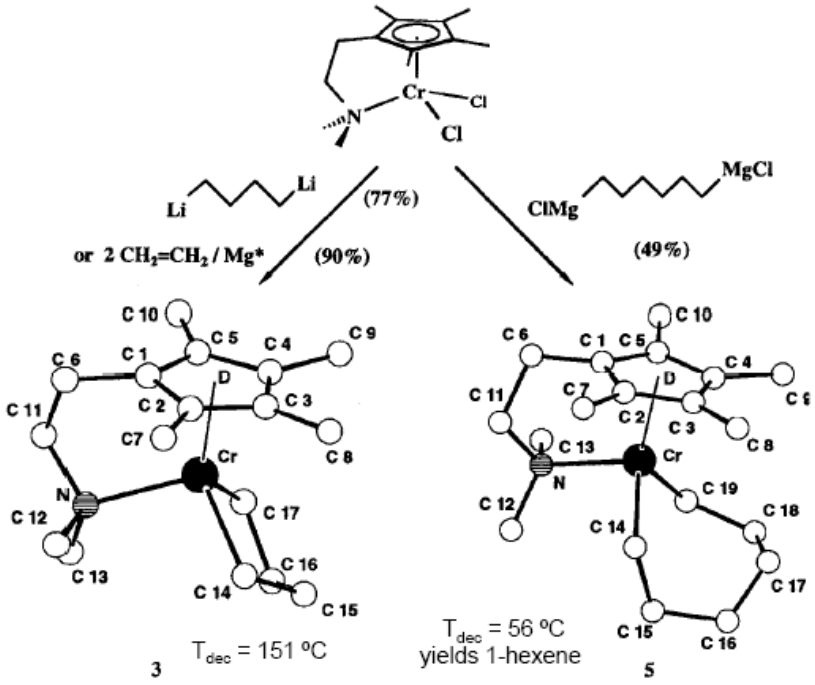

Figure 1.5: Isolated structure for chromacyclopentane and chromacycloheptane.[19]

Recent systematic mechanistic studies with deuterium labelling experiments performed by Bercaw,[20] Gibson[21] and McGuinness[22] also conclusively demonstrated the metallacycle mechanism hypothesis.

Despite the selective formations of certain α-olefins, mechanisms for the formations of non-selective oligomerization products are still in debate. Nonetheless, crossover experiments with C_2H_4 and C_2D_4 performed with tungsten, nickel, cobalt and iron based non-selective

catalytic systems are found to be consistent with the Cossee mechanisms,[23] while certain Cr-based non-selective systems are found to be consistent with the metallacycle mechanisms (Scheme 1.5).[24]

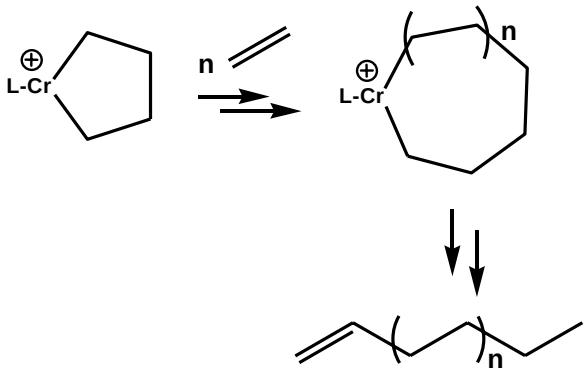

Scheme 1.5: Proposed extended metallocycle mechanism for Schulz-Flory distribution.

It seems unreasonable that non-selective Cr-based systems follow the extended metallacycle mechanisms. This is due to the fact that the transition state that leads to β-hydrogen elimination from the chromacyclopentane is expected to be rather strained compared to the ring expansion by ethylene insertion. Therefore, these systems seem to be more consistent with the chain-growth Cossee-type insertion mechanisms.

1.3.1.3 Proposed Bimetallic Mechanism for Ethylene Tetramerization:

As already mentioned, ethylene trimerization systems have made major breakthroughs with the preparation of highly active and selective systems, [25] with the ring expansion mechanistic hypothesis being widely accepted.[26] The same metallacycle mechanism is also used to explain the formation of 1-octene. Computational studies have revealed that the collapse of

metallacyclohepatane to generate 1-hexene is energetically favoured when compared to the use of ethylene insertion to produce metallacyclononane and eventually 1-octene. Therefore, it is unlikely that through a ring expansion mechanism a highly selective tetramerization catalyst will be obtained, and so, the search for a catalytic system capable of forming 1-octene with high selectivity poses a great challenge. As a result, there are only three homogeneous catalytic systems in all of patent and academic literature that are capable of producing large excesses of 1-octene.[27] Given the rarity of tetramerization catalysts, one might wonder if a selective tetramerization system producing 1-octene may be possible, without an alternate mechanistic pathway being followed.

Recently, an alternate mechanistic proposal for the formation of 1-octene has been reported in the literature involving dinuclear chromium complexes (Scheme 1.6).[28] This proposal is based on the observations made for acetylene trimerization and the formation of 1-octene upon thermal decomposition of tetralithium tetrabutanediyldichromate from dinuclear chromium complexes.[29]

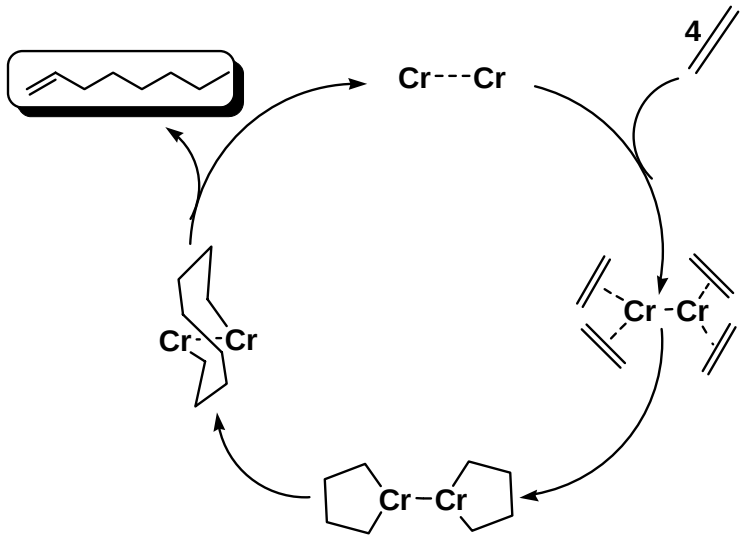

Scheme 1.6: Proposed bimetallic mechanism for selective tetramerization.

According to the proposal, monovalent dinuclear chromium centers should be held by the ligand in such a distance that in one hand it prevents formation of Cr-Cr quintuple bond and at the same time keeping the intermetallic distance sufficiently short enough to afford an internal reductive elimination of the two five membered rings to 1-octene (Scheme 1.6). This mechanism avoids an intermediate metallacycloheptane that is responsible for the formation of 1-hexene.

1.3.2 Chromium Based Selective Ethylene Oligomerization Systems

For the purpose and scope of this thesis work, related breakthrough systems and the most influencing commercial catalysts have been highlighted in this section.

1.3.2.1 The Phillips System – Pyrrolyl Ligands

Reagan, in Phillips Petroleum Company, was the pioneer researcher for developing highly active and selective commercial systems for ethylene trimerization. The *in situ* generated catalysts consist of mixture of 2,5-dimethylpyrrole (DMP), chromium-ethylhexanoate and DEAC/TEAL in hydrocarbon solvent, affording an outstanding activity (156,666 g/g Cr/h) with a purity as high as 93.2% of 1-hexene (Figure 1.6). [25a , 30, 31]

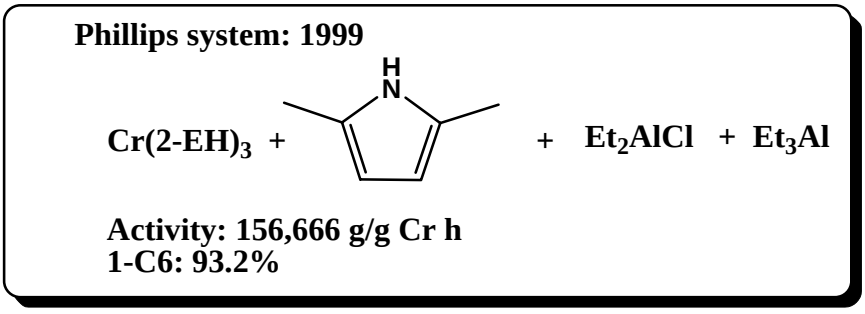

Figure 1.6: Phillips-Chromium Pyrrolyl catalyst for ethylene trimetization.

The most significant contributions to the Phillips system were made by Mitsubishi Chemical Corporation.[32] Their improvement consists on the use of chlorinated solvent, hexachloethane, and non-coordinating Lewis acid, $B(C_6F_5)_3$. With the same *in situ* protocol containing chromium(III)2-ethylhexanoate, 2,5-dimethylpyrrole and triethylaluminum in molar ratios of 1:6:4:40, the process afforded 95.4% pure 1-hexene. This method had a significantly higher activity of 3,780,000 g/g Cr/h in comparison to the Phillips system (Figure 1.7).[33]

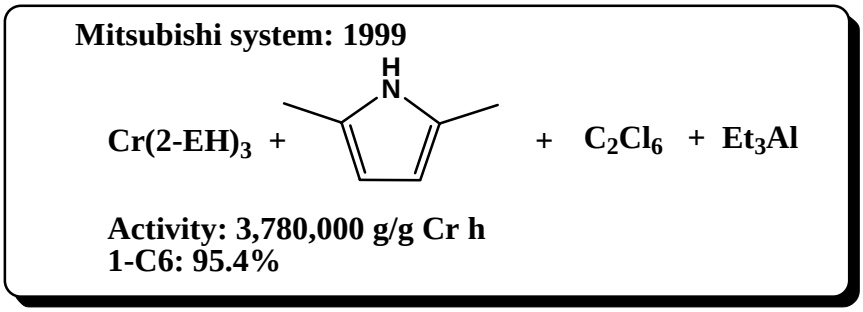

Figure 1.7: Mitsubishi improved Chromium Pyrrolyl catalyst for ethylene trimetization.

Despite the enormous commercial success of these systems, the system remained poorly understood until the catalytically active species were isolated from the Gambarotta's lab (Figure 1.8).[34] The findings relate the specific chromium oxidation states with the type of catalytic behaviours. For example, an active species of Cr(I)-pyrrolato system showed selective formation of 1-hexene with ethylene whereas Cr(II)-species showed the exclusive formation of polyethylene (Figure 1.8, A & B).

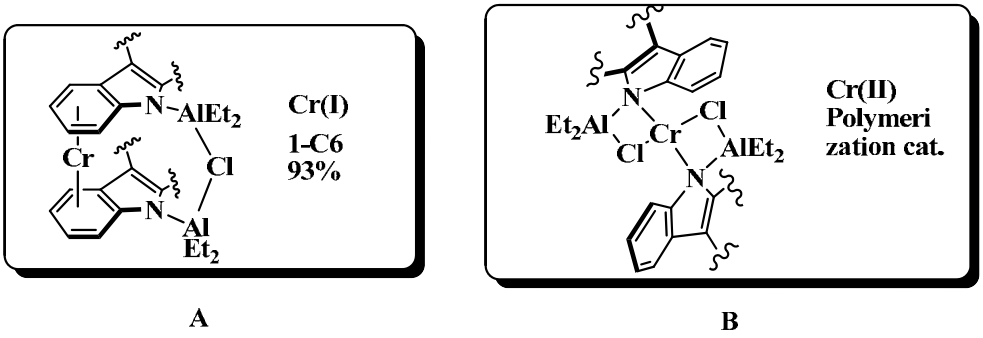

Figure 1.8: Isolated active species of Cr(I) and Cr(II)-pyrrolato system[34]

1.3.2.2 The Albemarle/Amoco System – Tris-Phosphorus Ligands

Following the Phillips patent, Amoco corporation filed another patent for selective trimerization of ethylene with asymmetric polydentate phosphorus ligands of the general formula $R_2P(CH_2)_aP(R')(CH_2)_bPR_2$ where (a = 2, b = 3). Their best results were obtained with a Cr(III) complex bearing the asymmetric $Me_2P(CH_2)_2P(Ph)(CH_2)_3PMe_2$ ligand when activated with 222 equivalents of butylaluminoxane (BuAO) and at 35 bar of ethylene pressure, at 60°C. A productivity of 48700 g/g Cr/h and selectivity of 98.3% of hexenes (99.0% of 1-hexene) was reported (Figure 1.9).[35] Nonetheless, high cost and difficulty in catalyst preparations challenge the commercialization of this system.

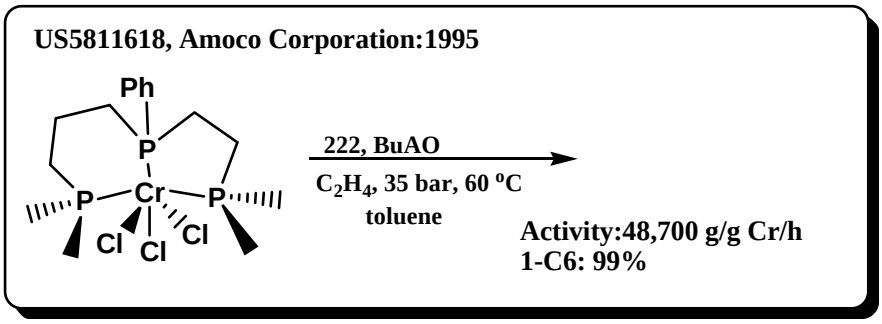

Figure 1.9: Amoco's tris (phospha)-Cr complex for selective trimerization.

1.3.2.3 Tosoh Corporation's System – Tris(pyrazolyl)methane Ligand

Tosoh Corporation's researcher added one more significant step in the discovery of highly active and selective ethylene trimerization systems by making use of already existing tris (pyrazolyl) methane ligands. This ligand adopts facial coordination geometry with the Cr-metal centre as opposed to the meridional ligation adopted by the above mentioned tris-phosphorus ligand systems. The Cr(III)-complex of this tris (pyrazolyl) methane ligand, upon activation with 360 molar equivalents of MAO as co-catalyst, showed the overall productivity of 40,100 g/g Cr/h and selectivity reaching 99.1% (Figure 1.10).[36] The significance of this system lies in the stability of the ligands making them easy to handle compared to the Phillips pyrrolato systems

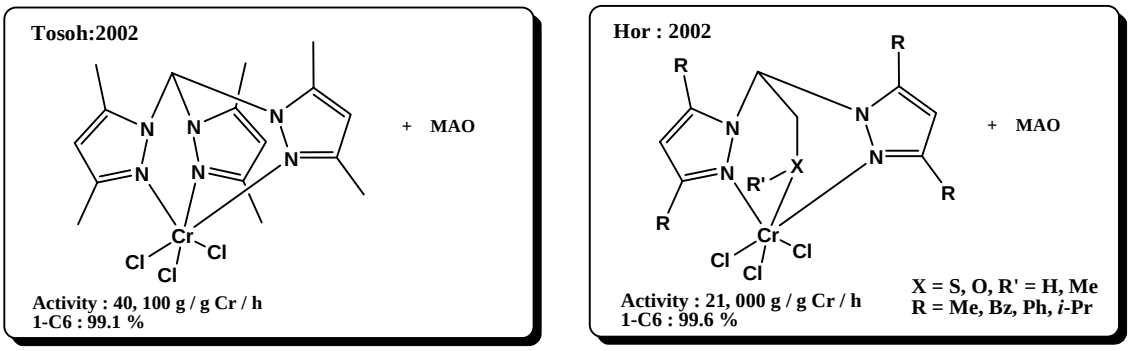

Figure 1.10: Tosoh's and Hor's Pyrazolylmethane system.

and Amoco tris-phosphorus systems.

Further modification of this system carried out by Hor and coworkers, consists of the replacement of central pyrazolyl ring with the functionalized pendant arm on the spacer link between the two pyrazolyl moieties, thereby giving so called "heteroscorpionate" ligand architecture. The ether functionalized arm was found to be more robust with the overall productivity and selectivity of 21,000 g/g Cr/h and 96.1% of 1-hexene, respectively. In contrast,

the case of the thioether functionalized pendant has a lower activity (16,200 g/g Cr/h), albeit higher selectivity (99.6%) was observed (Figure 1.10).[37]

1.3.2.4 The British Petroleum System – Hybrid Nitrogen and Phosphorus Ligands

It was Duncan Wass from British Petroleum (BP) that established the multidentate N and P hybrid ligands with Chromium (III) metal precursor for obtaining selective trimerization of ethylene. The systematic studies done on the effect of substituent on this ligand, showed that the breakthrough system was obtained upon *in situ* mixing of Cr(halide)-precursor with ortho $(methoxyphenyl)_2PN(Me)P(methoxyphenyl)_2$ ligand when activated with 300 equivalents of MAO in toluene solvent (Figure 1.11).

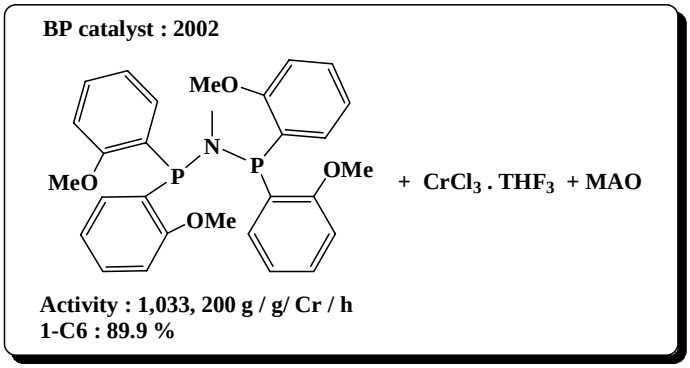

Figure 1.11: BP catalyst for selective ethylene trimerization.

The productivity from this system was significantly high enough (1,033,200 g/g Cr/h) with the remarkable selectivity of 1-hexene (89.9%) even with no polymer fouling in the reactor.[38] This activity is one order in magnitude higher than the Phillips system because it has an extremely low deactivation rate of catalyst.

1.3.2.5 The Sasol System – PNP and SNS hybrid Ligand

In their initial studies McGuinness and Wasserscheid found the hybrid N and P ligand of the general formula $R_2PCH_2CH_2N(H)CH_2CH_2PR_2$ to support very active ethylene trimerization while in combination with Cr(III)-halide source and MAO as an activator. Later on, Sasol technology improved the system even further and patented the systems. Less sterically crowded diethylphosphino substituent compared to sterically demanding dicyclohexyl substitutes showed increased activity (37, 400 g/g Cr/h) and 1- hexene selectivity (93.2%).[39] However, the drawback of this system is its requirement of a very high amount (850 equivalents) of MAO for activation (Figure 1.12).[39]

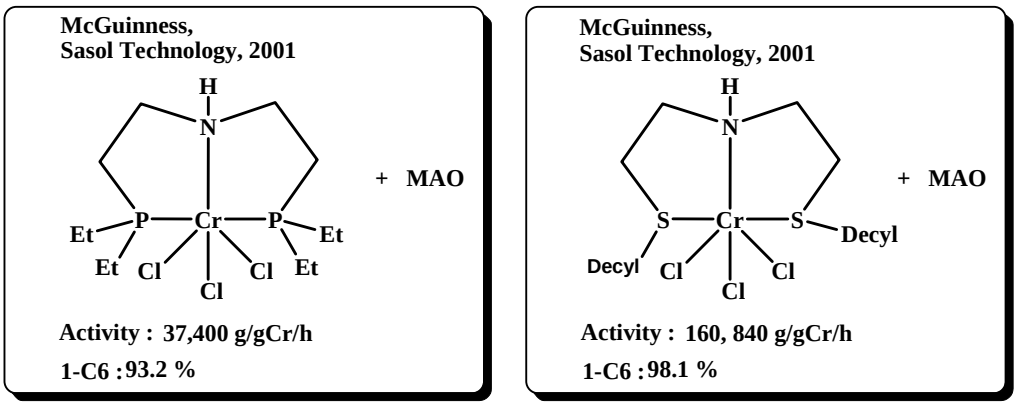

Figure 1.12: McGuiness system for selective ethylene trimerization.

Further modifications of the systems have been carried out by the same researchers by replacing the soft donor- Phosphorus, with another soft donor - Sulphur. The comparatively high activity (160, 840 g/g Cr/h) and selectivity (98.1%, 1- C6 purity) was obtained with [bis-(2-decylsulphanyl-ethyl)-amine]$CrCl_3$ complex upon activation with a small amount of MAO (280

equivalents) (Figure 1.12).[40] This discovery introduced the potential of sulphur based ligands as cost efficient and easily accessible systems.

Another breakthrough discovery in the field of ethylene oligomerizations was achieved by Bollmann *et. al* in the Sasol Technology by performing a slight modification on the Wass's trimerization catalyst, (orthomethoxy)-PNP.[41] Their discovery launched the first commercial tetramerization catalyst with a catalyst obtained by removing the substituent on the phenyl group at phosphorous and alkylating the centre nitrogen with an isopropyl group (Figure 1.13). The selectivity of 1-octene was up to a record 70% with an exceptionally high activity 285, 000 g /g Cr/h. Other side products were 1-hexene (16%), and methylcyclopentane and methylenecyclopentane in 1:1 ratio.

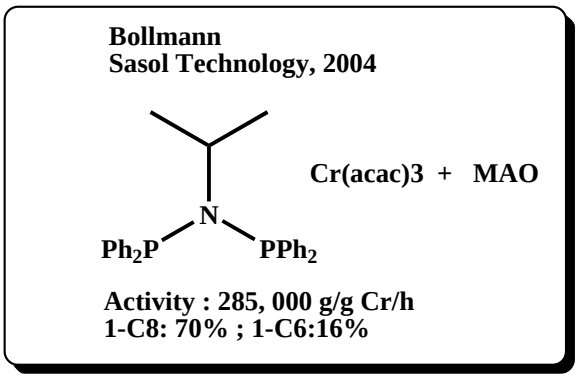

Figure 1.13: Sasol PNP system for tetramerization of ethylene.

1.3.2.6 The SK Energy System – Chiral PCCP Ligand

Following the slight modifications on the previously investigated less selective (39.7%, 1-C8) diphenylphosphinoethane (PCCP) ligand of Sasol, Kang at SK energy was able to achieve a remarkably active catalyst of productivity 1,929, 000 g/g Cr/h, while still maintaining the selectivity for 1-octene (64%) comparable to Sasol's PNP system. The ligand is based on the

PCCP framework containing a chiral scaffold, as shown in Figure 1.14. Among them, the *S, S-chiraphos* ligand showed the highest activity.[42]

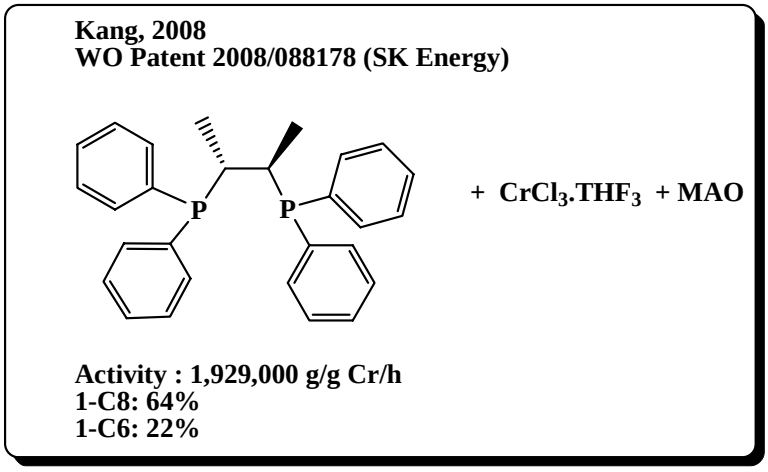

Figure 1.14: SK energy's S, S-chiraphos ligand for selective ethylene tetramerization.

1.3.2.7 Rosenthal and Wass System – New derivatives of PNP Ligand

A new derivative of Sasol PNP system has been reported by Rosenthal with tethered NH-moiety to one of the Phosphino arm to give a ligand of the type $Ph_2PN(i\text{-}Pr)P(Ph)(i\text{-}prNH)$.[43] Despite showing k_2-(P,P) coordination similar to PNP ligands without pendent donors, this ligand with $CrCl_3.THF_3$ and activated with MAO is proven to be a highly active and selective ethylene trimerization catalyst (Figure 1.15).

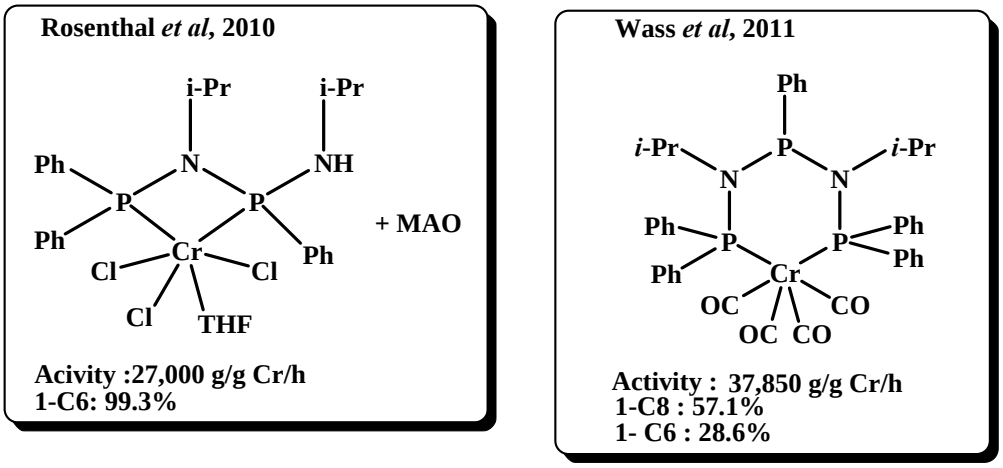

Figure 1.15: Rosenthal and Wass's tri-and tetramerization system.

Recently, an interesting variation of Rosenthal's system has been reported by Wass (Figure 1.15) via an unconventional route. He utilized Rosenthal's PNPNH ligand as a starting point to complex with $Cr(CO)_6$, and then treated with MeLi and Ph_2PCl to synthesize PNPNP ligand of the type shown in Figure 1.15. This system proved to be more selective towards 1-octene (57.1%) than 1-hexene (28.6%), with overall activity of 37,850 g/g Cr/h.[44]

1.3.3 Nickel Based Ethylene Oligomerization Catalysts

Apart from chromium, another extensively exploited oligomerization catalyst system is based on the element Nickel. Organonickel chemistry became the subject of immense scientific interest soon after the Ziegler's discovery that nickel can transfer Al-H from Al(*n*-Bu)$_3$ to ethylene, giving butene and $AlEt_3$.[45] Late transition metals, (Ni, Pd, Rh, Fe) being rich in electron density, are less electrophilic than early transition metals (Ti, Cr), thereby decreasing the attraction of the weakly basic ethylene molecules. Moreover, catalysts of late metals are more susceptible to β-hydrogen elimination due to instability of metal-carbon bonds. This property has

made them an attractive candidate for ethylene oligomerization processes. Shell had already been exploiting Nickel oligomerization catalysts for years since 1972. Keim *et al* discovered a nickel-Phosphorusoxide-based catalyst (Figure 1.16)[46]. This is the first worldwide commercial non-selective ethylene oligomerization catalyst in a process called "Shell Higher Olefin Process (SHOP)".[46] The activity of this process reaches 6000 moles of ethylene per mol of complex with 99% of linear α-olefins. The individual products require separation by fractional distillation in order to fulfill their market demand which is laborious and costly process.

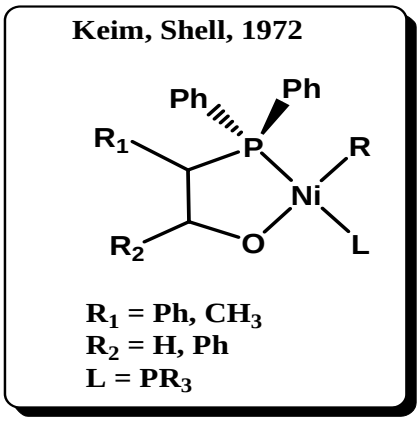

Figure 1.16 : Keim catalyst for ethylene oligomerization.

It is proposed that the non-selective oligomers are produced via a general Cossee-type mechanism (Scheme 1.7). The coordinatively unsaturated species generated after activation is stabilized by a *β*-agostic interaction from the hydride of the inserted ethylene molecule. The evidence for the formation of a hydride intermediate has been reported in the literature.[47] This process is followed by further insertion, and the final product is released after *β*-hydride elimination/chain transfer step. The selective formation of *α*-olefin product depends on the

ethylene pressure, as the rate of chain transfer relative to chain isomerization increases with the ethylene concentrations.[48]

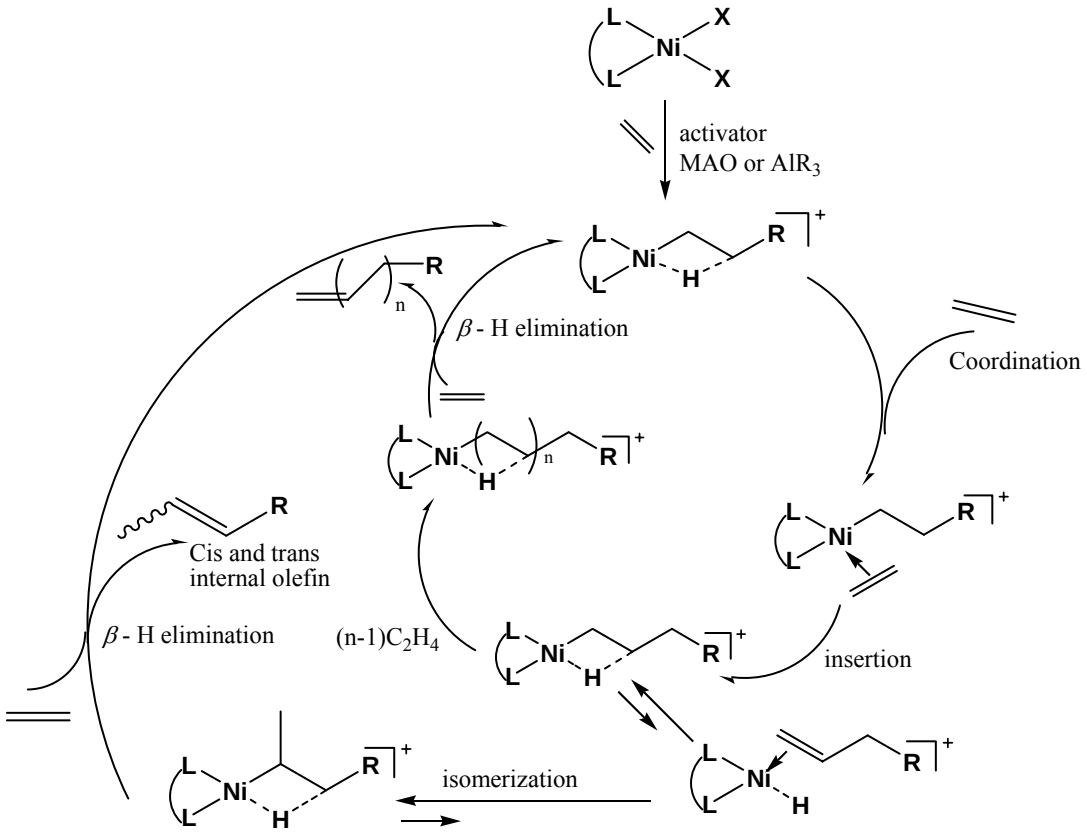

Scheme 1.7: Proposed Cossee-type mechanism for non-selective oligomerization by Ni(II) catalyst.[47]

Various Nickel (II) catalysts tend to favor chain termination over propagation, resulting in their application for dimerization of ethylene to butene. However, the challenge is to selectively isolate 1-butene from 2-butene, as nickel catalysts are prone to form internal olefins. The behavior of nickel catalysts could be fine tuned and modified by the judicious choice of ligands. As in the case of Cr-catalyst, a selective formation of 1-butene can only be explained via metallacycle mechanism.[48]

The paradigm that nickel catalysts can only be used for α-olefins production was challenged by the evolutionary discovery of Brookhart and Small that nickel catalysts could also be used for ethylene polymerization. By using already existing diimine ligands, they showed that late transition metals (e.g Ni) are able to polymerize ethylene and higher olefins to high molecular weight polymers with exceptionally high activities. This breakthrough has stimulated the research for understanding the unique abilities of this system to sustain catalytic activity at a late metal center and encouraged the development of other transition metal systems based on this family of ligands. Some examples are shown in the Figure 1.17.[49]

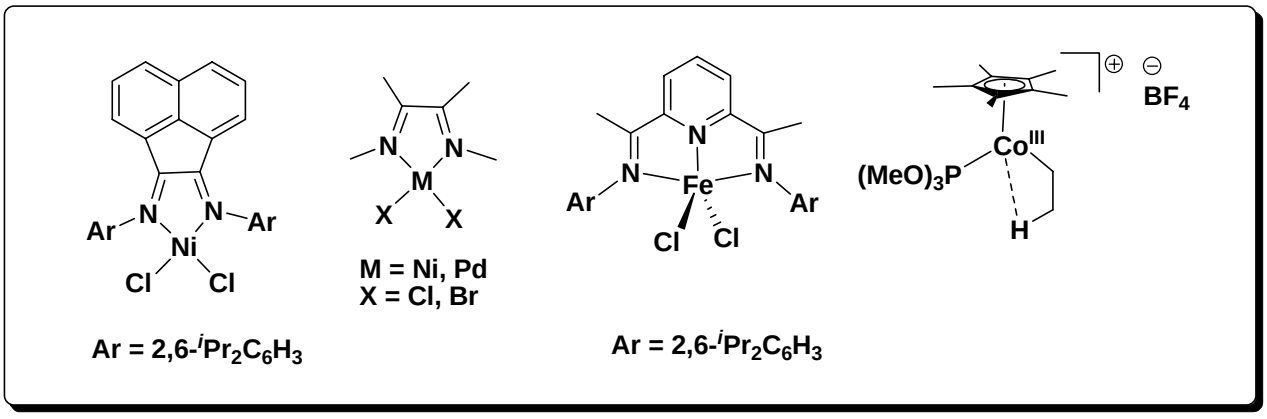

Figure 1.17: Late transition metal polymerization catalysts.[49]

The bis-iminopyridine ligand system received special attention with respect to steric and electronic parameters, as it was expected to lead to increased control during ethylene polymerizations. An attempt of understanding this ligand with respect to its bonding mode, electronic features and some unique chemical reactivity has been presented below in this thesis (Chapter 7).

1.4 The Activators

Since the first discovery of the aluminum alkyls as co-catalysts needed for polymerization, considerable effort was put towards understanding the actual role in catalysis. At the early stages, various Lewis acidic aluminum alkyls, or aluminum alkyl halides, were used as co-catalysts for the purpose of generating active species via alkylation and abstraction of halides or alkyls from the metal center creating co-ordinatively unsaturated cationic metal alkyl species. Later on, even stronger Lewis acids such as $B(C_6F_5)_3$ or trityl borate salts, $[(C_6H_5)_3C][B(C_6F_5)_4]$ were employed by the researchers to generate a cationic metal centres.[50] The improved activity shown by these co-catalysts is attributed to the presence of a large anionic borate that forms a solvent-separated ion pair and creates a vacant site adjacent to the M-C bonds.

The whole perspective of the polymerization and oligomerization industry has changed after the discovery of the highly efficient activator methyl aluminoxane (MAO) by Kaminski and Sinn in 1980's.[51] MAO, a hydrolyzed version of $AlMe_3$, is the preferred catalyst activator today. Even though MAO is widely used and studied as an important cocatalyst, the structure of MAO is still not fully understood due to the lack of well defined crystal structure. It is believed to be composed of –MeAlO- units in a polymeric form, containing variable amounts of free $AlMe_3$ ranging from 10-30%. The experimental and computational evidence suggests that, like other aluminum activators, the role of MAO is 1) to allow alkylation of the metal centers, and 2) to encourage halide or alkyl abstractions from the metal center, creating an electron deficient cationic metal centre. It is also believed that the large polymeric structure of the anionic MAO helps it to remain separate from the metal center, thereby maintaining the cationic nature of the active species, consequently increasing the catalytic activity. When used in excess, MAO is an

excellent scavenger of water; however, this large excess is expensive. Alternatively, some research is being seen for the use of stoichiometric amounts of boron reagents in combination with some alkylating agents such as TIBA, as an inexpensive alternative for MAO. For the purpose of this thesis work, different kinds of co-catalysts and alkylating agents were used apart from MAO, with the aim of isolating catalytically active species and to help to better understand the factors controlling the selectivity of the catalytic processes.

1.5 Aim and Objectives of the Thesis

At the start of this thesis work, some of the issues regarding the diverse behavior of the chromium catalysts, including selectivity as well as factors impacting selectivity (solvent effect, temperature, pressure, activators, and metal oxidation states) were still not conclusively determined. The key to obtaining selective trimerization catalysts is the possibility of generating monovalent derivatives. Thus, the initial aim was to address these issues. The ultimate goal of working with early transition metal, Chromium, and the late transition metal; Nickel, to gather some missing pieces of the mechanistic puzzle and to better understand the ethylene oligomerization process was quite ambitious. The knowledge gained from this study could be applied to the design of new and improved catalytic systems. It is however worth noting that we were able to isolate the first ever 99.9% selective tetramerization catalyst, an achievement once considered to be impossible. This was rewarded by World Intellectual Property Organization (WO) patent filled from commercial company (LyondellBasell). These findings in fact opened up the door for academic research to find an alternative mechanistic pathway, and give hope to the commercial world to develop a solely selective tetramerization catalyst.

To fulfill the aforementioned goal, the following objectives were laid out:

1. Screening of diverse ligands containing N, O and P such as NP, NCN, NCO, aminobispyridine, pyrrole as well as bis-aminopyridine ligands. From previous studies done in the Gambarotta lab and others, it appears that stabilization of low-valent states of the metal catalyst is highly dependent on the nature of ligands.

2. Isolation of well defined & catalytically active intermediates and assessment of their single component catalytic behavior with ethylene.

3. Isolation and assessment of well defined monovalent Cr(I) and Ni(I) complexes to address the issue of metal oxidation states in reactivity.

4. Utilization of all the isolated complexes in different oxidation states to understand the effect of variable pressure, temperature, co-catalysts and solvents on the activity and selectivity.

Detailed descriptions of the specific issues are addressed in the corresponding chapters.

1.5.1 Chapter 2

This chapter will discuss the isolation of a series of chromium complexes in different oxidation states, isolation of heterobimetallic Cr-aluminate complexes and few observations about single component and selective trimerization catalytic behavior of this system. A remarkable solvent effect on selective trimerization behavior is also presented. For this work, the anionic amidophosphine (NP) ligand has been selected. In a continued effort to address the issue of metal oxidation state and catalytic behavior type, I have isolated self-activating monovalent

Cr(I) complexes via an unconventional route of using a vinyl Grignard reagent. This chapter will also describe the reduction of the tetranuclear and divalent {[(*t*-Bu)NPPh$_2$]Cr[μ-(*t*-Bu)NPPh$_2$]$_2$Cr}$_2$(μ-Cl)$_2$ to an unusual mixed-valence, self-activating catalyst and its unprecedented switcheability from UHMW polymerization behavior to either selective 1-butene or 1-hexene depending on the type of activation.

1.5.2 Chapter 3

The previous chapter explains, anionic N-P ligands support a variety of polynuclear structures, from dimeric to tetrameric, showing an enhanced tendency to retain aluminate activators. Furthermore, they may also stabilize the monovalent state responsible for selective trimerization. No tetramerization activity has been determined for these derivatives. Given the importance of tetramerization catalysts, we have extended our research and probe the N-P ligand frame by replacing the acidic proton on the ligand with an additional alkyl and explored the corresponding R_2NPPh_2 ligands. In this chapter I have reported a catalytic tetramerization system that show with moderate activity a selectivity of over 90%. This chapter will also describe the further modification of above mentioned neutral NP ligand by adding a pyridine pendent. The isolation and catalytic assessments of the corresponding Cr(II)/Cr(III) complexes will also describe.

1.5.3 Chapter 4

The search for a catalytic system capable of forming 1-octene selectively indeed poses a great challenge. In this chapter a conclusive evidence for the formation of substantial amounts of

1-octene (>99%) using amino-bispyridine-Cr(III) complexes will be provided. Herein we discuss the implications of these findings.

1.5.4 Chapter 5

The elimination of the P atom from the ligand frame of the PN system and use of a regular amide anion as well as its impact on the catalytic behavior of the chromium complex has been studied. In this chapter, I have described the isolation, characterization and catalytic single component self-activating behavior of chromium amido-aluminate complexes for ethylene oligomerization in homogeneous system. Depending on the activators, the catalytic activity switched from polymerization to mixture of 1-hexene/1-octene to S-F distribution.

1.5.5 Chapter 6

As a part of our systematic exploration on ligands, their ability to stabilize a particular oxidation state and their role in catalytic behaviours, in this chapter, I am presenting our attempt to evaluate the hard donors bidentate and tridentate amidinates and amidate ligands and their ability to affect the stability of the chromium divalent state . The bimetallic and monometallic Cr(II)/Cr(III) complexes were isolated and fully characterized and their highly active polymer free non-selective oligomerization behavior is also presented in this chapter.

1.5.6 Chapter 7

After the breakthrough discovery of Brookhart *et al* that nickel catalysts can polymerize ethylene with exceptionally high activity, the whole research perspective for late metal catalysis changed. A body of work has been devoted to understand the special feature of these well known shiff-base ligands to stabilize late metal catalysts at the expense of β-hydrogen elimination. This

chapter will describe the "non-innocence" properties of bis(imino)pyridine ligand and its involvement in organometallic chemistry of the metal centre. Additionally, isolation of a novel Nickel dinitrogen, Nickel-hydride and alkyl complexes as well as their unprecedented ethylene oligomerization activity is also presented.

1.5.7 Chapter 8

Extending our concept of monovalent species that are particularly of interesting for taking part in variety of chemical transformations, a great effort has been put to isolated a rare example of Ni(I) species with dianionic tripyrrolide ligand. In this chapter I have described the preparation, isolation, characterization and the chemistry related to the formation of the novel monovalent heterobimetallic nickel species. Ethylene oligomerization activity of monovalent and divalent complexes is also presented.

1.5.8 Chapter 9

One of the characteristic of Ni catalyst is its ability to form a variety of C-C bonds. The versatility of nickel in engaging in both reductive elimination and oxidative addition is the basis of its catalytic behavior. In this chapter I have described an unprecedented example of nickel promoted reversible C-C coupling at the α-carbon of dimethylpyrrole, however, it was not the search for the initial aim. Highly selective ethylene dimerization to 1-butene behavior of the complex is also investigated.

References:

1. a) Severn, J.; Chadwick, J.; Duchateau, R.; Friederichs, N. *Chem. Rev*. **2005**, *105*, 4073. b) http://en.wikipedia.org/wiki/Bioplastic.
2. Bamberger, E.; Tschirner, F. *Chem. Ber*. **1900**, *33*, 955.
3. GB Patent 497, 643, **1938.**
4. Hogan, J. P.; Banks, R. L. U.S. Patent 2,825,721, **1958.**
5. a) Ziegler, K.; Holzkamp, E.; Breil, H.; Martin, H. *Angew. Chem*. **1955**, *67*, 541. b) Ziegler, K.; Breil, H.; Matin, H.; Holzkamp, E. GR 973,626, **1960**. c) Natta, G.; Pino, P.; Corradini, P.; Danusso, F.; Mantica, E.; Mazzanti, G.; Moraglio, G. *J. Am. Chem. Soc*. **1955**, *77*, 1708.
6. Kissin, Y. V. *in Alkene Polymerization Reactions with Transition Metal Catalysts.* First Edition, Elsevier: Amsterdam, **2008**. *173*, 2.
7. Nakayama, K.; Furumiya, A.; Okamoto, T.; Yagi, K.; Kaito, A.; Choe, C. R.; Wu, L.; Zhang, G.; Xiu, L.; Liu, D.; Masuda, T.; Nakajima, A. *Pure & Appl. Chem*. **1991**, *63*, 1793.
8. Bercaw, E. J. KFUPM, *Lecture Series on Organotransition Metal Chemistry and Olefin Polymerization,* **2011**.
9. a) Cossee, P. *Tetrahedron Lett*. **1960**, *8*, 86. b) Cossee, P. *in Proceedings of the 6th Int. Congress on Coordination Chemistry*. Macmillan: New York, **1961**, 241. c) Arlman, J. *Proc. Int. Congr. Catal. 3rd*, **1964**, *2*, 957.
10. a) Crabtree, R. H. *The organometallic Chemistry of Transition metals*, Wiley, 4th Edition, P. 140. b) Breslow, D. S.; Newberg, N.R. *J. Am. Chem. Soc.* **1957**, *79*, 5072.

c) Petros, R. A.; Norton, J. R. *Organometallics,* **2004**, *23*, 5105.

11. Cavallo, L.; Guerra, G. *Macromolecules* **1996**, *29*, 2729.
12. a) Britovsek, G. J. P.; Gibson, V.; wass, D. F. *Angew. Chem. Int. Ed*. **1999**, *38*, 428. b) Karbach, F. F. *Diplomarbeit,* Eindhoven University of Technology*,* **2010** and reference there in.
13. a) Lappin, G. R.; Sauer, J. D. *in Alpha Olefins Application Handbook*. Marcel Dekkers, INC: New York, **1989**. 37, 1. b) Vogt, D. Oligomerization of ethylene to higher linear α-olefins; *in Applied Homogeneous Catalysis with Organometallic Compounds*; Cornils, B., Herrmann, W. A., Eds.; Wiley-VCH: Weinheim, Germany, **2000**; Chapter 2, pp 245.
14. Morgan, D. in *PERP report 02/04*, Nexant Chem Systems, **2004**.
15. McGuinness, D. S. *Chem. Rev*. **2011**, *111*, 2321.
16. a) Cossee, P. *J. Catal*. **1964**, *3*, 80. b) Arlman, E. J.; Cossee*,* P. *J. Catal*. **1964**, *3*, 99.
17. Manyik, R. M.; Walker, W. E.; Wilson, T. P. *J. Catal*. **1977**, *47*, 197.
18. Agapie, T. *Coordination Chemistry Reviews.* **2011**, *255*, 861.
19. Emrich, R.; Heinemann, O.; Jolly, C. W.; Kruger, C.; Verhonok, G. p. *J. organometallics* **1997**, *16*, 1511.
20. a) Agapie, T.; Labinger, J. A.; Bercaw, J. E. *J. Am. Chem. Soc.* **2007**, *129*, 14281. b) Agapie, T.; Schofer, S. J.; Labinger, J. A.; Bercaw, J. E. *J. Am. Chem. Soc.* **2004**, *126*, 1304.
21. Tomov, A. K.; Chirinos, J. J.; Long, R. J.; Gibson, V. C.; Elsegood, M. R. J. *J. Am. Chem.*

Soc. **2006**, *128*, 7704.

22. McGuinness, D. S.; Suttil, J. A.; Gardiner, M. G.; Davies, N. W. *Organometallics* **2008**, *27*, 4238.
23. a) Flory, P. J. *J. Am. Chem. Soc*. **1940**, *62,* 1561. b) Skupinska, J. *Chem. Rev.* **1991**, *91,* 613.
24. Tomov, A. K.; Chirinos, J. J.; Jones, D. J.; Long, R. J.; Gibson, V. C. *J. Am. Chem. Soc.* **2005**, *127*, 10166.
25. a) Reagan,W. K. EP 0417477 (Phillips Petroleum Company), **1991**. b) Dixon, J. T.; Green, M. J.; Hess, F. M.; Morgan, D. H. *J. Organomet. Chem*. **2004**, *689*, 3641. c) Morgan, D. H.; Schwikkard, S. L.; Dixon, J. T.; Nair, J. J.; Hunter, R. *Adv. Synth. Catal.***2003**, *345*, 939. d) Temple, C.; Jabri, A.; Crewdson,P.; Gambarotta, S.; Korobkov, I.; Duchateau, R. *Angew. Chem. Int.Ed*. **2006**, *45*, 7050. e) Albahily, K.; Al-Baldawi, D.; Gambarotta, S.; Duchateau, R.; Koç E.; Burchell, T. J. *Organometallics* **2008**, *27*, 5708. f) Agapie, T.; Day, M.W.; Henling, L. M.; Labinger, J. A.; Bercaw, J. E. *Organometallics* **2006**, *25*, 2733. g) Schofer, S. J.; Day, M.W.; Henling, L. M.; Labinger, J. A.; Bercaw, J. E. *Organometallics* **2006**, *25*, 2743. h) Agapie, T.; Labinger, J. A.; Bercaw, J. E. *J. Am. Chem. Soc*. **2007**, *129*, 14281. i) Köhn, R. D.; Smith, D.; Mahon, M. F.; Prinz, M.; Mihan, S.; Kociok-Köhn, G. *J. Organomet. Chem.* **2003**, *683*, 200.
26. a) McDermott, J. X.; White, J. F.; Whitesides, G. M. *J. Am. Chem. Soc*. **1973**, *95*, 4451. b) McDermott, X. J.; White, F.; Whitesides, G. M. *J. Am. Chem. Soc*. **1976**, *98*, 6521. c) Manyik, R. M.; Walker, W. E.; Wilson, T. P. *J. Catal*. **1977**, *47*, 197. d) McDaniel, M. P. *Adv. Catal*. **1985**, *33*, 47. e) Briggs, J. R. *Chem. Commun*. **1989**, *11*, 674. f) Meijboom, N.;

Schaverien, C. J.; Orpen, A. G. *Organometallics* **1990**, *9*, 774. g) Emrich, R.; Heinemann, O.; Jolly, P. W.; Krüger, G.; Verhovnik, P. J. *Organometallics* **1997**, *16*, 544.

27. a) Blann, K.; Bolmann, A.; Dixon, J. T.; Hess, F.; Kilian, E.; Maumela, H.; Morgan, D. H.; Neveling, A.; Otto, S.; Overett, M. *Chem. Commun.* **2005**, 620. b) Mohamed, H.; Bollmann, A.; Dixon, J. T.; Gokul, V.; Griesel, L.; Grove, C.; Hess, F.; Maumela, H.; Pepler, L. *Appl.Catal*. *A* **2003**, *255*, 355. c) Kuhn, P.; Sémeril, D.; Matt, D.; Chetcuti, M. J.; Lutz, P. *Dalton Trans*. **2007**, 515. d) Overett, M. J.; Blann, K.; Bollmann, A.; Dixon, J. T.; Haasbroek, D.; Killian, E.; Maumela, H.; McGuinness, D. S.; Morgan, D. H. *J. Am. Chem. Soc*., **2005**, *127*, 10723.
28. Peitz, S.; Aluri, B. R.; Peulecke, N.; Müller, B. H.; Wöhl, A.; Müller, W.; Al-Hazmi, M. H.; Mosa, F. M.; Rosenthal, U. *Chem. A Eur. J.* **2010**, *16*, 7670.
29. Jolly, P.W. *Acc. Chem. Res.* **1996**, *29*, 544.
30. Mimura, H.; Aoyama, T.; Yamamoto, T.; Oguri, M.; Koie, Y. (Tosoh Corporation) JP 09268133, **1997**.
31. Freeman, J. W.; Buster, J. L.; Kundsen, R. D. (Phillips Petroleum Company) US 5,856,257, **1999**.
32. Tanaka, E.; Urata, H.; Oshiki, T.; Aoshima, T.; Kawashima, R.; Iwade, S.; Nakamura, H.; Katsuki, S.; Okanu, T. (Mitsubishi Chemical Corporation) EP 0611743, **1994**.
33. Araki, Y.; Nakamura, H.; Nanba, Y.; Okanu, T. (Mitsubishi Chemical Corporation) US 5,856,612, **1999**.
34. Jabri, A.; Mason, C. B.; Sim, Y. ; Gambarotta, S.; Burchell, T. J.; Duchateau, R. *Angew. Chem. Int. Ed*. **2008**, *47*, 9717.

35. Wu, F. J. (Amoco Corporation) US 5,811,618, **1995**.

36. Yoshida, T.; Yamamoto, T.; Okada, H.; Murakita, H. (Tosoh Corporation) US 2002/0035029, **2002**;

37. Zhang, J.; Braunstein, P.; Hor, A. T. S. *Organometallics* **2008**, *27*, 4277.

38. Carter, A.; Cohen, S. A.; Cooley, N. A.; Murphy, A.; Scutt, J.; Wass, D. F. *Chem. Commun.* **2002**, 858.

39. a) Dixon, J. T.; Grove, J. J. C.; Wasserscheid, P.; McGuinness, D. S.; Hess, F. M.; Maumela, H.; Morgan, D. H.; Bollmann, A. (Sasol Technology (Pty) Ltd) WO 03053891, **2001**. b) McGuinness, D. S.; Wasserscheid, P.; Keim, W.; Dixon, J. T.; Grove J. J. C.; Hu, C.; Englert, U. *Chem. Commun*. **2003**, 334.

40. McGuinness, D. S.; Wasserscheid, P.; Keim, W.; Morgan, D. H.; Dixon, J. T.; Bollmann, A.; Maumela, H.; Hess, F. M.; Englert, U. *J. Am. Chem. Soc*. **2003**, *125*, 5272.

41. Bollmann, A.; Blann, K.; Dixon, J. T.; Hess, F. M.; Killian, E.; Maumela, H.; McGuinness, D. S.; Morgan, D. H.; Neveling, A.; Otto, S.; Overett, M.; Slawin, A. M. Z.; Wasserscheid, P.; Kuhlmann S. *J. Am. Chem. Soc*. **2004**, *126*, 14712.

42. Han, T. K.; Ok, M. A.; Chae, S. S.; Kang,S. O.; Jung, J. H. WO Patent 2008/088178(SK Energy), **2008**.

43. Peitz, S.; Peulecke, N.; Aluri, B. R.; Hansen, S.; Müller, B. H.; Spannenberg, A.; Rosenthal, U.; Al-Hazmi, M. H.; Mosa, F. M.; Wöhl, A.; Müller, W. *Eur. J. Inorg. Chem*. **2010**, 1167.

44. Dulai, A.; McMullin, C. L.; Tenza, K.; Wass. D. F. *Organometallics* **2011**, *30*, 935.

45. Fischer, K; jonas, k; Misbach, P; Stabba, R; Wilke, G. *Angew. Chem., Int. Ed. Engl.* **1973**,

12, 943.

46. a) Freitas, E.; Gum, C. *Chem. Eng. Prog.* **1973**, 73. b) Keim, W. *Angew. Chem., Int. Ed. Engl.* **1990**, *29*, 235. c) Hirose, K.; Keim, W. *J. Mol. Catal.* **1992**, *73*, 271.
47. Muller, U.; Keim, W.; Kruger, C.; Betz, P. *Angew. Chem., Int. Ed. Engl.* **1989**, *28*, 1011.
48. Speiser, F.; Braunstein, P.; Saussine, L. *Acc. Chem. Res*. **2005**, *38*, 784.
49. Ittel, S. D.; Johnson, L. K. *Chem. Rev.* **2000**, *100*, 1169.
50. Chen, E. Y. X.; Marks, T. J. *Chem. Rev.* **2000**, *100*, 1391.
51. Andresen, A.; Cordes, H. G.; Herwig, J.; Kaminksy, W.; Merck, A.; Mottweiler, R.; Pein, J.; Sinn, H.; Vollmer, H. J. *Angew. Chem.* **1976**, *88*, 689.

Part I

Chromium Catalysts

Publications:

1) **Thapa, I**.; Gambarotta, S.; Duchateau, R.; Kulangara, S. V; Chevalier, R. *Organometallics* **2010**, *29*(18), 4080-4089.
2) **Thapa, I**.; Gambarotta, S.; Korobkov, I.; Murugesu, M.; Budzelaar, P. *Organometallics* **2012**, *31*(1), 486-494.

Switchable Chromium Catalysts Supported by Amido-Phosphine (N-P) Ligand: From Ethylene Polymerization to Selective and Non-Selective Oligomerization.

2.1 Introduction

Chromium is the feature component of commercially employed catalysts for selective tri-[1-10] and tetramerization,[10-13] non-selective oligomerization[14-18] and polymerization.[19-26] This versatility raises interesting questions about this metal's unique behavior. In principle, the three processes could be regarded as belonging to the same category of C-C bond forming reactions although, in reality, involve conceptually very different mechanisms. The selective trimerization is a redox process where a two-electron oxidative addition of ethylene forms an expandable chroma-metallacycle followed by a two-electron reductive elimination.[1-13,17,27-34] The ethylene reductive coupling is one of the key-steps of this catalytic cycle, in turn requiring a sufficiently reactive oxidation state of the metal center.[27-34] Polymerization is instead a non-redox process

where the Lewis acidity of the metal center is the drive for ethylene-precoordination, to be followed by insertion and chain growth.[35] However, evidence has been produced that, at least in some cases, polymerization may also proceed via a redox ring expansion mechanism.[15] Non-selective oligomerization was also found to proceed via both redox and non-redox mechanisms.[15,17] Controlling the selectivity of the ring expansion (e.g. towards either formation of 1-hexene versus 1-octene or statistical oligomerization) remains a formidable challenge.

Recent synthetic/mechanistic work on the Phillips trimerization system has linked the metal oxidation state to the type of catalytic performance.[8c,d] The isolation of intermediates capable of acting as a single component self-activating catalysts has pointed to the monovalent state as responsible for selective trimerization, and to divalent chromium for polymerization and non-selective oligomerization. Catalysts based on the neutral PNP and related PCCP ligands are the only existing systems capable of producing a sizable excess of 1-octene.[11-13] The active species of this selective system is believed to contain a cationic chromium(I) center.[33,36] One of the major difficulties in generalizing this crucial information consists of the remarkable redox dynamism existing between organo-chromium (I), (II) and (III), readily inter-converting via reduction and disproportionations.[8, 12, 37]

This chapter is describing the preparation of a series of chromium complexes in different valence states aiming at clarifying their interaction with aluminum alkyl species *vis-à-vis* the redox behavior of this particular metal. For this work, we have selected the anionic amidophosphine (NP) ligand to assess the role of the ligand's negative charge and number of donor atoms within the PNP ligand framework in determining the type of catalytic behavior in relation to the metal oxidation state. Furthermore, recent work by Rosenthal[38] on the closely

related NPNP ligand system has identified an excellent selectivity for the production of 1-hexene, thus reiterating the potential provided by the combination of these donor atoms.

2.2 Experimental

All reactions were carried out under a dry nitrogen atmosphere unless otherwise stated. Solvents were dried using an aluminum oxide solvent purification system. $CrCl_2(THF)_2$ and $CrCl_3(THF)_3$ were prepared according to published procedure.[39] Infrared spectra were recorded on an ABB Bomen FT-IR instrument from Nujol mulls prepared in a dry box except in the case of air stable compounds. Samples for magnetic susceptibility were weighed inside a dry box equipped with an analytical balance and sealed into calibrated tubes and measurements were carried out with a Johnson Matthey Magnetic Susceptibility balance at room temperature. Samples for variable temperature magnetic susceptibility measurement were pre-weighed inside a dry box equipped with an analytical balance and measured using Quantum Design SQUID magnetometer MPMS-XL7 operating between 1.8 and 300 K for dc-applied fields ranging from −7 to 7 T. NMR data were collected on a Bruker Avance 300 spectrometer. Data for X-ray crystal structure determination were obtained with a Bruker diffractometer equipped with a 1K Smart CCD area detector. Elemental analyses were carried out with a Perkin-Elmer 2400 CHN analyzer. Molecular weight and molecular weight distributions of the resulting polymers were determined by gel permeation chromatography on a PL-GPC210 equipped with a RI and viscosity detector and a 3 × PLgel 10 μm Mixed-B column set at 135°C using 1,2,4-trichlorobenzene as solvent. The molecular weight of the polyethylenes was referenced to polyethylene standards. Results of the oligomerization were assessed by NMR for activity and GC-MS for reaction mixture composition. Gas chromatography of oligomerization products was

conducted on a Varian 450-GC equipped with an autosampler and a factor four capillary column VF-5ms 25M×0.25MM. A gradient oven temperature program, starting from 50°C (for 2 min) to 280°C at a rate of 10°C/min and holding at the final temperature for 3 min was employed. The chromatograms were obtained via flame ionization detector (FID). As a transport gas helium was used. All single-point experiments were performed in duplicate. Aluminum and lithium reagents were purchased from Aldrich; Vinyl Grignard (Aldrich), MAO (10% wt, ALDRICH), Me_3Al and $Al(Et)_3$ (Strem) were used as received. DMAO was prepared by pumping in *vacuo* solution of MAO for three days and under moderate heating. NMR solutions were checked for eventual and residual presence of TMA.

2.2.1 Preparation of *t*-BuN(H)P(Ph)$_2$

A solution of *t*-$BuNH_2$ (20 mL, 173 mmol) in dry diethyl ether (150 mL) was cooled to -78 ^oC and treated dropwise with chlorodiphenylphosphine (16 mL, 86 mmol) under nitrogen. White precipitate of *t*-$BuNH_3Cl$ immediately separated. The reaction mixture was allowed to warm up to room temperature and stirred for 48 hours. The ammonium salt was eliminated by filtration and the resulting solution concentrated to small volume under reduced pressure. The title compound was isolated from the resulting solution as analytically pure crystals upon standing at room temperature overnight (36 g, 141.7 mmol, 81%). ^{1}H-NMR (300 MHz, $CDCl_3$, 25 ^oC) δ: 7.49 (4H, m), 7.37 (6H, m), 2.10 (1H, d, J = 11.4), 1.36 (9H, s). ^{13}C{1H}-NMR (300 MHz, $CDCl_3$, 25 ^oC) δ: 144.3, 144.1, 131.5, 131.2, 128.6, 128.5, 51.9, 51.6, 32.7, 32.6. ^{31}P{H}-NMR δ: 23.2. EI-MS m/z = 257.1(M^+).

2.2.2 Preparation of [(*t*-BuNPPh$_2$)Cr$_2$(μ-*t*-BuNPPh$_2$)$_3$]1.5(toluene) (2.1).

A solution of *t*-BuN(H)P(Ph)$_2$ (1.01 g, 4 mmol) in THF (15 mL) was treated with a solution of *n*-BuLi in hexane (1.64 mL, 4.1 mmol, 2.5 M) at -10 ^{o}C. The reaction mixture was stirred overnight at room temperature and then combined with a suspension of $CrCl_2(THF)_2$ (0.27 g, 1 mmol) in THF (5 mL). Stirring was continued for 18 hrs. Solvent was evaporated in *vacuo* and the solid residue was redissolved in toluene. A small amount of colorless insoluble material was separated by centrifugation, and the resulting brown solution was allowed to stand for three days at -35 ^{o}C. Brown paramagnetic crystals of **2.1** were filtered, washed with cold hexane and dried in vacuo (0.39 g, 0.3 mmol, 30%). Identical reaction using a ligand to chromium ratio of 2:1 also afforded **2.1** in higher yield (63%). Elemental Analysis Calcd. (Found) for $C_{74.50}H_{88}Cr_2N_4P_4$: C 70.60 (69.99), H 7.00 (6.94), N 4.42 (4.38). IR (Nujol mull, cm^{-1}): 3052s, 2955s, 2924s, 2854s, 1584m, 1457s, 1429m, 1376m, 1352m, 1191s, 1086m, 1055m, 1018s, 819m, 803m, 739, 733s, 724s, 695s. [μ_{eff} = 2.75 μ_B].

2.2.3 Preparation of [(μ-AlMe$_3$)$_2${(*t*-BuNP(Ph)$_2$}$_2$Cr]·(toluene) (2.2).

Method A: A solution of **2.1** (0.20 g, 0.16 mmol) in toluene (5 mL) was cooled to -35^{o}C for 10 minutes and treated with neat TMA (0.056 g, 0.79 mmol) dropwise while stirring. After 15 minutes at room temperature, the resulting solution was allowed to stand for 5 days at -35 ^{o}C. Blue paramagnetic crystals of **2.2** formed which were washed with cold hexane and dried *in vacuo* (0.12 g, 0.15 mmol, 95%). Elemental Analysis Calcd. (Found) for $C_{45}H_{64}Al_2CrN_2P_2$: C 67.48 (67.35), H 8.05 (7.99), N 3.50 (3.46). IR (Nujol mull, cm^{-1}): 3051s, 2922s, 2857s, 2716, 2667, 2032, 1960s, 1884s, 1812s, 1781s, 1607s, 1588s, 1466s, 1436s, 1375m, 1360s, 1303m, 1192b, 1097s, 1044m, 1014m, 991m, 919m, 839s, 778s, 744m, 696m. [μ_{eff} = 4.93 μ_B].

Method B: A solution of *t*-Bu-N(H)P(Ph)$_2$ (0.25 g, 1 mmol) in THF (10 mL) was treated with a solution of *n*-BuLi in hexane (0.44 mL, 1.1 mmol, 2.5M) at -10 ^{o}C. The reaction mixture was stirred overnight at room temperature and then combined with a suspension of $CrCl_2$ $(THF)_2$ (0.13 g, 0.5 mmol) in THF (5 mL). Stirring was continued for 18 hrs. The volatile materials were removed *in vacuo* and the solid residue was redissolved in toluene. Neat trimethylaluminium (0.36 g, 5 mmol) was added dropwise and the reaction mixture was stirred at room temperature for 10 minutes. A small amount of colourless insoluble material was separated by centrifugation. The resulting green/blue solution was allowed to stand for 7 days at -35 ^{o}C. Blue paramagnetic crystals of **2.2** were filtered, washed with cold hexane and dried *in vacuo* (0.20 g, 0.24 mmol, 49%).

Method C: A solution of **7** (0.20 g, 0.22 mmol) in toluene (5 mL) was cooled to -35 ^{o}C for 10 minutes. Neat TMA (0.16 g, 2.19 mmol) was added dropwise to the cold solution under stirring. Stirring was continued for 24 hours at room temperature and the resulting solution was allowed to stand for 5 days at -35 ^{o}C. Blue paramagnetic crystals of **2.2** were filtered, washed with cold hexane and dried *in vacuo* (0.10 g, 0.12 mmol, 57%).

2.2.4 Preparation of [(μ-AlMe$_2$Cl)$_2${(*t*-BuNP(Ph)$_2$}$_2$Cr]·(toluene) (2.3).

The complex was prepared and isolated in a similar manner and using same quantities as complex **2.4** by using trimethylaluminum (0.29 g, 4.0 mmol) to yield **2.3** as paramagnetic blue crystalline material (0.34 g, 0.4 mmol, 77%). Elemental Analysis Calcd. (Found) for $C_{43}H_{58}Al_2Cl_2CrN_2P_2$: C 61.36 (61.19), H 6.95 (6.88), N 3.33 (3.29). IR (Nujol mull, cm^{-1}): 3205b, 2908b, 1961b, 1899, 1774, 1607b, 1459b, 1381s, 1354m, 1307m, 1190s, 1093s, 1042m, 995m, 905m, 850s, 785s, 737s, 689s, 672b. [μ_{eff} = 4.86 μ_B].

2.2.5 Preparation of {μ-AlEt$_2$Cl)$_2$[(*t*-BuNP(Ph)$_2$]$_2$Cr}·(toluene) (2.4).

Neat triethylaluminum (0.11 g, 1 mmol) was added dropwise to a solution of *t*-Bu-N(H)P(Ph)$_2$ (0.25 g, 1 mmol) in toluene (5 mL) at room temperature during the period of 10 minutes. The resulting solution was then combined with a suspension of $CrCl_2(THF)_2$ (0.13 g, 0.5 mmol) in toluene (5 mL). Stirring was continued for one hour and during this period additional triethylaluminum was added (0.34 g, 3 mmol). Stirring was continued for additional 48 hours at room temperature. A small amount of insoluble material was separated by centrifugation and the resulting blue solution was allowed to stand overnight at -35 ^{o}C. Blue paramagnetic crystals of **2.4** were collected by filtration, washed with cold hexane and dried in vacuo (0.37 g, 0.41 mmol, 82%). Elemental Analysis Calcd. (Found) for $C_{47}H_{63}Al_2Cl_2CrN_2P_2$: C 63.09 (63.01), 7.10 (7.03), N 3.13 (3.08). IR (Nujol mull, cm^{-1}): 3052s, 2908, 1961, 1899, 1774, 1607, 1459s, 1381s, 1354s, 1307s, 1190s, 1093s, 1042s, 995m, 905m, 850s, 785s, 737s, 697s, 672s. [μ_{eff} = 4.87 μ_B].

2.2.6 Preparation of [{[(*t*-BuNP(Ph)$_2$]$_3$Cr$_2$(μ-Cl)}$_2$]·2(toluene) (2.5).

A solution of *t*-Bu-N(H)P(Ph)$_2$ (0.25 g, 1 mmol) in THF (5 mL) was treated with a solution of *n*-BuLi in hexane (0.44 mL, 1.1 mmol, 2.5 M) at -10 ^{o}C. The reaction mixture was stirred overnight at room temperature and a suspension of $CrCl_2(THF)_2$ (0.27 g, 1 mmol) in THF (5 mL) was added. Stirring was continued for additional 18 hrs. The solvent was evaporated *in vacuo* and the solid residue redissolved in toluene. A small amount of colorless insoluble material was separated by centrifugation, and the resulting greenish brown solution was allowed to stand for three days at -35 ^{o}C. Green paramagnetic crystals of **2.5** were filtered, washed with cold hexane and dried in vacuo (0.17 g, 0.10 mmol, 10%). Elemental Analysis Calcd. (Found)

for $C_{110}H_{130}Cl_2Cr_4N_6P_6$: C 66.03 (65.97) H 6.55 (6.46), N 4.20 (4.19). IR (Nujol mull, cm^{-1}): 3054m, 1952m, 1895m, 1819m, 1770m, 1588s, 1479s, 1432s, 1361s, 1220s, 1093m,1025s, 978 s, 839b, 734b, 696b. [μ_{eff} = 8.15 μ_B per tetrameric unit].

2.2.7 Preparation of [{(μ-AlMe$_2$)[*t*-BuNP(Ph)$_2$]$_2$}Cr(μ-Cl)]$_2$· 1.7 (toluene) (2.6).

A cooled solution of **2.5** (0.20 g, 0.10 mmol) in toluene (5 mL) was treated at -35 ^oC with TMA (0.014 g, 0.20 mmol). The reaction mixture was allowed to stir for 15 minutes at room temperature while the initial brown-greenish color turned green. Green crystals of **2.6** (0.08 g, 0.053 mmol, 54%) separated from the resulting solution upon standing at -35 ^oC for 5 days. Elemental Analysis Calcd. (Found) for $C_{81.30}H_{103.20}Al_2Cl_2Cr_2\ N_4P_4$: C 65.57 (65.49) H 6.98 (6.96) N 3.76 (3.71). [μ_{eff} = 3.31 μ_B per dimeric unit].

2.2.8 Preparation of [(*t*-BuNPPh$_2$)$_3$Cr]·(toluene) (2.7).

A solution of *t*-Bu-N(H)P(Ph)$_2$ (1.01 g, 4.0 mmol) in THF (15 mL) was treated with a solution of *n*-BuLi in hexane (1.64 mL, 4.1 mmol, 2.5M) at -10 ^oC. The reaction mixture was stirred overnight at room temperature and combined with a suspension of $CrCl_3(THF)_3$ (0.49 g, 1.3 mmol.) in THF (5 mL). Stirring was continued for 18 hrs. The solvent was evaporated *in vacuo* and the resulting solid residue redissolved in toluene. A small amount of colorless insoluble material was removed by centrifugation, and the resulting green solution was allowed to stand at -35 ^oC for 5 days. Green paramagnetic crystals of **2.7** were filtered, washed with cold hexane and dried *in vacuo* (0.085 g, 0.93 mmol, 46%). Higher yield of **2.7** were obtained from the reaction of $CrCl_3(THF)_3$ with three equivalents of ligand (90%). Elemental Analysis Calcd. (Found) for $C_{55}H_{65}CrN_3P_3$: C 72.35 (72.29), H 7.18 (7.16), N 4.60 (4.57). IR (Nujol mull, cm^{-1}):

3058, 2849b, 2724, 1960s, 1892b, 1816b, 1588, 1464s, 1434s, 1377s, 1357s, 1303, 1265, 1193bm, 1093m, 1063s, 1025s, 979m, 911, 843b, 820, 740s, 696s. [μ_{eff} = 3.83 μ_B].

2.2.9 Preparation of [μ-$Al_2(Et)_2$ $(Cl)_2${(*t*-BuNP$(Ph)_2$}$_2$$(Cl)_2$Cr].toluene (2.8).

A solution of **2.7** (0.30 g, 0.33 mmol) in toluene (5 mL) was cooled to -35 ^oC for 10 minutes. Neat DEAC (0.20 g, 1.64 mmol) was added dropwise to the cold solution under stirring. Stirring was continued for 5 minutes at room temperature and the resulting solution was allowed to stand for seven days at -35 ^0C. Blue paramagnetic crystals of **2.8** were filtered, washed with cold hexane and dried *in vacuo* (0.19 g, 0.22 mmol, 67%). Elemental Analysis Calcd. (Found) for $C_{39.50}H_{52}Al_2Cl_4$ CrN_2P_2: C 54.87 (54.80), H 6.06 (6.00), N 3.24 (3.21). [μ_{eff} = 4.86 μ_B].

2.2.10 Preparation of $(Me_3P)Cr[\mu$-(*t*-Bu)$NPPh_2]_3Cr$ (**2.9**).

Method A: A solution of *t*-BuN(H)P$(Ph)_2$ (0.25 g, 1.0 mmol) in THF (5 mL) was treated with a solution of n-BuLi in hexane (0.41 mL, 1.02 mmol, 2.5 M) at -10 ^oC. The reaction mixture was stirred overnight at room temperature and then combined with a suspension of $CrCl_2$ $(THF)_2$ (0.27 g, 1 mmol) in THF (5 mL). Stirring was continued for 18 hrs. Neat trimethylphosphine (0.10 mL, 1 mmol) was added to the reaction mixture under continuing stirring at room temperature. After 30 minutes, the color of the solution turned into brown. Freshly prepared potassium graphite (0.27 g, 2.0 mmol) was added and stirring continued at room temperature for further 48 hours. The solvent was evaporated *in vacuo* and the solid residue was redissolved in diethyl ether. A small amount of insoluble gray material was separated by centrifugation, and the resulting brown solution was allowed to stand for 5 days at -35 ^oC. Brown paramagnetic crystals of **2.9** were filtered, washed with cold hexane and dried *in vacuo* (0.02 g, 0.02 mmol, 20%).

Elemental Analysis Calcd. (Found) for $C_{51}H_{66}Cr_2N_3P_4$: C 64.55 (64.35), H 7.01 (6.88), N 4.43 (4.23). IR (Nujol mull, cm^{-1}): 2923b, 2854b (Nujol), 1975s, 1892m, 1819s, 1766m, 1580m, 1466m, 1430s, 1383s, 1358s, 1354s, 1203m, 1178s, 1085m, 1049m, 1025s, 950s, 819m, 747s, 725s, 697s. [$\mu_{eff} = 1.875\ \mu_B$].

Method B: A green solution of **2.5** (0.23 g**,** 0.11 mmol) in THF (5 mL) was treated with neat trimethylphosphine (0.012 mL, 0.11 mmol) and stirred at room temperature for 30 minutes. Freshly prepared potassium graphite (0.03 g, 0.23 mmol) was added to the solution and the resulting mixture was stirred at room temperature for further 48 hours. The solvent was evaporated in vacuo and the solid residue was redissolved in diethyl ether. A small amount of insoluble gray material was separated by centrifugation, and the resulting brown solution was allowed to stand for 5 days at -35 ^oC. Brown paramagnetic crystals of **2.9** were filtered, washed with cold hexane and dried *in vacuo* (0.09 g, 0.09 mmol, 85%).

Method C. A solution of *t*-BuN(H)P(Ph)$_2$ (0.25 g, 1 mmol) in THF (5 mL) was treated with a solution of *n*-BuLi in hexane (0.41 mL, 1.02 mmol, 2.5 M) at -10 ^oC. The reaction mixture was stirred overnight at room temperature and then combined with a suspension of $CrCl_2$ $(THF)_2$ (0.27 g, 1 mmol) in THF (5 mL). Stirring was continued for 18 hrs. Neat trimethylphosphine (0.10 mL, 1 mmol) was added to the reaction mixture and stirring was continued at room temperature for further 30 minutes. By this time, the green color of the solution changed into brown. A solution of vinyl magnesium chloride (1.25 mL, 2mmol, 1.6 M in THF) was added and stirring was continued at room temperature for further 18 hours. Anhydrous dioxane (0.26 mL, 3mmol) was then added. The solid formed during 12 hours was removed by centrifugation. The solvent was evaporated *in vacuo* and the solid residue was redissolved in diethyl ether. A small amount of colorless insoluble material was further eliminated by centrifugation, and the

resulting brown solution was allowed to stand for 5 days at -35 ^{o}C. Brown paramagnetic crystals of **2.9** were filtered, washed with cold hexane and dried *in vacuo* (0.20 g, 0.21 mmol, 21%).

Method D: A green solution of **2.5** (0.23 g, 0.11 mmol) in THF (5 mL) was added with neat trimethylphosphine (0.12 mL, 0.11 mmol). After 30 minutes, the mixture was added with vinylmagnesium chloride (0.14 mL, 0.23 mmol, 1.6 M in THF) and stirred at room temperature for 18 hours. Dry dioxane (0.03 mL, 0.34 mmol) was added. After centrifugation, the solvent was evaporated *in vacuo* and the solid residue redissolved in diethyl ether. A small amount of colorless insoluble material was separated by centrifugation, and the resulting brown solution was allowed to stand for 5 days at -35 ^{o}C. Brown paramagnetic crystals of **2.9** were filtered, washed with cold hexane and dried in *vacuo* (0.10 g, 0.10 mmol, 92%).

2.2.11 Isolation of {[(η^4-butadiene)Cr(μ,η^4-butadien-di-yl)(μ-NP)Mg]$_2$(μ-Cl)$_4$Mg(THF)$_2$}{[(THF)$_3$Mg]$_2$ (μ-Cl)$_3$}$_2$ (THF)$_{2.5}$ (2.10).

A solution of **2.9** (0.12 g, 0.1 mmol, 1.6 M) in THF (10 mL) was treated with vinylmagnesium chloride (2.5 mL, 1.6 M in THF) at room temperature. The reaction mixture was stirred for 2 hrs at room temperature. The color changed to dark brown and dioxane was added (0.026 g, 0.3 mmol). A small amount of insoluble material was separated by centrifugation, and the resulting brown solution was allowed to stand for two days at -35 °C. A few orange colored paramagnetic crystals of **2.10** were obtained which were washed with cold hexane and dried *in vacuo* (0.0125 g, 0.005 mmol, 5%). The amount was too small for further analysis and characterization other than crystallographic.

2.3 X-ray Data

Table 2.1: Crystal Data and Structure Analysis Results.

	2.1	**2.2**	**2.3**	**2.4**
Formula	$C_{74.50}H_{88}Cr_2N_4P_4$	$C_{45}H_{64}Al_2CrN_2P_2$	$C_{43}H_{58}Al_2Cl_2CrN_2P_2$	$C_{47}H_{63}Al_2Cl_2CrN_2P_2$
FW	1267.37	800.88	841.71	894.79
Space group	Monoclinic, P2(1)/c	Monoclinic, C2/c	Triclinic, P-1	Triclinic, P-1
a (Å)	20.633(3)	29.849(9)	9.3772(15)	9.8866(19)
b (Å)	16.034(2)	11.978(3)	11.5117(19)	11.738(2)
c (Å)	21.309(3)	14.055(4)	11.6769(19)	12.036(2)
α(deg)	90	90	112.718(3)	112.373(3)
β(deg)	105.518(2)	115.175(4)	98.557(3)	102.186(3)
γ(deg)	90	90	100.060(3)	100.069(3)
V (Å^3)	6792.4(14)	4548(2)	1111.9(3)	1211.2(4)
Z	4	4	1	1
radiation (Kα, Å)	0.71073	0.71073	0.71073	0.71073
D_{calcd} (g cm^{-3})	1.239	1.170	1.257	1.227
μ_{calcd} (mm^{-1})	0.459	0.392	0.520	0.482
F_{000}	2684	1712	444	473
R, R_w[2 a]	0.0534, 0.1261	0.0565, 0.1444	0.0454, 0.1220	0.0992, 0.2908
GoF	1.024	1.049	1.058	1.084

[a] $R = \Sigma||Fo| - |Fc||/\Sigma|F|$. $Rw = [\Sigma(|Fo| - |Fc|)^2/\Sigma wFo^2]^{1/2}$.

	2.5	**2.6**	**2.7**	**2.8**
Formula	$(C_{55}H_{65}ClCr_2N_3P_3)_2$	$C_{81.30}H_{103.20}Al_2Cl_2Cr_2N_4P_4$	$C_{55}H_{65}CrN_3P_3$	$C_{39.50}H_{52}Al_2Cl_4CrN_2P_2$
FW	(1000.46)2	1489.22	913.01	864.53
space group	Triclinic, P-1	Triclinic, P-1	Trigonal, P-3	Triclinic, P-1
a (Å)	11.752(5)	12.6373(16)	21.772(3)	9.790(16)
b (Å)	12.928(6)	13.0520(17)	21.772(3)	11.692(9)
c (Å)	18.525(8)	14.8046(19)	18.456(3)	11.832(9)
α (deg)	85.416(7)	107.041(2)	90	111.259(12)
β (deg)	79.728(7)	106.809(2)	90	101.514(15)
γ (deg)	70.844(7)	102.044(2)	120	99.885(16)
V (Å^3)	2615(2)	2117.0(5)	7576(2)	1192(2)
Z	2	1	6	1
Radiation (Kα, Å)	0.71073	0.71073	0.71073	0.71073
T (K)	203(2)	203(2)	202(2)	200(2)
D_{calcd} (g cm^{-3})	1.270	1.168	1.201	1.205
μ_{calcd} (mm^{-1})	0.596	0.458	0.360	0.595
F_{000}	1052	787	2910	451
R, R_w[2 a]	0.0516, 0.1355	0.0763, 0.1624	0.0665, 0.1556	0.0815, 0.2150
GoF	1.021	1.018	1.049	1.002

	2.9	**2.10**
Formula	C_{51} H_{66} Cr_2 N_3 P_4	C_{114} H_{194} Cl_{10} Cr_2 Mg_7 N_2 $O_{16.50}$ P_2
FW	948.95	2547.32
space group	Cubic, Pa-3	Triclinic, P-1
a (Å)	21.7483(6)	12.4175(6)
b (Å)	21.7483(6)	16.4579(8)
c (Å)	21.7483(6)	18.4679(9)
α (deg)	90	67.111(3)
β (deg)	90	81.574(3)
γ (deg)	90	81.574(3)
V (Å^3)	10286.7(5)	3438.4(3)
Z	8	1
Radiation (Kα, Å)	0.71073	0.71073
T (K)	200(2)	200(2)
D_{calcd} (g cm^{-3})	1.225	1.230
μ_{calcd} (mm^{-1})	0.582	0.463
F_{000}	4008	1356
R, R_w [2 a]	0.0426, 0.1121	0.0651, 0.1123
GoF	1.035	1.038

[a] $R = \Sigma||Fo| - |Fc||/\Sigma|F|$. $Rw = [\Sigma(|Fo| - |Fc|)^2/\Sigma wFo^2]^{1/2}$.

2.4 Results and Discussion

2.4.1 Switchable Chromium (II) Complexes of a Chelating Amido-phospine (N-P) for Selective and Non-Selective Ethylene Oligomerization.

The reaction of the lithium salt of *t*-BuN(H)PPh_2 in THF with $CrCl_2(THF)_2$ afforded the dinuclear $[(t\text{-BuNPPh}_2)Cr_2(\mu\text{-}t\text{-BuNPPh}_2)_3]\cdot 1.5$(toluene) (**2.1**) as dark brown paramagnetic crystals (Scheme 2.1). The dimeric formulation of the complex was elucidated by a crystal structure (Figure 2.1) and confirmed by satisfactory combustion analysis data.

The structure of **2.1** (Figure 2.1) shows four *t*-$BuNPPh_2$ anions asymmetrically located around a dichromium unit. Three ligands adopt the bridging mode with the nitrogen atoms connected to the same chromium [Cr(2)-N(4) = 2.007(3)Å, Cr(2)-N(2) = 2.009(3)Å, Cr(2)-N(3) = 2.033(3)Å] and their corresponding phosphorous bonding the second metal [Cr(1)-P(4) =

2.5319(12)Å, Cr(1)-P(3)= 2.5583(12)Å, Cr(1)-P(2) = 2.6698(12)Å]. The fourth ligand solely chelates the second chromium atom [Cr(1)-P(1) = 2.3756(12)Å, Cr(1)-N(1) = 2.088(3)Å]. As a result, the coordination of the chromium atom exclusively surrounded by the nitrogen atoms is trigonal planar with a minor deviation of the metal from the planarity [N(4)-Cr(2)-N(2) = 117.34(14)°, N(4)-Cr(2)-N(3) = 110.28(14)°, N(2)-Cr(2)-N(3) = 132.37(14)°]. The second chromium shows instead a severely distorted trigonal bypyramidal geometry with the trigonal equatorial plane defined by two P atoms of two bridging ligands and the phosphorous of the chelating ligand [P(1)-Cr(1)-P(2) = 106.27(4)°, P(3)-Cr(1)-P(2) = 104.13(4)°, P(1)-Cr(1)-P(3) = 140.18(4)°]. The axial positions are occupied by one P atom of the third bridging ligand and the N atom of the chelating ligand [N(1)-Cr(1)-P(4) = 140.14(9)°, P(4)-Cr(1)-P(3) = 98.02(4)°, P(1)-Cr(1)-P(4) = 100.23(4)°]. The Cr-Cr distance [Cr(1)…Cr(2) = 2.7688(9)Å] is remarkably long for this type of dimeric structure somewhat reminiscent of the paddlewheel complexes of divalent chromium and outside the M-M bonding range.[40]

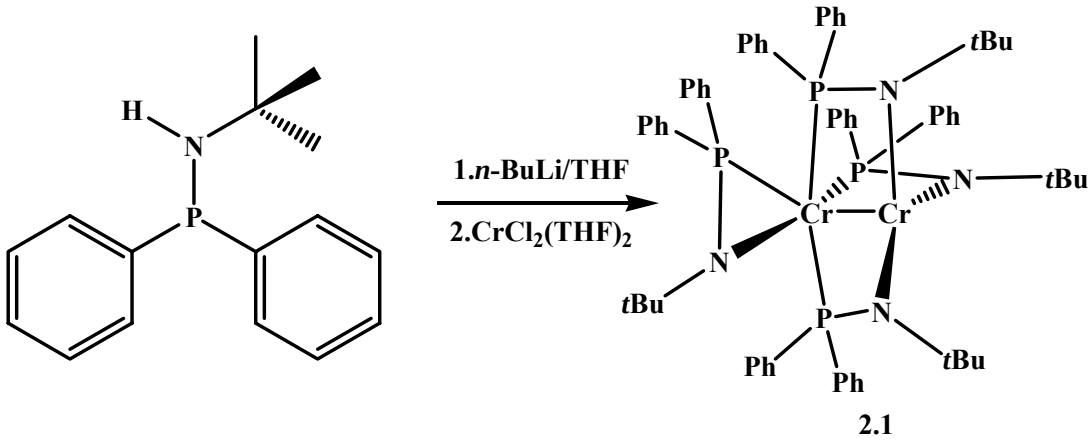

2.1

Scheme 2.1: Synthesis of complex 2.1

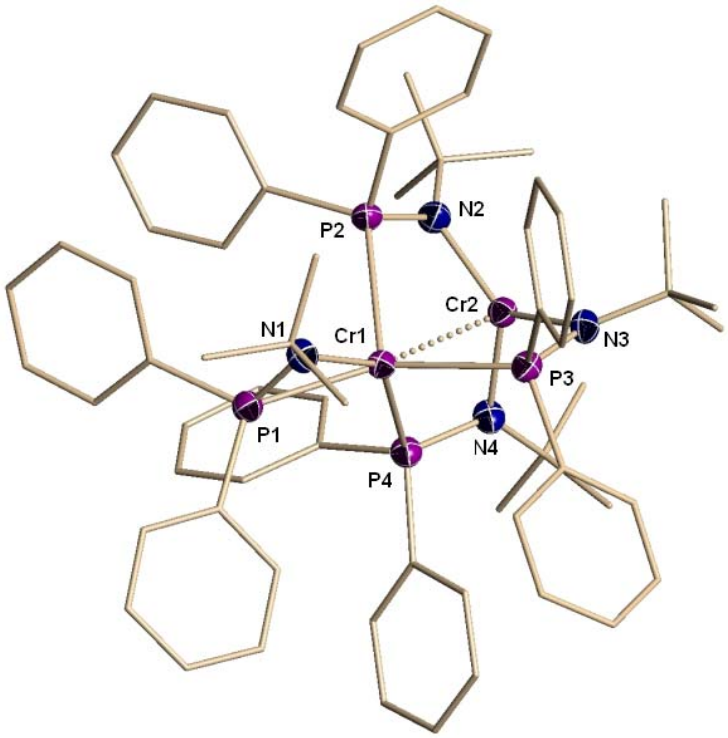

Figure 2.1: Partial thermal ellipsoids drawing of 2.1(50% probability level) with carbon atom ellipsoids omitted for clarity.

The strange asymmetry observed in the dimeric structure and the completely different coordination geometries of the two Cr atoms are probably the result of steric repulsions as also emphasized by the folding of the Cr(1)-Cr(2)-N-P plane. The steric encumbrance of the three large *t*-Bu groups is likely responsible for the trigonal planar arrangement of one of the two chromium atoms.[41] The possibility for a terminally bonded hydride to be present in the seemingly void space opposed to the Cr-Cr vector was ruled out by degradation experiments showing no evolution of hydrogen gas under hydrolytic conditions. The value of the magnetic moment at room temperature [$\mu_{eff} = 2.57\ \mu_B$] was as expected for a dinuclear structure of divalent chromium without direct metal-metal ligation.

As described in the section below, complex **2.1** acts as a moderately active ethylene polymerization catalyst precursor. Depending on the activation conditions, 1-hexene was

observed aside the formation of the polymer. Thus, in an attempt to discriminate between the factors leading to each of the two catalytically active species (respectively forming polymer and 1-hexene) and with the hope of improving activity and selectivity of the system, we have embarked on a study to assess the interaction of **2.1** with alkyl aluminum reagents. Regrettably, the reaction with MAO (the most preferred activator) only afforded oily intractable materials. In the case of the reaction with five equivalents of trimethyl aluminum (TMA) instead, the crystalline and paramagnetic $[(\mu\text{-}AlMe_3)_2\{(t\text{-}BuNP(Ph)_2\}_2Cr]\cdot(toluene)$ (**2.2**) was isolated and fully characterized. The complex could also conveniently be prepared in a one-pot synthesis (Scheme 2.2). The chemical connectivity was clarified by an X-ray crystal structure (Figure 2.2) and the magnetic moment was in agreement with the high-spin configuration of d^4 Cr(II) complex in a square planar environment.

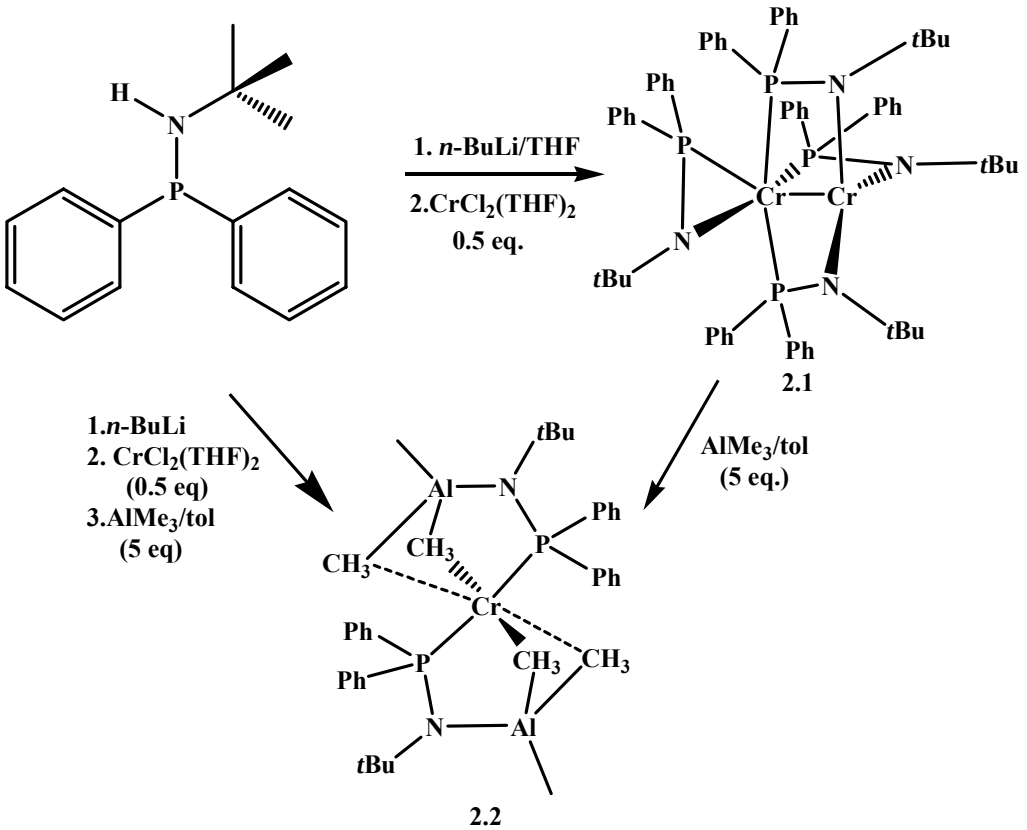

Scheme 2.2: Synthesis of complex 2.2

Complex **2.2** is monomeric (Figure 2.2) and features two ligands and two $AlMe_3$ units surrounding the chromium metal center. Each ligand adopted the bridging-chelating bonding mode with the N atom bonding the organoaluminium residue [N(1)-Al(1) = 1.896(3)Å] and the P atom connected to chromium [P(1)-Cr(1) = 2.536(1)Å]. In turn, one of the three methyl group on each Al is reaching a bonding contact with chromium [Cr(1)-C(1) = 2.283(5)Å]. The square-planar environment of the transition metal [C(1)-Cr(1)-P(1) = 86.38(13)°] is provided by two methyl groups and the two P atoms in *trans* to each other [C(1)-Cr(1)-C(1a) = 179.99(1)°, P(1)-Cr(1)-P(1a) = 180.0(1)°]. Two other methyl groups, each from one Al, are oriented on the axial position of a severely distorted octahedron centered on chromium. However, the Cr-C distances with these two methyl groups are well beyond the bonding range [Cr(1)-C(2) = 2.960(5)Å, C(2)-Cr(1)-C(2a) = 180.00(0)°].

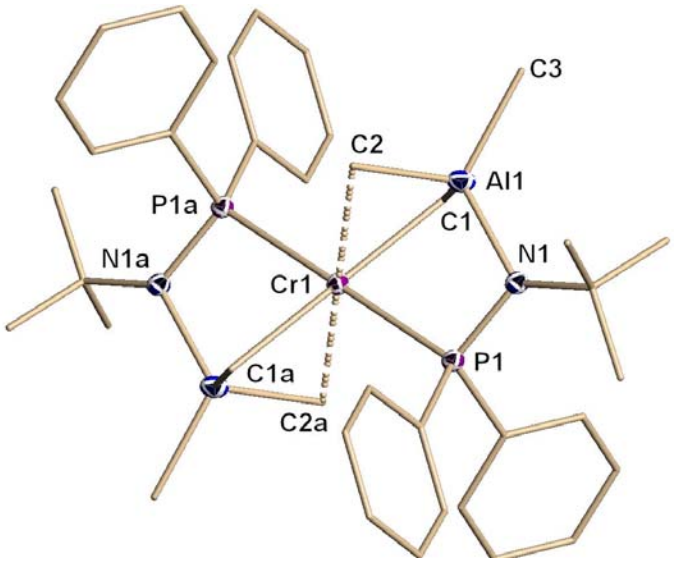

Figure 2.2: Partial thermal ellipsoids drawing of 2.2 (50 % probability level) with carbon atom ellipsoids omitted for clarity.

As mentioned above, complex **2.2** could be conveniently prepared in a one-pot synthesis by treating the lithiated phosphineamine ligand with $CrCl_2(THF)_2$ followed by treatment with

TMA. When the sequence of addition was reverted and the ligand was used in its protonated rather than lithiated form, two new species formulated as $[(\mu\text{-}AlMe_2Cl)_2\{(t\text{-}BuNP(Ph)_2\}_2Cr]\cdot$(toluene) (**2.3**) and $[(\mu\text{-}AlEt_2Cl)_2\{(t\text{-}BuNP(Ph)_2\}_2Cr]\cdot$(toluene) (**2.4**) were isolated in good and reproducible yield while using TMA and triethyl aluminum (TEAL), respectively (Scheme 2.3). Both complexes display the magnetic moments as expected for the high spin d^4 electronic configuration of monomeric divalent chromium in square-planar environments.

The two complexes display very similar geometries (Figure 2.3) the only difference consisting of the presence of a Me versus Et groups attached to the Al residue. As in

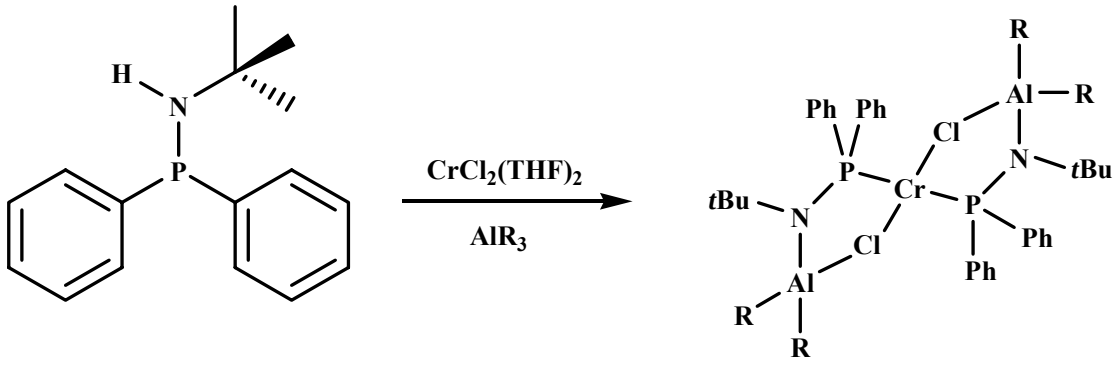

Scheme 2.3: Synthesis of complex 2.3 and 2.4

complex **2.2**, the metal center is surrounded by two ligands bonding the chromium center with the P atom [**2.3**:Cr-Cl = 2.3429(9)Å, and Cr – P = 2.5733(8)Å, **2.4**: Cr(1)-Cl(1) = 2.3321(18)Å, Cr(1)-P(1) = 2.5572(13)Å] and retain an Al group with the N atom [**2.3**: N(1)-Al(1) = 1.889(3) Å, **2.4**: N(1)-Al(1) = 1.874(5)Å]. Different from **2.2**, the Al residues retained one chlorine atom and which is used to bridge the central chromium [**2.3**: Cl(1)-Cr(1) = 2.3429(9)Å, Al(1)-Cl(1) =

2.3274(14)Å, Al(1)-Cl(1)-Cr(1) = 90.10(4)°, **2.4**: Cl(1)-Cr(1) = 2.3321(18)Å, Al(1)-Cl(1) = 2.282(3)Å, Al(1)-Cl(1)-Cr(1) = 99.26(10)°]. No further interaction is visible for the chromium center with any of the organic group of the aluminum atoms. As a result, in both cases the coordination geometry around the metal center is square-planar and defined by the two *trans* located P and Cl atoms [**2.3**: Cl(1)-Cr-Cl(1a) = 180.00(3)°, P(1)-Cr(1)-P(1a) = 180.0°, **2.4**: Cl(1)-Cr-Cl(1a) = 180.000(1)°, P(1)-Cr(1)-P(1a) = 180.0°].

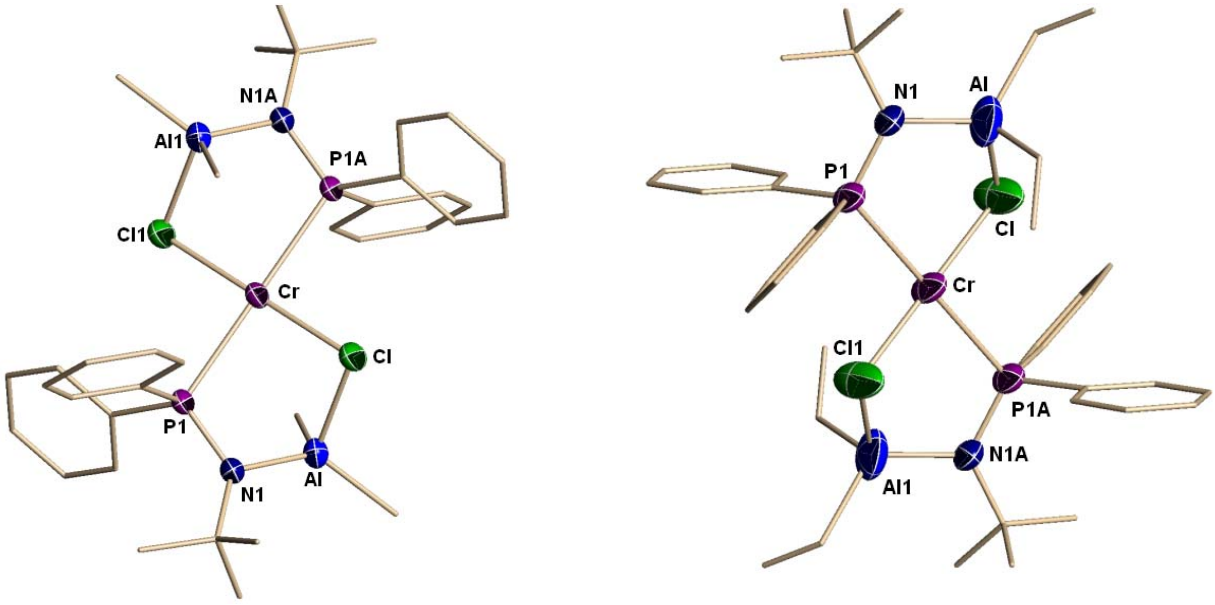

2.3 **2.4**

Figure 2.3: Partial thermal ellipsoids drawing of 2.3 and 2.4 with carbon atom ellipsoids omitted for clarity (50 % probability level).

When the reaction affording **2.1** was carried out with a 1:1 ratio of ligand to $CrCl_2(THF)_2$, the new tetrameric cluster $\{[(t\text{-BuNP(Ph)}_2]_3Cr_2(\mu\text{-Cl})\}_2]\cdot 2$(toluene) (**2.5**) was

formed (Scheme 2.4). As usual, the magnetic moment was lower than theoretically expected, which most likely is the consequence of antiferromagnetic exchange between the metal centers.

The molecular structure was elucidated by X-ray diffraction analysis (Figure 2.4). The structure consists of a symmetry generated tetramer composed by two identical dimetallic units each surrounded by three P-N ligands and linked by two bridging chlorine atoms [Cr(2)-Cl(1) = 2.4993(16) Å; Cr(2)-Cl(1a) = 2.6917(16)Å]. The three ligands of the dimetallic unit adopted an

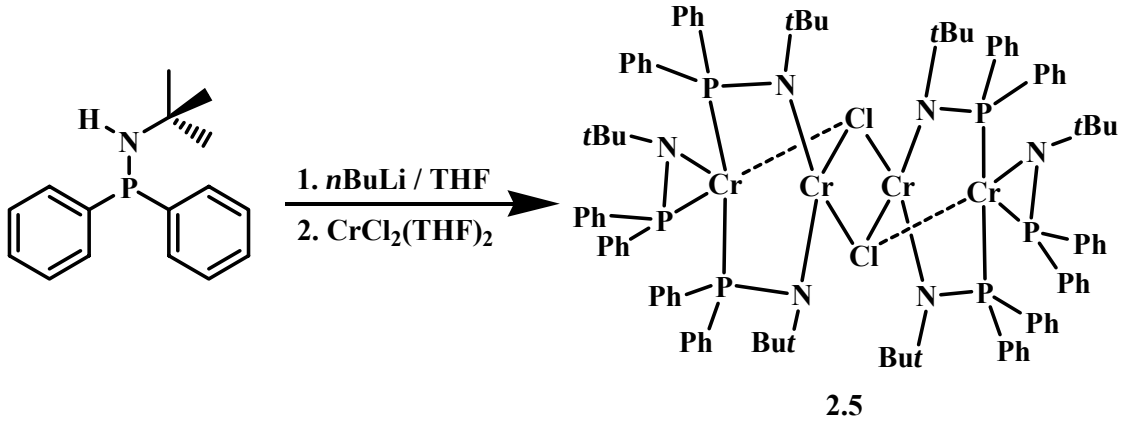

2.5

Scheme 2.4: Synthesis of complex 2.5

arrangement similar to that observed in **2.1**. Two ligands bridge the two metals by orienting the P atoms towards the same chromium [Cr(1)-P(3) =2.4637(14)Å, Cr1-P2= 2.4867(14)Å] and the nitrogens towards the second [Cr(2)-N(3) = 2.019(3)Å, Cr(2)-N(2) = 2.020(3)Å]. The third instead simply chelates the chromium atom placed at the periphery of the cluster [Cr(1)-N(1) = 2.020(3)Å, Cr(1)-P(1) = 2.3780(14)Å] and surrounded by the phosphorous atoms. The coordination geometry might be regarded as severely distorted square-planar [N(1)-Cr(1)-P(1) = 42.70(10)^{o}, N(1)-Cr(1)-P(3) = 143.77(10)^{o}, N(1)-Cr(1)-P(2) = 113.73(11)^{o}, P(2)-Cr(1)-P(3) = 99.31(5)^{o}, P(1)-Cr(1)-P(3) = 101.94(5)^{o}, P(1)-Cr(1)-P(2) =139.43(5)^{o}]. The chlorine atom

bonded to the second chromium and used for the bridging interaction with a second dimetallic unit, is reaching a short non-bonding contact and is located on the apex of an ideal square pyramid [Cr(1)..Cl(1) = 2.8223(16)Å, Cl(1)-Cr(1)-P(1) = 109.63(5)^{o}, Cl(1)-Cr(1)-P(2) = 104.42(4)^{o}, Cl(1)-Cr(1)-P(3) = 90.16(4)^{o}, Cl(1)-Cr(1)-N(1) = 95.37(10)^{o}]. The coordination geometry of the second chromium atom is very distorted square-planar, or flattened tetrahedral, and is defined by the two nitrogen of the two bridging ligands [N(2)-Cr(2)-N(3) = 111.43(13)^{o}] and the two bridging chlorine atoms [Cl(1)-Cr(2)-Cl(1a) = 79.80(4)^{o}, Cl(1)-Cr(2)-N(2) = 133.37(10)^{o}, Cl(1)-Cr(2) - N(3) = 103.84(10 ^{o}]. The Cr..Cr distances within each dimetallic unit are long and outside the bonding range [Cr(1)..Cr(2) = 2.7670(13)Å].

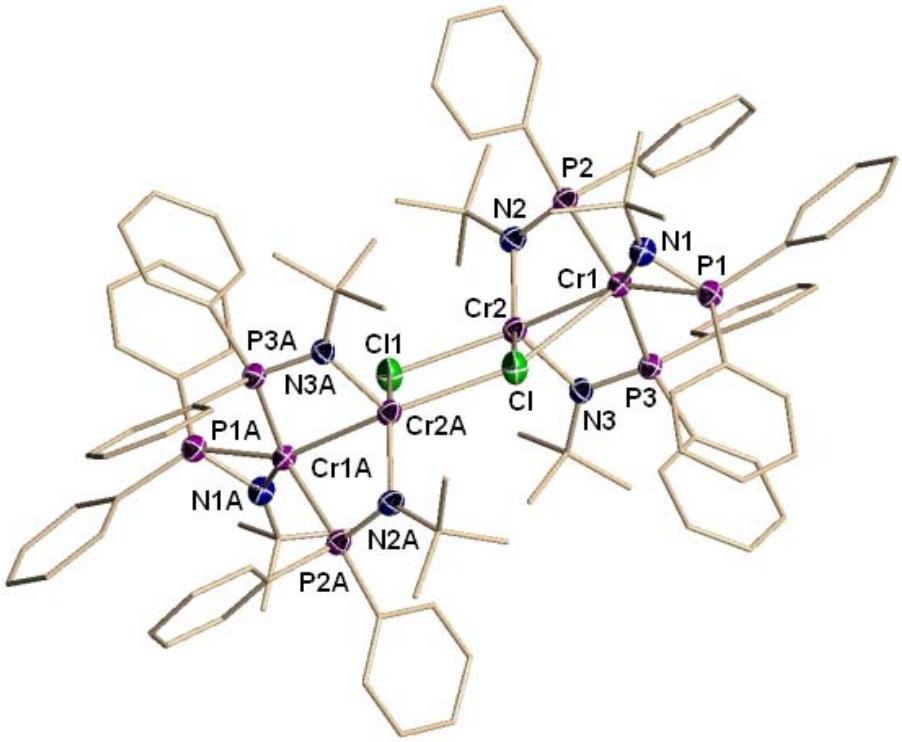

Figure 2.4: Partial thermal ellipsoids drawing of 2.5 (50 % probability level) with carbon atom ellipsoids omitted for clarity.

As usual, the reactions with R_3Al proved to be difficult affording only intractable materials. Just in the case of TMA it was possible to obtain a crystalline product formulated as a dinuclear $[\{(\mu\text{-}AlMe_2)[t\text{-}BuNP(Ph)_2]_2\}Cr(\mu\text{-}Cl)]_2 \cdot 1.7(toluene)$ (**2.6**) on the basis of the X-ray crystal structure (Scheme 2.5).

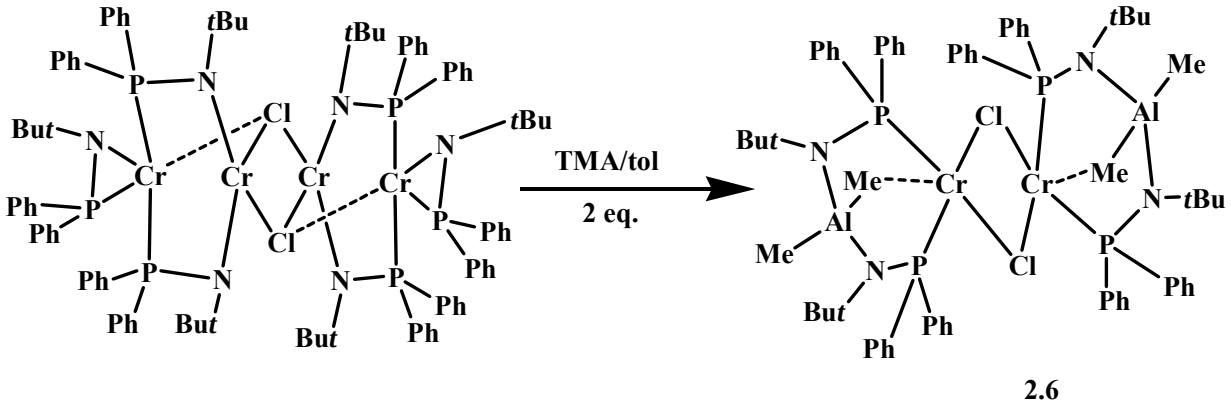

Scheme 2.5: Synthesis of complex 2.6

The structure indicated that the reaction has taken a surprisingly different pathway with respect to those leading to **2.2**, and **2.3**. The symmetry generated dimer (Figure 2.5) has two chromium-containing units linked by two bridging chloride [Cr(1)-Cl(1) = 2.3866(17) Å; Cr(1)-Cl(1a) = 2.3795(16) Å]. Each unit consists of a chromium atom bonded to two phosphorous of two ligands [Cr(1)-P(1) = 2.4471(17) Å; Cr(1)-P(2) = 2.5193(17) Å] and which in turn use the N atoms to link one Me_2Al unit [Al(1)-N(2) = 1.916(5) Å; Al(1)-N(1) = 1.929(5) Å].

The coordination geometry around the chromium center is therefore square-planar and is defined by two chlorine atoms placed in *cis* [Cl(1)-Cr(1)-Cl(1a) = 86.45(6)^o] and the two P atoms of the two ligands [P(1)-Cr(1)-P(2) = 95.52(6)^0, Cl(1)-Cr(1)-P(2) = 172.37(7)^o]. Once again, one of the two Me groups of the Me_2Al unit is oriented towards the metal center and occupies the axial position of an ideal square pyramid based on the chromium atom. However, the Cr…Me

distance [C(33)-Cr(1) = 2.805(6)Å] is outside the normal bonding range. The magnetic moment of **2.6** was in line with that of the other polynuclear complexes reported in this work with a room temperature value lower than expected as a possible result of an antiferromagnetic interaction.

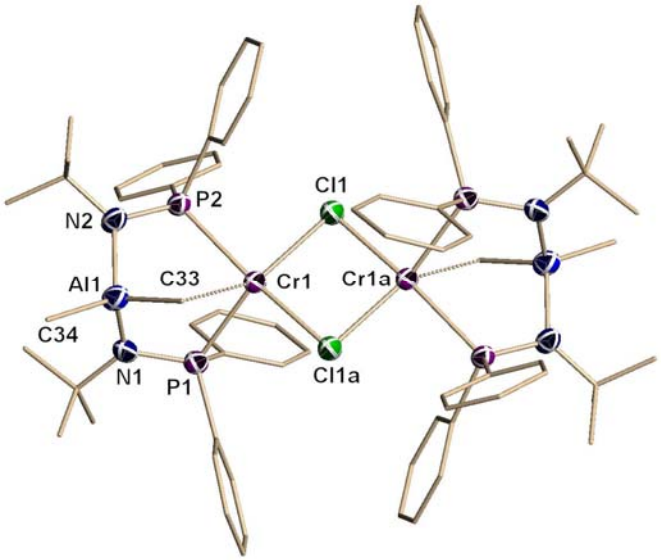

Figure 2.5: Partial thermal ellipsoids drawing of 2.6 (50 % probability level) with carbon atom ellipsoids omitted for clarity.

As previously mentioned, recent work on chromium pyrrolide[8c,d] has established a link between the metal oxidation state and catalytic behavior (selective trimerization versus polymerization and non-selective oligomerization). It is for this reason that in addition to the divalent species described above, we have also attempted to prepare and test the trivalent derivative of the same ligand system. Treatment of three equivalents of the lithium salt of aminophosphine ligand with one equivalent of $CrCl_3(THF)_3$ (Scheme 2.6) afforded green-colored, X-ray quality paramagnetic crystals of [(*t*-BuNPPh$_2$)$_3$Cr]·(toluene) **(2.7**). The room temperature magnetic moment was as expected for the high spin d^3 electronic configuration of trivalent chromium in an octahedral field.

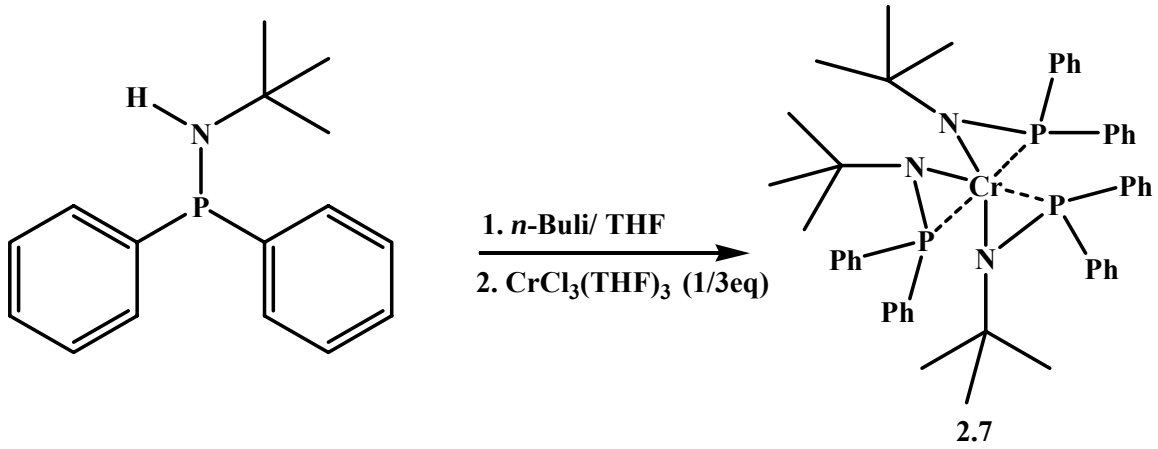

Scheme 2.6: Synthesis of complex 2.7

The structure of **2.7** (Figure 2.6) confirmed the monomeric nature of the complex with three ligands surrounding the metal center in a distorted octahedral geometry with the three ligands in a propeller-type of arrangement [P(1)-Cr(1)-N(1) = 41.54(10)^{o}, P(1A)-Cr(1)-N(1A) = 41.54(10) ^{o}, P(1A)-Cr(1)-N(1A) = 41.54(10)^{o}]. Of interest is that the three phosphorous [Cr(1)-P(1) = 2.4151(12)Å, Cr(1)-P(1A) = 2.4151(12)Å, Cr(1)-P(1A) = 2.4151(12)Å] and

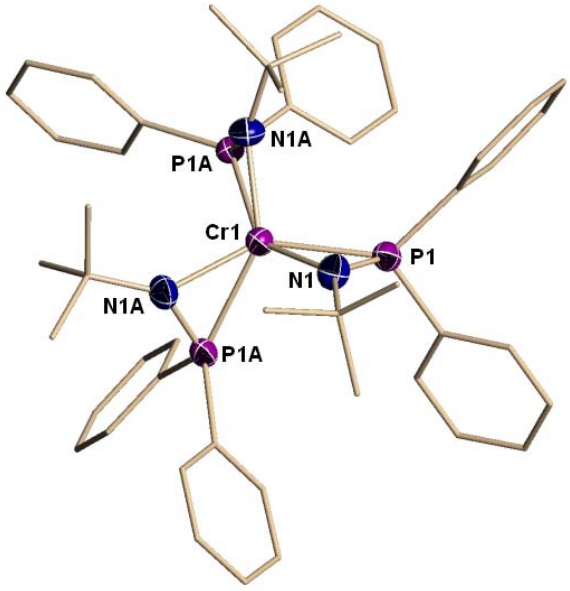

Figure 2.6: Partial thermal ellipsoids drawing of 2.7 (50 % probability level) with carbon atom ellipsoids omitted for clarity.

nitrogen atoms [Cr(1)-N(1) = 2.024(3)Å, Cr(1)-N(1a) = 2.024(3)Å, Cr(1)-N(1A) = 2.024(3)Å] are facially oriented [N(1)-Cr(1)-N(1A) = 111.67(10)^{o}, N(1)-Cr(1)-N(1A) =111.67(10)^{o}, N(1A)-Cr(1)-N(1A) = 111.67(9)^{o}, P(1)-Cr(1)-P(1A) = 108.96(4)^{o}, P(1)-Cr(1)-P(1A) = 108.96(4)^{o}, P(1A)-Cr(1)-P(1A) = 108.96(4) ^{o}].

The catalytic behavior of **2.7** is by any mean closely related to that of all the other divalent complexes reported in this work (*vide infra*). Therefore, it is conceivable that one of the preliminary steps of the catalyst activation is in fact the reduction of the trivalent species to a Cr(II) derivative rather than a monovalent chromium species as anticipated. To conclusively demonstrate this point**, 2.7** was treated with the same aluminum alkyls described earlier in this work (Scheme 2.7)**.**

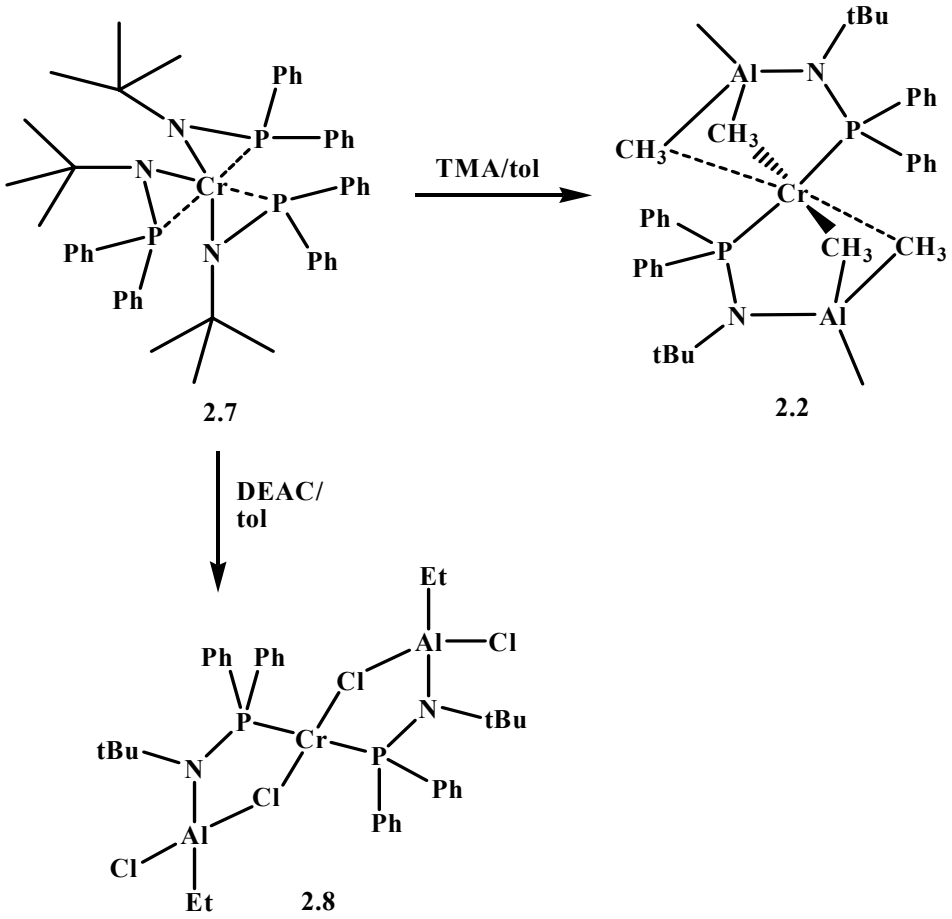

Scheme 2.7: Reduction of Cr(III) to Cr(II) complexes

Reaction with TMA under the usual reaction conditions afforded **2.2,** while the reaction with DEAC gave the new complex **2.8** whose structure is closely related to those of **2.3** and **2.4** with comparable bond distances and angles (Figure 2.7). The value of the magnetic moment of **2.8** was in the expected range.

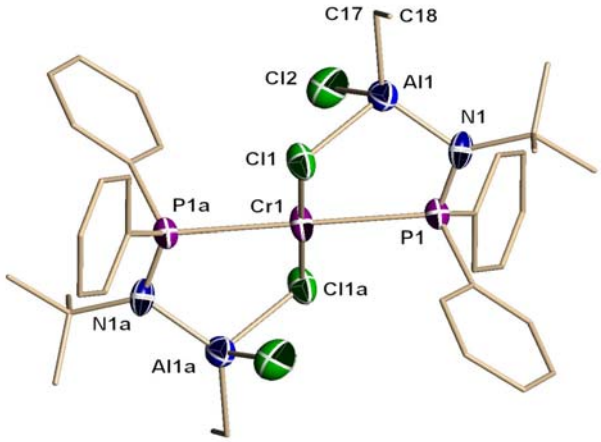

Figure 2.7: Partial thermal ellipsoids drawing of 2.8 (50 % probability level) with carbon atom ellipsoids omitted for clarity.

Catalytic behavior

The catalytic behavior of all the complexes above was tested *vis-à-vis* of their ability to oligo- or polymerizes ethylene with and without alkyl aluminum activators. Complex **2.1** behaved as a moderately active ethylene polymerization catalyst upon activation with MAO (Table 2.2). However, what makes this catalyst potentially interesting is that, aside the formation of polymer, a visible amount of 1-hexene was formed as the *only* byproduct. In turn, this indicates that the activator converts **2.1** into two separate catalytically active species, respectively responsible for polymer formation and selective trimerization. Attempts to activate **2.1** with different activators such as TMA and TIBA afforded only a small amount of 1-hexene with no

traces of polymer. Similar behavior was observed with TEAL albeit that a substantially larger amount of 1-hexene was produced. The overall activity remained, however, rather low even under a variety of reaction conditions.

Table 2.2 Effect of Temperature on Catalytic behavior of of **2.1.** [a]

Temp. (°C)	Activity g/mmol, Cat.h	Polymer (g)	Oligomers (mL)	Mol %						
				C6	C8	C10	C12	C14	C16	C18
25	0	0	0	-	-	-	-	-	-	-
50	1,580	5.5	2.4	99.9	-	-	-	-	-	-
75	5,400	11.3	15.7	27.9	23.4	20.5	18.2	12.5	8	2
100	6,560	6.0	26.8	23.9	33.2	26.6	20.1	15.7	11.7	3.5
50*	320	-	1.6	99.9	-	-	-	-	-	-

*Conditions [a]: MAO activator1000 eq,,10 µmol catalyst loading, 40 bar ethylene, 30 mins reaction time, total volume 100 mL in toluene. * Activated with TEAL (100 equiv)*

Increasing the temperature had a rather strong effect on improving the activity (Table 2.2) by one order of magnitude. However, the selectivity towards formation of 1-hexene was lost as a S-F distribution of oligomers was formed instead. This implies that another catalytically active species is generated at a temperature of 75 °C and higher. This remarkable sensitivity to the temperature is also responsible for the remarkable dependence on the amount of catalyst employed. By increasing the loading of **2.1** (Table 2.3) the production of polymer was more than doubled but 1-hexene was replaced by a much larger amount of a F-S distribution of oligomers. This is clearly a temperature effect that can no longer be properly controlled when a large amount of polymer is being formed.

Complex **2.5** is closely related to **2.1** from which it differs only for the nuclearity and the presence of one chlorine atom per dimeric unit. In spite of displaying a very similar ligand arrangement, **2.5** shows a substantially better catalytic performance giving a large amount of S-F distribution of oligomers, interestingly, with octene as the major component (Table 2.3).

Among the complexes containing AlR_2 residues, only **2.2** act as a single-component self-activating catalyst (Table 2.3). Upon exposure to ethylene at 100 °C, **2.2** produced a mixture of 1-butene (~75%), 1-hexene and 1-octene with a minor amount of polymer. Complexes containing organo-aluminum residues, such as **2.3, 2.4, 2.6** and **2.8**, were instead inactive as single-component catalysts. When activated with MAO though, they showed outstanding activity as non-selective oligomerization catalysts producing a large amount of a F-S distribution of oligomers alongside some polymer. Complex **2.6** in particular displayed high activity with only traces of waxy higher α-olefins accompanying the production of oligomers.

Table 2.3. Catalytic behavior of **2.1-2.7.** [a]

Cat (μmol)	MAO (eq)	Activity g/mmol, Cat.h	Polymer (g)	Mw	PDI	Oligomers (mL)	Mol %						
							C6	C8	C10	C12	C14	C16	C18
2.1(10)	1000	1,560	5. 5	42,180	3.8	2. 4	99.9	-	-	-	-	-	-
2.1(25)	1000	2,800	13			22	37.87	20.03	14.00	10.90	7.6	5.6	0.5
2.2(50)[c]	0	236	1. 2			4.7[b]	25.0	10.0	-	-	-	-	-
2.2(25)	1000	4,616	2.7	72,150	2.5	55	14.08	26.35	23.42	19.77	15.61	12.76	0.636
2.3(50)[c]	0	0	-			-	-	-	-	-	-	-	-
2.3(10)	1000	7,200	8			28.0	18.9	24.9	20.2	15.8	11.3	6.6	2.2
2.3(25)	1000	6,200	9. 5	969,950	17.6	68	20.00	27.2	16.7	10.3	6.1	2.9	1.1
2.4(50)[c]	0	0	-			-	-	-	-	-	-	-	-
2.4(25)	1000	6,280	8. 5	561,380	8.6	70	35.6	22.2	16.71	10.3	6.1	2.9	1.1
2.5(5)	1000	14,000	2			33	12.7	26.3	19.8	15.9	11.5	8.1	5.6
2.5(5)[d]	1000	19,200	5			43	22.08	27.70	22.91	17.70	13.12	9.58	7.5
2.5(25)	1000	5,384	12.7	1,225,580	7.1	54.6	15.36	23.32	18.09	14.04	10.4	7.9	6.12
2.6(50)[c]	0	20	0. 5			-	-	-	-	-	-	-	-
2.6(10)	1000	10,400	0.2			51	15.02	21.53	18.5	14.5	11.01	8.18	6.34
2.7(10)	1000	3,688	6.43			12.01	37.8	20.6	14.4	11	8.1	5.5	2.3
2.7(10)	300	7,634	30	567,880	18.6	8.17	27	23	20	18	12	8	2
2.8(10)	1000		1-wax			68	22.2	23.9	19.2	14.9	11.2	8.0	6.4
Blank	1000	-	0.08			-	-	-	-	-	-	-	-

[a] *Conditions: MAO activator, 40 bar ethylene, 30 minutes reaction time, total volume 100 mL in toluene*

[b] *large amount of 1-butene (~65%) not reliably quantifiable due to volatility.*

[c] *Single component catalyst runs were carried out with 50μmol catalyst loading to minimize the destructive impact of impurities and T= 100 °C.*

[d] *T = 75 °C*

Complex **2.4** gave the highest activity producing a F-S distribution of oligomers aside a substantial amount of polymer. The trivalent **2.7** produced a very large amount of polymer and a F-S distribution of α-olefins (Table 2.3). Lower amount of MAO substantially increased the amount of polymer. As mentioned above, treatment of **2.7** with several activators including TMA and DEAC afforded **2.2** and **2.8**, respectively. While in comparison with the other compounds (Table 2.3), complex **2.8** is not a single-component catalyst since it gave a catalytic activity similar to those of **2.3** and **2**.**4**. Its desirable feature is that, aside the outstanding activity as a non-selective catalyst only a negligible amount of polymer was produced.

By changing the solvent to methylcyclohexane[8c], all the complexes display an interesting behavior as they all are selective ethylene trimerization catalysts upon activation with MAO (Table 2.4). Interestingly, this is a complete turnaround with respect to the behavior of Rosenthal's PNPN systems,[38] which produced high selectivity in toluene.

Table 2.4. Effect of the Solvent**.** [a]

Cat (μmol)	MAO (eq)	Activity g/mmol, Cat.h	Oligomers (mL)	1-C_6 (%)	Polymer (g)	Mw	PDI
2.1(25)	150	720	4. 0	>99.9	5. 0	42,000	3.1
2.2(25)	150	1,760	6. 0	>99.9	16	90040	2.9
2.3(10)	1000	2,660	5. 3	>99.9	8. 0		
2.3(25)	150	1,880	4. 5	>99.9	19	241880	8.5
2.3(10)[b]	1000	860	2.3	>99.9	2. 0		
2.4(25)	150	2,160	9. 0	>99.9	18	1645820	3.9
2.4(10)[b]	1000	2,560	7. 4	>99.9	5. 4		
2.5(25)	150	1,120	5. 0	>99.9	9. 0	501150	58
2.5(25)[b]	500	920	3.5	>99.9	8. 0		
2.6(11)	150	5,700	1.5	>99.9	27	237,280	32
2.7(25)	150	2,160	8. 0	>99.9	19	134690	6.5
2.8(10)	150	2,120	5.5	>99.9	20	551790	10.1

[a]Conditions: MAO activator, T = 60 °C, 40 bar ethylene, 30 mins reaction time, total volume 100 mL in methylcyclohexane.[b] MMAO activator

This may tentatively be explained with the presence of an additional P atom in PNPN ligands, preventing the reoxidation of the monovalent intermediates via disporportionation. In the case of **2.4** the formation of 1-hexene was the highest observed in this work. It is therefore unfortunate that a large amount of polymer was ubiquitously present. Interestingly though, complex **2.6** switched its selectivity from S-F distribution to waxy high molecular weight linear α-olefins (Table 2.4).

Given the trend, it is rather strange that **2.1** is the only one of this class of complexes to give a selective trimerization catalyst in toluene. This can be tentatively ascribed to the low productivity with consequent low exothermicity that prevented thermal degradation of the catalyst (see Table 2.2). With the only exception of **2.2** as single component catalyst (which also seems to give some selectivity), all the other compounds produced a substantially larger amount of S-F distribution of products in toluene as a reaction solvent. This reiterates the prominent role played by the temperature in deactivating the trimerization catalyst when toluene is used as solvent. Finally, the ability of the solvent to switch the catalytic outcome from a S-F distribution to selective formation of 1-hexene clearly indicates that the same catalytically active species responsible for the formation of 1-hexene in methylcyclohexane cannot be responsible for the S-F distribution observed in toluene. Further ring expansion leading to heavier α-olefins in toluene cannot possibly be hindered by methylcyclohexane. Therefore, we hypothesize that either a different mechanism or a different active species should be operational for the efficient nonselective oligomerization in toluene as graphically depicted below.

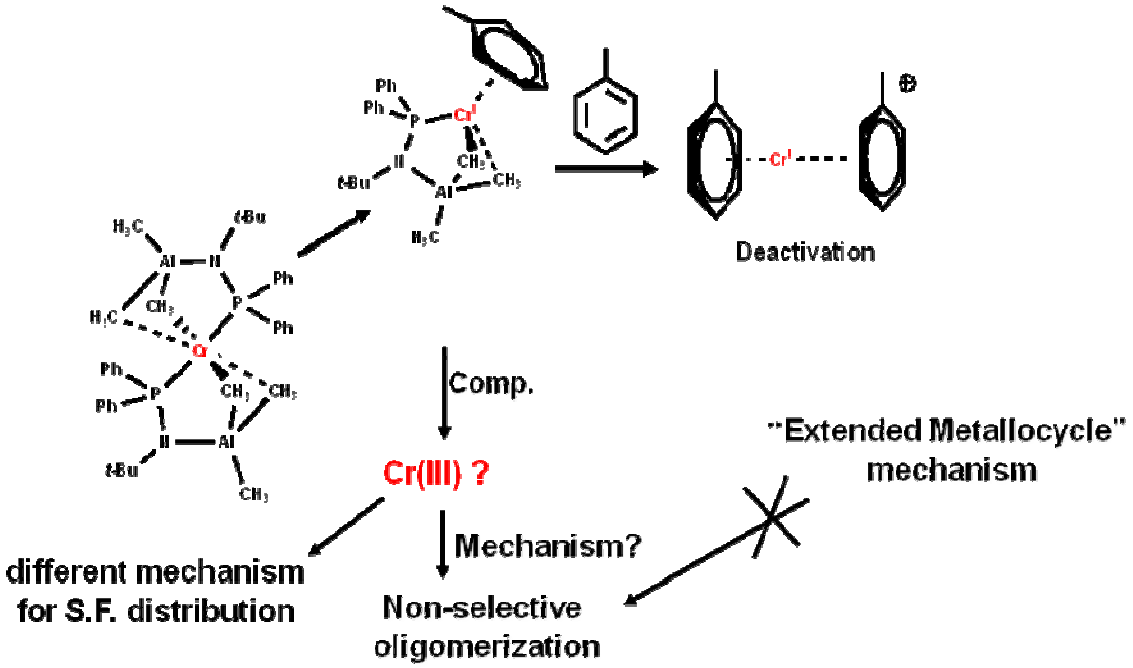

On the other hand, from these observations we infer that catalytically active monovalent Cr(I) species formed *in situ* is sufficiently stable in methylcyclohexane to undergo metallacycle mechanism for selective formation of 1-hexene as assumed in the following plausible mechanistic pathway (Scheme 2.8).

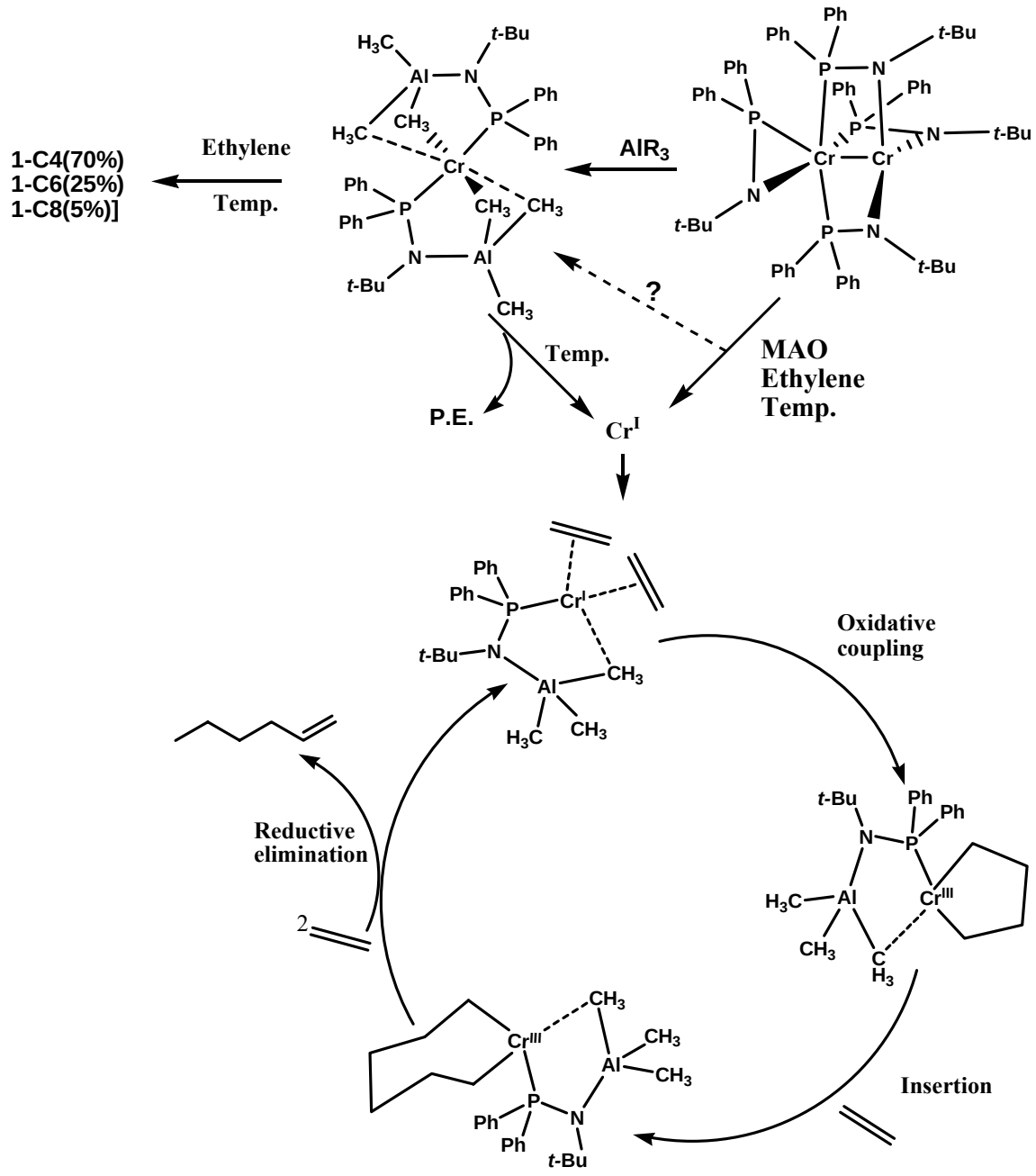

Scheme 2.8: Plausible pathway for the formation of 1-hexene selectively from NP complexes.

In order to prove this hypothesis, a great effort has been put to isolate a well defined catalytically active monovalent Cr(I) species. By endeavoring the isolation of such compounds we hope to obtain self-activating catalysts, which in turn could deepen our understanding of this

fascinating catalytic process. Towards this end, we are presenting a detailed study of the reduction of the above mentioned tetranuclear and divalent {[(*t*-Bu)NPPh$_2$]Cr[μ-(*t*-Bu)NPPh$_2$]$_2$Cr}$_2$(μ-Cl)$_2$ (**2.5**) to an unusual Cr(I)/Cr(II) mixed-valence, self-activating catalyst (**2.9**), in the following section. In this case it was possible to isolate, albeit in very low yield, an intriguing butadiene/butadiene-di-yl cluster {[(η^4-butadiene)Cr(μ,η^4-butadien-di-yl)(μ-NP)Mg]$_2$(μ-Cl)$_4$Mg(THF)$_2$}{[(THF)$_3$Mg]$_2$(μ-Cl)$_3$}$_2$ (**2.10**) which is a highly selective self-activating trimerization catalyst.

2.4.2 Isolation and Characterization of a Class-II Mixed-Valence Cr(I)/Cr(II) Self - Activating Ethylene Trimerization Catalyst.

The reduction of **2.5** was easily achieved by stirring its THF solutions with freshly prepared KC_8 and in the presence of small excess of PMe_3. The reaction afforded the new mixed valence species (Me_3P)Cr[μ-(*t*-Bu)NPPh$_2$]$_3$Cr (**2.9**) in crystalline form (Scheme 2.9).

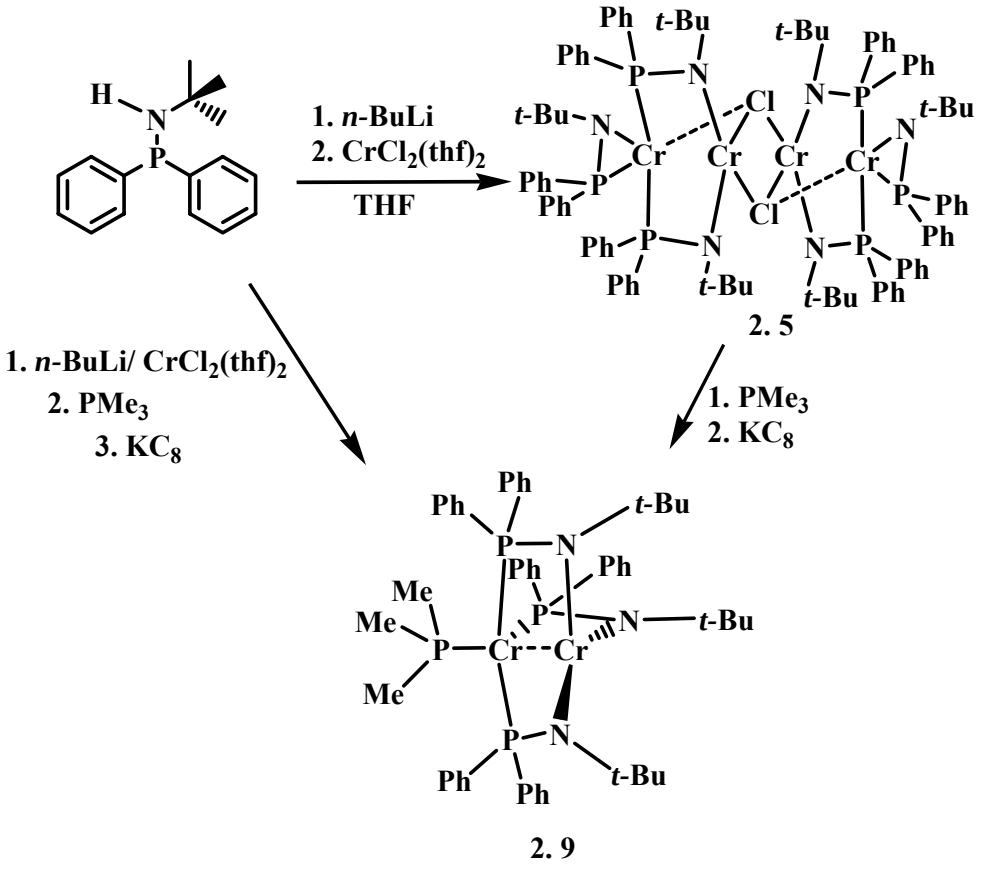

Scheme 2.9: Different route to complex 2.9

The connectivity of **2.9** was revealed by an X-Ray crystal structure (Figure 2.8) showing a dinuclear core with the two metal centers bridged by three *t*-BuNPPh$_2$ anions. The ligands are identically placed with respect to the dimetallic unit in the sense that one metal is exclusively bonded to the P atoms and the second only to the nitrogens. The chromium bonded to the phosphorus atoms [Cr(1)-P(1) = 2.4431(4)Å, P(1)-Cr(1)-P(2) = 108.569(13)°] is also coordinated to the P atom of a Me_3P unit [Cr(1)-P(2) = 2.5008(8)Å] in an overall tetrahedral environment [P(1)-Cr(1)-P(1a) = 110.356(13)°, P(1)-Cr(1)-P(1b) = 110.359(13)°, P(1a)-Cr(1)-P(1b) = 110.357(13)°]. The three nitrogen atoms of the three ligand amino residues chelate the second chromium atom [Cr(2)-N(1) = 2.0172(13)Å,] and provide a trigonal planar coordination

geometry [N(1)-Cr(2)-N(1a) = 119.814(6)°]. The Cr-Cr distance [Cr(1)…Cr(2) = 2.3124(6)Å] is short and falls in what is normally regarded as a Cr-Cr multiple bonding range.

Charge count of complex **2.9** suggests two different interpretations of the structure that can be either regarded as a Cr(III)/Cr(0) or a Cr(II)/Cr(I) mixed valence species. The two distinctively different coordination environments indicate that in any scenario the complex may be regarded as a class II mixed-valence species. The trigonal planar environment of the chromium atom surrounded by the three nitrogens is strongly reminiscent of that of a few existing Cr(III) amido complexes.[42] In turn this will require the second chromium atom being zerovalent. However, the close proximity at Cr-Cr bonding distance makes such a large charge unbalance between the two metals unlikely. Therefore, a Cr(II)/Cr(I) formulation is perhaps more realistic.

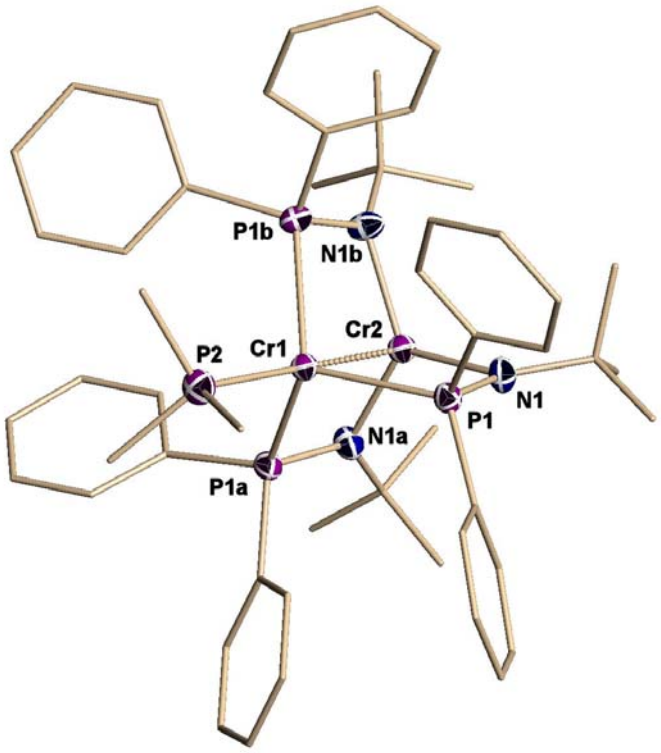

Figure 2.8: Partial thermal ellipsoids drawing of complex 2.9 (50 % probability level).

Magnetic properties measured at variable temperature were not particularly informative with this respect (Figure 2.9) only showing a Curie-Weiss type of behavior (C = 0.4 and θ = - 2.8 K) with the value of the magnetic moment leveling at room temperature over the 1.7 μ_{BM} as expected for a S = 1/2 species.

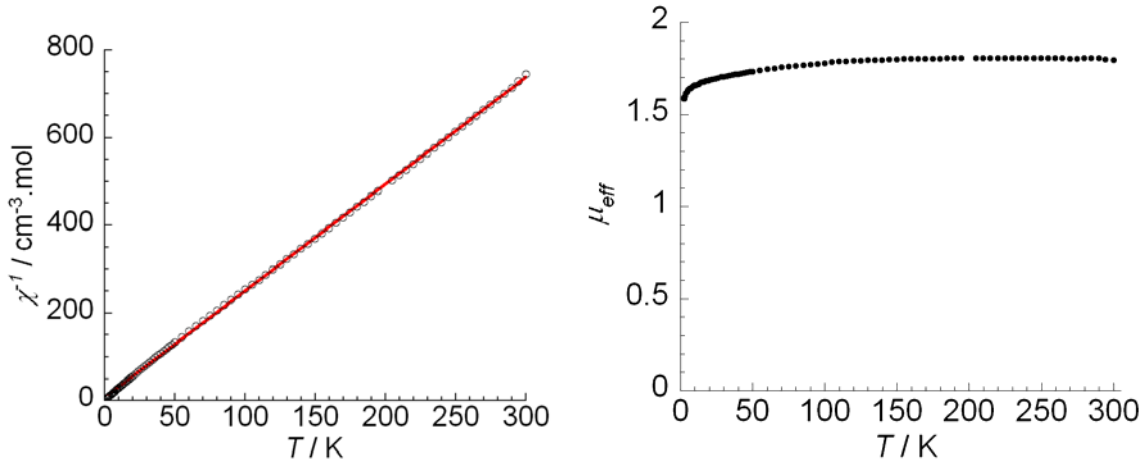

Figure 2.9: Diagrams of the inverse of the magnetic susceptibility (left) and of the magnetic moment (right) versus temperature. Solid line represent the fit obtained using Curie-Weiss law.

Also the behavior of the magnetization against the field did not reveal unexpected features (found in the supporting information of reference 43)[43] other than the presence of less than 5% of paramagnetic impurities. These impurities are most likely inherent to the sample preparation technique of a material of such enhanced air-sensitivity.

Computational Methods.

Unrestricted DFT calculations were undertaken to elucidate the electronic structure and the oxidation states of the two metals in **2.9**. All calculations used the program Turbomole[44] in combination with the external Baker optimizer.[45] For the energy profile shown in Figures 2.10 and 2.11, all geometries were initially fully optimized at the b3-lyp[46]/TZVP[47] level. Vibrational

analyses (analytical second derivatives) were carried out to check the nature of all stationary points (minima or transition states), and to calculate thermal corrections (enthalpy and entropy, gas phase, 273K 1 bar). Since the calculations were not intended to model any specific experiment, no solvent corrections were applied, but entropies were scaled by a factor of 0.67 to represent the effect of reduced freedom in solution.[48] For all systems, improved single-point energies at the optimized geometries were then calculated at the b3-lyp/TZVPP[49] level. Final free energies were obtained by combining the b3-lyp/TZVPP electronic energy with the enthalpy and scaled entropy values obtained at the b3-lyp/TZVP level. Structures of model compounds $(Me_3P)Cr[\mu\text{-}MeNPMe_2]_3Cr$ (for **2.9**), (η^4-butadiene)Cr(μ,η^4-butadien-di-yl)[μ-$MeNPMe_2$]$Mg(THF)_2$ and (η^4-butadiene)Cr(μ,η^4-butadien-di-yl)[μ-$MeNPMe_2$]$MgCl_2^{2-}$ (for **2.10**) were only optimized at the b3-lyp[C]/SV(P)[50] level, and no higher-level single-point calculations were performed. Orbital plots were generated using Molden.[51]

The results for the simplified models $Cr^{II}(\mu\text{-}MeNPMe_2)_3Cr^{I}(PMe_3)$ and $Cr^{II}(\mu\text{-}{}^{t}BuNPMe_2)_3Cr^{I}(PMe_3)$ gave very similar results and only the former one (which give cleaner MO pictures) will be discussed here. The three NP ligands are best considered as bearing a charge of -1 each. That results in a total oxidation state of +III divided over the two Cr atoms. The experimentally observed doublet ground state would be compatible with either two low-spin Cr centers or antiferromagnetic coupling between two high-spin Cr centers. In view of the low coordination numbers of both chromium atoms, the latter interpretation seems more reasonable. According to the calculations, the electronic structure is best interpreted as having the N-bound Cr in the +II oxidation state, while the P-bound Cr is assigned an oxidation state of +I. The pattern of occupied orbitals (see Table 2.5) is entirely consistent with an interpretation of antiferromagnetic coupling between a high-spin Cr(I) and a high-spin Cr(II) centre. For such

Table 2.5. Occupied α and β orbitals for $Cr^2(\mu\text{-MeNPMe}_2)_3Cr^1(PMe_3)$.[a]

α (HOMO = 119)		β (HOMO = 118)	
119 Cr^1 d_{xz}	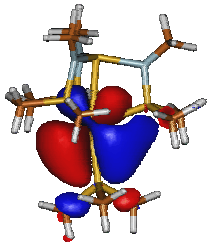	118 Cr^1 d_{xz}	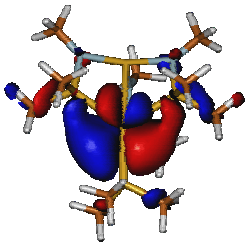
118 Cr^2 d_{xy}	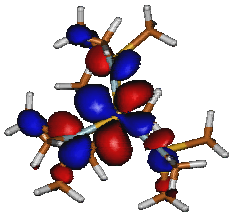	117[b] Cr^1 d_{z2}+...	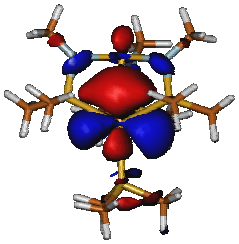
117 Cr^2 d_{z2}+...	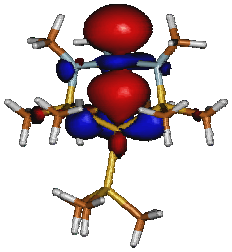	116 Cr^1 d_{yz}-NP	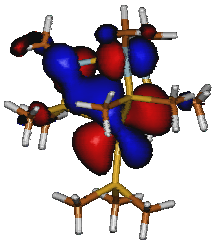
115 Cr^2 d_{xz}	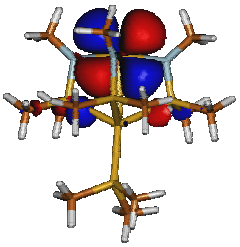	115 Cr^1 d_{yz}+NP	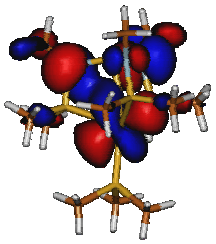
114 Cr^2 d_{yz}	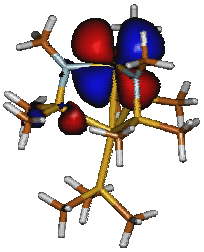	114[b] Cr^1 d_{x2-y2}	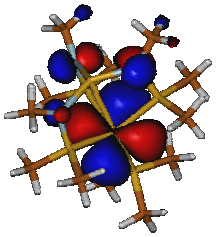

[a] α116 is a combination of N p_π orbitals. For orbital labelling, the z axis was chosen along the Cr-Cr vector; x and y labels are arbitrary. Orientations are different for the different orbitals to better illustrate their shapes. [b] Orientations of β117 and β114 are not nicely aligned with coordinate axes.

one would expect a Jahn-Teller distortion, and indeed the optimized structure is not perfectly symmetric. However, the deviations from perfect C_{3v} symmetry are modest even for the model complexes. It seems reasonable to assume that for the highly sterically hindered real systems steric factors will maximize the distances between the NP ligands and hence favor an even more symmetric structure, thus explaining the observed threefold symmetry.

The occupied orbitals show very little evidence of metal-metal bonding. In both α117 and β117 (occupied Cr d_{z2} orbitals) there is only a small contribution from the second Cr center (contributing to the Cr-Cr σ-bond). The other orbitals show even less evidence for metal-metal π and/or δ bonding. Thus, this complex seems to be another example of a Cr dimer where the short Cr-Cr distance is enforced or promoted by the ligand skeleton (with no "objection" by the Cr atoms) rather than by a strong metal-metal bond.[40b] Accordingly, one could envisage that ligand rearrangement/redistribution could easily lead to fragmentation of the dimer into two monometallic fragments.

Catalytic Activity

Complex **2.9** shows an interesting catalytic behavior for ethylene oligo- and polymerization (Table 2.6). As expected for a reduced species capable of feeding the catalytic cycle with low-valent chromium, the complex is also self-activating. Under pressure of ethylene gas, the complex produces a mixture of 1-butene and 1-hexene and no polymer. As commonly observed for self-activating catalysts, the activity was low, likely due to both the difficulties to eliminate impurities from the reaction mixture and also to the fact that only one of the two metal

centers may produce catalytic behavior under the self-activating conditions. Assuming that the catalytically self-activating species is the unit containing the monovalent center, the formation of 1-hexene as a major component has to be expected.

Table 2.6 Catalytic testing.[a]

Cat. Solv.	Co-cat. (eq.)	Activity g/mmol/Cat/h	PE (g)	Oligo. (g)	C_4 (%)	C_6 (%)	C_8 (%)	$>C_{10}$ (%)
2.9,**To**luene	-	60	-	1.5	30	70	-	-
2.9, MeCy	-	120	-	3.0	30	65	5	-
2.9, Toluene	MAO (500)	160	4	traces	-	-	-	-
2.9, MeCy	MAO (150)	340	8	traces	-	-	-	-
2.9, MeCy	DMAO (400)	1,504	38	-	-	-	-	-
2.9, MeCy	TMA(10)	40	-	1.0	52	48	-	-
2.9, MeCy	DMAO(400)/ TEAL (20)	200	-	5	-	95	5	-
2.9, MeCy	TEAL (20)	120	traces	3	99	traces	-	-
2.9, MeCy	C_2H_3MgCl (2)	240	-	6	53	45	2	-
2.10, MeCy*	-	280	-	7.5	traces	99	-	-

*Conditions[a]: 50 µmol catalyst loading, 40 bar ethylene, 30 mins reaction time, total volume 100 mL at 100 °C. * 5 µmol catalyst loading.*

Instead the formation of the relatively large amount of 1-butene could be generated through a different path. In fact, in the ring expansion mechanism, reductive elimination is not expected to occur at the level of the five-membered ring.[52] The fact that the reaction is sensitive to the nature of the solvent fits instead with the poisoning effect of toluene on monovalent chromium catalysts.[8a, c, 12, 37a]

Activation with MAO only produced small amounts of PE. However an interesting catalytic activity was observed upon activation with TMA-depleted MAO (DMAO). The polymer formed with this activator was near to perfectly linear with reasonable polydispersity and a very high molecular weight (Mw = 980,423, PDI = 2.7). In addition, the high-T ^{13}C-NMR spectrum showed the polymer being highly linear. To assess the role of TMA present in MAO,

we have also tested **2.9** with pure TMA. The reaction in this case produced no polymer and only comparable amount of 1-butene and 1-hexene with low activity. By adding to DMAO a small amount of the more reducing TEAL, highly pure 1-hexene free of 1-butene and polymer was obtained, the only contaminant being small amount of 1-octene. Remarkably, activation by TEAL alone resulted in the exclusive formation of 1-butene.

The self-activating behavior of **2.9** is intriguing and it can be rationalized with the ability of **2.9** to feed monovalent species directly into the catalytic cycle. The switchable behavior observed as a function of the nature of the activator is instead hard to comprehend. It indicates that the aluminates may clearly trigger formation of two different catalytically active species, namely full reduction (as in the case of DMAO/TEAL) or disproportionative oxidation (as in the case of DMAO).

In search for clues, possible trimerization and dimerization cycles, briefly highlighted in Scheme 2.10, were computationally investigated. For the trimerization cycle we have examined the minimal [Me_2PNMe]Cr catalytic center, assuming that [Ph_2PNtBu]Cr fragments may be generated by the dissociation of **2.9** in the presence of ethylene.

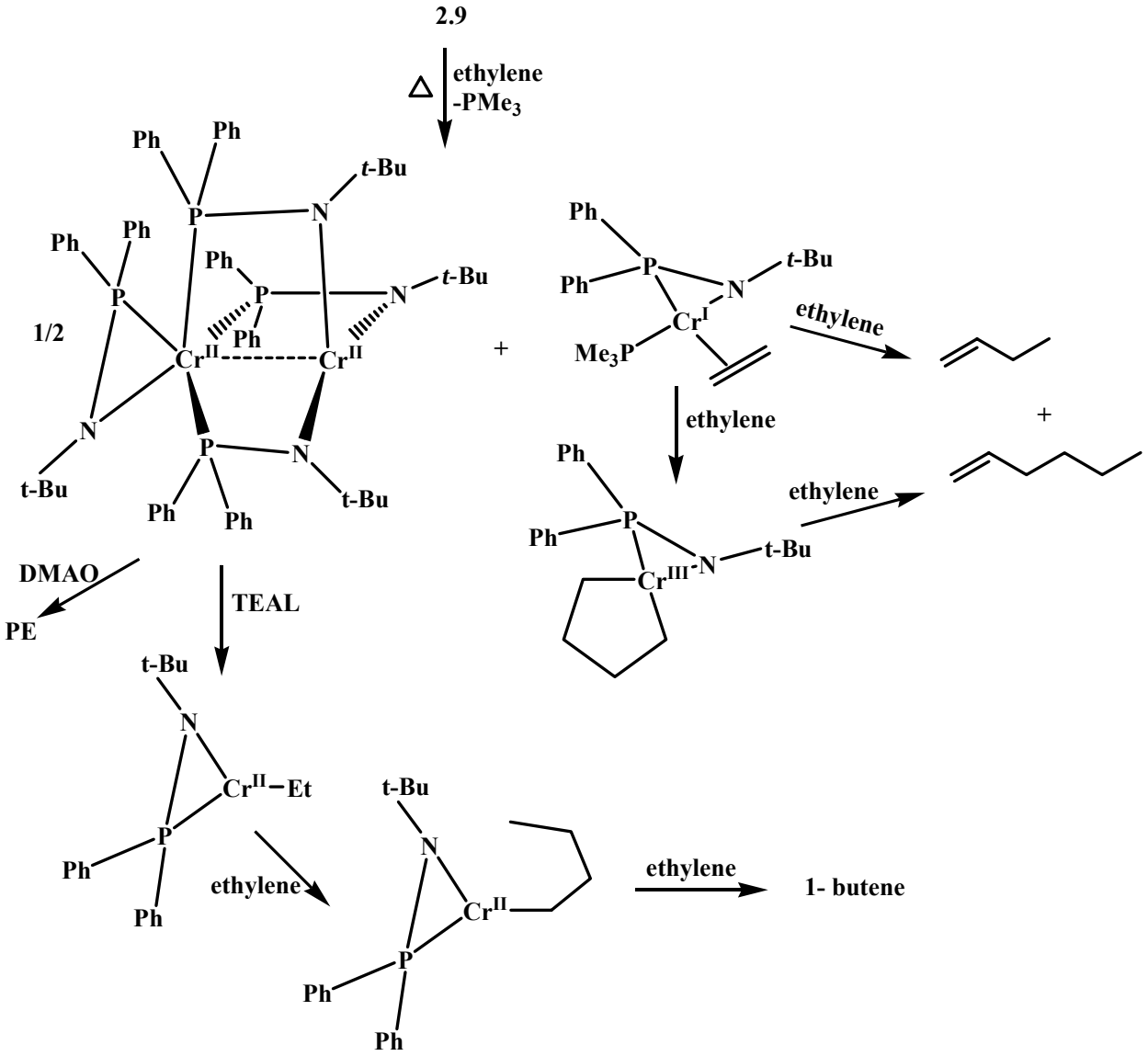

Scheme 2.10: Computationally investigated possible di-and trimerization cycle.

Spin states S = 1/2, 3/2 and 5/2 were considered. The S = 3/2 spin state was found to be lowest in energy for all stages of the reaction except the mono-olefin complexes, where S = 5/2 was preferred. S = 1/2 states were systematically about 20 kcal/mol higher in energy than S = 3/2 states. The reaction profile is summarized in Figure 2.10, and energies are collected in Table 2.7.

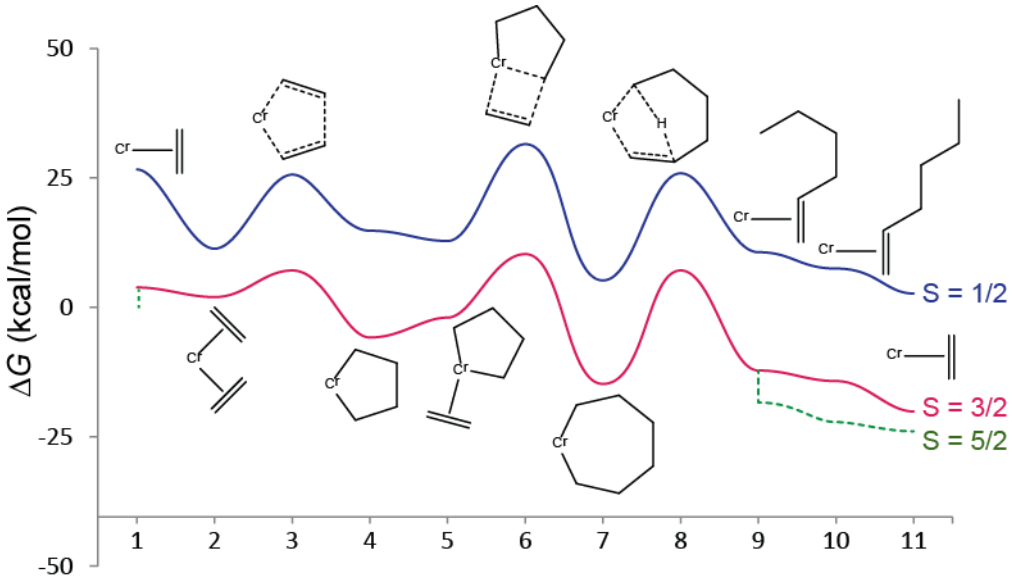

Figure 2.10: Free energy profile (kcal/mol) for 1-hexene formation at a [Me$_2$PNMe]Cr centre. The S = 5/2 state is only relevant for Cr(I) mono-olefin complexes. The final Cr(C$_2$H$_4$) complex is shown lower than the initial one because on going from 1 to 11 one molecule of 1-hexene has been produced.

The initially formed [Me$_2$PNMe]Cr(C$_2$H$_4$) prefers the S = 5/2 spin state. However, in this state the system does not bind a second ethene molecule. After a switch to S = 3/2, a second ethene molecule does bind, at a free energy close to the starting S = 5/2 mono-ethene complex. [Me$_2$PNMe]Cr(C$_2$H$_4$)$_2$ undergoes very easy C-C coupling to the corresponding metallacyclopentane complex, with a barrier of only about 5 kcal/mol. Binding an additional ethene molecule is now endergonic by just 4 kcal/mol, and its insertion has a barrier of 12 kcal/mol. The subsequent β→ω hydrogen transfer is the most difficult step of the reaction, with a calculated free energy barrier of 22 kcal/mol. After that, a spin flip back to S = 5/2 occurs, and the final step is exchange of ethene for hexene. Geometries of the various stages of the reactions are found in the supporting information of reference 43 (Figure S1)[43].

Ligand hemilability seems to be a common theme for trimerization catalysts. Indeed, the PN model ligand used here also displays rather variable Cr-P distances, which are not dictated by

steric effects. Interestingly, there is also no obvious link with electronic unsaturation. Thus, we see relatively short Cr-P distances for the bis(ethene) complex, the metallacyclopentane, its ethene complex, the insertion TS and the resulting metallacyclohexane, but longer Cr-P distances for the ethene coupling TS and the H transfer TS. Inspection of preferred relative orientations of amide and hydrocarbon fragments suggests that the amide nitrogen also functions as a π-donor, so the complexes studied are less electronically unsaturated than one might expect for such low coordination numbers.

Table 2.7 Calculated relative free energies (kcal/mol) for catalytic 1-hexene formation.

Stage[a]	S = 1/2	S = 3/2	S = 5/2
1	26.61	3.85	0.00
2	11.30	2.01	
3	25.64	7.14	
4	14.79	-5.83	
5	12.79	-2.00	
6	31.51	10.28	
7	5.22	-14.80	
8	25.89	7.12	
9	10.65	-12.18	-18.37
10	6.81	-14.25	-22.19
11	2.64	-20.12	-23.97

[a] For structures, see Figure 2.10.

In addition to trimerization, we have also studied a simple model for the selective ethene dimerization observed upon activation (following the traditional insertion mechanism). Given that elimination of 1–butene from the five-membered metallacycle is energetically less favored (but not impossible),[52] we have considered the possibility that the divalent partner of the initial dissociation of **2.9** might be responsible for it. Upon activation with TEAL, such a species might be transformed into [Me_2PNMe][Me_3P]Cr(Et) (a species such as [Me_2PNMe]Cr(Et) was considered to be too unsaturated to be realistic). As long as the PN ligand remains N-monodentate, one would expect standard square-planar Cr(II) insertion chemistry for [Me_2PNMe][Me_3P]Cr(Et) upon coordination of ethylene, and we assumed an S = 2 spin state throughout the cycle. Indeed, we see this coordination mode for most of the cycle (Figure 2.11, Table 2.8)[43]. Only the coordinatively unsaturated CrEt and CrH species preferentially adopt geometries in which the PN ligand becomes η^2-bound, thus relieving the electronic unsaturation. In addition, for some olefin complexes we located geometries which are closer to 5-coordinate, with the H or Et in a fac orientation relative to N and the phosphine ligand. These do not appear to play a prominent role in the insertion chemistry.

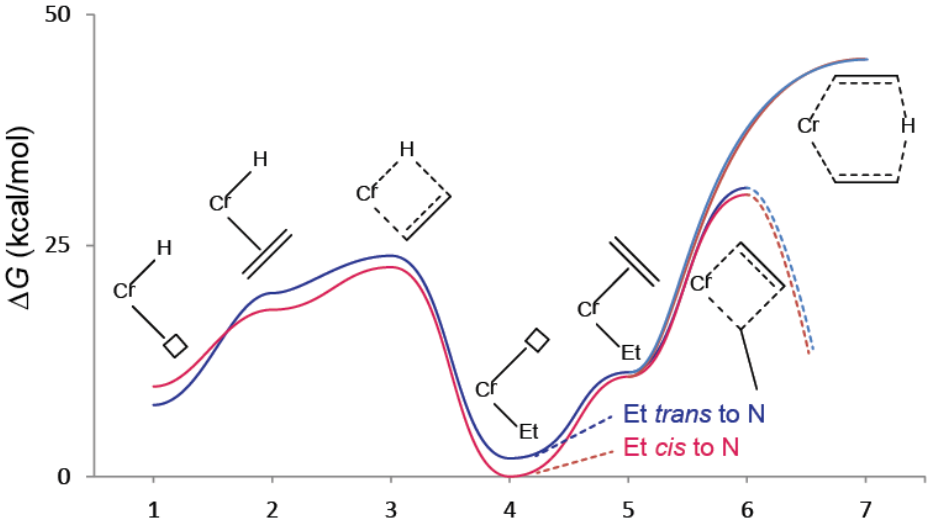

Figure 2.11: Free energy profile for 1-butene formation at [Me_2PNMe][Me_3P]Cr(Et) (S = 2).

Table 2.8. Calculated relative free energies (kcal/mol) for 1-butene formation at [Me_2PNMe][Me_3P]Cr(Et).

	Et trans to N	Et cis to N
1	7.76	9.74
2	19.87	18.06
3	23.90	22.67
4	1.97	0.00
5	11.30	10.80
6	31.25	30.49
7	45.31	45.31

[a] For structures, see Figure 2.11.

Therefore, 1-butene formation in this system appears to follow the standard insertion/elimination mechanism, although insertion barriers are rather high, perhaps reflecting the low electrophilicity of the metal centre. The *β*–elimination from the ethyl complex to give the hydride-ethene complex, and even subsequent loss of ethene, are easier than insertion. Interestingly, concerted β-H transfer to monomer is very difficult for this system. The transition state for this step does not involve any close Cr-H interaction but rather resembles the "alternative" transfer TS geometry studied systematically by Talarico and Budzelaar.[40b]

We have also tried to model alternative chain growth mechanisms involving Cr(I), as well as possible trimerization cycles involving Cr(II)/Cr(IV) or Cr(0)/Cr(II), but none of these variations produced a viable cycle. Therefore, we believe the above results at least suggest that a Cr(I)/Cr(III) cycle is reasonable for 1-hexene and, to minor extent, 1-butene formation, while insertion chemistry is more consistent with a Cr(II) species. One new idea derived from the

above data is that for these species of low electrophilicity β-H elimination rather than β-H transfer may be responsible for low molecular weight polymers, oligomers or S-F distributions.

We have also attempted the activation of **2.9** with vinyl Grignard. This was advised by recent results from our lab showing that the oxidative coupling of two vinyl anions bonded to chromium may trigger two-electron reduction to the monovalent state, thus producing self-activating selective trimerization catalysts.[53] Upon treatment of **2.9** with two equivalents of vinyl Grignard and exposure to ethylene, the catalytic system displayed a behavior very comparable to that observed with TMA affording the same mixture of 1-butene and 1-hexene, just with higher activity. We further observed that during the activation process of **2.9** with vinyl Grignard the color changed from reddish-brown to brown. Occasionally, a few crystals of a new compound were formed with very low yield. Regrettably, attempts to improve the reaction yield to enable complete characterization failed and even the reproducibility of the crystal formation was random. Nonetheless, the quality of the crystals was always sufficient for crystal structure determination allowing to formulate this new species as {[(η^4-butadiene)Cr(μ–η^4:η^1-butadien-di-yl)(μ-NP)Mg]$_2$(μ-Cl)$_4$Mg(THF)$_2$}{[(THF)$_3$Mg]$_2$(μ-Cl)$_3$}$_2$ (**2.10**).

Complex **2.10** is a symmetry generated dimer (Figure 2.12) where each of the two identical (η^4-butadiene)Cr(μ–η^4:η^1-butadien-di-yl)(μ-NP)Mg units is connected to a central magnesium cation via two bridging chlorine atoms. Two unconnected {[(THF)$_3$Mg]$_2$(μ-Cl)$_3$} cations per dimeric unit complete the structure. The chromium containing unit shows the chromium atom sandwiched between two π–bonded butadiene units. The first butadiene residue displays the expected bond distances [C(21)-C(22) = 1.406(9)Å, C(22)-C(23) = 1.432(10)Å, C(23)-C(24) = 1.400(9)Å, Cr(1)-C(21) = 2.204(7)Å, Cr(1)-C(22) = 2.095(7)Å, Cr(1)-C(23) = 2.083(7)Å, Cr(1)-C(24) = 2.179(7)Å] and angles [C(22)-Cr(1)-C(21) = 38.1(2)°, C(23)-Cr(1)-

C(22) = 40.1(3)°, C(23)-Cr(1)-C(24) = 38.3(2)°, C(22)-Cr(1)-C(24) = 70.0(3)°, C(23)-Cr(1)-C(21) = 69.6(3)°, C(24)-Cr(1)-C(21) = 79.9(3)°] well comparing with those of other Cr butadiene derivatives. The second instead appears to be unusual in the sense that one C-C bond with the terminal C σ–bonded to a Mg cation displays a distance indicative of a C-C single bond [C(17)-C(18) = 1.471(8)Å]. The other two carbon-carbon distances in the same ligand are closer to what would be expected for C-C double bonds [C(18)-C(19) = 1.400(9)Å, C(19)-C(20) = 1.384(8)Å]. In addition, the Cr-C distances to the internal two C atoms of this ligand are relatively short [Cr(1)-C(18) = 2.105(7)Å, Cr(1)-C(19) = 2.088(7)Å]. The NP ligand bridges chromium to magnesium [N(1)-Mg(1)-Cr(1) = 87.06(17)°, P(1)-Mg(1)-Cr(1) = 50.99(6)°]. However, only the P atom is bonded to chromium while both donor atoms are in the bonding range with magnesium [Cr(1)-P(1) = 2.398(2)Å, Mg(1)-N(1) = 2.002(6)Å, Mg(1)-P(1) = 2.733(3)Å]. Two unconnected $[Mg_2Cl_3(THF)_6]^+$ countercations complete the structure.

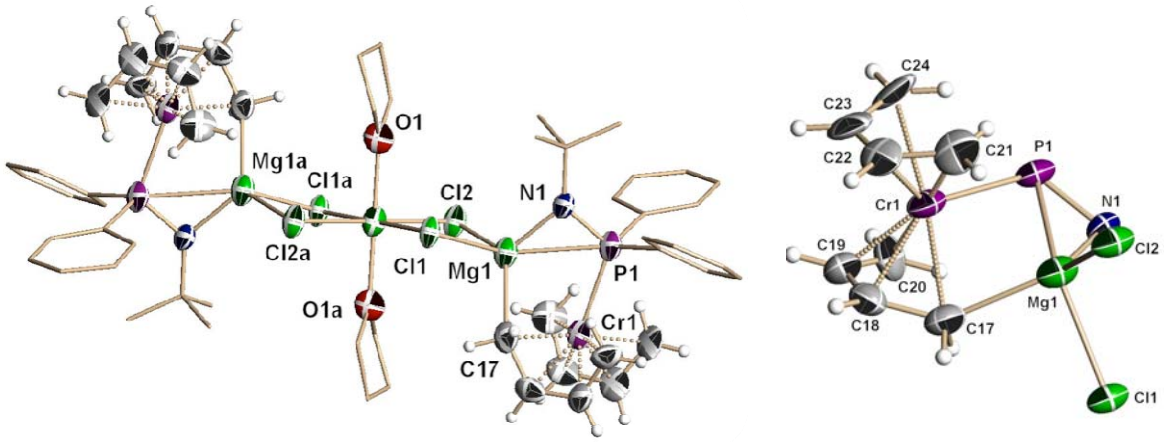

Figure 2.12: (Left) Partial thermal ellipsoids drawing of the di-anionic moiety of complex 2.10 (50 % probability level) and (Right) simplified view of the chromium containing unit. The two {[(THF)$_3$Mg]$_2$(μ-Cl)$_3$} cations have been omitted for clarity.

The hydrogen atoms positions of the two C_4 units were yielded by difference Fourier maps and satisfactorily refined with a minor decrease of the convergence factors and thus lending some credibility to their positions. Optimized structures of simplified, mono-chromium models (η^4-butadiene)Cr(μ,η^4-butadien-di-yl)(μ-Me_2PNMe)Mg(THF)$_2$ and (η^4-butadiene)Cr(μ,η^4-butadien-di-yl)(μ-Me_2PNMe)$MgCl_2^{2-}$ reproduced the observed structural features well and also support the above-mentioned H atom locations (found in the supporting information of reference 43, Figure S-5).[43]

The formation of **2.10** from **2.9** has no simple explanation (Scheme 2.11). We have recently described the utilization of vinyl Grignard for the formation of mono-valent chromium butadiene complexes[53] and butadiene-di-yl derivatives. In the present case, each chromium atom in the dimetallic dianion of **2.10** bears both units.

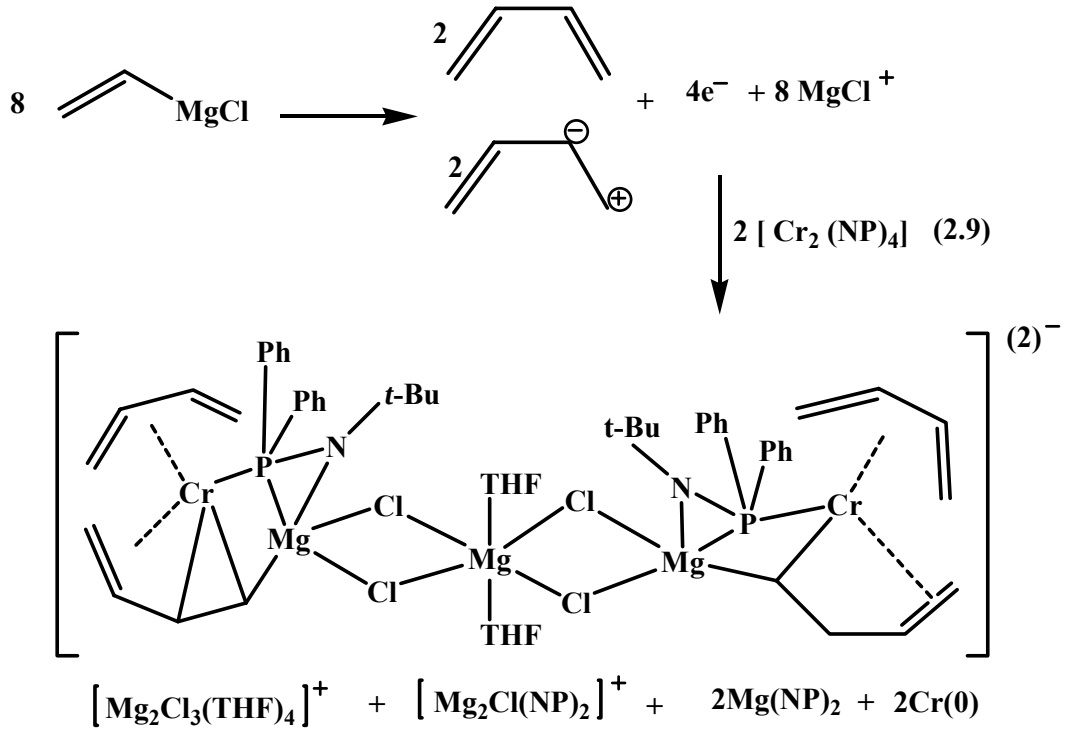

Scheme 2.11: Possible route for the formation of mono-valent chromium butadiene complex 2.10 with vinyl Grignard.

The difference with the previously reported butadiene-di-yl compound is that the two formal negative charges appear to be located on two continuous C atoms rather than on the two terminal ones.[53] The coordination of Mg at the terminal carbon atom is probably responsible for this oddity. In any event, the vinyl coupling generates the electrons necessary for the reduction of the four chromium atoms to the two formally monovalent centers present in **2.10**, and to metallic chromium that unavoidably was observed during the reactions of **2.9** with activators. Due to the lower-than-stoichiometric amount of chlorine, the reaction stoichiometry can be balanced only by assuming that the magnesium countercations may redistribute in the reaction mixture among several species, with only that containing fully chlorinated $[Mg_2Cl_3(THF)_6]^+$ cations being able to crystallize into **2.10**. Incidentally, this could well explain the very low yield and difficulty in reproducing the crystallization. Nonetheless, the structure is of interest given the unprecedented arrangement around the chromium center. Also in agreement with the presence of the formal monovalent state, the complex is a self-activating catalyst exclusively producing 1-hexene under the usual reaction conditions. Different from the activation of **2.9** with vinyl Grignard, no 1–butene has been detected even in traces during the self-activation of **2.10**, consistent with the complex containing only Cr(I).

2.5 Conclusions

In conclusions, the anionic N-P ligand system has shown some interesting and promising behavior by allowing the preparation of a variety of organochromium complexes, assembling unprecedented molecular and polynuclear structures and enabling to elucidate the retention of AlR_x residues. In the series of complexes isolated and characterized in this work, all species showed catalytic behavior. The single component catalytic activity observed in the case of **2.2** is

particularly attractive given that this sort of behavior is exceedingly rare in chromium chemistry.[8] The lack of single-component behavior for **2.3** and **2.4** is likely to be due to the presence of chlorine, building in these complexes robust bridges between the Al and Cr atoms. The outstanding activity observed for some of these species as S-F oligomerization catalysts is useful especially when, as in the cases of **2.6** and **2.8**, no high molecular weight polymeric byproducts are formed. The limited formation of 1-hexene in some of the runs, as the only oligomer detectable besides the polymer, is clearly due to the predominant stability of the divalent oxidation state, which allows in this case only limited accessibility to the monovalent state responsible for the selective trimerization. The transformation of the trivalent **2.7** into the divalent **2.2** and **2.8** upon exposure to the aluminum alkyl activators also reiterates the greater stability of the divalent state for these species. Instead, the switching of catalytic behavior from trimerization to an occasionally potent nonselective oligomerization catalyst is likely the result of diproportionation toward the divalent state. Even though this seems to be contradicted by the ease of the reduction of the trivalent organochromium derivatives as discussed above, previous mechanistic work on a highly performing trimerization system[37a] has clearly indicated the existence of the redox dynamism via continuous reduction and reoxidation of the chromium catalytic center during the catalytic cycle. The almost ubiquitous presence of polymer besides either 1-hexene or the S-F distribution of oligomers is again an indication that the three oxidation states, responsible for each of these three processes, may coexist or rapidly interconvert in the catalytic mixture. The change of solvent from toluene to methylcyclohexane transformed these catalytic systems into selective trimerization catalysts, producing in some case significant amounts of 1-hexene.

We have herein also reported the isolation and full characterization of a Cr(I)/Cr(II) mixed valence derivative of the anionic NP ligand. As expected for a reduced species, this complex is a self-activating catalyst. DFT calculations supported the idea that the monovalent species generates 1-hexene and 1-butene to lesser extent, while the divalent unit is likely to be responsible for 1-butene through a different mechanism. The ability of activators to switch the behavior from polymerization to selective tri- or dimerization is in agreement is just the result of their ability to trigger the chromium redox dynamism. [8a,c,12,37a]

In the next chapter the anionic N-P ligand system was further modified by replacing the acidic proton in the ligand frame with an additional alkyl and used the corresponding R_2NPPh_2 ligand to further evaluate the effect of ligand charge on catalytic performances.

References

1. a) Reagan, W. K. (Phillips Petroleum Company)EP 0417477, **1991**. b) Tanaka, E.; Urata, H.; Oshiki, T.; Aoshima, T.; Kawashima, R.; Iwade, S.; Nakamura, H.; Katsuki, S.; Okanu, T. (Mitsubishi Chemical Corporation) EP 0611743, **1994**. c) Wu, F. J. (Amoco Corporation) US 5811618, **1998**. d) Yoshida, T.; Yamamoto, T.; Okada, H.; Murakita, H. (Tosoh Corporation) US2002/0035029, **2002**. e) Grove, J. J. C.; Mahome, H. A.; Griesel, L. (Sasol Technology) WO 03/004158, **2002**.
2. a) K€ohn, R. D.; Haufe, M.; Kociok-K€ohn, G.; Grimm, S.; Wasserscheid, P.; Keim, W. *Angew. Chem., Int. Ed*. **2000**, *39*, 4337. b) K€ohn, R. D.; Smith, D.; Mahon, M. F.; Prinz, M.; Mihan, S.; Kociok-K€ohn, G. *J. Organomet. Chem*. **2003**, *683*, 200.
3. Carter, A.; Cohen, S. A.; Cooley, N. A.; Murphy, A.; Scutt, J.; Wass, D. F. *Chem. Commun*. **2002**, 858.
4. a) McGuinness, D. S.; Wasserscheid, P.; Keim, W.; Hu, C.; Englert, U.; Dixon, J. T.; Grove, C. *Chem. Commun*. **2003**, 334. b) McGuinness, D. S.;Wasserscheid, P.; Keim,W.; Morgan, D. H.; Dixon, J. T.; Bollmann, A.; Maumela, H.; Hess, F. M.; Englert, U. *J. Am. Chem. Soc.* **2003**, *125*, 5272. c) McGuinness, D. S.; Wasserscheid, P.; Morgan, D. H.; Dixon, J. T. *Organometallics* **2005**, *24*, 552.
5. a) Morgan, D. H.; Schwikkard, S. L.; Dixon, J. T.; Nair, J. J.; Hunter, R. Adv. *Synth. Catal*. **2003**, *345*, 939. b) Mahomed, H. A.; Bollmann, A.; Dixon, J. T.; Gokul, V.; Griesel, L.; Grove, J. J. C.; Hess, F.; Maumela, H.; Pepler, L. *Appl. Catal., A* **2003**, *225*, 355.
6. Bluhm, M. E.; Walter, O.;D€oring, M. *J. Organomet. Chem*. **2005**, *690*, 713.
7. Nenu, C. N.; Weckhuysen, B. M. *Chem. Commun*. **2005**, 1865.
8. a) Temple, C.; Jabri, A.; Crewdson, P.; Gambarotta, S.; Korobkov, I.; Duchateau, R. *Angew.*

Chem., Int. Ed. **2006,** *45*, 7050. b) Albahily, K.; Koc, E.; Al-Baldawi, D.; Savard, D.; Gambarotta, S.; Burchell, T. J.; Duchateau, R. *Angew. Chem., Int. Ed.* **2008,** *47,* 5816. c) Jabri, A.; Mason,C.B.; Sim,Y.; Gambarotta, S.; Burchell, T. J.; Duchateau, R. *Angew. Chem., Int. Ed.* **2008**, *47*, 9717. d) Vidyaratna, I.; Nikiforov, G. B.; Gorelsky, S. I.; Gambarotta, S.; Duchateau, R.; Korobkov, I. *Angew. Chem., Int. Ed*. **2009**, *48*, 6552.

9. a) Zhang, J.; Braunstein, P.; Hor, T. S. A. *Organometallics* **2008**, *27*, 4277. b) Zhang, J.; Li, A.; Hor, T. S. A. *Organometallics* **2009**, *28*, 2935.
10. Klemps, C.; Payet, E.; Magna, L.; Saussine, L.; Le Goff, X. F.; Le Floch, P. *Chem.;Eur. J.* **2009**, *15*, 8259.
11. a) Bollmann, A.; Blann, K.; Dixon, J. T.; Hess, F. M.; Killian, E.; Maumela, H.; McGuinness, D. S.; Morgan, D. M.; Neveling, A.; Otto, S.; Overett, M.; Slawin, A. M. Z.; Wasserscheid, P.; Kuhlman, S. *J. Am. Chem. Soc*. **2004**, *126*, 14712. b) Blann, K.; Bolmann, A.; Dixon, J. T.; Hess, F.; Kilian, E.; Maumela, H.; Morgan, D. H.; Neveling, A.; Otto, S.; Overett, M. *Chem. Commun*. **2005**, 620. c) Blann, K.; Bollmann, A.; Dixon, J. T.; Hess, F. M.; Killian, E.; Maumela, H.; Morgan, D. H.; Neveling, A.; Otto, S.; Overett, M. *J. Chem. Commun*. **2005**, 622. d) Overett, M. J.; Blann, K.; Bollmann, A.; Dixon, J. T.; Haasbroek, D.; Killian, E.; Maumela, H.; McGuinness, D. S.; Morgan, D. H. *J. Am. Chem. Soc.* **2005**, *127*, 10723. e) Kuhlmann, S.; Blann, K.; Bollmann, A.; Dixon, J. T.; Killian, E.; Maumela, M. C.; Maumela, H.; Morgan, D. H.; Pr_etorius, M.; Taccardi, N.; Wasserscheid, P. *J. Catal.* **2006**, *245*, 279. f) Walsh, R.; Morgan, D. H.; Bollmann, A.; Dixon, J. T. *Appl. Catal. A*: Gen. **2006**, *306*, 184. g) Kuhlmann, S.; Dixon, J. T.; Haumann, M.; Morgan, D. H.; Ofili, J.; Spuhl, O.; Taccardi, N.; Wasserscheid, P. *Adv. Synth. Catal.***2006**, *348*, 1200. h) Kuhlmann, S.; Blann, K.; Bollmann, A.; Dixon, J.

T.; Killian, E.; Maumela, M. C.; Maumela, H.; Morgan, D. H.; Pretorius, M.; Taccardi, N.; Wasserscheid, P. *J. Catal*. **2007**, *245*, 279. i) Killian, E.; Blann, K.; Bollmann, A.; Dixon, J. T.; Kuhlmann, S.; Maumela, M. C.; Maumela, H.; Morgan, D. H.; Nongodlwana, P.; Overett, M. J.; Pretorius, M.; H€ofener, K.; Wasserscheid, P. J. *Mol. Catal. A: Chem*. **2007**, *270*, 214. j) McGuinness, D. S.; Overett, M.; Tooze, R. P.; Blann, K.; Dixon, J. T.; Slawin, A. M. Z. *Organometallics* **2007**, *26*, 1108.

12. Jabri, A.; Crewdson, P.; Gambarotta, S.; Korobkov, I.; Duchateau, R. *Organometallics* **2006**, *25*, 715.
13. Han, T.K.; Ok, M. A.; Chae, S. S.; Kang, S. O. (SK Energy Corporation) WO 2008/088178, 2008.
14. Greiner, E.; Gubler, R.; Inoguchi, Y. Linear Alpha Olefins, CEH Marketing Research Report, *Chemical Economics Handbook*; *SRI International: Menlo Park,* CA, May **2004**.
15. a) Tomov, A. K.; Chirinos, J. J.; Long, R. J.; Gibson, V. C.; Elsegood, M. R. J. *J. Am. Chem. Soc.* **2006**, *128*, 7704. b) Tomov, A. K.; Chirinos, J. J.; Long, R. J.; Gibson, V. C. *J. Am. Chem. Soc.* **2005**, *127*, 10166.
16. a) Crewdson, P.; Gambarotta, S.; Djoman, M.-C.; Korobkov, I.; Duchateau, R. Organometallics **2005**, *24*, 5214. b) Albahily, K.; Koc, E.; Al-Baldawi, D.; Savard, D.; Gambarotta, S.; Burchell, T. J.; Duchateau, R. *Angew. Chem., Int. Ed.* **2008**, *47*, 5816.
17. McGuinness,D. S.; Suttil, J. A.; Gardiner,M. G.; Davies, N. W. Organometallics **2008**, *27*, 4238.
18. Kirillov, E.; Roisnel, T.; Razavi, A.; Carpentier, J.-F. *Organometallics* **2009**, *28*, 2401.
19. a) Hogan, J. P.; Banks, R. L. (Phillips Petroleum Co.) U.S. Patent 2,825,721, **1958**. b) Karapinka, G. L. (Union Carbide Corp.) Ger. Offen. DE 1,808,388, **1970**. c) Karol, F. J.;

Karapinka, G. L.; Wu, C.; Dow, A. W.; Johnson, R. N.; Carrick, W. L. *J. Polym. Sci*., *Polym. Chem. Ed*. **1972**, *10*, 2621. d) Karapinka, G. L. (Union Carbide Corp.) U.S. Patent 3,709,853, **1973**.

20. a) MacAdams, L. A.; Buffone, G. P.; Incarvito, C. D.; Rheingold, A. L.; Theopold, K. H. *J. Am. Chem. Soc*. **2005**, *127*, 1082. b) Theopold, K. H. *Eur. J. Inorg. Chem*. **1998**, *15*. c) Bhandari, G.; Kim,Y.; McFarland, J. M.; Rheingold, A. L.; Theopold, K. H. *Organometallics* **1995**,*14*, 738. d) MacAdams, L. A.; Kim,W. K.; Liable-Sands, L. M.; Guzei, I. A.; Rheingold, A. L.; Theopold, K. H. *Organometallics* **2002**, *21*, 952.
21. D€ohring, A.; Gohre, J.; Jolly, P. W.; Kryger, B.; Rust, J.; Verhovnik, G. P. J. Organometallics **2000**, *19*, 388.
22. a) Rogers, J. S.; Bu, X. H.; Bazan, G. C. *Chem. Commun*. **2000**, 1209. b) Bazan, G. C.; Rogers, J. S.; Fang, C. C. *Organometallics* **2001**, *20*, 2059.
23. Enders, M.; Fernandez, P.; Ludwig, G.; Pritzkow, H. *Organometallics* **2001**, *20*, 5005.
24. a) Gibson, V. C.; Maddox, P. J.; Newton, C.; Redshaw, C.; Solan, G. A.; White, A. J. P.; Williams, D. J. *Chem. Commun*. **1998**, 1651. b) Gibson, V. C.; Mastroianni, S.; Newton, C.; Redshaw, C.; Solan, G. A.; White, A. J. P.; Williams, D. J. *Dalton Trans*. **2000**,1969.
25. Esteruelas, M. A.; Lopoez, A. M.; Mendez, L.; Olivan, M.; Onate, E. *Organometallics* **2003**, *22*, 395.
26. Vidyaratne, I.; Scott, J.; Gambarotta, S.; Duchateau, R. *Organometallics* **2007**, *26*, 3201.
27. a) McDermott, J. X.; White, J. F.; Whitesides, G. M. *J. Am. Chem. Soc*. **1973,** *95*, 4451. b) McDermott, X.; White, J. F.; Whitesides, G. M. *J. Am. Chem. Soc*. **1976**, *98*, 6521.
28. Manyik, R.M.; Walker, W. E.; Wilson, T. P. *J. Catal*. **1977**, *47*, 97.
29. Briggs, J. R. *Chem. Commun*. **1989**, *11*, 674.

30. Meijboom, N.; Schaverien, C. J.; Orpen, A. G. *Organometallics* **1990**, *9*, 774.

31. Emrich, R.; Heinemann, O.; Jolly, P. W.; Kr€uger, C.; Verhovnik, G. P. J. *Organometallics* **1997**, *16*, 544.

32. a) Blok, A. N. J.; Budzelaar, P. H. M.; Gal, A. W. *Organometallics* **2003**, *22*, 2564. b) Tobisch, S.; Ziegler, T. *Organometallics* **2003**, *22*, 5392. c) Tobisch, S.; Ziegler, T. *J. Am. Chem. Soc*. **2004,** *126*, 9059. d) Van Rensburg, W. J.; Grove, C.; Seynberg, J. P.; Stark, K. B.; Huyser, J. J.; Steynberg, P. J. *Organometallics* **2004**, *23*, 1207.

33. a) Agapie, T.; Schofer, S. J.; Labinger, J. A.; Bercaw, J. E. *J. Am.Chem. Soc*. **2004**, *126*, 1304. b) Agapie, T.; Day, M. W.; Henling, L. M.; Labinger, J. A.; Bercaw, J. E. *Organometallics* **2006**, *25*, 2733. c) Agapie, T.; Labinger, J. A.; Bercaw, J. E. *J. Am. Chem. Soc.* **2007**, *129*, 14281. d) Schofer, S. J.; Day, M.W.; Henling, L. M.; Labinger, J. A.; Bercaw, J. E. *Organometallics* **2006**, *25*, 2743.

34. Tomov, A. K.; Chirinos, J. J.; Jones, D. J.; Long, R. J.; Gibson, V. C. *J. Am. Chem. Soc*. **2005**, *127*, 10166.

35. a) Cossee, P. J. Catal. **1964**, *3*, 80. b) Arlman, E. J.; Cossee, P. *J. Catal*. **1964**, *3*, 99. c) Skupinska, *J. Chem. Rev*. **1991**, *91*, 613.

36. Rucklidge, A. J.; McGuinness, D. S.; Tooze, R. P.; Slawin, A. M. Z.; Pelletier, J. D. A.; Hanton, M. J.; Webb, P. B. *Organometallics* **2007,** *26*, 2782.

37. a) Jabri, A.; Temple, C.; Crewdson, P.; Gambarotta, S.; Korobkov, I.; Duchateau, R. *J. Am. Chem. Soc*. **2006**, *128*, 9238.

38. a) Peitz, S.; Peulecke, N.; Aluri, B. P.; Hansen, S.; Muller, B. H.; Spannenberg, A.; Rosenthal, U.; Al-Hazmi, M. H.; Mosa, F. M.; Wohl, A.; Muller, W. *Eur. J. Inorg. Chem*. **2010**, 1167. b) Wohl, A.; Muller, W. Peitz, S.; Peulecke, N.; Aluri, B. P.; Muller, B. H.;

Heller, D.; Rosenthal, U.; Al-Hazmi, M. H.; Mosa, F. M. *Chem. Eur. J*. **2010**, *16*, 7837. c) Peitz, S.; Peulecke, N.; Aluri, B. P.; Muller, B. H.; Spannenberg, A.; Rosenthal, U.; Al-Hazmi, M. H.; Mosa, F. M.; Wohl, A.; Muller, W. *Organometallics* **2010**, *29,* 5263. d) Muller, W.; Wohl, A.; Peitz, S.; Peulecke, N.; Aluri, B. P.; Muller, B. H.; Heller, D.; Rosenthal, U.; Al-Hazmi,M. H.; Mosa, F. M. *Dalton Trans*. **2010**, 7911. e) Peulecke, N.; Muller, W.; Peitz, S.; Aluri, B. P.; Rosenthal, U.; Wohl, A.; Muller, B. H.; Al-Hazmi, M. H.; Mosa, F. M. *Chem.Cat.Chem*, **2010**, *2*, 1079.

39. a) K€ohler, F. H.; Prossdorf, W. Z. *Naturforsch.* **1977**, *32*, 1026. b) Kern, R. J. *J. Inorg. Nucl. Chem.* **1962**, *24*, 1105.
40. a) Cotton, F. A.; Walton, R. A. *Metal-metal Multiple bonds in dinuclear clusters. Struct. Bonding (Berlin)* **1985**, *62*, 1. b) Horvath, S.; Gorelsky, S. I.; Gambarotta, S.; Korobkov, I. *Angew. Chem., Int. Ed*. **2008**, *47*, 9937, and references therein.
41. Ruppa, K. B. P.; Feghali, K.; Kovacs, I.; Aparna, K.; Gambarotta, S.; Yap, G. P.A.; Bensimon, C. *Dalton Trans*. **1998**, 1595, and references therein.
42. Reardon, D.; Kovacs, I.; Ruppa, K. B. P.; Feghali, K.; Gambarotta, S.; Petersen, *J. Chemistry, Eur. J.* **1997**, *3*, 1482.
43. Thapa, I.; Gambarotta, S.; Korobkov, I.; Murugesu, M.; Budzelaar, P. *Organometallics* **2012***, 31*(1), 486.
44. a) Ahlrichs, R.; Bär, M.; Baron, H.-P.; Bauernschmitt, R.; Böcker, S.; Ehrig, M.; Eichkorn, K.; Elliott, S.; Furche, F.; Haase, F.; Häser, M.; Hättig, C.; Horn, H.; Huber, C.; Huniar, U.; Kattannek, M.; Köhn, A.; Kölmel, C.; Kollwitz, M.; May, K.; Ochsenfeld, C.; Ohm, H.; Schäfer, A.; Schneider, U.; Treutler, O.; Tsereteli, K.; Unterreiner, B.; Von Arnim, M.; Weigend, F.; Weis, P.; Weiss, H.

Turbomole, 5 ed., *Theoretical Chemistry Group, University of Karlsruhe,* **2002.**

b) Treutler, O.; Ahlrichs, R. *J. Chem. Phys*. **1995**, *102*, 346.

45. a) Baker, J. *J. Comput. Chem.* **1986**, *7*, 385. b) Baker, J. PQS, 2.4 ed., *Parallel Quantum Solutions,* Fayetteville, AR, **2001**.

46. a) Becke, A.D. *J. Chem. Phys*. **1993**, *98*, 5648. b) Becke, A.D. *J. Chem. Phys.* **1993**, *98*, 1372. c) Lee, C.T.; Yang, W.T.; Parr, R.G. *Phys. Rev.* B **1988**, 37, 785.

47. Schafer, A.; Huber, C.; Ahlrichs, R. *J. Chem. Phys.* **1994**, *100*, 5829.

48. a) Raucoules, R.; de Bruin, T.; Raybaud, P.; Adamo, C. *Organometallics* **2009**, *28*, 5358. b) Tobisch, S.; Ziegler, T. *J. Am. Chem. Soc*. **2004**, *126*, 9059.

49. Weigend, F.; Furche, F.; Ahlrichs, R. *J. Chem. Phys.* **2003**, *119*, 12753.

50. Schafer, A.; Horn, H.; Ahlrichs, R. *J. Chem. Phys.* **1992**, *97*, 2571.

51. Schaftenaar, G.; Noordik, J.H. *J. Comput. Aid. Mol. Des.* **2000**, *14*, 123.

52. The unrestricted calculation result has Cr(I) with 1 α and 4 β electrons, and Cr(II) with 4 α electrons. This is likely an artifact of the use of a single determinant instead of a well-defined spin state.

53. a) Albahily, K.; Shaikh, Y.; Sebastiao, E.; Gambarotta, S.; Korobkov, I.; Gorelsky, S. *J. Am. Chem. Soc.* **2011**, *133*, 6388. b) Albahily. K.; Fomitcheva, V.; Gambarotta, S.; Korobkov, I.; Murugesu, M.; Gorelski, S. *J. Am. Chem. Soc*. **2011**, *133*, 638.

Publications:

1) **Thapa, I**.; Gambarotta, S.; Descour, C.; Duchateau, R. *Organometallics* (Submission in process)
2) **Thapa, I**.; Doiseau, A. C; Gambarotta, S.; Korobkov, I. *Organometallics* (Submitted)

Selective Ethylene Tetramerization based on a $Cr(R_2NPPh_2)$ Catalytic System.

3.1 Introduction

Catalytic ethylene oligomerization is an industrially useful process for which we have today a reasonably deep level of understanding.[1] Apart from dimerization, the majority of oligomerization catalytic systems are based on chromium[2] and highly active systems are used for the commercial production of LAO.[3] Even the technical problem of unwanted formation of polymeric materials fouling the reactors has been solved with the judicious selection of the appropriate ligand systems and stabilization of chromium oxidation state.[4] However, introducing selectivity in the catalytic cycle remains challenging even though a few highly active and selective trimerization systems have been established.[5] The mechanism of the reaction is well known[6] and the isolation and characterization of intermediates of the catalytic cycles has allowed to identify the metal oxidation state in turn enabling to target efforts aiming at the preparation of new catalytic systems.[7]

Ethylene tetramerization remains instead indefinable compared to trimerization. The Sasol[8] and the SK-Energy[9] processes produce 1-octene with unsurpassed activity although the selectivity remains only in the range of 70%. The moderate selectivity of these systems contrasts with the trimerization where formation of 1-hexene polymer-free may reach near to quantitative levels.[10] This striking discrepancy is likely to be ascribed to the ring expansion mechanism believed to operate also for tetramerization. In fact, very high selectivity of the reductive elimination is unlikely to be achieved when rings have tendency to expand over the seven-membered. The Rosenthal's bimetallic proposal[11] is a fascinating working hypothesis to solve the impasse. Although the mechanism was never substantiated by kinetic, theoretical or synthetic work, it has guided the discovery of two tetramerization systems of high selectivity.[12] Common characteristic among these two systems was in fact the utilization of ligands with dinucleating ability. Regrettably, the moderate activity and formation of polymeric material (in one case the major product) make these systems unsuitable for commercial purposes. On the other hand, these results indicate that very high selectivity is indeed achievable for tetramerization. Hence, we are multiplying our efforts for the systematic analysis of ligand features that may help the refinement of tetramerization catalysts.

Ligands containing nitrogen and phosphorus donor atoms and especially those with a direct N-P bond seems to be versatile for introducing selectivity in the oligomerization cycle,[5] including tetramerization.[8,12] Ligands belonging to the NP family are abundant and provide the advantage of easy and large scale preparation as well as the fine-tuning of the steric features.[13] We observe that in the four existing tetramerization systems, including the Sasol and SK-Energy's, the ligands lack the anionic charge that is

often (but not necessarily) present in ligands used for ethylene trimerization or non-selective oligomerization. Our recent work on [R(H)N-PPh_2], (as mentioned in the previous chapter 2) the simplest member of this family of ligands, has highlighted its main characteristics.[14] Firstly, they support a variety of polynuclear structures, from dimeric to tetrameric, showing an enhanced tendency to retain aluminate activators.[14] Secondly, they may sufficiently stabilize the monovalent state which has been conclusively linked to the selectivity of the oligomerization process.[15] Yet, no tetramerization activity has been determined for these derivatives. Therefore, we have now replaced the acidic proton in the ligand frame with an additional alkyl and used the corresponding R_2NPPh_2.

Herein we report a catalytic tetramerization system, closely related to the previously reported trimerization and non-selective systems which, albeit with moderate activity, displays selectivity over 90%.

3.2 Experimental Section:

All reactions were carried out under a dry nitrogen atmosphere. Solvents were dried using an aluminum oxide solvent purification system. Elemental analyses were carried out with a Perkin-Elmer 2400 CHN analyzer. Samples for magnetic susceptibility were weighed inside a dry box equipped with an analytical balance and sealed into calibrated tubes and measurements were carried out with a Johnson Matthey Magnetic Susceptibility balance at room temperature. Data for X-ray crystal structure determination were obtained with a Bruker diffractometer equipped with a 1K Smart CCD area detector. Mass spectra were recorded on a Micromass Quattro-LC

Electrospray-Triple Quadrupole Mass Spectrometer. MAO (10% wt, Aldrich), Me_3Al, MMAO (7% wt) and $Al(Et)_3$ (Strem) were used as received. DMAO was prepared by pumping *in vacuo* solution of MAO for three days and under moderate heating. NMR solutions were checked for eventual and residual presence of TMA. $CrCl_3(THF)_3$ and $CrCl_2(THF)_2$ were prepared according to standard procedures. The NP and (pyridine)-NP ligands were prepared according to published procedures[16].

3.2.1 Preparation of $(Me)_2NP(Ph)_2$ (1)

Lithium salt of dimethyl amido was prepared according to the published procedure. To the lithium salt (1 g, 19.6 mmol) in dry THF (15 mL) at 0 ^oC added dropwise chlorodiphenylphosphine (3.6 mL, 19.6 mmol) under nitrogen atmosphere and allowed to stir at room temperature for further 18 hours. Lithium chloride was separated out from filtration. The filtrate was concentrated to a small volume under reduced pressure. The title compound was isolated from the resulting solution as analytically pure viscous oil (4.4 g, 19.2 mmol, 98%).

^{1}H-NMR (300 MHz, $CDCl_3$, 25°C) δ: 7.39 – 7.37 (10H, m), 2.64 (6H, d, J = 9.6 Hz).

^{13}C{1H}-NMR (300 MHz, $CDCl_3$, 25°C) δ: 132.0, 131.8, 128.3, 128.1, 128.0, 41.9, 41.7.

^{31}P{H}-NMR δ: 61.6. EI-MS Calcd. for $C_{14}H_{16}NP$: m/z = 229.10 (M^+), Found 229.1.

3.2.2 Preparation of $(Et)_2NP(Ph)_2$ (2)

A solution of diethylamine, Et_2NH (4.15 mL, 59.5 mmol) in dry tetrahydrofuran (100 mL) was cooled to 0 ^oC and treated dropwise with chlorodiphenylphosphine (5 mL, 27 mmol) under nitrogen. White precipitate of Et_2NH_2Cl immediately separated out. The reaction mixture was allowed to warm up to room temperature and stirred for 48 hours.

The ammonium salt was separated by filtration and the resulting solution was concentrated to small volume under reduced pressure. The title compound was isolated from the resulting solution as an analytically pure viscus oil (6.7 g, 26.0 mmol, 96.5%). ^{1}H-NMR (300 MHz, $CDCl_3$, 25°C) δ: 7.48 (4H, m), 7.37 (6H, m), 3.14 (4H, m), 1.01 (6H, t, J = 6.9 Hz). ^{13}C{1H}-NMR (300 MHz, $CDCl_3$, 25°C) δ: 140.3, 140.1, 131.9, 131.7, 128.0, 127.9, 127.9, 44.4, 44.2, 14.5, 14.5. ^{31}P{H}-NMR δ: 58.4. EI-MS Calcd. for $C_{16}H_{20}NP$: m/z = 257.13 (M^+), Found 257.1.

3.2.3 Preparation of (*i*-pr)$_2$NP(Ph)$_2$ (3)

A solution of diisopropylamine (*i*-pr)$_2$NH (17.5 mL, 123.9 mmol) in dry THF (100 mL) was cooled to (0 ^{o}C) and treated dropwise with chlorodiphenylphosphine (10 mL, 53.9 mmol) under nitrogen. White precipitate of (*i*-pr)$_2$NH$_2$Cl immediately separated out. The reaction mixture was allowed to warm up to room temperature and stirred for 72 hours. The ammonium salt was separated by filtration and the resulting solution was washed with dry diethylether (20 mL) concentrated to small volume under reduced pressure to isolate an analytically pure title compound (14 g, 49.0 mmol, 91%).

^{1}H-NMR (300 MHz $CDCl_3$, 25°C) δ: 7.77 (4H, m), 7.34 (6H, m), 3.46 (2H, septet), 1.23(12H, d, J = 6.6 Hz). ^{13}C{1H}-NMR (300 MHz $CDCl_3$, 25°C) δ: 141.1, 140.9, 132.6, 132.4, 47.5, 47.3, 23.7, 23.6. ^{31}P{H}-NMR δ: 35.1. EI-MS Calcd. for $C_{18}H_{24}NP$: m/z = 285.16 (M^+), Found 285.1.

3.2.4 Preparation of (Ph)$_2$NP(Ph)$_2$ (4)

Title compound was synthesized in an analytically pure solid by using corresponding amine (5 g, 29.5 mmol), triethylamine (4.4 mL, 32.4 mmol) and

diphenylchlorophosphine (5.4 mL, 29.5 mmol) from the above mentioned procedure (9.4 g, 26.5 mmol, 90%). ^{1}H-NMR (300 MHz, $CDCl_3$, 25°C) δ: 7.40 (4H, m), 7.29 (6H, m), 7.12 (5H, m), 7.00 (5H, m). ^{13}C{1H}-NMR (300 MHz, $CDCl_3$, 25°C) δ: 132.7, 132.4, 129.3, 128.8, 128.1, 128.0, 124.4, 124.3, 122.8, 120.9, 117.7. ^{31}P{H}-NMR δ: 51.5. EI-MS Calcd. for $C_{24}H_{20}NP$: *m/z* = 353.13 (M^+), Found 353.1.

3.2.5 Preparation of $(Et)_2NP(i\text{-}pr)_2$ (5)

Title compound was synthesized in an analytically pure oil by using corresponding amine (6.1 mL, 59.5 mmol), and diisopropylchlorophosphine (4.3 mL, 27 mmol) from the above mentioned procedure (4.6 g, 24.5 mmol, 91%). ^{1}H-NMR (300 MHz, $CDCl_3$, 25°C) δ: 2.93 (4H, m), 1.79 (2H, m), 1.01 (18H, m). ^{13}C{1H}-NMR (300 MHz, $CDCl_3$, 25°C) δ: 45.4, 45.3, 27.5, 27.1, 21.0, 20.0, 16.2 16.0. ^{31}P{H}-NMR δ: 80.0. EI-MS Calcd. for $C_{10}H_{24}NP$: *m/z* = 189.13 (M^+), Found 189.1.

3.2.6 Preparation of complex (1)-$CrCl_3$(THF) (3.1)

Ligand **1** (0.229 g, 1 mmol) was mixed with $CrCl_3(THF)_3$ (0.188 g, 0.5 mmol) in toluene (5 mL) at room temperature and continue stirring for further 18 hours. To the resulting brown solution added hexane (2 mL) affording brown precipitate. The solid was filtered, washed and dried in *vacuo* to obtain **(1)-$CrCl_3$ (THF)** as brown solid (0.16 g, 0.35 mmol, 70%). ESI-MS Calcd. for $C_{18}H_{24}Cl_3CrNPO$: *m/z* = 458.01(M^+), Found 550.01 $[M+tol]^+$, 389.95 $[M+2H\text{-}THF]^+$.

3.2.7 Preparation of (2)-[CrCl] (3.2)

Ligand **2** (0.257 g, 1 mmol) was mixed with $CrCl_3(THF)_3$ (0.188 g, 0.5 mmol) in toluene and heated to the boiling while stirring until all the solvent was evaporated resulting brown solid which was then washed with hexane followed by toluene to get the pure material (0.188 g, 0.2 mmol, 40%). ESI-MS Calcd. for $C_{48}H_{60}Cl_2Cr_2N_3P_3$: *m/z* = 945.22 ($M^+$), (assignment, rel. intensity %) Found: 944.4 {$[M-H]^+$ 1.67}, 875.55 {$[M-2Cl]^+$ 1.27}, 799.44 {$[M-2Cl-C_6H_4]^+$ 100.00}.

3.2.8 Preparation of complex (3)-$CrCl_3$ (THF) (3.3)

Identical procedure as described for **3.2** and amount as above were used affording **(3)-$CrCl_3$ (THF)** brown solid (0.113 g, 0.22 mmol, 44%). ESI-MS Calcd. for $C_{22}H_{32}NPCrCl_3O$: *m/z* = 516.07 (M^+), Found 426.94 $[M-2Cl-CH_3-3H]^+$.

3.2.9 Preparation of (4)-$CrCl_3$ (THF) (3.4)

Identical procedure as described for **3.2** and amount as above were used affording **(4)-$CrCl_3$ (THF)** as brown solid (0.110 g, 0.19 mmol, 38%). ESI-MS Calcd. for $C_{28}H_{28}Cl_3CrNPO$: *m/z* = 582.04 (M^+), Found 513.73 $[M-THF+2H]^+$.

3.2.10 Preparation of (5)-$CrCl_3$(THF) (3.5)

Identical procedure as described for **3.2** and amount as above were used affording **(5)-$CrCl_3$(THF)** as brown solid (0.08 g, 0.19 mmol, 38%). ESI-MS Calcd. for $C_{14}H_{32}Cl_3CrNPO$: *m/z* = 420.07 (M^+), Found 554.54 $[M+ tol + C_3H_7]^+$.

3.2.11 Preparation of {[(2-pyridine)N(Me)PPh$_2$]CrCl$_2$}$_2$(μ-Cl)$_2$ (3.6)

A solution of (2-Pyridine)N(Me)P(Ph)$_2$ (0.292 g, 1 mmol) in THF (15 mL) was combined with a suspension of $CrCl_3$ (THF)$_3$ (0.376 g, 1 mmol,) in THF (5 mL). Stirring was continued for 18 hrs. Solvent was evaporated resulting the blue solid residue which was washed with hexane, dried in *vacuo* (0.44 g, 0.49 mmol, 49%). Elemental Analysis Calcd. (Found) for $C_{36}H_{34}Cr_2Cl_6N_4P_4$: C 44.89 (44.78), H 3.56 (3.49), N 5.82 (5.87). ESI-MS Calcd. 899.92 (M^+), Found (*m/z*, ret. intensity) = {900, 65.81; 899, 21.21; 387, 100 $[M/2 -3Cl+C_2H_4N]^+$ }. [μ_{eff} = 3.12 μ_B].

3.2.12 Preparation of {[(2-pyridine)N(Me)PPh$_2$]CrCl$_3$(NCCH$_3$)} (3.7)

Blue paramagnetic X-ray quality crystals were isolated upon cooling the blue clear acetonitrile solution of **3.6** (0.1 g, 0.11 mmol) at -20 ^oC for overnight. The analytically pure crystals were obtained by filtering, washing with cold hexane and dried under *vacuo* to yield (0.053 g, 0.1 mmol, 99%). Elemental Analysis Calcd. (Found) for C_{22} H_{23} Cl_3 Cr N_4 P: C 49.60 (49.52), H 4.35 (4.28), N 10.52 (10.50). [μ_{eff} =3.85 μ_B].

3.2.13 Preparation of {[(2-pyridine)N(Me)PPh$_2$]CrCl$_3$[(2-pyridine)N(Me)H]}. {(CH$_3$CN). (CH$_2$Cl$_2$)} (3.8)

To the blue powder of **3.6** (0.1 g, 0.1 mmol) added dichloromethane (3 ml) and acetonitrile drop wise until all the blue suspension dissolved resulting a clear blue solution. Blue X-ray quality crystals were formed upon cooling the blue solution at -25 ^oC for 7 days resulting paramagnetic crystals of **3.8** which were collected, filtered, washed with cold hexane and dried in *vacuo* (0.06 g, 0.05 mmol, 50% yield). Elemental

Analysis Calcd. (Found) for $C_{50.75}H_{54.50}Cl_{7.50}Cr_2N_9P_2$: C 49.87(49.78), H4.49 (4.32), N 10.31(10.28). [μ_{eff} = 3.80 μ_B].

3.2.14 Preparation of {[(2-pyridine)N(Me)PPh$_2$]Cr}$_2$(μ-Cl)$_2$][AlCl$_3$Et]$_2$ (3.9)

Method A

A solution of (2-Pyridine)N(Me)P(Ph)$_2$ (0.292 g, 1 mmol) in toluene (5 mL) was combined with a suspension of $CrCl_2(THF)_2$ (0.27 g, 1 mmol) in toluene (5 mL), followed by the addition of neat diethylaluminium chloride (0.6 g, 5 mmol). Stirring was continued at room temperature for 5 minutes. Blue X-ray quality crystals were formed upon cooling the resulting solution at -35 ^oC for 10 days. Paramagnetic crystals of **3.9** were collected, filtered, washed with cold hexane and dried in *vacuo* (0.47 g, 0.43 mmol, 43%). Elemental Analysis Calcd. (Found) for $C_{40}H_{44}Al_2Cl_8Cr_2N_4P_2$: C 44.31(44.23), H 4.09 (4.01), N 5.17 (5.11). [μ_{eff} = 4.01 μ_B].

Method B

A solution of (2-Pyridine)N(Me)P(Ph)$_2$ (0.292 g, 1 mmol) in toluene (5 mL) was combined with a suspension of $CrCl_3(THF)_3$ (0.376 g, 1 mmol) in toluene (5 mL), followed by the addition of neat diethylaluminium chloride (0.6 g, 5 mmol). Stirring was continued at room temperature for 5 minutes. Green solution was concentrated to reduce the volume up to 5 mL and layer with pentane. Blue X-ray quality crystals were formed upon cooling the resulting solution at -35 ^oC for 10 days. Blue paramagnetic crystals of **3.9** were collected, filtered, washed with cold hexane and dried in *vacuo* (0.42 g, 0.4 mmol, 40%).

3.2.15 Preparation of {[(2-pyridine)N(Me)]$_4$Cr$_2$}.{Li$_2$Cl$_2$(THF)$_4$)} (3.10)

A solution of (Pyr)N(Me)P(Ph)$_2$ (0.292 g, 1 mmol) in Toluene (5 mL) was combined with a suspension of $CrCl_2$ (THF)$_2$ (0.27 g, 1 mmol) in toluene (5 mL), followed by addition of ethyl lithium (2 mL, 1 mmol, 0.5M in benzene/cyclohexane). Stirring was continued at room temperature for 30 minutes. Brown crystals of X-ray quality were formed upon cooling the resulting solution at -35 ^{o}C for 5 days. Brown crystals of **3.10** were collected, filtered, washed with cold hexane and dried in *vacuo* (0.28 g, 0.3 mmol, 32%). Elemental Analysis Calcd. (Found) for C_{40} H_{60} Cl_2 Cr_2 Li_2 N_8 O_4: C 53.04 (52.91), H 6.68 (6.43), N 12.37 (12.19). ^{1}H NMR lines were too broad for assignment, [μ_{eff} = 1.48 μ_B].

3.2.16 Preparation of [(Me$_3$Cr)$_2$(μ-Me)$_3$][μ-Li(THF)]$_2$ (3.11)

A solution of ligand (0.29 g, 1 mmol) in THF (8 mL) was treated with $CrCl_3$(THF)$_3$ (0.19 g, 0.5 mmol) with stirring. The solution was cooled at -20 °C for 10 mins. Methyl lithium (2.5 mL, 4.0 mmol) was added drop wise while stirring. After 5 mins the resulting solution was filtered and cool to -20 ^{o}C. Orange crystals were formed in overnight which were then separated, washed with cold hexane followed by toluene, dried under *vacuo* to yield (0.24 g, 0.3 mmol, 29%). ^{1}H-NMR (300 MHz, C_6D_6, 25°C) δ: 2.83-2.54 (27H, m), 5.83-5.81 (8H, m), 6.33-6.17(8H, m). ^{13}C{1H}-NMR (300 MHz, C_6D_6, 25°C) δ: 22.1 33.8, 33.9, 103.7, 107.1. (Aromatic impurities present, crystal lattice also contains {LiCl(THF)$_4$}.

3.2.16 Preparation of {[(2-Pyridine)NP(Ph)$_2$]$_3$Cr$_2$Cl$_3$(THF)} 2.6 (toluene) (3.12)

To the cold solution of (2-Pyridine)N(H)P(Ph)$_2$ (0.278 g, 1 mmol) in THF (5 mL) added drop wise *n*-butyllithium (0.44 mL, 1.1 mmol, 2.5 M in hexane) and continued stirring for 12 hours. The lithium salt of ligand was then combined with a suspension of $CrCl_3(THF)_3$ (0.376 g, 1 mmol) in THF (5 mL) and further continued stirring at room temperature for 18 hours. Solvent was evaporated in reduced vacuum. The resulting green residue re-dissolved in toluene. White Lithium chloride salt and small amount of intractable solid were removed through centrifugation. Mother liquor was decanted and concentrated to 5 mL. Upon standing the green solution at -35 ^{o}C paramagnetic crystals of **3.12** were collected, filtered, washed with cold hexane and dried in vacuo (0.65 g, 0.48 mmol, 48%). Elemental Analysis Calcd. (Found) for $C_{73.20}H_{70.80}Cl_3Cr_2N_6OP_3$: C 64.94 (64.81), H 5.27 (5.21), N 6.21 (6.18). [μ_{eff} = 3.11 μ_B].

3.2.17 Preparation of {[(2-Pyridine)NP(Ph)$_2$]$_2$Cr}$_2$.3 (toluene) (3.13)

To the cold solution of (2-Pyridine)N(H)P(Ph)$_2$ (0.278 g, 1 mmol) in THF (5 mL) added drop wise *n*-butyllithium (0.44 mL, 1.1 mmol, 2.5 M in hexane) and continued stirring for 12 hours. The lithium salt of ligand was then combined with a suspension of $CrCl_2(THF)_2$ (0.13 g, 0.5 mmol) in THF (5 mL) and continued further stirring at room temperature for 18 hours. Solvent was evaporated off in *vacuo* and the brown residue re-dissolved in toluene. White Lithium chloride salt and small amount of intractable solid were removed through centrifugation. Mother liquor was decanted and concentrated to 5 mL. Upon standing the brown solution at -35 ^{o}C diamagnetic X-ray quality crystals of **3.13** were collected, filtered, washed with cold hexane and dried in *vacuo* (0.67 g, 0.45

mmol, 45%). Elemental Analysis Calcd. (Found) for C_{89} H_{80} Cr_2 N_8 P_4: C 71.76(71.79) H 5.41(5.47) N 7.52 (7.53). ^{1}H-NMR (300 MHz, THF-d_8, 25°C) δ: 5.62 (4H, m), 5.31-5.20 (40H, m), 4.97 (4H, m), 4.48 (4H, m), 3.90 (4H, m). ^{13}C{1H}-NMR (25°C, THF-d_8, 300 MHz) δ: 168.0, 144.4, 136.9, 136.6, 132.0, 128.3, 128.2, 128.1, 125.7, 125.0, 144.1, 107.0, ^{31}P{H}: 9.91. (NMR shows coordinated ligand only).

3.3 X-ray data

Table 3.1: Crystal Data for Complexes **3.7 -3.13.**

	3.7	**3.8**	**3.9**	**3.10**
Formula	C_{22} H_{23} Cl_3 Cr N_4 P	$C_{50.75}$ $H_{54.50}$ $Cl_{7.50}$ Cr_2 N_9 P_2	C_{40} H_{44} Al_2 Cl_8 Cr_2 N_4 P_2	C_{40} H_{60} Cl_2 Cr_2 Li_2 N_8 O_4
FW	532.76	1222.35	1084.29	905.74
Space group	Monoclinic, P2(1)/n	Monoclinic, P2(1)	Triclinic, P-1	Tetragonal, P4nc
a (Å)	9.7929(6)	10.4846(7)	11.9272(3)	13.2716(8)
b (Å)	18.3610(11)	17.4391(14)	12.3609(3)	13.2716(8)
c (Å)	13.7933(8)	17.0211(13)	17.2699(5)	13.5668(10)
α (deg)	90	90	96.3990(10)	90
β (deg)	91.989(3)	95.649(4)	102.0750(10)	90
γ (deg)	90	90	91.1540(10)	90
V (Å^3)	2478.6(3)	3097.1(4)	2471.80(11)	2389.6(3)
Z	4	2	2	2
radiation(Kα, Å)	0.71073	0.71073	0.71073	0.71073
T (K)	200(2)	200(2)	200(2)	200(2)
D_{calcd} (g cm^{-3})	1.428	1.311	1.457	1.259
μ_{calcd} (mm^{-1})	0.867	0.766	1.006	0.611
F_{000}	1092	1255	1104	952
R, R_w [2 a]	0.0435, 0.1064	0.0865, 0.2243	0.0567, 0.1283	0.0468, 0.1136
GoF	1.043	1.024	1.011	1.052

[a] $R = S||Fo| - |Fc||/S|F|$. $Rw = [S(|Fo| - |Fc|)^2/SwFo^2]^{1/2}$

	3.11	**3.12**	**3.13**
Formula	$C_{38.40}H_{85.80}Cl_{0.50}Cr_2Li_{3.50}O_{7.35}$	$C_{73.20}H_{70.80}Cl_3Cr_2N_6OP_3$	$C_{89}H_{80}Cr_2N_8P_4$
FW	811.29	1353.82	1489.49
Space group	Orthorhombic, P nna	Triclinic, P-1	Triclinic, P-1
a (Å)	17.6340(5)	12.8235(12)	9.4428(2)
b (Å)	41.3359(11)	13.1794(12)	13.4319(2)
c (Å)	13.6627(4)	19.8185(18)	15.8049(3)
α (deg)	90	93.035(4)	67.9540(10)
β (deg)	90	101.320(4)	81.0660(10)
γ (deg)	90	102.966(4)	89.5830(10)
V (Å^3)	9959.0(5)	3184.0(5)	1832.65(6)
Z	8	2	1
radiation(Kα, Å)	0.71073	0.71073	0.71073
T (K)	200(2)	200(2)	200(2)
D_{calcd} (g cm^{-3})	1.082	1.412	1.350
μ_{calcd} (mm^{-1})	0.501	0.594	0.438
F_{000}	3536	1408	778
R, R_w[2 a]	0.0684, 0.1858	0.0722, 0.1778	0.0341, 0.0883
GoF	1.043	1.014	1.030

3.4 Results and Discussion

3.4.1 Exploration of R_2NPPh_2 Ligands

The ligands $(R')_2PN(R)_2$ [R' = Ph; R = Me (**1**); Et (**2**); *i*-Pr (**3**); Ph (**4**); R = Et, R' = *i*-Pr (**5**)] do not react with chromium salts in THF. However, Ligand **1** is readily ligating trivalent chromium salts in toluene as indicated by color change and dissolution upon mixing. Instead ligands **2**, **3, 4** and **5** required forcing conditions and boiling toluene to observe color change. All complexes were isolated as microcrystalline materials from toluene solutions after centrifugation and upon layering with hexane. ESI-MS data were in support with simple ligand coordination to the $CrCl_3(THF)_3$ residue. Reactions carried out on the ligand-$CrCl_3$ adducts showed no difference in catalytic behavior with the *in situ* generated species. Therefore, catalytic testings were carried out with *in situ* generated

complexes, easily obtained by mixing either $CrCl_3(THF)_3$ or $CrCl_2(THF)_2$ with the appropriate ligand, activator and reaction solvent in the reactor pressurized with ethylene.

The reactions carried out in toluene using TMA-depleted MAO, (d-MAO) as co-catalyst produced S-F distributions of oligomers with high activity. Interestingly, the product mixtures were polymer-free in three cases (Table 3.2).

Table 3.2. Catalytic behaviour of complexes **(3.1-3.5)-$CrCl_3$**

Ligand	Co-cat.	Co-cat (eq.)	PE(g)	Oligomers (mL)	Activity g/mmol cat./h	Mol %		
						C6	C8	C10-C18
1	d-MAO/toluene	500	-	13	1,056	19	24	57
1	d-MAO/MeCy	500	1.9	1.0	232	50	50	-
1	d-MAO/TEAl	500/100	1.3	1.5	224	48	52	-
2	d-MAO/toluene	500	-	40	3,200	22	25	55
2	d-MAO/MeCy	500	0.7	3.5	336	21	79	-
2	d-MAO/TEAl	500/100	0.5	4.4	392	6.8	93.2	-
2	d-MAO/ Et_2Zn	500/100	0.9	3.5	400	20	80	-
2*	d-MAO/TEAl	500/100	0.5	3.0	280	10	90	-
2	d-MAO/TEAl	400/100	0.4	1.8	176	28	72	-
2	d-MAO/TEAl	500/250	0.7	2	216	20	80	-
3	d-MAO/toluene	500	0.3	26	2,104	20	26	54
3	d-MAO/MeCy	500	1.6	1.5	248	43	57	-
3	d-MAO/TEAl	500/100	1	2	240	38	62	-
4	d-MAO/toluene	500	-	23	1,840	24	28	48
4	d-MAO/MeCy	500	2.3	2	344	60	40	-
4	d-MAO/TEAl	500/100	1.5	5	520	60	40	-
5	d-MAO/toluene	500	1.0	30	2,480	19	22	77
5	d-MAO/MeCy	500	1.3	1.5	224	75	25	-
5	d-MAO/TEAl	500/100	0.8	1.5	184	75	25	

Conditions: 25 µmol catalyst (2:1, ligand: Cr), 40 bar ethylene pressure, 80 (^oC) T, 30 min. reaction time, $Cr(NCyl_2)_3$ as Cr source, methylcyclohexane solvent.*

Conversely, when MeCy was used as solvent and under the same reaction conditions, mixtures of 1-hexene, 1-octene and polymer were obtained. Higher oligomers were not detected even in traces. The addition of TEAl (100 equiv.) to d-MAO (also in MeCy) did not change the outcome of the catalytic cycle in the case of ligand **4** and **5**.

It slightly improved the selectivity of **1** and **3.** In the case of **2** instead the amount of 1-octene increased substantially at the expenses of 1-hexene, without modifying the activity other than for an increased production of polymer. The selectivity for 1-octene was strongly depending on the nature of the ligand substituent, the maximum having been reached with ligand **2**.

Experiments carried out at lower ethylene pressure showed a decrease of both activity and selectivity (Table 3.3).

Table 3.3: Ethylene Pressure Effect on catalytic behavior of (**3.2)**

Co-cat. d-MAO/TEAl	T (^{o}C)	Pressure (bar)	PE(g)	Oligomers (mL)	Activity g/mmol cat./h	Mol %	
						C6	C8
500/100	80	15	-	traces	-	-	-
500/100	80	30	1.02	2.4	273.6	49	51
500/100	80	40	0.5	4.4	392	6.8	93.2

Conditions: 25 µmol catalyst (2:1, ligand: Cr), 80 (^{o}C) T, 30 min. reaction time, methylcyclohexane solvent.

Finally reaction carried out under the best conditions, at variable temperature and monitoring the ethylene uptake, showed an almost linear behavior suggesting a rather constant productivity as a function of time (Figure 3.1).

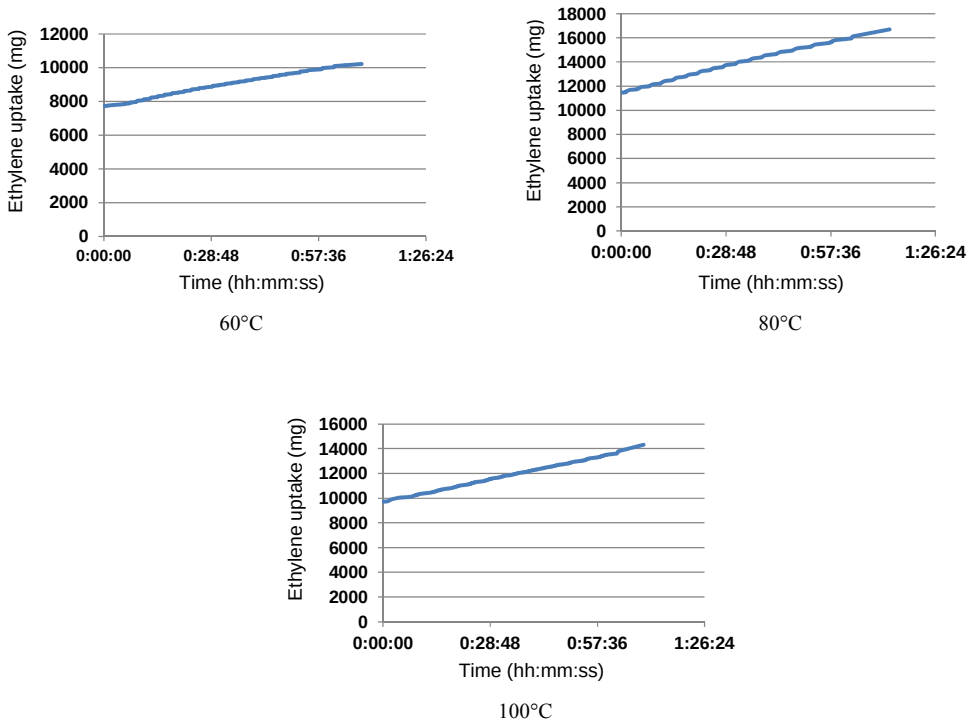

Figure 3.1. Rate of Ethylene Uptake at Different Temperatures.

The switching of activity from a general S-F distribution to 1-hexene/1-octene as a function of the solvent employed for the reaction (toluene *versus* MeCy) is often encountered among the chromium-based oligomerization catalysts.[12b,14] It may be explained with the poisoning effect of toluene on the Cr(I) intermediate responsible for the selective behaviour. The almost ubiquitous presence of polymeric material in variable amount clearly speaks for the ability of these species to disproportionate.[4c-g,12a] The fact that in MeCy the S-F distribution of oligomers is replaced by a mixture of only 1-hexene and 1-octene is also an indication about the formation of monovalent chromium.[4,12,14,17] The seemingly poor ability of this catalyst to distinguish between 1-hexene and 1-octene is

possibly an indication that the selective oligomerization proceed via ring expansion mechanism where the expansion from 7- to 9-membered ring has activation barrier comparable to that of the reductive elimination. The predominance of 1-octene and complete absence of superior homologues is however intriguing. In consequence, we cannot exclude the possibility that the tetramerization occurs via the Rosenthal dimeric dimetallic mechanism, 1-hexene being produced by monomeric species in a dissociation equilibrium with the tetramerization. The reason why TEAl may so substantially boost the selectivity for tetramerization just in the case of ligand **2** remains unclear.

3.4.2 Exploration of (Pyridyl)N(R)PPh_2 Ligand

As mentioned, understanding the mechanistic details of a catalytic cycle is central to narrow the search for appropriate ligand systems of new performing catalysts. Towards this end, a large library of PN based ligand systems is now available and the selective behavior, frequently observed with their chromium derivatives, is likely to be ascribed to the ability of these combinations of donor atoms to stabilize the monovalent state and possibly encourage formation of dimetallic species.[14,15] Pyridine rings as coordinating units are also versatile for the purpose while the presence/absence of anionic charge in the ligand may also be a factor determining the selectivity.[12a] For this reason we have further modified the simple N-P ligand to the neutral (2-pyridine)N(Me)PPh_2 and anionic phosphine-amidopyridyl [(2-pyridine)$NPPh_2$]$^{(-)}$ ligands to assess the ability of this ligand to sustain selectivity for the ethylene oligomerization cycle *vis-à-vis* possible tetramerization activity.

The ligand (2-pyridine)N(Me)PPh_2 was readily prepared via reaction of the deprotonated form of methylaminopyridine with $ClPPh_2$. It readily bonds $CrCl_3(THF)_3$ in THF as indicated by immediate color change to blue upon mixing. The reaction afforded homogeneous, crystalline, paramagnetic, blue complex formulated as {[(2-pyridine)N(Me)PPh_2]$CrCl_2$}$_2$(μ-Cl)$_2$ (**3.6**) on the basis of its analytical data (Scheme 3.1).

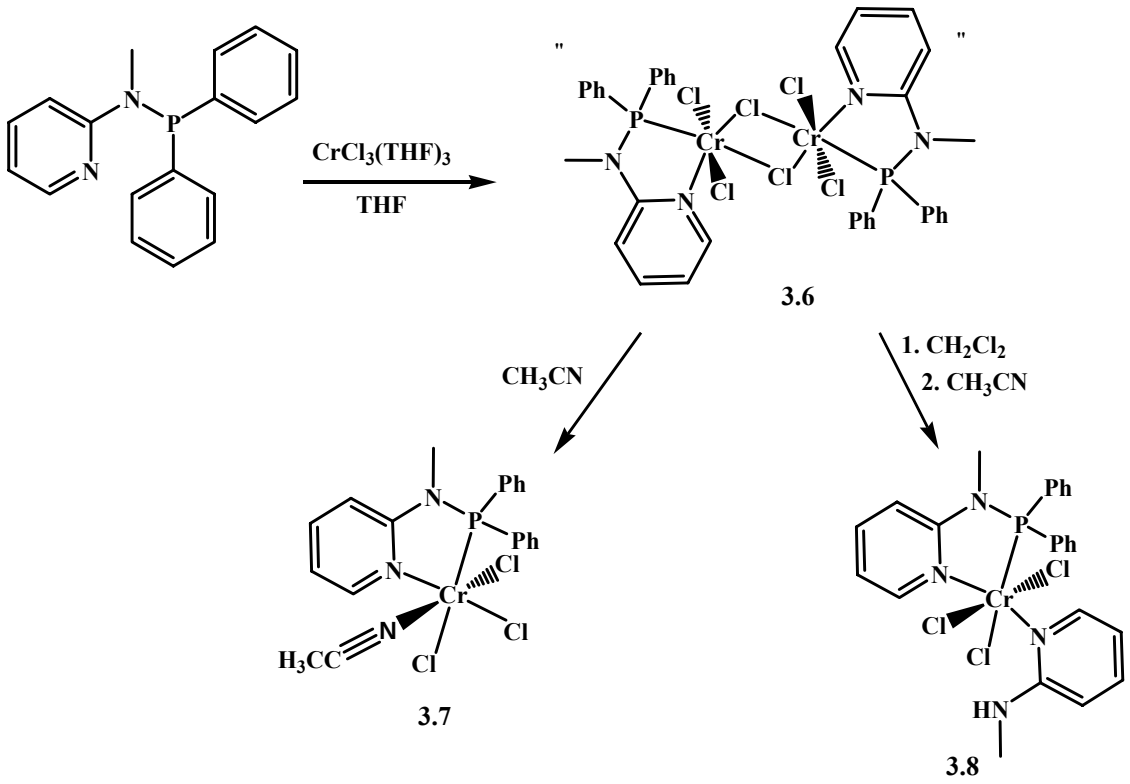

Scheme 3.1: Synthesis of complexes 3.7 and 3.8 from 3.6

While attempting to obtain crystals suitable for X-ray diffractions have been frustrated by unfavorable crystal shape, the dimetallic structure is hereby proposed on the basis of the low value of the magnetic moment [μ_{eff} = 3.12 μ_B]. Furthermore, the structure of **3.6** was also indirectly supported by the result of the reaction with CH_3CN which afforded the mononuclear {[(2-pyridine)N(Me)PPh_2]$CrCl_3(NCCH_3)$} (**3.7**) isolated as

pale blue crystals. Similar observation with coordinating acetonitrile is also reported in literature by the group of Kang with PCCP ligand of the SK-Energy tetramerization system.[18]

The structure of **3.7** (Figure 3.2) shows a distorted octahedral geometry around the trivalent metal center defined by the three facially placed chlorine atoms [Cr1-Cl2 = 2.2865(7)Å, Cr1-Cl1 = 2.3115(7)Å, Cr1-Cl3 = 2.3169(7)Å, Cl2-Cr1-Cl1 = 93.55(3)^o] and the N atom of the coordinated CH_3CN molecule [Cr1-N3 = 2.074(2)Å, N3-Cr1-Cl1 = 92.50(6)^o, N3-Cr1-Cl3 = 87.93(6)^o]. The P and pyridine N donor atoms of the ligand systems [Cr1-P1 = 2.4144(7)Å, Cr1-N2 = 2.117(2)Å] complete the coordination polyhedron [N3-Cr1-N2 = 85.89(8)^o, N3-Cr1-Cl2 = 172.67(6)^o, N2-Cr1-Cl2 = 87.32(6)^o, N2-Cr1-Cl1 = 167.68(6)^o, N2-Cr1-Cl3 = 97.82(6)^o].

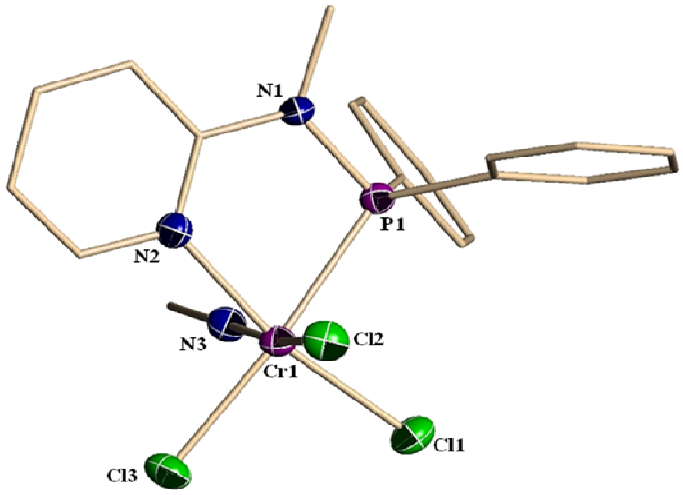

Figure 3.2: Partial thermal ellipsoids drawing of complex 3.7 (50 % probability level).

A different complex was isolated during attempts to crystallize **3.6** in CH_2Cl_2 followed by treatment with acetonitrile (Scheme 3.1). The crystal structure of the new

complex revealed this new species as {[(2-pyridine)N(Me)PPh_2]$CrCl_3$[(2-pyridine)N(Me)H]}.{(CH_3CN) (CH_2Cl_2)} (**3.8**). The ligand fragmentation observed due to the exposure of a mixture of CH_2Cl_2 and acetonitrile is puzzling and indicated the lability of the phosphine residue as an unanticipated feature of this ligand system.

The crystal structure of **3.8** (Figure 3.3) did not show any particular feature other than the mildly distorted octahedral geometry around the Cr(III) metal [P1-Cr1-N1 = 77.17(17)°, P1-Cr1-Cl1 = 92.67(7)°, P1-Cr1-N3 = 94.9(2)°, P1-Cr1-Cl2 = 172.66(8)°, P1-Cr1-Cl2 = 172.66(8)°, P1-Cr1-Cl3 = 83.20(7)°] as defined by the three meridionally oriented chlorine atoms [Cl2-Cr1 = 2.3365(19)Å, Cl3-Cr1 = 2.297(2)Å, Cl1-Cr1 = 2.347(2)Å] the N and P donor atom of one intact ligand [P1-Cr1 = 2.4790(19)Å, N1-Cr1 = 2.106(6)Å] and the N atom of the pyridine ring of the fragmented ligand [N3-Cr1 = 2.123(6)Å].

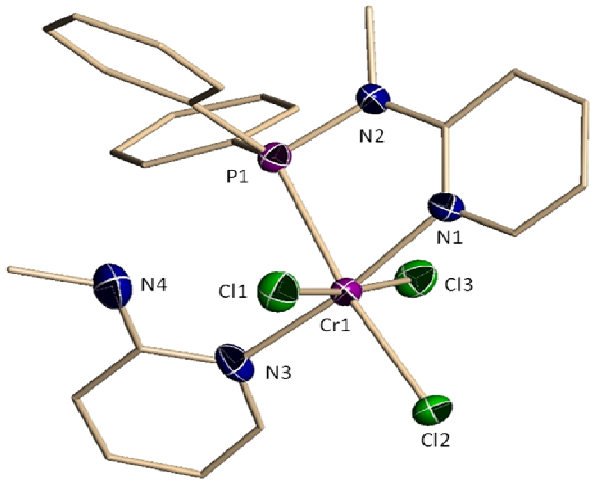

Figure 3.3: Partial thermal ellipsoids drawing of complex 3.8 (50 % probability level).

When ligand complexation was carried out with either $CrCl_2(THF)_2$ or $CrCl_3(THF)_3$ and in presence of diethylaluminum chloride (DEAC), the paramagnetic,

dimeric and divalent $\{[(2\text{-pyridine})N(Me)PPh_2]Cr\}_2(\mu\text{-}Cl)_2][AlCl_3Et]_2$ (**3.9**) was obtained (Scheme 3.2).

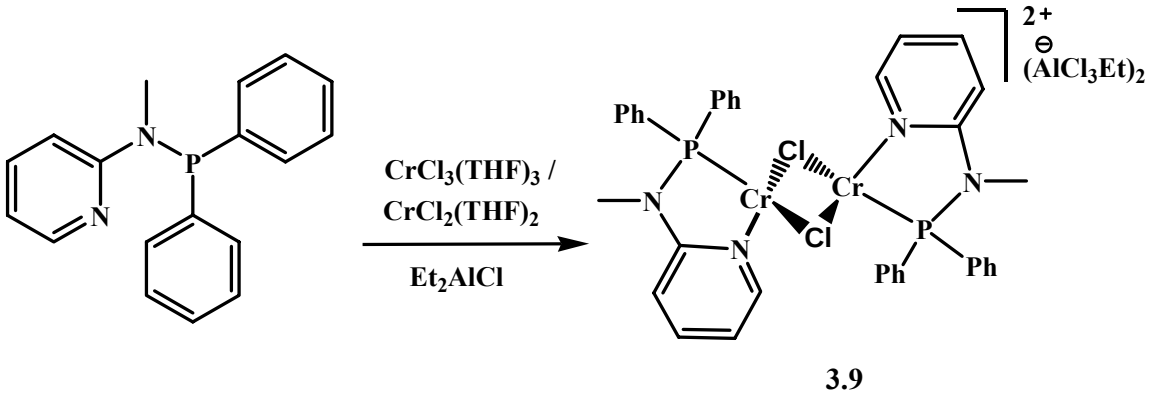

Scheme 3.2: Preparation of complex 3.9

The chemical connectivity of **3.9** was clarified by an X-ray crystal structure (Figure 3.4). The complex is a symmetry-generated dimer composed of two identical chromium units bridged by two chlorine atoms [Cr1-Cl1 = 2.4277(11)Å, Cr1-Cl1a = 2.3569(12)Å, Cr1a-Cl1a = 2.4200(12)Å] and each surrounded by one ligand [Cr1-N1 = 2.102(3)Å, Cr1-P1 = 2.4428(11)Å]. The coordination geometry of the two metal centers in square-planar [Cl1a-Cr1-Cl1 = 89.45(4)°, N1-Cr1-P1 = 78.66(9)°, N1-Cr1-Cl1 = 100.56(9)°, Cl1a-Cr1-P1 = 91.33(4)°]. Two $AlCl_3Et$ anions, unconnected to the dimetallic dication, are also present in the unit cell. The Cr…Cr distance is unusually short for a chlorine bridged Cr(II) dimeric species [Cr(1)-Cr(2) = 2.3570(12)Å].

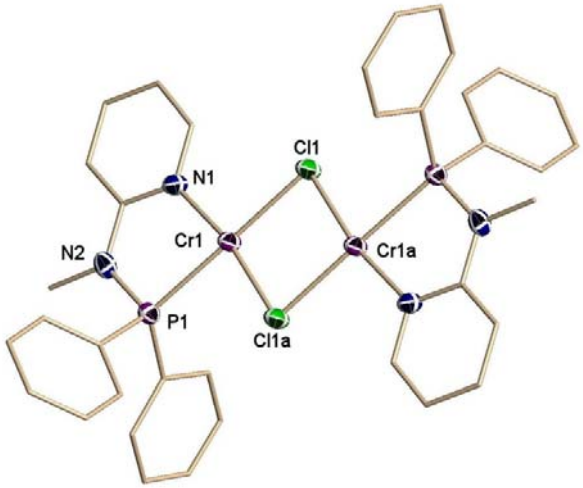

Figure 3.4: Partial thermal ellipsoids drawing of the cationic portion of 3.9 (50 % probability level). The two $AlCl_3Et$ anions have been omitted for clarity.

The lack of formation of Cr-C bonds during the alkylation of DEAC prompted to attempt the same complexations in the presence of stronger alkylating agents such as EtLi and MeLi (Scheme 3.3).

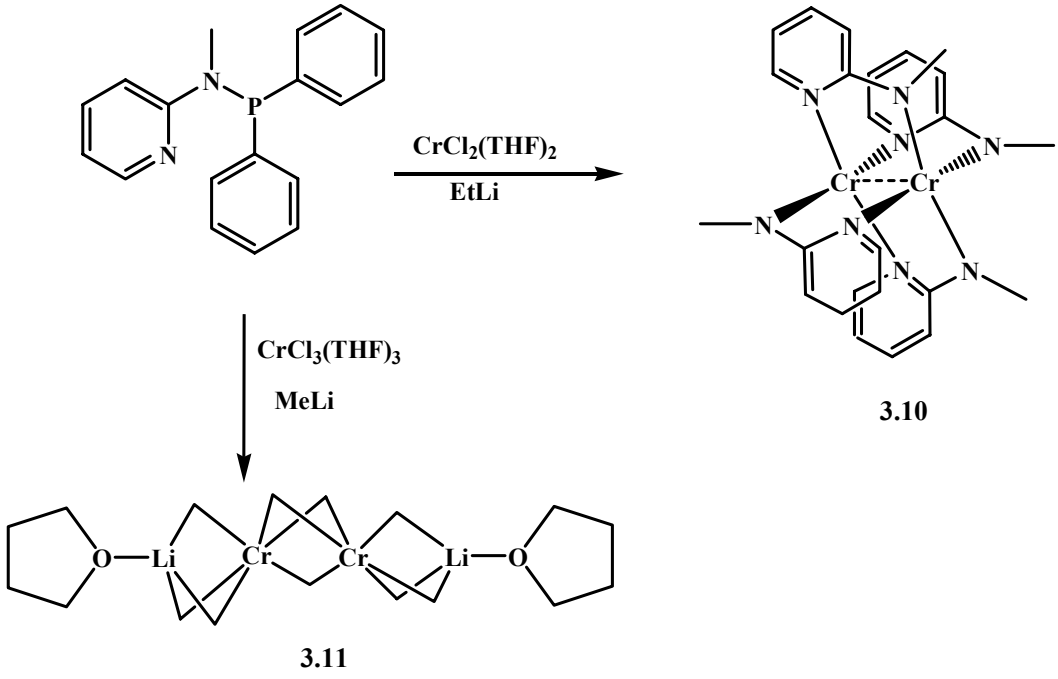

Scheme 3.3: Isolation of complexes 3.10 and 3.11, showing labile nature of ligand

In the case of $CrCl_2(THF)_2$, a crystalline material was isolated from the reaction with ethyl lithium. The complex was formulated as the dinuclear {[(2-pyridine)N(Me)]$_4Cr_2$}.{$Li_2Cl_2(THF)_4$)} (**3.10**) on the basis of its crystal structure. The ^{1}H-NMR shows resonances of the coordinated ligand at the expected regions for the Me group (2.67 ppm) and the pyridine ring (7.02, 6.26 and 5.80), however these linings are too broad to satisfactory assignment of the spectra.

The crystal structure of **3.10** (Figure 3.5) shows the typical paddle-wheel structure as expected for the methylpyridine amido anion with a Cr…Cr distance is the so-called supershort Cr-Cr bonding range [1.8619(13)Å]. The geometry around the metal centre is the usual distorted square planar with the two metal pulled inward the molecular core [Cr1-Cr2-N1b = 95.0(3)^o, N1a-Cr2-N1b = 89.57(6)^o, Cr1-Cr2-N1c = 95.0(3)^o, N1a-Cr2-N1c = 170.0(7)^o, N1b-Cr2-N1c = 89.57(6)^o, Cr1-Cr2-N1 = 95.0(3)^o, N1a-Cr2-N1 = 89.57(6)^o, N1b-Cr2-N1 = 170.0(7)^o, N1c-Cr2-N1 = 89.57(6) ^{o}] .

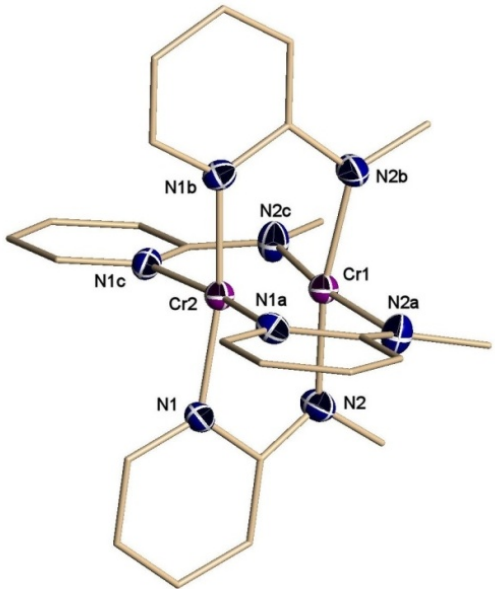

Figure 3.5: Partial thermal ellipsoids drawing of complex 3.10 (50 % probability level). ($Li_2Cl_2(THF)_4$ is omitted for clarity).

An intersting feature in the formation of **3.10** is that ligand fragmentation ocuurred even in this case as a probable result of a nucleophilic attack of EtLi to the ligand P atom. This of course reiterates that ligand lability could be a systematic problems for the catalytic systems based on this ligand. The result of the reaction of $CrCl_3(THF)_3$ with MeLi also reiterates ligand lability. The reaction in this case afforded the homoleptic Cr(III) derivative $[(Me_3Cr)_2(\mu\text{-}Me)_3][\mu\text{-}Li(THF)]_2$ **(3.11)** (Figure 3.6).

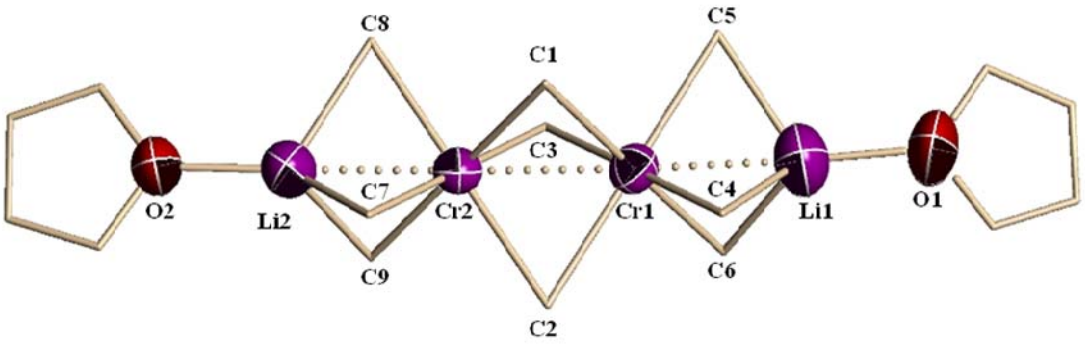

Figure 3.6: Partial thermal ellipsoids drawing of complex 3.11 (50 % probability level).

Complex **3.11** is basically isostructural with the previously reported mononuclear divalent $[(Me_4Cr)(\mu\text{-}Me)_2][\mu\text{-}Li(TMEDA)]_2$, the only difference being the solvation of the two alkali metal at the periphery of the structure.[19] Krausse was the first to report homoleptic divalent chromium with super short Cr…Cr contact [1.980Å] stabilized by bridging methyl and alkali cations.[20] As of our knowledge complex **3.11** is the first structurally characterized homoleptic dimer of Cr(III) stabilized by bridging methyl and alkali metal with non-bonded Cr…Cr contact 2.5164(14)Å.

Catalytic Activity

All the above mentioned isolated complexes were tested for ethylene oligomerization/polymerization activity at optimized reaction conditions (Table 3.4). Upon activation with MAO, complex **3.6** behaves as non-selective catalyst producing Schulz-Flory distribution of products. Unlike $Cr(R_2NPPh_2)$ described earlier, complex **3.6** showed non-selective behavior even with TMA-depleted MAO (DMAO) and also upon activation with TEAl. Nonetheless, upon activation with MMAO the system showed some selectivity towards 1-octene which reaches up to ~ 50% and with an overall selectivity of 1-hexene/1-octene is ~70 %.

Table 3.4: Catalytic behaviour[a] of complexes **3.6-3.11**.

Cat. (μmol)	Co-cat. (eq)	Temp (°C)	Activity g/mmol, cat.h	PE (g)	Oligomer (mL)	Mol %						
						C6	C8	C10	C12	C14	C16	C18
3.6(20)*	MAO (150)	60	1,700	5	12	30.33	36.72	10.12	7.62	6.47	5.35	3.40
3.6(20)	MAO (150)	60	4,500	7	38	35.20	35.39	11.46	7.54	4.86	3.29	2.25
3.6(20)	MMAO (400)	70	900	0.9	8	19.40	49.86	12.9	8.14	5.33	3.61	0.69
3.6(20)	d-MAO (400) /TEAl (100)	70	3,800	2	36	29.14	21.73	14.21	11.3	9.72	8.01	5.85
3.6(20)	d-MAO (500)	70	3,100	3.8	27	26.38	32.90	13.1	9.14	8.38	5.90	4.24
3.6(20)	MMAO (400)	60	940	1	8.4	20.30	43.59	12.93	9.07	6.58	4.53	3.00
3.6(20)	MMAO (400)	45	660	1.6	5	23.26	33.03	16.94	10.9	7.29	4.99	3.58
3.7(20)	MMAO (400)	70	1,270	-	12.7	33.40	34.66	12.13	8.35	5.59	3.68	2.20
3.8(20)	d-MAO (400) /TEAl (100)	70	5,360	1.6	52	27.84	25.15	16.80	12.0	8.11	6.02	4.05
3.8(20)	MMAO (400)	70	200	traces	2	57	43	traces	-	-	-	-
3.9(20)*	MAO (150)	60	450	0.5	4	25.68	31.64	12.11	10.1	8.65	7.57	4.28
3.9(20)	MMAO (400)	70	-	traces	traces	trace	trace	-	-	-	-	-
3.10(20)	MMAO (400)	70	-	traces	traces	trace	trace	trace	-	-	-	-
3.11(20)*	MAO (150)	60	1,200	2	10	32.62	27.56	17.71	12.7	5.12	2.82	1.48
3.11(20)	MMAO (400)	70	-	-	-	-	-	-	-	-	-	-

Conditions[a] : 40 bar ethylene, 30 mins. reaction time, total volume 100 mL, in methylcyclohexane; toluene*

The excess of both 1-octene and 1-hexene implies that a metallacycle mechanism is operational during the catalytic cycle. In turn, this indicates the formation of monovalent chromium intermediates along with some divalent Cr(II). Divalent Cr(II) is most likely responsible for the heavier oligomers (S-F distribution). The invariable presence of polymer is instead likely to ascribe to the trivalent state in the end indicating the three oxidation states actively interconvert under the conditions required by the catalytic cycle.[4c,e, 7a,b]

On the other hand upon activation with MMAO, monomeric complex **3.7** showed lower selectivity towards 1-octene (34%) and increased selectivity for 1-hexene (33%) compared to the dimeric complex **3.6** (50% 1-octene, 19% 1-hexene). Even though we have no conclusive evidence, we speculate that the different selectivity could be ascribed to the co-existence of dimeric and monomeric structures in equilibrium. Each of the two arrangements accounts for the formation of either of 1-hexene or 1-octene. The comparatively higher selectivity for 1-octene when MMAO was used as a co-catalyst could be explained with the use of strongly reducing *i*-BuAl capable of generating some monovalent species. Lower activity shown by the cationic complex **3.9** could be simply the result of lower solubility in non polar solvent.

The lability of the ligand scaffold, as highlighted by the unexpected formation of complexes **3.7**, **3.10** and **3.11** prompted us to investigate the behavior of the anionic analogue of the ligand system $[(2\text{-pyridine})NPPh_2]^{(-)}$.

Complex $\{[(2\text{-Pyridine})NP(Ph)_2]_3Cr_2Cl_3(THF)\}$ **(3.12)** was readily prepared by the reaction of lithium salt of ligand (2-Pyridine)N(H)PPh_2 with $CrCl_3(THF)_3$ in THF (Scheme 3.4).

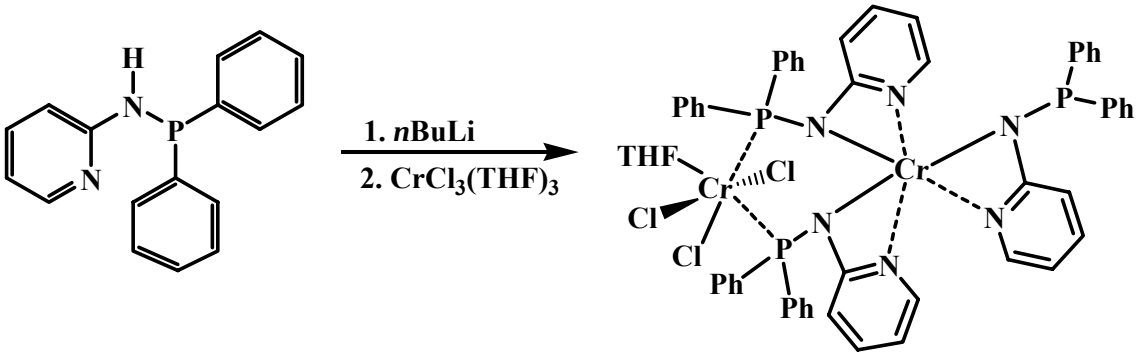

3.12

Scheme 3.4: synthesis of complex 3.12

The chemical connectivity was yielded by an X-ray crystal structure determination (Figure 3.7). Complex **3.12** displays an interesting dimeric trivalent Cr(III) species asymmetrically coordinated to three ligands. One of the two Cr centres is ligated by only nitrogen atoms of the three ligands in a distorted octahedral environment [Cr2-N1 = 2.045(4)Å, Cr2-N2 = 2.047(4)Å, Cr2-N3 = 2.049(4)Å, Cr2-N4 = 2.028(4)Å, Cr2-N5 = 2.061(4)Å, Cr2-N6 = 2.044(4)Å, N1-Cr2-N2 = 65.68(16)^{o}, N4-Cr2-N3) = 65.70(15)^{o}, N6-Cr2-N5 = 65.30(17)^{o}]. Another Cr centre is bonded to two phosphorus atoms of the ligands [Cr1-P1 = 2.5889(15)Å, Cr1-P2 = 2.4859(15)Å]. The other four coordination sites are occupied by three meridionally oriented chlorine atoms [Cr1-Cl1 = 2.2940(16)Å, Cr1-Cl3 = 2.3018(15)Å, Cr1-Cl2 = 2.3183(15)Å, Cl(1)-Cr(1)-Cl(3) = 169.44(6)^{o}] and one THF molecule [Cr1-O1 = 156(4)Å, O1-Cr1-Cl2 = 87.07(12)^{o}, O1-Cr1-P1 = 85.59(11)^{o}] in an overall distorted octahedral environment.

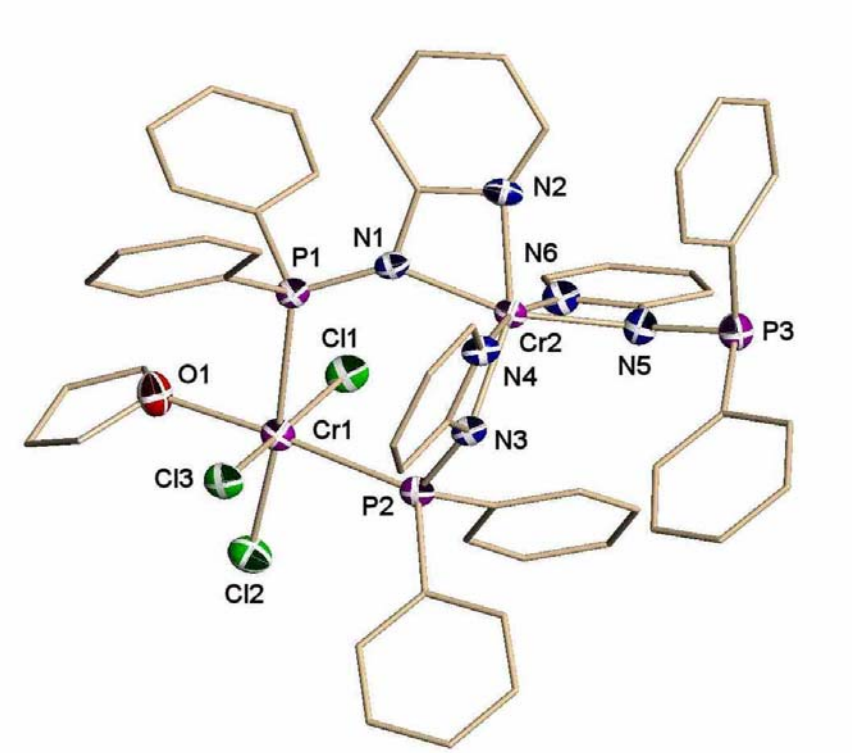

3.12

Figure 3.7: Partial thermal ellipsoids drawing of complex 3.12 (50 % probability level).

While the reaction was carried out with $CrCl_2(THF)_2$ a lantern-type dimeric divalent complex $\{[(2\text{-Pyridine})NP(Ph)_2]_2Cr\}_2$ **(3.13)**, similar to **3.10** with very short Cr…Cr distance [1.877Å] was obtained (Scheme 3.5). The diamagnetic character of the complex was highlighted by the sharp phosphorus resonance at 9.91 ppm of $^{31}P\{H\}$-NMR spectrum and the series of well-solved multiplets in the ^{1}H-NMR spectrum at 5.62, 4.97, 4.48 for the pyridine ring and at 5.31 ppm for the phenyl groups. Unlike complex **3.12** all the phosphorus atoms are oriented away from the metal centres.

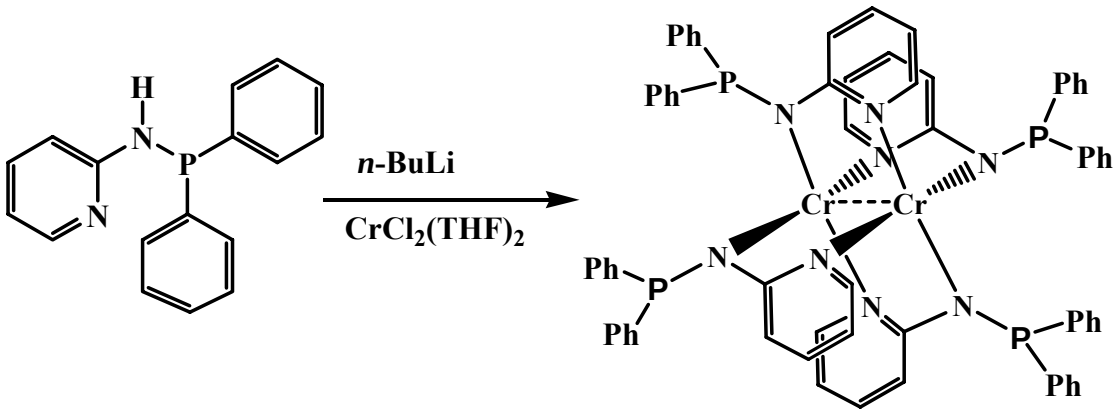

3.13

Scheme 3.5: Preparation of complex 3.13

The structure was determined by X-ray analysis (Figure 3.8). The geometry around the metal centre is the usual distorted square planar with the two metal pulled inward the molecular core [Cr1-N3 = 2.0537(4)Å, Cr1-N1 = 2.0578(5)Å, Cr1-N2a = 2.0608(3)Å, Cr1-N4a = 2.0717(6)Å, N2-Cr1a = 2.0608(4)Å, N4-Cr1a = 2.0717(5)Å, Cr1a-Cr1-N3 = 94.1(15)^{o}, Cr1a-Cr1-N1 = 94.6(13)^{o}, N3-Cr1-N1 = 95.4(14)^{o}, Cr1a-Cr1-N2a = 96.6(17)^{o}, N3-Cr1-N2a = 88.3(3)^{o}, N1-Cr1-N2a = 167.9(13)^{o}, Cr1a-Cr1-N4a = 96.8(6)^{o}, N3-Cr1-N4a = 167.3(7)^{o}, N1-Cr1-N4a = 90.1(5)^{o}, N2a-Cr1-N4a = 84.1(5)^{o}].

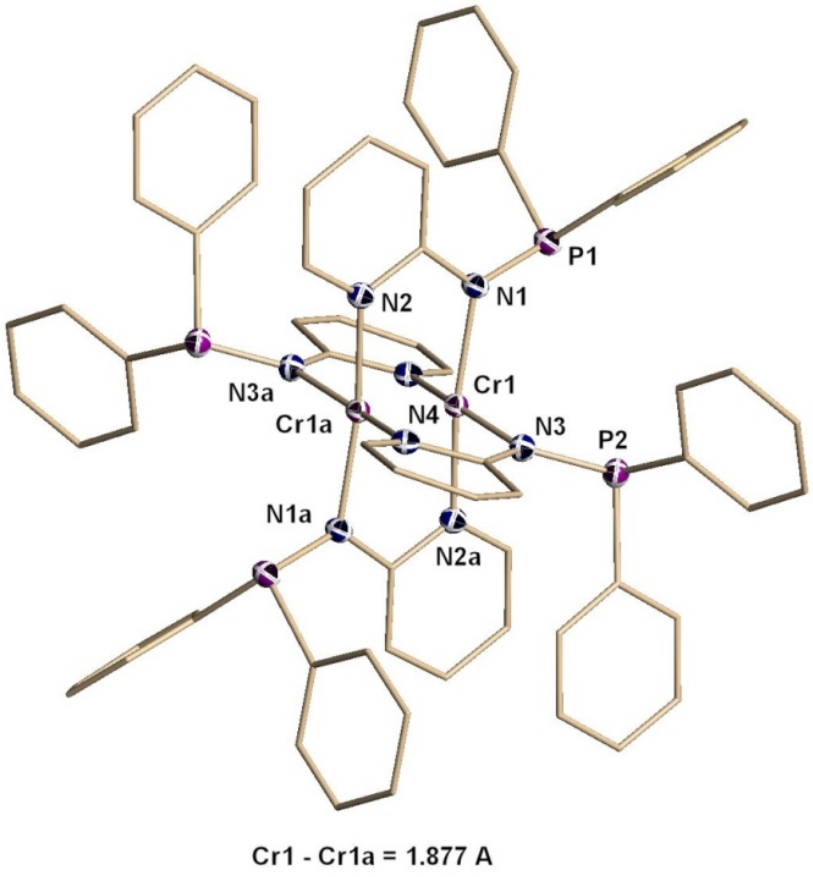

3.13

Figure 3.8: Partial thermal ellipsoids drawing of complex 3.13 (50 % probability level).

Both complexes were tested for ethylene oligomerization under optimized reaction conditions. Upon activation with MAO in methylcyclohexane, **3.12** and **3.13** showed highly active but non-selective ethylene oligomerization behavior with formation of a small amount of polymers (Table 3.5). This result is completely different from the simple anionic N-P complexes described earlier in chapter 2 and which selectively formed 1-hexene (99%).[14] The behaviour clearly indicates reduction of trivalent state to divalent and no further reduction. Both complexes unlike their neutral analogue, showed very low

activity upon activation with MMAO, therefore, indicating that no reduction towards the divalent state occurs with this anionic ligand.

Table 3.5. Catalytic behavior of of **3.12** and **3.13.**[a]

Cat. (μmol)	Co-cat.	Co-cat (eq.)	Activity g/mmol, Cat.h	PE (g)	Oligo. (mL)	Mol % C6	C8	C10	C12	C14	C16	C18
3.12(20)	MAO	150	5,046.0	2.8	55	16.8	21.8	15.6	14.6	13.0	11.3	6.9
3.12(10)	MMAO	400		traces	traces							
3.13(10)	MAO	150	2,581.3	3.1	27	27.4	27.5	17.5	11.3	9.1	5.2	2.1
3.13(10)	MMAO	400		traces	traces							

Conditions[a]: 40 bar ethylene, 30 mins reaction time, total volume 100 mL, in methylcyclohexane; 70 ^{o}C.

3.5 Conclusions

In summary, we have now studied the effect of ligand substituent on a small series of neutral NP ligand finding in one case a remarkably high selectivity for 1-octene. Although these findings do not shed any additional light on the reaction mechanism and do not allow distinguishing among the ring expansion and the bimetallic mechanism, they confirm that high selectivity in the tetramerization cycle is indeed possible. Findings from this study suggest that a small modification on a ligand has a profound effect on the selectivity of ethylene tetramerization product. It is likely that the tendency of (Pyridyl)N(R)PPh_2 ligand to stabilize divalent Cr(II) could be the reason for decreased selectivity in the system. The ligand lability under thermal condition seems to be at the basis of the disappointing catalytic behaviour. It is also evident that the anionic nature of (Pyridyl)N(H)PPh_2 ligand provided strong stabilization to divalent state of Cr(II) and thereby preventing further reduction to monovalent state producing in turn Schulz-Flory

distribution of the oligomers. It is worth noting that presence/absence of anionic charge in the ligand may also is a factor affecting the selectivity.

In the next chapter we will be describing our continuous effort for searching a highly selective tetramerization catalyst and exploration of a neutral 2,2'-dipyridylamine ligand system with binucleating ability for the purpose.

References:

1. a) Manyik, R. M.; Walker, W.E.; Wilson, T. P. *J. Catal*. **1977**, *47*, 197. b) Rensburg, W. J.; Grove, C.; Stark, K. B.; Huyser, J. J.; Steynberg, P. J. *Organometallics* **2004**, *23*, 1207. and references therein. c) Tomov, A. K.; Chirinos, J. J.; Jones, D. J.; Long, R. J.; Gibson, V. C. *J. Am. Chem. Soc.* **2005**, *127*, 10166. d) Overett, M. J.; Blann, K.; Bollmann, A.; Dixon, J. T.; Haasbroek, D.; Killian, E.; Maumela, H.; McGuinness, D. S., Morgan, D. H. *J. Am.Chem. Soc,* **2005**, *127*, 10723. e) Rensburg, W. J.; Berg, J.A.; Steynberg, P. J. *Organometallics* **2007**, *26*, 1000. f) Köhn, R. D. *Angew. Chem. Int. Ed.* **2007**, *46*, 2. g) Blom, B.; Klatt, G.; Fletcher, J. C. Q.; Moss, J. R. *Inorg. Chim. Acta.* **2007**, *360*. 2890. h) Bhaduri, S.; Mukhopadhyay, S.; Kulkarni, S. A. *J. Organomet. Chem.***2009**, *694*, 1297. i) Beweries, T.; Fischer, C.; Peitz, S.; Burlakov, V. V.; Perdita, A.; Baumann, W.; Spannenberg, A.; Heller, D.; Rosenthal, U. *J. Am. Chem. Soc.* **2009**, *131*, 4463. j) Zhang, J.; Li, A.; Hor, T. S. A. *Organometallics* **2009**, *28*, 2935. k) Aluri, B. R.; Peulecke, N.; Peitz, S.; Spannenberg, A.; Müller, B. H.; Schulz, S.; Drexler, H. J.; Heller, D.; Al-Hazmi, M. H.; Mosa, F. M.; Wöhl, A.; Müller, W.; Rosenthal, U. *Dalton Trans.* **2010**, *39*, 7911. l) Alpha Olefins (02/03-4) *PERP Report*, Nexant Chem. Systems. m) Lutz, E. F. *J. Chem. Educ.* **1986**, *63*, 202. n) Weissermel,K. H. Arpe in *Industrial Organic Chemistry*, 3rd ed, Wiley, New York, **1997**. o) Wittcoff, H.; Reuben, B. G.; Plotkin, J. S.in *Industrial Organic Chemicals*, 2nd ed, Wiley- Interscience, New York, **2004**. p) Kuhn, P.; Semeril, D.; Matt, D.; Chetcuti, M. J.; Lutz, P. *Dalton Trans*. **2007**, 515. q) McDermott, J. X.; White, J. F.; Whitesides, G. M. *J. Am. Chem. Soc.* **1976**, *98*, 6521.

2. a) Dixon, J. T.; Green, M. J.; Hess. F. M.; Morgan, D. H. *J. Organomet. Chem*. **2004**, *689*, 3641. b) Crewdson, P.; Gambarotta, S.; Djoman, M.C.; Korobkov, I.; Duchateau, R. *Organometallics* **2005**, *24*, 5214. c) Agapie, T.; Day, M. W.; Henling, L. M.; Labinger, J. A.; Bercaw, J. E. *Organometallics* **2006**, *25*, 2733. d) Schofer, S. J.; Day, M. W.; Henling, L. M.; Labinger, J. A.; Bercaw, J. E. *Organometallics* **2006**, *25*, 2743. e) Agapie, T. *Coord.Chem. Rev*. **2011**, *255*, 861. f) McGuinness, D. S. *Chem. Rev*. **2011**, *111*, 2321, and references therein.
3. a) Hogan, J. P.; Banks, R. L. (Phillips Petroleum Co.) U.S. Patent 2,825,721, **1958**. b) Karapinka, G. L. (Union Carbide Corp.) Ger. Offen. DE 1,808,388, **1970**. c) Karapinka, G.L. (Union Carbide Corp.) U.S. Patent 3,709,853, **1973**. d) Reagan, W. K. (Phillips Petroleum Company) EP 0417477, **1991**. e) Tanaka, E.; Urata, H.; Oshiki, T.; Aoshima, T.; Kawashima, R.; Iwade, S.; Nakamura, H.; Katsuki, S.; Okan, T. (Mitsubishi Chemical Corporation) EP 0611743, **1994**. f) Mimura, H.; Aoyama, T.; Yamamoto, T.; Oguri, M.; Koie, Y. (Tosoh Corporation) JP 09268133, **1997**. g) Wu, F. J. (Amoco Corporation) US 5811618, **1998.** h) Dixon, J. T.; Wasserscheid, P.; McGuinness, D. S.; Hess, F. M.; Maumela, H.; Morgan, D.H.; Bollmann, A. (Sasol Technology (Pty) Ltd) WO 03053890, **2001**. i) Yoshida, T.; Yamamoto, T.; Okada, H.; Murakita, H. (Tosoh Corporation) US2002/0035029, **2002**. j) Grove, J. J. C.; Mahome, H. A.; Griesel, L. (Sasol Technology) WO 03/004158, **2002**. k) Wass, D. F. (BP Chemicals Ltd) WO 02/04119, **2002**. l) Han, T. K.; Ok, M. A.; Chae, S. S.; Kang, S. O.; Jung, J. H. WO Patent 2008/088178(SK Energy), **2008**.
4. a) Blann, K.; Bollmann, A.; Dixon, J. T.; Hess, F. M.; Killian, E.; Maumela, H.; Morgan, D. H.; Neveling, A.; Otto, S.; Overett, M. *Chem. Commun.* **2005**, 620. b)

Bowen, L. E.; Haddow, M. F.; Orpen, A. G.; Wass, D. *Dalton Trans* **2007**, 1160. c) Jabri, A.; Mason, C. B.; Sim, Y.; Gambarotta, S.; Burchell, T. J.; Duchateau, R. *Angew. Chem. Int. Ed.* **2008**, *47*, 9717. d) Klemps, C.; Payet, E.; Magna, L.; Saussine, L.; Le Goff, X.F.; Le Floch, P. *Chem A Eur. J*. **2009**, *15*, 8259; See for example: e) Vidyaratne, I. ; Nikiforov, G. B.; Gorelski, S. I.; Gambarotta, S.; Duchateau, R.; Korobkov, I. *Angew. Chem. Int. Ed.* **2009**, *48*, 6522. f) Skobelev, I. Y.; Panchenko, V. N.; Lyakin, O. Y.; Bryliakov, K. P. V.; Zakharov, A.; Talsi, E. P. *Organometallics* **2010**, *29*, 2943. g) Dulai, A.; de Bod, H.; Hanton, M. J.; Smith, D. M.; Downing, S.; Mansell, S. M.; Wass, D. F. *Organometallics* **2009**, *28*, 4613.

5. a) Bollmann, A.; Blann, K.; Dixon, J. T.; Hess, F. M.; Killian, E.; Maumela, H.; McGuinness, D. S.; Morgan, D. H.; Neveling, A.; Otto, S.; Overett, M.; Slawin, A. M. Z.; Wasserscheid, P.; Kuhlmann S. *J. Am. Chem. Soc*. **2004**, *126*, 14712. b) Albahily, K.; Koç, E.; Al-Baldawi, D.; Savard, D.; Gambarotta, S.; Burchell, T. J.; Duchateau, R. *Angew. Chem. Int. Ed. Engl.* **2008**, *47*, 5816. c) Albahily, K.; Al-Baldawi, D.; Gambarotta, S.; Duchateau, R.; Koç, E.; Burchell, T. J. *Organometallics* **2008**, *27* , 5943.
6. a) Mohamed, H.; Bollmann, A.; Dixon, J.; Gokul, V.; Griesel, L.; Grove, C.; Hess, F.; Maumela, H.; Pepler, L. *Appl. Catal. A.* **2003**, *255*, 355. b) McGuinness, D. S.; Wasserscheid, P.; Keim, W.; Morgan, D. H.; Dixon, J. T.; Bollmann, A.; Maumela, H.; Hess, F. M.; Englert, U. *J. Am. Chem. Soc*. **2003**, *125*, 5272. c) Agapie, T.; Schofer, S. J.; Labinger, J. A.; Bercaw, J. E. *J. Am. Chem. Soc.* **2004**, *126*, 1304. d) Tomov, A. K.; Chirinos, J. J.; Long, R. J.; Gibson, V. C.; Elsegood, M. R. J. *J. Am. Chem. Soc.* **2006**, *128*, 7704. e) Agapie, T.; Labinger, J. A.; Bercaw, J. E. *J. Am.*

Chem. Soc. **2007**, *129*, 14281. f) McGuinness, D. S.; Suttil, J. A.; Gardiner, M. G.; Davies, N. W. *Organometallics* **2008**, *27*, 4238.

7. a) Temple, C.; Jabri, A.; Crewdson, P.; Gambarotta, S.; Korobkov, I.; Duchateau, R. *Angew. Chem.* **2006**, *118*, 7208; *Angew. Chem. Int. Ed*. **2006**, *45*, 7050. b) Jabri, A.; Temple, C.; Crewdson, P.; Gambarotta, S.; Korobkov, I.; Duchateau, R. *J. Am. Chem.Soc.* **2006**, *128*, 9238. c) Emrich, R.; Heinemann, O.; Jolly, C. W.; Kruger, C.; Verhonok, G. p. *J.Organometallics* **1997**, *16*, 1511.
8. a) Kuhlmann, S.; Blann, K.; Bollmann, A.; Dixon, J. T.; Killian, E.; Maumela, M. C.; Maumela, H.; Morgan, D. H.; Pr_torius, M.; Taccardi, N.; Wasserscheid, P. *J. Catal.* **2006**, *245,* 279, and references therein. b) Bollmann, A.; Blann, K.; Dixon, J. T.; Hess, F. M.; Killian, E.; Maumela, H.; McGuinness, D. S.; Morgan, D. H.; Neveling, A.; Otto, S.; Overett, M.; Slawin, A. M. Z.; Wasserscheid, P.; Kuhlmann S. *J. Am. Chem. Soc*.**2004**, *126*, 14712.
9. Han, T.K. M.; Ok, A.; Chae, S. S.; Kang, S. O. (SK Energy Corporation), WO 2008/088178, **2008**.
10. a) Carter, A.; Cohen, S. A.; Cooley, N. A.; Murphy, A.; Scutt, J.; Wass, D. F. *Chem. Commun.* **2002**, 858. b) McGuinness, D. S.; Wasserscheid, P.; Keim, W.; Hu, C.; Englert, U.; Dixon, J. T.; Grove, C. *Chem. Commun*. **2003**, 334. c) Zhang, J.; Braunstein, P.; Hor, T. S. A.; *Organometallics* **2008**, *27*, 4277.
11. Peitz, S.; Aluri, B. R.; Peulecke, N.; Müller, B. H.; Wöhl, A.; Müller, W.; Al-Hazmi, M. H.; Mosa, F. M.; Rosenthal, U. *Chem. Eur. J.* **2010**, *16*, 7670.
12. a) Licciulli, S.; Thapa, I.; Albahily, K.; Korobkov, I.; Gambarotta, S.; Duchateau, R.; Chevalier, R.; Schuhen, K. *Angew. Chem. Int. Ed*. **2010,** *49* (48), 9225. b)

Shaikh, Y.; Albahily, K.; Sutcliffe, M.; Fomitcheva, V.; Gambarotta, S.; Korobkov, I.; Duchateau, R. *Angew. Chem. Int. Ed.* **2012**, *51*, 1366.

13. a) Overett, M. J.; Blann, K.; Bollmann, A.; Dixon, J. T.; Hess, F. M.; Killian, E.; Maumela,.M. C.; Morgan, D. H.; Neveling, A.; Otto, S. *Chem.Commun.* **2005**, 622. b) Peitz, S.; Peulecke, N.; Aluri, B. R.; Hansen, S.; Müller, B. H.; Spannenberg, A.; Rosenthal, U.; Al-Hazmi, M. H.; Mosa, F. M.; Wöhl, A.; Müller, W. *Eur. J. Inorg. Chem*. **2010**, 1167. c) Bluhm, M. E.; Walter, O.; Doring, M. *J. Organomet. Chem*. **2005**, *690*, 713. d) Blann, K.; Bollmann, A.; Dixon, J. T.; Neveling, A.; Morgan, D. H.; Maumela,H.; Killian, E.; Hess, F.; Otto, S.; Pepler, L.; Mahomed, H.; Overett, M. WO Patent 04056479A1 (Sasol Technology), **2004**. e) Gao, X.; Carter, C. A. G.; Henderson, L.D. WO Patent 2010/034102 (Nova Chemicals), **2010**. f) Elowe, P. R.; McCann, C.; Pringle, P. G.; Spitzmesser, S. K.; Bercaw, J. E. *Organometallics* **2006**, *25*, 5255.

14. Thapa, I.; Gambarotta, S.; Duchateau, R.; Kulangara, S. V; Chevalier, R. *Organometallics* **2010**, *29*(18), 4080.

15. Thapa, I.; Gambarotta, S.; Korobkov, I.; Murugesu, M.; Budzelaar, P. *Organometallics* **2012**, *31*(1), 486.

16. Blank, B; Madalska, M; Kempe, R. *Advanced synthesis & catalysis*, **2008**, *350* (5), 749.

17. K. Albahily, Y. Shaikh, E. Sebastiao, S. Gambarotta, I. Korobkov, S. I. Gorelsky, *J. Am. Chem. Soc*.**2011**, *133*, 6388.

18. Kim, S.G.; Kim, T.J.; Chung, J.H.; Hahn, T.K.; Chae, S.S.; Lee, H.S.; Cheong, M.; Kang, S. O. *Organometallics* **2010**, *29*, 5805.

19. Hao, S.; Gambarotta, S.; Bensimon, C. *J. Am. Chem. Soc*. **1992**, *114*, 3556.

20. Krausse, J.; Mark, G.; Schoedl, G. *J. Organomet. Chem.* **1970**, *21*, 159.

Publication:

Licciulli, S.; **Thapa, I**.; Albahily, K.; Korobkov, I.; Gambarotta, S.; Duchateau, R.; Chevalier, R.; Schuhen, K. *Angew. Chem. Int. Ed*. **2010,** *49*(48), 9225-9228.

Patent:

Schuhen, K; Chevalier, R; Gambarotta, S; Licciulli, S; **Thapa, I**; Duchateau, R.
PCT Int. Appl. (**2011**), WO 2011085951 A1 20110721

Towards Selective Ethylene Tetramerization

4.1 Introduction

As already mentioned in the previous chapters the metallacycle mechanism formulated to account for the excellent selectivity of catalytic ethylene-trimerization processes is well-established today.[1-3] Further ring expansion through the insertion of a fourth ethylene unit is believed to afford 1-octene.[4] However, selectivity becomes a major challenge in this event. If a fourth molecule of ethylene can be inserted readily into a seven-membered ring, it is clearly very difficult to prevent further expansion of the nine-membered ring (and thus the formation of heavier oligomers). In fact, in the entire patent and academic literature, only two homogeneous catalytic systems, discovered by researchers at Sasol[4a] and SK Energy,[4b] have been described that are capable of producing a substantial excess of 1-octene (about 70%) over other α-olefins and hence used for the commercial production of 1-octene.

The search for a catalytic system capable of producing 1-octene as the only product is still being pursued actively. One may even question whether selective tetramerization to produce solely 1-octene may ever be possible, unless an alternate mechanistic pathway is followed. In our

search for highly selective ethylene-tetramerization catalysts, we selected the 2,2'-dipyridylamine ligand with an alkylated central nitrogen atom. Alkylation of the central N atom to prevent anionization was deemed necessary to maintain the possibility of cationizing the monovalent metal center, as necessary for catalytic activity.[1p] Alkylation of the central nitrogen atom was also expected to diminish the established tendency of the ligand to form multiply bonded dimers or higher aggregates,[5] because of sterically induced deformation of the ligand backbone.[6]

Herein we report our discovery of an unprecedented tetramerization chromium catalyst displaying selectivity up to 99% by using an alkylated 2'2-dipyridylamine ligand. Its structure, activity and a possible deactivation pathway during the oligomerization process are also described.

4.2 Experimental Section

All reactions were carried out under a dry nitrogen atmosphere in Schlenk line or in a purified nitrogen-filled drybox. Solvents were dried using an aluminum oxide solvent purification system except for anhydrous DMF which was purchased from Sigma-Aldrich and used as received. 2,2'-dipyridylamine, 1-chloro-2,2-dimethylpropane and any other alkyl halide used for the synthesis of the ligands were purchased from Sigma-Aldrich and used without further purification. KH was purchased from Strem Chemicals, washed with hexane and dried prior to use. $CrCl_3(THF)_3$, $CrCl_2(THF)_2$ and $Cr(NCy_2)_3$ were prepared according to standard procedures. MAO (10% wt in Toluene) was purchased from Sigma-Aldrich. Ethylene was purchased from BOC Gases (polymer grade 3.0) and used as received. GC-MS analysis of the ligands and the oligomers was obtained with a Hewlett–Packard HP 5973 gas chromatograph using an Agilent DB1 column. Elemental analyses were carried out with a Perkin-Elmer 2400

CHN analyzer. Infrared spectra were recorded on ABB Bomem FT-IR instrument from Nujol mulls prepared in a dry box. Samples for magnetic susceptibility were weighed inside a dry box equipped with an analytical balance and sealed into calibrated tubes and measurements were carried out with a Johnson Matthey Magnetic Susceptibility balance at room temperature. Data for the X-ray crystal structure determinations were obtained with a Bruker diffractometer equipped with a Smart CCD area detector and with Bruker Kappa APEXII CCD diffractometer. NMR spectra were recorded on Varian Inova 500 MHz, Bruker Avance 500 and 300 spectrometers; all chemical shifts have been quoted relative to deuterated solvent signals, δ in ppm. All the polymerization reactions were performed in a Büchi high pressure 300 ml reactor.

4.2.1 N-neopentyl-N-(pyridin-2-yl)pyridine-2-amine (b)

A solution of 2,2'-dipyridylamine (10.0 g, 54.5 mmol) in dry DMF (100 mL) was stirred under N_2 at 0°C for 15 min. Solid KH (2.62 g, 65.4 mmol) was added portion wise and the resulting mixture was stirred at 0°C for 1.5h. 1-chloro-2,2-dimethylpropane (6.57 g, 71.0 mmol) was added and the resulting yellow/green solution was refluxed at 70-75°C for 2 days. EtOH (10 mL) was added to quench the reaction (**CAUTION**). The resulting mixture was stirred for 20 min and all the solvents were evaporated under reduced pressure. The resulting thick yellow oil was treated with Et_2O (30 mL) forming a yellow suspension which was filtered. The liquid organic phase was separated and evaporated under reduced pressure to give yellow oil which was purified by column chromatography on silica gel (Hexane/AcOEt 8/2). Pure **b** was obtained as white crystalline material (9.72 g, 40.3 mmol, 74% yield). ^{1}H-NMR (300 MHz, $CDCl_3$, 25^{o}C) δ: 0.87 (9H, s, -*t*Bu), 4.19 (2H, s, CH_2-*t*Bu), 6.84 (2H, m, Py), 7.04 (2H, d, J = 8.1 Hz, Py), 7.49 (2H, t, J = 7.7 Hz, Py), 8.33 (2H, d, J = 3.9 Hz, Py). ^{13}C{H}-NMR (300 MHz, $CDCl_3$, 25^{o}C) δ:

28.5 (-CH_3), 34.3 (-C-), 57.7 (-CH_2-), 115.4 (Py), 116.9 (Py), 136.9 (Py), 148.8 (Py), 158.7 (Py). ES-MS *m/z* = 241.2 ($M^+ + H^+$), 184.1, 78.0.

4.2.2 N-(trimethylsilyl)methyl-N-(pyridin-2-yl)pyridine-2-amine (c)

The same procedure as for **b** was followed by replacing 1-chloro-2,2-dimethylpropane with (chloromethyl)trimethylsilane and the crude yellow oil was purified by column chromatography on silica gel (Hexane/AcOEt 9/1). The pure product was obtained as pale yellow oil (11.72 g, 45.5 mmol, 83% yield). ^{1}H-NMR (300 MHz, $CDCl_3$, 25^{o}C) δ: -0.02 (9H, s, -$Si(CH_3)_3$), 3.78 (2H, s, CH_2-$Si(CH_3)_3$), 6.80 (2H, ddd, J_1 = 0.9 Hz, J_2 = 4.9 Hz, J_3 = 7.2 Hz, Py), 7.13 (2H, d, J = 8.5 Hz, Py), 7.48 (2H, ddd, J_1 = 2.1 Hz, J_2 = 7.2 Hz, J_3 = 8.5 Hz, Py), 8.31 (2H, ddd, J_1 = 0.8 Hz, J_2 = 1.9 Hz, J_3 = 4.9 Hz, Py). ^{13}C{1H}-NMR (300 MHz, $CDCl_3$, 25^{o}C) δ: -1.1 (-CH_3), 39.7 (-CH_2-), 114.2 (Py), 116.3 (Py), 136.7 (Py), 147.9 (Py), 157.8 (Py). ES-MS *m/z* = 257.1 ($M^+ + H^+$), 242.1 ($M^+ + H^+ - CH_3$), 184.1, 150.1, 78.0.

4.2.3 N-hexadecyl-N-(pyridin-2-yl)pyridine-2-amine (d)

The same procedure as for **b** was followed by replacing 1-chloro-2,2-dimethylpropane with 1-bromohexadecane and the crude brown oil was purified by column chromatography on silica gel (Hexane/AcOEt 9/1). The pure product was obtained as white crystalline material (17.25 g, 43.6 mmol, 80% yield). ^{1}H-NMR (300 MHz, $CDCl_3$, 25^{o}C) δ: 0.87 (3H, t, J = 6.5 Hz, -CH_3), 1.23-1.38 (26H, m, -$(CH_2)_{13}$-), 1.65-1.77 (2H, m, -CH_2-($C_{14}H_{29}$), 4.15 (2H, t, J = 7.6 Hz, -CH_2-($C_{15}H_{31}$), 6.83 (2H, dd, J_1 = 5.4 Hz, J_2 = 6.7 Hz, Py), 7.07 (2H, d, J = 8.4 Hz, Py), 7.47-7.55 (2H, m, Py), 8.33 (2H, d, J = 3.0 Hz, Py). ^{13}C{1H}-NMR (300 MHz, $CDCl_3$, 25^{o}C) δ: 14.1 (-CH_3), 22.6, 27.0, 28.3, 29.3, 29.4, 29.6, 31.9 (-CH_2-), 48.3 (N-CH_2-), 114.6 (Py), 116.7 (Py),

137.0 (Py), 148.2 (Py), 157.5 (Py). ES-MS *m/z* = 395.3 ($M^+ + H^+$), 317.3, 275.3, 198.0, 184.1, 171.2, 106.1, 78.0.

4.2.4 N-(triethoxysilyl)propyl-N-(pyridin-2-yl)pyridine-2-amine (f)

The same procedure as for **b** was followed by replacing 1-chloro-2,2-dimethylpropane with (3-chloropropyl)triethoxysilane and the crude brown oil was purified by column chromatography on silica gel (Hexane/AcOEt 9/1). The pure product was obtained as colorless oil (15.35 g, 40.9 mmol, 75% yield). ^{1}H-NMR (300 MHz, $CDCl_3$, 25^{o}C) δ: 0.65-0.71 (2H, m, -CH_2-Si), 1.18 (9H, t, *J* = 7.0 Hz, -CH_3), 1.75-1.86 (2H, m, -CH_2-), 3.78 (6H, q, *J* = 7.0 Hz, O-CH_2-), 4.16 (2H, t, *J* = 7.8 Hz, N-CH_2-), 6.82 (2H, ddd, J_1 = 0.9 Hz, J_2 = 4.9 Hz, J_3 = 7.2 Hz, Py), 7.09 (2H, dt, J_1 = 0.9 Hz, J_2 = 8.4 Hz, Py), 7.50 (2H, ddd, J_1 = 2.0 Hz, J_2 = 7.2 Hz, J_3 = 8.4 Hz, Py), 8.31 (2H, ddd, J_1 = 0.9 Hz, J_2 = 2.0 Hz, J_3 = 4.9 Hz, Py). ^{13}C{1H}-NMR (300 MHz, $CDCl_3$, 25^{o}C) δ: 7.4 (Si-CH_2-), 18.2 (-CH_3), 21.2 (-CH_2-), 50.7 (N-CH_2-), 58.2 (O-CH_2-), 114.6 (Py), 116.7 (Py), 136.9 (Py), 148.1 (Py), 157.3 (Py). ES-MS *m/z* = 375.2 ($M^+ + H^+$), 330.2, 255.1, 198.1, 184.1, 171.2, 119.1, 78.0.

4.2.5 N-(4-ethoxybutyl)-N-(pyridin-2-yl)pyridine-2-amine (g)

The same procedure as for **b** was followed by replacing 1-chloro-2,2-dimethylpropane with 1-chloro-4-ethoxybutane and the crude brown oil was purified by column chromatography on silica gel (Hexane/AcOEt 9/1). The pure product was obtained as colourless oil (10.94 g, 40.3 mmol, 74% yield). ^{1}H-NMR (300 MHz, $CDCl_3$, 25^{o}C) δ: 1.16 (3H, t, *J* = 7.0 Hz, -CH_3), 1.57-1.68 (2H, m, -CH_2-), 1.69-1.81 (2H, m, -CH_2-), 3.42 (2H, t, *J* = 6.6 Hz, O-CH_2-), 3.44 (2H, q, *J* = 7.0 Hz, O-CH_2-), 4.20 (2H, t, *J* = 7.5 Hz, N-CH_2-), 6.83 (2H, ddd, J_1 = 0.9 Hz, J_2 = 4.9 Hz, J_3 = 7.2 Hz, Py), 7.08 (2H, dt, J_1 = 0.9 Hz, J_2 = 8.4 Hz, Py), 7.49 (2H,ddd, J_1 = 2.0 Hz, J_2 = 7.2 Hz, J_3

= 8.4 Hz, Py), 8.32 (2H, ddd, J_1 = 0.9 Hz, J_2 = 2.0 Hz, J_3 = 4.9 Hz, Py). ^{13}C{1H}-NMR (300 MHz, $CDCl_3$, 25^{o}C) δ: 15.2 (-CH_3), 25.0 (-CH_2-), 27.2 (-CH_2-), 48.0 (-CH_2-N), 66.0 (-CH_2-O), 70.4 (-CH_2-O), 114.7 (Py), 116.8 (Py), 137.0 (Py), 148.3 (Py), 157.4 (Py). ES-MS *m/z* = 271.2 ($M^+ + H^+$), 242.1, 226.1, 198.1, 184.1, 170.1, 147.1, 78.0.

4.2.6 6-methyl-N-(6-methylpyridin-2-yl)-N-(3-(triethoxysilyl)propyl) pyridyne-2-amine (h).

A solution of 2-Br-6-Me-pyridine (5.0 g, 29.0 mmol) and 2-amino-6-Me-pyridine (3.44 g, 31.9 mmol) in anhydrous toluene (450 ml) was treated with $Pd_2(dba)_3$ (1.33 g, 1.45 mmol), BINAP (0.68 g, 1.1 mmol) and *t*BuOK (5.29 g, 47.3 mmol) added in rapid sequence. The resulting brown mixture was refluxed at 90°C overnight. Et_2O (240 ml) was added to the reaction mixture after cooling to room temperature. The inorganic salts are removed by filtration through Celite and the organic layer evaporated at reduced pressure to give crude 6,6'-dimethyl-2,2'-dipyridylamine as orange/brown crystaline material. The compound was sufficiently pure (^{1}H-NMR analysis) to be used for the next alkylation step. The same procedure as for **b** was followed for the alkylation of 6,6'-dimethyl-2,2'-dipyridylamine by replacing 1-chloro-2,2-dimethyl propane with (3-chloropropyl)triethoxysilane. The crude brown thick oil obtained after work-up was purified by column chromatography on silica gel (Hexane/AcOEt 9/1). The pure product was obtained as yellow oil (7.02 g, 17.4 mmol, 60% overall yield). ^{1}H-NMR (300 MHz, $CDCl_3$, 25^{o}C) δ: 0.65-0.71 (2H, m, -CH_2-Si), 1.19 (9H, t, *J* = 7.0 Hz, -CH_3), 1.75-1.88 (2H, m, -CH_2-), 2.43 (6H, s, CH_3-Py), 3.79 (6H, q, *J* = 7.0 Hz, O-CH_2-), 4.16 (2H, t, *J* = 7.7 Hz, N-CH_2-), 6.66 (2H, d, *J* = 7.3 Hz, Py), 6.86 (2H, d, *J* = 8.2 Hz, Py), 7.35 (2H, t, *J* = 7.8 Hz, Py). ^{13}C{1H}-NMR (300 MHz, $CDCl_3$, 25^{o}C) δ: 7.5 (Si-CH_2-), 18.2 (-CH_3), 21.3 (-CH_2-), 24.4 (CH_3-Py), 50.7 (N-CH_2-), 58.2 (O-CH_2-), 111.4 (Py), 115.7 (Py), 137.0 (Py), 156.9 (Py), 157.0 (Py). ES-MS *m/z* = 403.2 ($M^+ + H^+$), 358.2, 269.1, 226.1, 212.1, 199.0, 184.1, 163.1, 119.1, 92.0, 65.0.

4.2.7 4-methyl-N-(4-methylpyridin-2-yl)-N-(3-(triethoxysilyl)propyl) pyridine-2-amine (i)

The same procedure as for 6,6'-dimethyl-2,2'-dipyridylamine was followed by replacing 2-Br-6-Me-pyridine with 2-Br-4-Me-pyridine and 2-amino-6-Me-pyridine with 2-amino-4-Me-pyridine. The usual work-up gave crude 4,4'-dimethyl-2,2'-dipyridylamine as brownish crystalline material which was sufficiently pure according to ^{1}H-NMR analysis for the following step. The same procedure as for ligand **b** was followed for the alkylation of 4,4'-dimethyl-2,2'-dipyridylamine by replacing 1-chloro-2,2-dimethylpropane with (3-chloropropyl)triethoxy silane and the crude brown thick oil was purified by column chromatography on silica gel (Hexane/AcOEt 9/1). The pure product was obtained as yellow viscous oil (5.85 g, 14.5 mmol, 50% overall yield). ^{1}H-NMR (300 MHz, $CDCl_3$, 25^{o}C) δ: 0.61-0.71 (2H, m, -CH_2-Si), 1.16 (9H, t, *J* = 7.0 Hz, -CH_3), 1.69-1.83 (2H, m, -CH_2-), 2.22 (6H, s, CH_3-Py), 3.77 (6H, q, *J* = 6.9 Hz, O-CH_2-), 4.09 (2H, t, *J* = 7.5 Hz, N-CH_2-), 6.64 (2H, d, *J* = 4.8 Hz, Py), 6.84 (2H, s, Py), 8.14 (2H, d, *J* = 4.8 Hz, Py). ^{13}C{1H}-NMR (300 MHz, $CDCl_3$, 25^{o}C) δ: 7.3 (Si-CH_2-), 18.1 (-CH_3), 21.1 (CH_3-Py), 21.2 (-CH_2-), 50.9 (N-CH_2-), 58.2 (O-CH_2-), 115.1 (Py), 118.1 (Py), 147.8 (Py), 147.9 (Py), 157.6 (Py). ES-MS *m/z* = 403.2 ($M^+ + H^+$), 358.2, 269.1, 226.1, 212.1, 199.0, 184.1, 121.1, 92.1.

4.2.8 N-(4-fluoro-N-(pyridin-2-yl)pyridine-2-amine (j)

The same procedure as for **b** was followed by replacing 1-chloro-2,2-dimethylpropane with 1-chloro-4-fluorobutane and the crude brown oil was purified by column chromatography on silica gel (Hexane/AcOEt 9/1). The pure product was obtained as colorless oil (12 g, 48.8 mmol, 86.2% yield). ^{1}H-NMR (300 MHz, $CDCl_3$, 25^{o}C) δ: 1.57-1.68 (2H, m, -CH_2-), 1.69-1.72 (2H, m, -CH_2-), 4.17-4.20 (2H, m, -CH_2-F), 4.75 (2H, m, -CH-N), 6.63 (2H, ddd, J_1 = 0.9 Hz, J_2

= 4.9 Hz, J_3 = 7.2 Hz, Py), 7.46 (2H, dt, J_1 = 0.9 Hz, J_2 = 8.4 Hz, Py), 7.56 (2H, ddd, J_1 = 2.0 Hz, J_2 = 7.2 Hz, J_3 = 8.4 Hz, Py), 8.37 (2H, ddd, J_1 = 0.9 Hz, J_2 = 2.0 Hz, J_3 = 4.9 Hz, Py). ^{13}C{1H}-NMR (300 MHz, $CDCl_3$, 25^{o}C) δ: 25.1 (-CH_2-), 28.2 (-CH_2-), 29.4 (-CH_2-), 45.6 (-CH-N), 84.7, 88.5 (-CH_2-F), 109.4 (Py), 119.8 (Py), 136.0 (Py), 147.5 (Py), 161.2 (Py). ES-MS *m/z* = 245.1 ($M^+ + H^+$), ^{19}F NMR: -60.73.

4.2.9 N-(2- ethoxyethyl)-N-(pyridin-2-yl)pyridine-2-amine (k)

The same procedure as for **b** was followed by replacing 1-chloro-2,2-dimethylpropane with 1-chloro-2- ethoxyethyl and the crude brown oil was purified by column chromatography on silica gel (Hexane/AcOEt 9/1). The pure product was obtained as colorless oil (9.2 g, 38.1 mmol, 70% yield). ^{1}H-NMR (300 MHz, $CDCl_3$, 25^{o}C) δ: 1.16 (3H, t, J = 7.0 Hz, -CH_3), 3.42 (2H, t, J = 6.6 Hz, O-CH_2-), 3.44 (2H, q, J = 7.0 Hz, O-CH_2-), 4.20 (2H, t, J = 7.5 Hz, N-CH_2-), 6.83 (2H, ddd, J_1 = 0.9 Hz, J_2 = 4.9 Hz, J_3 = 7.2 Hz, Py), 7.08 (2H, dt, J_1 = 0.9 Hz, J_2 = 8.4 Hz, Py), 7.49 (2H, ddd, J_1 = 2.0 Hz, J_2 = 7.2 Hz, J_3 = 8.4 Hz, Py), 8.32 (2H, ddd, J_1 = 0.9 Hz, J_2 = 2.0 Hz, J_3 = 4.9 Hz, Py). ^{13}C{1H}-NMR (300 MHz, $CDCl_3$, 25^{o}C) δ: 15.2 (-$CH_{3)}$, 48.0 (-CH_2-N), 66.0 (-CH_2-O), 70.4 (-CH_2-O), 114.7 (Py), 116.8 (Py), 137.0 (Py), 148.3 (Py), 157.4 (Py). ES-MS *m/z* = 243.3 (M^+).

4.2.10 2-(2-Pyridylmethyl)pyridine (l)

Prepared according to the published literature.[6d]

4.2.11 (Trimethylsilyl)methyl-N-(pyridin-2-yl)pyridine (m)

Ligand **m** is alkylated as mentioned in **b** affording (10.0 g, 39.2 mmol, 72%).

^{1}H-NMR (300 MHz, $CDCl_3$, 25^{o}C) δ: -0.21 (9H, s, -Si(CH_3)$_3$), 1.58 (2H, s, CH_2-Si(CH_3)$_3$), 4.43-4.51 (1H, m, -CH-), 7.01 (2H, ddd, J_1 = 0.9 Hz, J_2 = 4.9 Hz, J_3 = 7.2 Hz, Py), 7.42 (d, J = 8.5 Hz, 2H, Py), 7.58 (2H, ddd, J_1 = 2.1 Hz, J_2 = 7.2 Hz, J_3 = 8.5 Hz, Py), 8.0 (2H, ddd, J_1 = 0.8 Hz, J_2 = 1.9 Hz, J_3 = 4.9 Hz, Py). ^{13}C{1H}-NMR (300 MHz, $CDCl_3$, 25^{o}C) δ: -0.03 (-CH_3), 19.7 (-CH_2-), 39.9 (-CH-), 115.2 (Py), 121.3 (Py), 136.7 (Py), 149.9 (Py), 164.3 (Py). ES-MS *m/z* = 256.1 (M^+).

4.2.12 Neopentyl-N-(pyridin-2-yl)pyridine (n).

Ligand **n** was prepared as mentioned in **b** affording (9.1 g, 38.2 mmol, 65%).

^{1}H-NMR (300 MHz, $CDCl_3$, 25^{o}C) δ: 0.86 (9H, s, -*t*Bu), 2.19 (2H, m, CH_2-*t*Bu), 3.42 (1H, m, -CH-), 6.64 (2H, m, Py), 7.5 (2H, d, J = 8.1 Hz, Py), 7.6 (2H, t, J = 7.7 Hz, Py), 8.53 (2H, d, J = 3.9 Hz, Py). ^{13}C{1H}-NMR (300 MHz,$CDCl_3$, 25^{o}C) δ: 22.5 (-C-), 31.3 (-CH_3), 42.64 (-CH_2-), 43.0(-CH-), 115.9 (Py), 122.9 (Py), 136.7 (Py), 149.8 (Py), 162.5 (Py). ES-MS *m/z* = 240.1(M+).

4.2.13 2-(2-Pyridylethyl)pyridine (**o**)

Purchased from commercial sources and used as obtained.

4.2.14 Preparation of Complex [{(2-$C_5H_4N)_2$NMe}$CrCl_3$(thf)] (4.1a)

The preparation was carried out following the same procedure as per **4.1c** affording **4.1a** as a light green powder (1.151 g, 2.77 mmol, 94%). Elemental Analysis Calcd. (Found) for $C_{15}H_{19}Cl_3CrN_3O$: C 43.34 (42.04), H 4.61 (4.43), N 10.11 (9.81). [μ_{eff} = 3.86 μ_B].

4.2.15 Preparation of Complex [{(2-$C_5H_4N)_2$N(CH_2CMe_3)}$CrCl_3$(thf)] (4.1b)

A solution of **b** (1.98 g, 7.7 mmol) in THF (10 mL) was added to a preheated (60 ºC) suspension of $CrCl_3(THF)_3$ (2.88 g, 7.7 mmol) in THF (50 mL). The resulting mixture was stirred and refluxed until the purple solid $CrCl_3(THF)_3$ disappeared (ca. 10 minutes). The mixture was cooled to room temperature and stirring continued for 6 hours. The green **1b** (1.37 g, 2.90 mmol, 90%) was filtered, washed with THF (5 x 5 mL) and dried in vacuum. Single crystals suitable for X-ray crystallography were grown from a diluted THF solution stored at room temperature. Elemental Analysis Calcd. (Found) for $C_{19}H_{27}Cl_3CrN_3O$: $C_{19}H_{27}Cl_3\,CrN_3O$: C 48.37 (48.13), H 5.77 (5.73), N 8.91 (8.62). [μ_{eff} = 3.81 μ_B].

4.2.16 Preparation of Complex [{(2-$C_5H_4N)_2N(CH_2SiMe_3)$}$CrCl_3$(thf)] (4.1c)

$CrCl_3(THF)_3$ (0.750 g, 2.0 mmol) was added to a solution of **c** (0.514 g, 2.0 mmol) in THF (10 mL) and the mixture stirred overnight. The color turned slowly from purple to green. The clear green solution was separated through centrifugation from the insoluble materials and evaporated to dryness. The resulting **4.1c** was isolated as a fine green solid which was washed with hexane (5 x 5 mL) and dried in vacuum (0.937 g, 1.92 mmol, 96%). Elemental Analysis Calcd. (Found) for $C_{18}H_{27}Cl_3CrN_3OSi$: C 44.31 (44.66), H 5.58 (5.54), N 8.61 (8.35.). [μ_{eff} = 3.94 μ_B].

4.2.17 Preparation of Complex [{(2-$C_5H_4N)_2N(C_{16}H_{33})$}$CrCl_3$(thf)] (4.1d)

The preparation was carried out following the same procedure as per **4.1c** affording **4.1d** as green powder (1.202 g, 1.92 mmol, 96%). Elemental Analysis Calcd. (Found) for $C_{30}H_{49}Cl_3CrN_3O$: C 57.55 (57.26), H 7.89 (7.84), N 6.71 (6.76). [μ_{eff} = 3.83 μ_B].

4.2.18 Preparation of Complex [{(2-$C_5H_4N)_2N$(benzyl)}$CrCl_3$(thf)] (4.1e)

The preparation was carried out following the same procedure as per **4.1c** affording **4.1e** as green powder (0.915 g, 1.86 mmol, 93%). Elemental Analysis Calcd. (Found) for $C_{21}H_{23}Cl_3CrN_3O$: C 51.29 (51.60), H 4.71 (4.75), N 8.54 (8.57). [μ_{eff} = 3.82 μ_B]. Single crystals suitable for X-ray crystallography were grown from a saturated THF solution stored at room temperature.

4.2.19 Preparation of Complex [{(2-$C_5H_4N)_2NC_3H_6$Si(OEt)$_3$}$CrCl_3$(thf)] (4.1f)

The preparation was carried out following the same procedure as per **4.1c** affording **4.1f** as a greysh powder (1.151 g, 1.90 mmol, 95%). Elemental Analysis Calcd. (Found) for $C_{23}H_{37}Cl_3CrN_3O_4Si$: C 45.59 (45.31), H 6.15 (6.08), N 6.93 (6.79). [μ_{eff} = 3.81 μ_B].

4.2.20 Preparation of Complex [{(2-$C_5H_4N)_2N(C_4H_8OEt)$}$CrCl_3$(thf)] (4.1g)

The preparation was carried out following the same procedure as per **4.1c** affording **4.1g** as a green powder (0.923 g, 1.84 mmol, 92%). Elemental Analysis Calcd. (Found) for $C_{20}H_{29}Cl_3CrN_3O_2$: C 47.87 (47.58), H 5.82 (5.76), N 8.37 (8.20). [μ_{eff} = 3.83 μ_B]. Single crystals suitable for X-ray crystallography were grown from a diluted THF solution stored at room temperature.

4.2.21 Preparation of Complex [{(2-$C_5H_4N)_2NCH_2SiMe_3$}$CrMeCl_2$(thf)] (4.2c)

A solution of MeLi (1.1 mmol, 1.6 M in Et_2O) was added to a suspension of $CrCl_3(THF)_3$ (0.376 g, 1 mmol) in THF (10 mL) at 0 ^oC. The resulting brown solution was stirred at room temperature for 15 minutes after which a solution of **c** (0.257 g, 1 mmol) in THF (5 mL) was added dropwise at room temperature. The resulting mixture was stirred for 5 minutes. The clear brown solution was separated through centrifugation from the insoluble materials and concentrated to 5 mL. Single crystals of **4.2c** suitable for X-ray crystallography were isolated

upon standing at -35°C for 2 days (0.416 g, 0.89 mmol, 89%). Elemental Analysis Calcd. (Found) for $C_{19}H_{30}Cl_2CrN_3OSi$: C 48.82 (48.48), H 6.47 (6.39), N 8.99 (8.78). [μ_{eff} = 3.94 μ_B].

4.2.22 Preparation of Complex [{(2-$C_5H_4N)_2NCH_2SiMe_3$}$CrCl_2$(DMF)] (4.3b)

The preparation was carried out following the same procedure as per **4.1c** affording **4.3b** as a green powder (0.707 g, 1.94 mmol, 97%). Elemental Analysis Calcd. (Found) for $C_{15}H_{19}Cl_2CrN_3$: C 49.46 (49.16), H 5.26 (5.19), N 11.54 (11.40). [μ_{eff} = 4.90 μ_B]. Single crystals suitable for X-ray crystallography were grown from a DMF/Et_2O solution stored at -15°C.

4.2.23 Preparation of Complex [{(2-$C_5H_4N)_2NC_3H_6Si(OEt)_3$}$CrCl_2$(DMF)] (4.3f)

The preparation was carried out following the same procedure as per **4.1c** affording **4.3b** as a light grey fine powder (0.957 g, 1.92 mmol, 96%). Elemental Analysis Calcd. (Found) for $C_{19}H_{29}Cl_2CrN_3O_3Si$: C 45.78 (46.14), H 5.86 (5.93), N 8.43 (8.64). [μ_{eff} = 4.88 μ_B].

4.2.24 Preparation of Complex [{2-(6-Me-$C_5H_4N)_2NC_3H_6$Si-$(OEt)_3$}$CrCl_3$(thf)] (4.4f)

The preparation was carried out following the same procedure as per **4.1b** affording **4.4f** as a purple fine powder (1.166 g, 1.84 mmol, 97%). Elemental Analysis Calcd. (Found) for $C_{25}H_{41}Cl_3CrN_3O_4Si$: C 47.36 (47.12), H 6.52 (6.41), N 6.63 (6.57). [μ_{eff} = 3.86 μ_B].

4.2.25 Preparation of Complex [{2-(6-Me-$C_5H_4N)_2NC_3H_6$Si-$(OEt)_3$}$CrCl_2$(thf)] (4.5f)

The preparation was carried out following the same procedure as per **4.1b** affording **4.5f** as a violet fine powder (1.021 g, 1.94 mmol, 97%). Elemental Analysis Calcd. (Found) for $C_{25}H_{41}Cl_2CrN_3O_3Si$: C 47.91 (48.43), H 6.32 (6.35), N 7.98 (8.12). [μ_{eff} = 4.91 μ_B].

4.2.26 Preparation of Complex [{2-(4-Me-$C_5H_4N)_2NC_3H_6Si$-$(OEt)_3$}$CrCl_3$(thf)] (4.6f)

The preparation was carried out following the same procedure as per **4.1c** affording **4.6f** as a light grey fine powder (1.078 g, 1.70 mmol, 85%). Elemental Analysis Calcd. (Found) for $C_{25}H_{41}Cl_3CrN_3O_4Si$: C 47.36 (47.22), H 6.52 (6.47), N 6.63 (6.54). [μ_{eff} = 3.83 μ_B].

4.2.27 Preparation of Complex [{(2-$C_5H_4N)_2NC_4H_9F$}$CrCl_3$(thf)] (4.7j)

The preparation was carried out following the same procedure as per **4.1c** affording **4.7j** as a green crystal (0.940 g, 1.84 mmol, 92%). Elemental Analysis Calcd. (Found) for C_{20} H_{28} Cl_3 Cr F N_3 $O_{1.5}$: C 46.97 (46.93), H 5.62 (5.51), N 8.37 (8.21). [μ_{eff} = 3.84 μ_B]. Single crystals suitable for X-ray crystallography were grown from a diluted THF solution on standing at room temperature.

4.2.28 Preparation of Complex [{(2-$C_5H_4N)_2N(C_2H_4OEt)$}$CrCl_3$(thf)] (4.8k)

The preparation was carried out following the same procedure as per **4.1c** affording **4.8k** as a green crystals (0.923 g, 1.84 mmol, 92%). Elemental Analysis Calcd. (Found) for C_{20} H_{29} Cl_3 Cr N_3 $O_{2.5}$: C 47.35 (47.12), H 5.82 (5.73), N 8.39 (8.24). [μ_{eff} = 3.86 $\mu_{B]}$. Single crystals suitable for X-ray crystallography were grown from a diluted THF solution at room temperature.

4.2.29 Preparation of Complex [{(2-$C_5H_4N)_2CH_2$}$CrCl_3$(thf)] (4.9l)

The preparation was carried out following the same procedure as per **4.1c** affording **4.9l** as a green powder (0.721 g, 1.80 mmol, 90%). Elemental Analysis Calcd. (Found) for C_{15} H_{18} Cl_3 Cr N_2 O: C 45.23 (44.97), H 4.85 (4.53), N 7.15(6.99). [μ_{eff} = 3.85 μ_B]. Single crystals suitable for X-ray crystallography were grown from a diluted THF solution on standing at room temperature.

4.2.30 Preparation of Complex [{(2-$C_5H_4N)_2CH_2SiMe_3$}$CrCl_3$(thf)] (4.10m)

The preparation was carried out following the same procedure as per **4.1c** affording **4.10m** as a green powder (0.946 g, 1.78 mmol, 89%). Elemental Analysis Calcd. (Found) for $C_{21.5}H_{33}Cl_3CrN_2O_{1.62}Si$: C 48.89 (48.55), H 6.42 (6.25), N 5.37 (5.27). [μ_{eff} = 3.86 μ_B]. Single crystals suitable for X-ray crystallography were grown from a diluted THF solution at room temperature.

4.2.31 Preparation of Complex [{(2-$C_5H_4N)_2CH_2CMe_3$}$CrCl_3$(thf)] (4.11n)

The preparation was carried out following the same procedure as per **4.1c** affording **4.11n** as a green powder (0.822 g, 1.75 mmol, 87%). Elemental Analysis Calcd. (Found) for $C_{20}H_{27}Cl_3CrN_2O$: C 51.34 (51.13), H 5.81 (5.79), N 6.27 (5.96). [μ_{eff} = 3.84 μ_B]. Single crystals suitable for X-ray crystallography were grown from a diluted THF solution stored at room temperature.

4.2.32 Preparation of Complex [{(2-$C_5H_4N)_2$}$CrCl_3$(thf)] (4.12)

The preparation was carried out following the same procedure as per **4.1c** affording **4.12** as a green powder (0.698 g, 1.81 mmol, 90.5%). Elemental Analysis Calcd. (Found) for $C_{14}H_{15}Cl_3CrN_2O$: C 43.87 (43.60), H 4.13 (3.92), N 7.37 (7.26). [μ_{eff} = 3.87 μ_B]. Single crystals suitable for X-ray crystallography were grown from a diluted THF solution stored at room temperature.

4.2.33 Preparation of Complex [{(2-$C_5H_4N)_2C_2H_4$}$CrCl_3$(thf)] (4.13o)

The preparation was carried out following the same procedure as per **4.1c** affording **4.13 o,** as a green powder (0.690 g, 1.67 mmol, 83.5%). Elemental Analysis Calcd. (Found) for $C_{16}H_{19}Cl_3CrN_2O$: C 46.77 (46.45), H 4.84 (4.63), N 6.93 (6.77), [μ_{eff} = 3.83μ_B].

4.2.34 Preparation of Complex [{(2-$C_5H_4N)_2NC_4H_8OEt\}_2CrMe_2$].[$AlMe_4$] (4.14g)

A solution of $Cr(NCy_2)_3$ (0.563 g, 1.0 mmol) in toluene (10 mL) was allowed to cool to -35 ^oC for 10 minutes. The cold solution of $Cr(NCy_2)_3$ was then treated with a neat solution of trimethylaluminium (0.364 g, 5.05 mmol) followed by a solution of ligand **g** (0.271g, 1 mmol) in toluene (5 mL) and allowed to stir at room temperature for 10 minutes. Upon standing at -35 °C for overnight brown paramagnetic crystals of **4.14g** were formed. Analytically pure crystals were collected, filtered, washed with cold hexane and dried in vacuo (0.257 g, 0.33 mmol, 33%). Elemental Analysis Calcd. (Found) for $C_{43.25}$ H_{66} Al Cr N_6 O_2: C 66.73 (66.51), H8.72 (8.52), N 10.89 (10.76). [μ_{eff} = 3.86 μ_B].

4.2.35 Preparation of Complex [{(2-$C_5H_4N)_2CHCH_2CMe_3\}_2$CrMeCl][$Li(THF)_3$] (4.15n)

A solution of $CrCl_3(THF)_3$ (0.376 g, 1 mmol) in Et_2O (10 mL) was allowed to cool to -35 ^oC for 10 minutes. The cold solution of $CrCl_3(THF)_3$ was then treated with solution of MeLi (1.25 mL, 2 mmol, 1.6 M in Et_2O) followed by a solution of ligand **n** (0.240 g, 1 mmol) in Et_2O (5 mL) and allowed to stir at room temperature for 10 minutes. Upon standing at -35 °C for 5 days brown/red paramagnetic crystals of **4.15n** were formed. Analytically pure crystals were collected, filtered, washed with cold hexane and dried in vacuo (0.33 g, 0.35 mmol, 35%). Elemental Analysis Calcd. (Found) for C_{53} H_{81} Cl Cr Li N_4 O_5: C 53 (52.94), H 81 (80.92), N 4 (3.93). [μ_{eff} = 3.83 μ_B].

4.3 Crystal Data

Table 4.1: Crystal structure analysis data

	4.1b	**4.1g**	**4.2c**	**4.3b**
Formula	$C_{19}H_{27}Cl_3CrN_3O$	$C_{42}H_{62}Cl_6Cr_2N_6O_{4.50}$	$C_{23}H_{38}Cl_2CrN_3O_2Si$	$C_{21}H_{33}Cl_2CrN_5O_2$
FW	471.79	1039.68	539.55	510.42
space group	Monoclinic, P2(1)/c	Monoclinic, P2(1)/c	Monoclinic, P2(1)/c	Triclinic, P-1
a (Å)	11.616(2)	25.370(4)	12.3822(7)	8.750(18)
b (Å)	15.117(3)	15.099(3)	16.5625(10)	10.89(2)
c (Å)	13.741(3)	13.767(2)	14.0934(8)	14.89(3)
α (deg)	90	90	90	84.79(3)
β (deg)	114.394(2)	104.341(3)	108.5870(10)	84.19(3)(2)
γ (deg)	90	90	90	75.29(3)
V (Å^3)	2197.5(8)	104.341(3)	2739.5(3)	1363(5)
Z	4	4	4	2
Radiation (Kα, Å)	0.71073	0.71073	0.71073	0.71073
T (K)	203(2)	203(2)	220(2)	200(2)
D_{calcd} (g cm^{-3})		1.352		1.244
μ_{calcd} (mm^{-1})	0.899	0.784	0.680	0.640
F_{000}		2168		
R, R_w [2 a]	0.0393, 0.1111	0.0783, 0.1855	0.0492, 0.1384	0.0516, 0.1184
GoF	1.031	1.037	1.025	1.025

	4.7j	**4.8k**	**4.9l**
Formula	$C_{20}H_{28}Cl_3CrFN_3O_{1.5}$	$C_{20}H_{29}Cl_3CrN_3O_{2.5}$	$C_{15}H_{18}Cl_3CrN_2O$
FW	511.805	509.81	400.66
Space group	Monoclinic, P2(1)/n	Monoclinic, P2(1)/n	Monoclinic, P2(1)/c
a (Å)	11.9011(12)	8.8597(3)	8.9762(4)
b (Å)	27.658(3)	10.9850(5)	13.9276(5)
c (Å)	15.0581(15)	24.2944(8)	13.6579(5)
α (deg)	90	90	90
β (deg)	109.292(2)	99.678(2)	98.263(2)
γ (deg)	90	90	90
V (Å^3)	4678.3(8)	2330.77(15)	1689.74(11)
Z	4	4	4
radiation (Kα, Å)	0.71073	0.71073	0.71073
T (K)	200(2)	200(2)	200(2)
D_{calcd} (g cm^{-3})	1.453	1.453	1.575
μ_{calcd} (mm^{-1})	0.859	0.858	1.153
F_{000}	2120	1060	820
R, R_w [2 a]	0.0536, 0.1278	0.0405, 0.0978	0.0417, 0.0806
GoF	1.040	1.022	1.012

	4.10m	**4.14g**	**4.15n**
Formula	$C_{21.5}H_{33}Cl_3CrN_2O_{1.62}Si$	$C_{43.25}H_{66}AlCrN_6O_2$	$C_{53}H_{81}ClCrLiN_4O_5$
FW	531.94	781.00	948.61
Space group	Monoclinic, P2(1)/n	Monoclinic, P2(1)/n	Triclinic, P1
a (Å)	14.5667(2)	11.810(2)	9.6213(16)
b (Å)	15.1706(2)	18.365(3)	11.1607(19)
c (Å)	26.0020(4)	22.137(4)	14.404(2)
α (deg)	90	90	69.629(3)
β (deg)	103.8550(10)	104.896(3)	76.333(3)
γ (deg)	90	90	68.253(3)
V (Å^3)	5578.88(14)	4639.8(15)	1336.5(4)
Z	4	4	1
radiation (Kα, Å)	0.71073	0.71073	0.71073
T (K)	200(2)	200(2)	200(2)
D_{calcd} (g cm^{-3})	1.267	1.118	1.179
μ_{calcd} (mm^{-1})	0.758	0.304	0.311
F_{000}	2224	1682	511
R, R_w [2 a]	0.0575,0.1450	0.0741, 0.1823	0.1288, 0.2862
GoF	1.011	1.027	1.013

[a] $R = \Sigma|Fo| - |Fc|/\Sigma|F|$. $Rw = [\Sigma(|Fo| - |Fc|)^2/\Sigma wFo^2]^{1/2}$.

4.4 Results and Discussion

A range of substituted $(2\text{-}C_5H_4N)_2NR$ derivatives and the corresponding trivalent chromium complexes $[\{(2\text{-}C_5H_4N)_2NR\}CrCl_3(thf)]$ (**4.1a:** R=Me; **4.1b:** $R=CH_2CMe_3$; **4.1c:** $R=CH_2SiMe_3$; **4.1d:** $R=C_{16}H_{33}$; **4.1e:** R=benzyl; **4.1f:** $R= C_3H_6Si(OEt)_3$; **4.1g:** $R=C_4H_8OEt$) were synthesized readily. The monomethyl Cr(III) derivative $[\{(2\text{-}C_5H_4N)_2NCH_2SiMe_3\}CrMeCl_2(thf)]$ (**4.2c**) was prepared by treating **4.1c** with a stoichiometric amount of MeLi in THF or by the direct treatment of $[CrMeCl_2(thf)_3]$ with the ligand. The structures were all very similar (Figure 4.1).

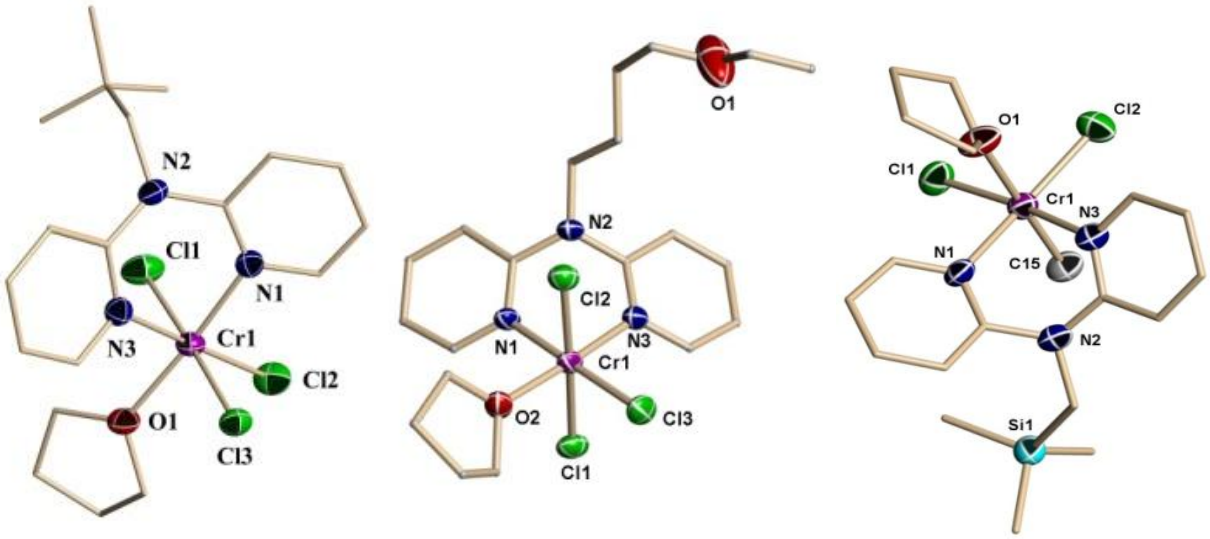

4.1b **4.1g** **4.2c**

Figure 4.1: Thermal-ellipsoid (50% probability) plots of 4.1b, 4.1g, 4.2c [11]

When activated with methylaluminoxane (MAO) at 50 ^{o}C, all trivalent complexes underwent a vigorously exothermic reaction after an induction period of several minutes to form large amounts of a heavy α-olefin. In all cases, the ^{13}C NMR spectrum showed the presence of a vinylic residue and a complete lack of branching: features indicative of linear α-olefins. Under isothermal conditions, with temperatures rising to a maximum of 110 ^{o}C, we observed that, aside from polyethylene (PE) wax, a sizeable amount of highly pure 1- octene was formed, as shown by NMR spectroscopy and GC– MS (Figure 4.2). The thermal behavior of the reaction was remarkable. After an induction period of about 4 min, the temperature increased very rapidly to reach about 110 ^{o}C. When the reaction temperature was maintained constant at 80 ^{o}C with the aid of a cooling coil in the interior of the reactor, the waxy α-olefin appeared to be the sole product of the reaction (only traces of 1-octene were detected; Table 4.2, entry 7). A lower catalyst loading and variable pressure did not affect the activity significantly.[7] Attempts to

diminish the amount of PE wax by carrying out the catalytic reaction in the presence of hydrogen gas did not affect the outcome. MAO appears to be the only usable activator, since no catalytic activity was observed with other common alkyl aluminum compounds, including trimethylaluminum (TMA), triisobutylaluminum, tetraisobutyldialuminoxane, triethylaluminum, and diethylaluminum chloride.[8] Interestingly, even the use of TMA-depleted MAO gave no reaction. Conversely, when a small amount of TMA (10%) was added to the TMA-depleted system, the original catalytic behavior was restored, which indicates that both TMA and MAO are required to generate the active species. The necessity for the presence of TMA indicates its role as the alkylating agent, whereas MAO simply provides adequate Lewis acidity. However, attempts to activate the precursors with alkyl aluminum compounds and trityl borate[8a] resulted in no activity.

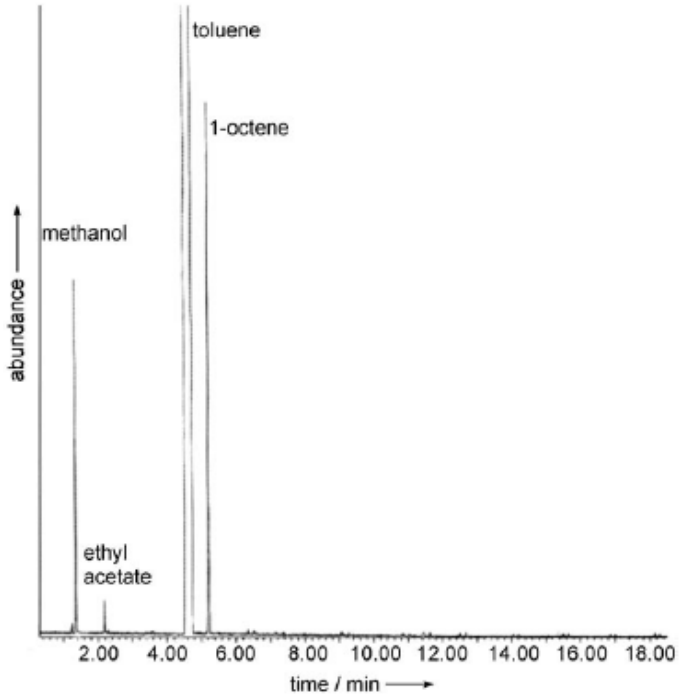

Figure 4.2: Gc-MS chromatogram of the solution phase (Table 4.2, entry 10) showing the presence of MeOH (quenching agent) ethyl acetate (needle-ringing agent), toluene (solvent) and 1-octene.

The nature of the amine substituent significantly affected the catalytic behavior of the catalyst (Table 4.2), as also observed in the Sasol system.[9] In the present case, this behavior can be ascribed to differences in solubility of the catalyst precursors.

The formation of 1-octene only at elevated temperatures under isoparabolic conditions (and not under isothermal conditions at 80 ^{o}C) clearly indicated that one catalytically active species (responsible for the formation of the PE wax) is primarily generated at 50 ^{o}C, and a second catalytically active species responsible for the selective formation of 1-octene is generated exclusively at higher temperature (>80 ^{o}C). However, experiments carried out at 100 ^{o}C as the initial temperature gave no 1-octene, thus indicating that the tetramerization catalyst is also rapidly deactivated at high temperature. This behavior is in agreement with the hypothesis that the thermolysis of organochromium(III) generates the catalytically active chromium(I) species.

Table 4.2: Results of the catalytic runs. [a]

Entry	complex	T [°C]	wax [g]	M_n [g/mol]	PDI	C_6 [mL]	C_6 [%]	C_8 [mL]	C_8 [wt %]	Other oligomers (>C_{10}) [mL]
1	**4.1a**	50-110	42	2233	2.1	traces	< 1	3.3	5.4	0.2
2	**4.1b**	50-110	60	2691	1.8	traces	< 1	5.8	6.4	-
3	**4.1c**	50-110	32	1954	2.2	-	-	2.6	5.6	-
4	**4.1d**	50-110	80	2283	1.9	traces	< 1	10.2	8.4	-
5	**4.1e**	50-110	55	3948	2.2	traces	< 1	4.2	5.2	-
6	**4.1f**	35-110	37	1974	2.0	0.8	1.2	4.1	6.8	2.2 (α=0.92)
7[(b)]	**4.1f**	80	80	4236	2.2	-	-	2.7	2.2	-
8	**4.1f**	50-110	60	2631	2.0	traces	< 1	13.1	13.5	-
9[(c)]	**4.1f**	50-110	-	-	-	-	-	-	-	-
10	**4.1g**	50-110	35	2566	2.2	-	-	6.9	12.3	traces
11	**4.2c**	50-110	62	1709	2.1	-	-	1.5	1.7	-
12	**4.3b**	50-110	25	2127	2.3	traces	< 1	traces	-	traces
13	**4.3f**	50-110	40	1411	2.3	0.4	< 1	2.1	3.5	1.2 (α=0.92)
14	**4.4f**	50-110	25	4848	2.6	9.0	19.6	traces	-	-
15	**4.4f**	35-110	12	1590	2.3	8.0	35.1	traces	-	-
16	**4.5f**	50-110	-	-	-	-	-	-	-	-
17	**4.6f**	60-110	57	1463	1.7	0.5	<1	7.9	8.9	-

[a] Reaction conditions: catalyst (20 mmol), MAO (400 equiv), toluene (solvent, 150 mL), ethylene (40 bar), 1 h. Longer reaction times did not lead to a further increase in the amount of product formed. "Traces" means less than 1%. [b] Catalyst loading: 10 mmol. [c] The complex was activated with TMA (40 equiv) and $[Ph_3C][B(C_6F_5)4]$ (3 equiv). Mn=number-average molecular weight, PDI=polydispersity index.

To exclude the possible role of divalent chromium in this complex system, we prepared the divalent precursors [{(2-$C_5H_4N)_2NCH_2SiMe_3$}$CrCl_2$(DMF)] **4.3b** and [{(2-$C_5H_4N)_2NC_3H_6Si(OEt)_3$}$CrCl_2$(DMF)] **4.3f** through the treatment of [$CrCl_2(thf)_2$] with the appropriate ligand (2-$C_5H_4N)_2NR$ (R=CH_2CMe_3 and $C_3H_6Si(OEt)_3$, respectively) in THF. Suitable crystals could be grown only upon treatment with N,N'-dimethylformamide (DMF; Figure 4.3). Catalytic testing of **4.3b** and **4.3f** under the usual reaction conditions showed that aside from the usual formation of large amounts of wax, only a small amount of *α*-olefins (Schulz–Flory distribution) was produced. The lack of selectivity for light oligomers not only excludes the possibility that divalent chromium might tetramerize ethylene, but also indicates that in this particular case, Cr(II) is not even a precursor for the tetramerization catalyst. Therefore, thermolysis is most likely to occur directly at a trivalent organochromium center and

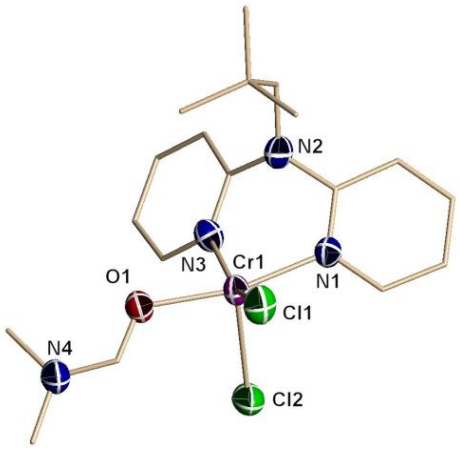

Figure 4.3 Thermal ellipsoid (50% probability) plot of the DMF adduct of 4.3b.

bypass the divalent species through a double alkylation and consequent two-electron reduction to form the monovalent species. A divalent complex may have been generated from **4.1f** (which produced the most 1-octene) only when treatment with the activator was carried out at 35 ^oC for about 20 min, before the temperature was increased to 50 ^oC, followed by the usual isoparabolic

increase to 100 ^{o}C (Table 4.2, entry 6). In this case, instead of the selective formation of 1-octene, a small amount of a Schulz–Flory distribution of oligomers was obtained, as observed with the other divalent precursors. Although a ring-expansion mechanism could effectively produce larger excesses of 1-octene, it is unlikely that it would enable selective tetramerization (e.g. >99%), in the way it enables selective ethylene trimerization. Further expansion of the seven-membered ring (responsible for 1-hexene formation) to generate heavier oligomers could lead to the formation of a range of larger metallacycles, whose stability and activation energy of formation are not expected to be much different from those of the nine-membered ring. Therefore, we considered that the weakly binucleating nature of the ligand in the assembly of a non-Cr-Cr-ligated dinuclear Cr(I) species might be a factor responsible for the selective formation of 1-octene (i.e. by the coupling of two neighboring chromacyclopentane units within a bimetallic structure and subsequent elimination of 1-octene). If this hypothesis is true, the introduction of substituents that prevent dinuclear aggregation could affect the selectivity of the present system. We therefore tested the effect of methyl substituents at the ortho positions of the pyridine rings (Scheme 4.1). The corresponding complex [{2-(6-Me-$C_5H_4N)_2NC_3H_6$Si-$(OEt)_3$}$CrCl_3$(thf)] (**4.4f**) was synthesized and tested under the usual optimal reaction conditions (Table 4.2). Remarkably, complex **4.4f** behaved in a very similar manner to complexes **4.1's**, but

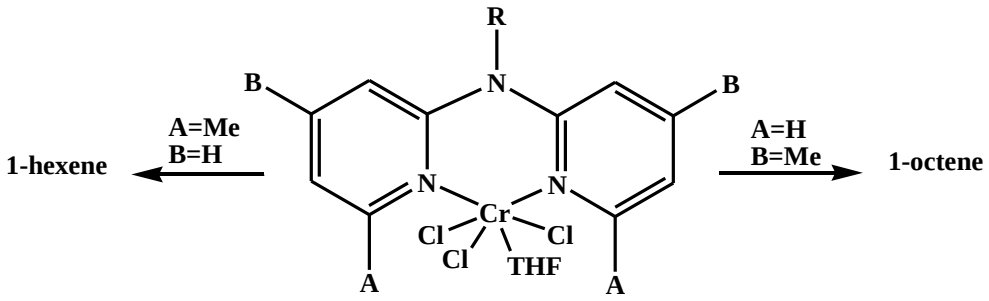

Scheme 4.1: Effect of methyl substituents at the ortho and para positions of the pyridine rings on the oligomerization.

produced much less wax and a sizeable amount of pure 1-hexene (Table 4.2, entry 15). Interestingly, the divalent congener [{2-(6-Me-$C_5H_4N)_2NC_3H_6$Si-$(OEt)_3$}$CrCl_2$(thf)] **5f** was catalytically inactive. We also prepared a similar ligand in which the methyl groups were placed in the para rather than ortho positions of the pyridine rings. The corresponding trivalent complex [{2-(4-Me-$C_5H_4N)_2NC_3H_6$Si-$(OEt)_3$}$CrCl_3$(thf)] (**4.6f**) showed the usual formation of 1-octene and a large amount of the waxy solid (Table 4.2,entry 17). This observation is particularly informative, since the repositioning of the methyl substituents from the ortho to the para positions of the aromatic rings is not expected to affect the electronic properties of the ligand. Thus, the switching of the selectivity from the selective formation of 1-octene to the selective formation of 1-hexene when the catalyst contains ortho- Me groups can be ascribed exclusively to steric factors.

4.5 Structure Activity Relationship (SAR)

The above mentioned studies have encouraged us for further modifications on the ligand backbone to evaluate electronic parameters. The modifications have been done systematically in the following positions on the ligand and studied their behavior towards catalysis.

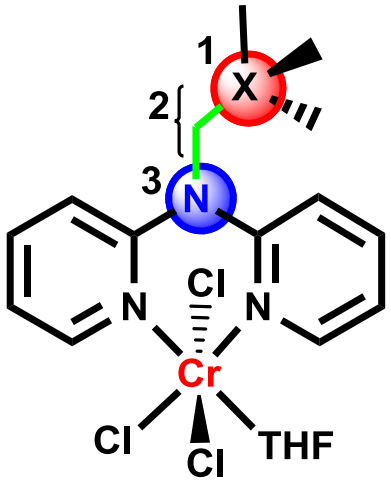

1. Heteroatom at the pendent

As mentioned above amine substituents have greater effect on the behavior of the catalysts (Table 4.2). In order to clarify the issue whether this behavior can be ascribed to differences in solubility of the catalyst precursors or the electronic effect of the associated atoms at the pendent tail, we prepared the complexes containing the electropositive Silicon to the most electronegative Fluorine atom shown in Figure 4.4.

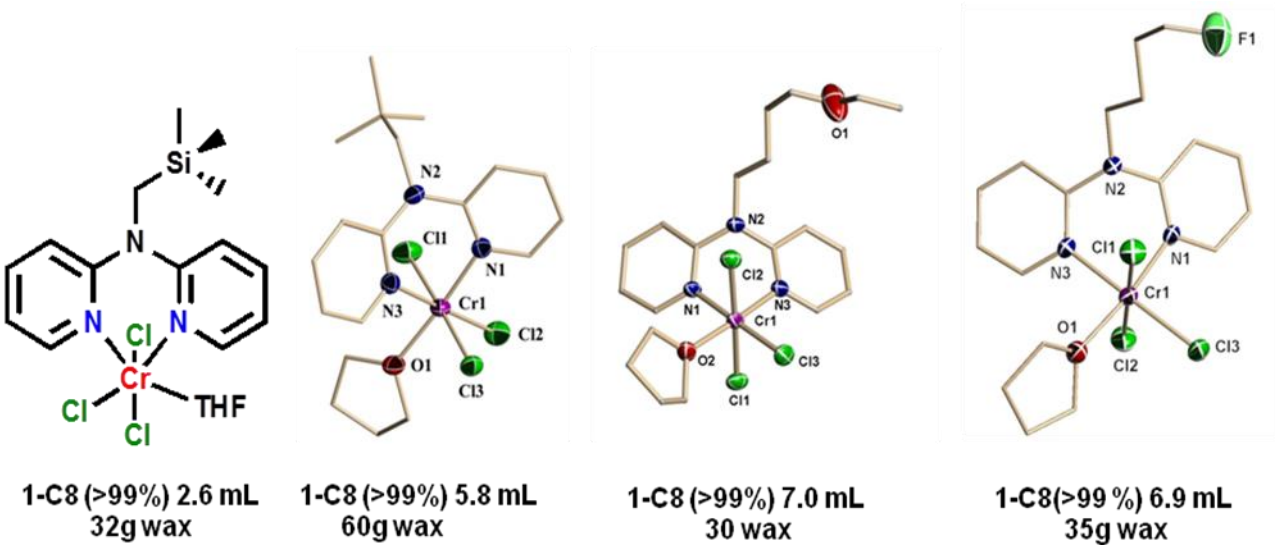

Figure 4.4 : Complexes with different heteroatoms at the pendent tail from Si to F.

As shown in Figure 4.4 the activity from Si-analogue to carbon-analogue increases almost the double in terms of 1-octene and the waxy solid formation. Additionally, Oxygen-analogue showed comparable activity towards 1-octene formation, however decreased amount of waxy solid with an order of magnitude by half, compared to its carbon-analogue. Same trend was observed with its fluorine analogue. The selectivity on the other hand remains the same in all cases. The result shows that the electronegativity of the pendant atoms do not have pronounced effect on the catalytic activity and selectivity of the systems.

2. Chain length

The next modification was done by decreasing the number of chain length between the bridging nitrogen and the pendant oxygen atoms from four carbon chain to two carbons. The modification was designed in such a way that the coordinating oxygen is in the perfect geometry to form a stable 5-membered ring with the chromium centre. The isolated two carbon chain Cr(III) complex [{(2-$C_5H_4N)_2N(C_2H_4OEt)$}$CrCl_3$(thf)] **(4.8k)**, however, showed the usual octahedral coordination geometry similar to its four carbon chain congener. Quite interestingly, though the complex showed completely non-selective (for example: 14 mL S-F, 4 g wax) catalytic behavior under the standard conditions. Although we do not have any conclusive evidence, we could speculate the formation of a stable monomeric complex during catalysts activation (Figure 4.5) which could undergo another activation pathway or generate different active species responsible for the formation of non-selective oligomerization products which would be different from the presumed "bimetallic" pathway producing selective 1-octene.

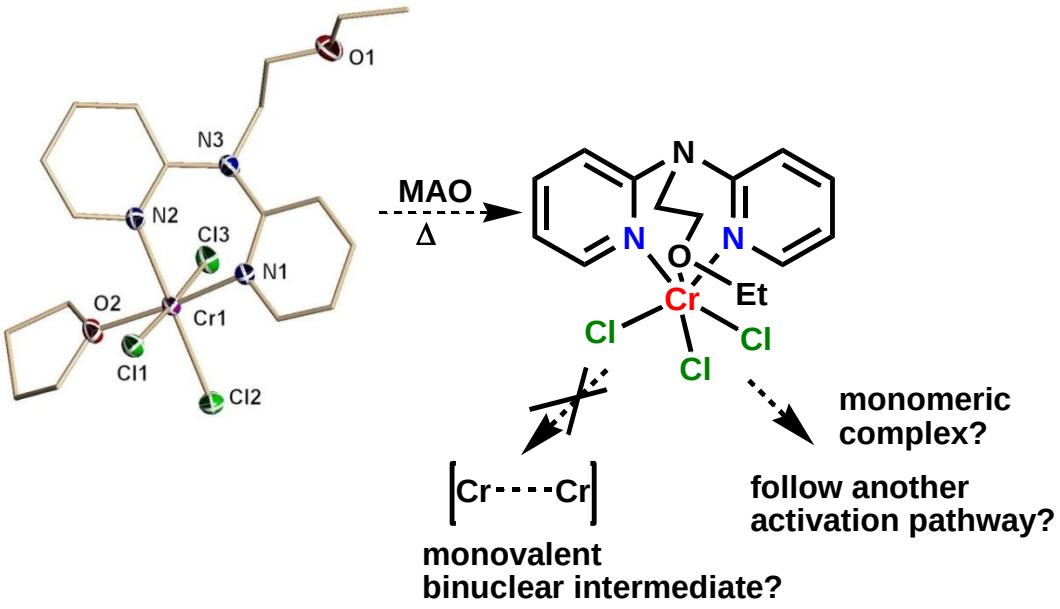

Figure 4.5: Two carbon chain Cr(III)-complex (4.8k) and hypothetical route of activation.

3. Bridging atoms

The next parameter to be examined was the effect of bridging nitrogen, for which we synthesized unsubstituted [{(2-$C_5H_4N)_2CH_2$}$CrCl_3$(thf)] (**4.9l**), trimethylsilyl substituted [{(2-$C_5H_4N)_2CH_2SiMe_3$}$CrCl_3$(thf)] (**4.10m**) and neopentyl substituted [{(2-$C_5H_4N)_2CH_2CMe_3$}$CrCl_3$(thf)] (**4.11n**) carbon analogues of aminobispyridine-Cr(III) complexes. These complexes showed comparable activity and selectivity with their nitrogen-analogues (Figure 4.6). The unsubstituted carbon-analogue showed the lowest activity among them. This could be explained simply because of the lower solubility of the catalyst precursor compared to others. The result shows that nitrogen and carbon analogs behave similarly in terms of activity and selectivity.

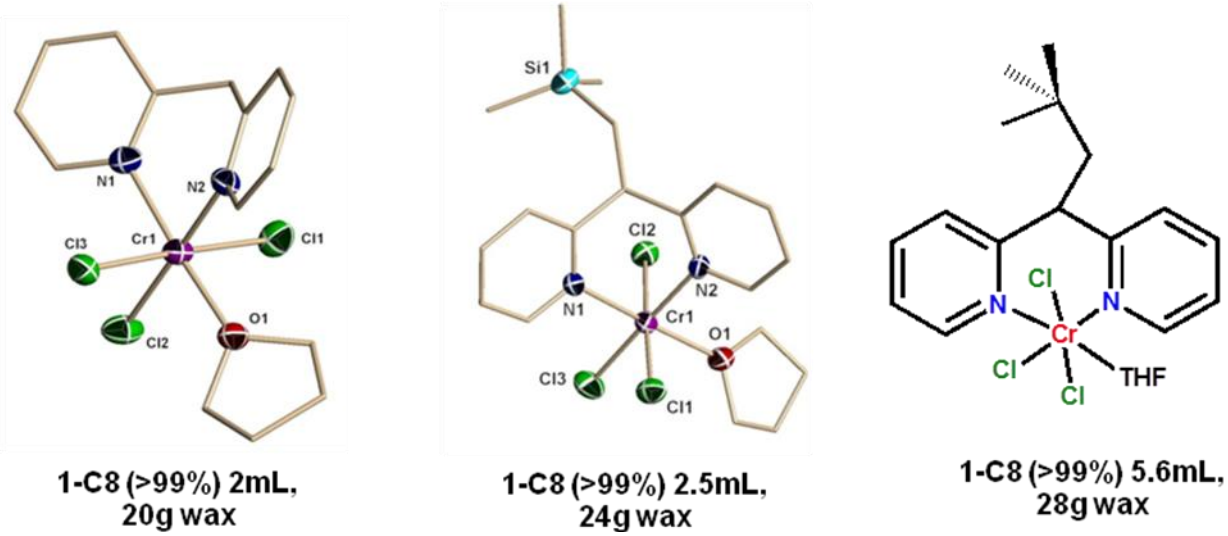

4.9l ***4.10m*** ***4.11n***

Figure 4.6: Carbon analogues of Cr(III)-Aminobispyridine complex.

4. Number of bridging atoms

The other modification was carried out by changing the number of bridging carbon atoms between the two pyridine rings. Bispyridine complex with no bridging atom [{(2-

$C_5H_4N)_2\}CrCl_3(thf)]$ **(4.12)** showed very low activity with decreased 1-octene (60%) selectivity (Figure 4.7). On the other hand, increased number of bridging carbon atoms by two, $[\{(2\text{-}C_5H_4N)_2C_2H_4\}CrCl_3(thf)]$ **(4.13o),** switched the selectivity completely towards Schulz-Flory distribution (Figure 4.7) rather than 99% of 1-octene as was observed in case of one carbon bridge analogue **4.9l** . The result shows that the optimum number of bridging carbon atoms between the two pyridine rings are essential to direct the catalytic activity and selectivity towards the desired direction in this system.

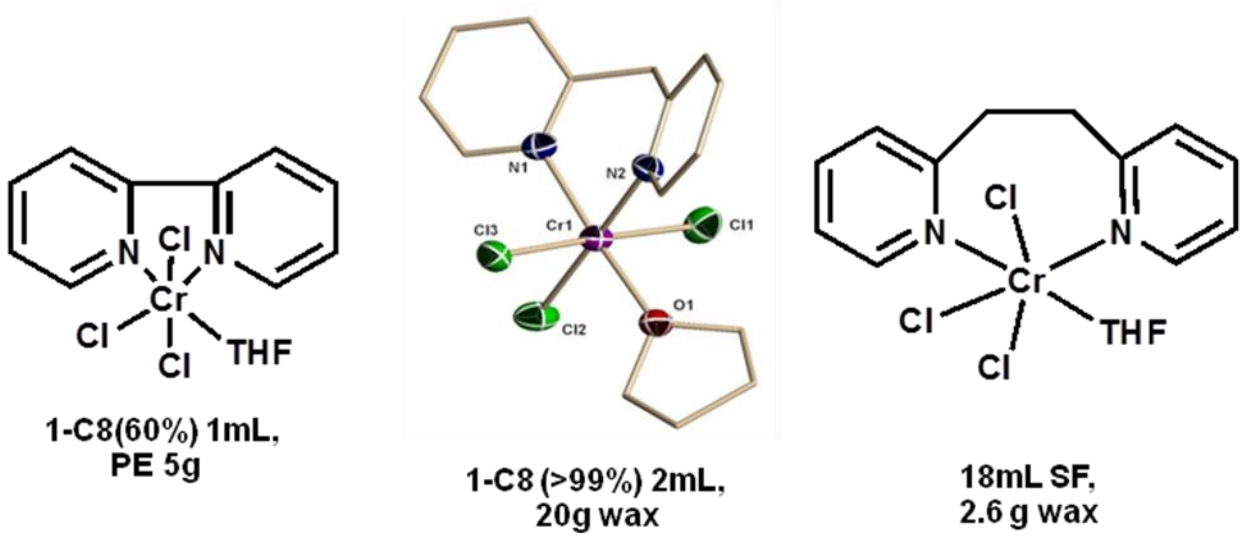

4.12 **4.9l** **4.13o**

Figure 4.7: Cr(III)-complexes with different number of carbon bridges.

4.6 Catalyst Deactivation

As mentioned earlier the Cr(III) complexes of the aminobispyridine ligand showed activity and selectivity towards 1-octene only when activation was carried out with MAO as a co-catalyst in toluene. Conversely, with other co-catalysts including TMA, these complexes were found to be inactive. To comprehend this behavior we have embarked on interaction of trivalent

chromium precursor, the ligand and Me_3Al reagent and were able to isolate a well defined Cr(III)-cationic complex $[\{(2\text{-}C_5H_4N)_2NC_4H_8OEt\}_2CrMe_2].[AlMe_4]$ **(4.14g)** (Figure 4.8). The crystal structure analysis illustrated that the coordination geometry of the complex **4.14g** was determined as octahedral defining by the four N atoms of two bispyridine ligands and remaining two is occupied by two methyl groups.

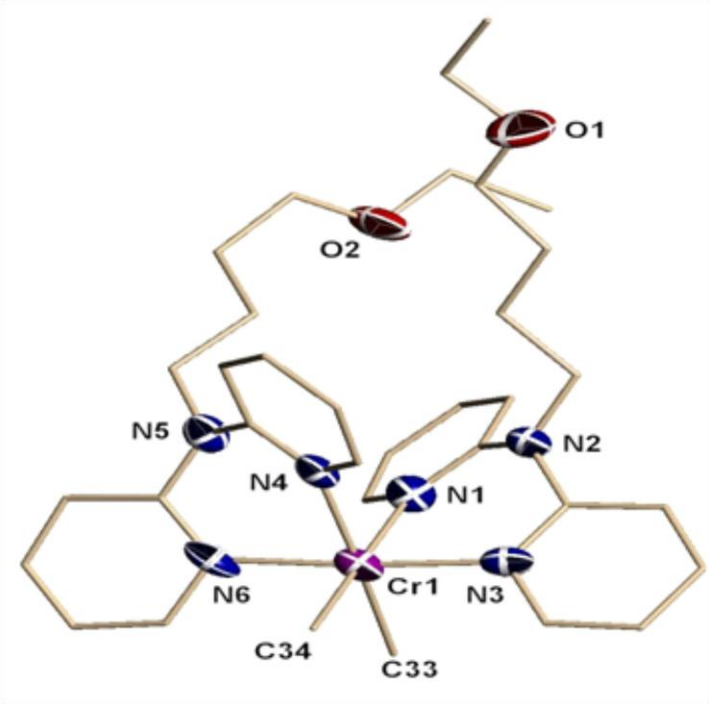

Figure 4.8: Cationic Cr(III)-dialkyl complex 4.14g. The anionic tetramethyl aluminum is removed for clarity.

The cationic dialkyl complex is counter balanced by tetramethylaluminum anion. This complex was found to be catalytically inert even with or without the activation of MAO. The result suggests that the formation of thermally stable Cr(III) complex might be the deactivation pathway for this catalytic system (Figure 4.9).

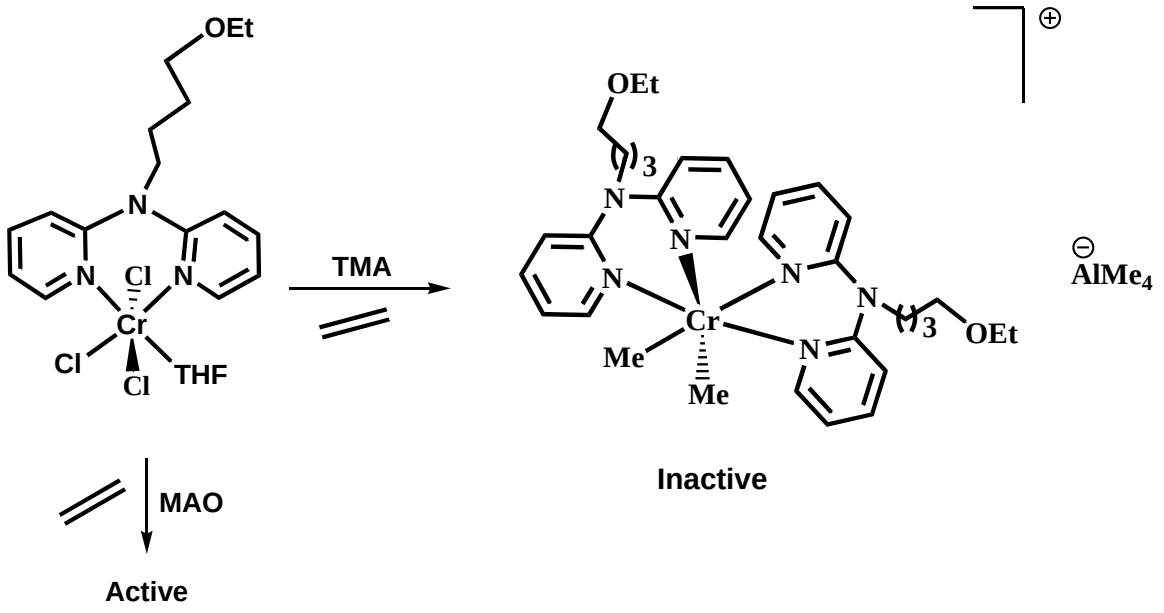

Figure 4.9: Possible route for catalyst deactivation.

Similar result was obtained upon activation of monomethylated octahedral Cr(III)-complex of carbon analogue $[\{(2\text{-}C_5H_4N)_2CHCH_2CMe_3\}_2CrMeCl][Li(THF)_3]$ **(4.15n)** with MAO (Figure 4.10). The result reiterates the fact that formation of thermally stable Cr(III) complex deactivates the catalyst in this case.

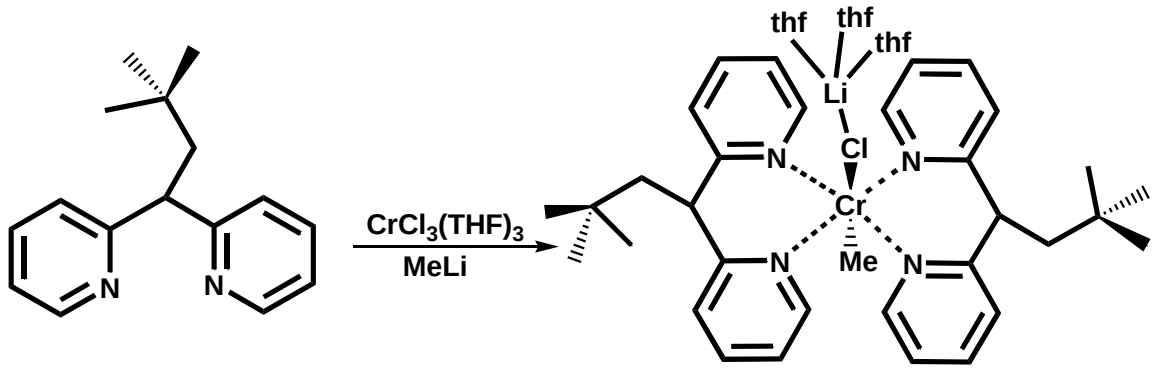

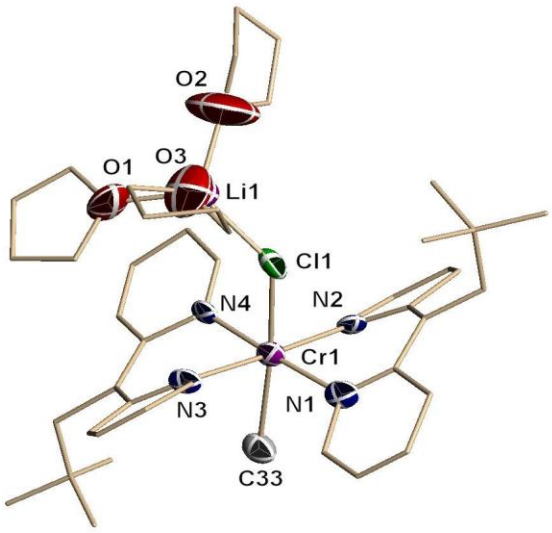

4.15n

Figure 4.10: Carbon analogue of aminobispyridine Cr(III)-complex, thermally stable and catalytically inactive.

4.7 Conclusions

In conclusion, we have described the intriguing formation of pure 1-octene alongside low-molecular-weight polyethylene wax. This observation suggests that a truly selective ethylene-tetramerization catalyst may indeed exist. As a working hypothesis, we concur with the mechanistic concept recently proposed by Rosenthal and co-workers[10] that a dinuclear monovalent species, possibly without a Cr-Cr multiple bond, might be formed with the aid of a non-anionic bidentate ligand and promote the formation of 1-octene through a bimetallic reductive elimination. The structure-activity relationship study in fact provided some experimental support to the proposed bimetallic concept of Rosenthal.

In search of clue for introducing selectivity in the catalytic cycle, in the next chapter, we will discuss the chemistry of trivalent chromium amides as a part of our systematic exploration on ligand systems.

References

1. a) Reagan, W. K. (Phillips Petroleum Company), EP 0417477, **1991**. b) Tanaka, E.; Urata, H.; Oshiki, T.; Aoshima, T.; Kawashima, R.; Iwade, S.; Nakamura,H.; Katsuki, S.; Okanu, T.; (Mitsubishi Chemical Corporation), EP 0611743, **1994**. c) Wu, F. J.; (Amoco Corporation), US 5811618, **1998**. d) Yoshida, T.; Yamamoto, T.; Okada, H.; Murakita, H.; (Tosoh Corporation), US2002/0035029, **2002**. e) Carter, A.; Cohen, S. A.; Cooley, N. A.; Murphy, A.; Scutt, J.; Wass, D. F. *Chem. Commun*. **2002**, 858. f) McGuinness, D. S.; Wasserscheid, P.; Keim,W.; Hu, C.; Englert, U.; Dixon, J. T.; Grove, C.; *Chem. Commun*. **2003**, 334. g) McGuinness, D. S.; Wasserscheid, P.; Keim,W.; Morgan, D. H.; Dixon, J. T.; Bollmann, A.; Maumela, H.; Hess, F. M.; Englert, U. *J. Am. Chem. Soc.* **2003**, *125*, 5272. h) Khn, R. D.; Haufe, M.; Kociok-Khn, G.; Grimm, S.; Wasserscheid, P.; Keim,W *Angew.Chem.* **2000**, *112*, 4519; *Angew. Chem. Int. Ed*. **2000**, *39*, 4337. i) Morgan, D. H.; Schwikkard, S. L.; Dixon, J. T.; Nair, J. J.; Hunter, R.; *Adv. Synth. Catal.* **2003**, *345*, 939. j) McGuinness, D. S.; Wasserscheid, P.; Morgan, D. H.; Dixon, J. T.; *Organometallics* **2005**, *24*, 552. k) Bluhm, M. E.; Walter, O.; M. ring, D. *J. Organomet. Chem*. **2005**, *690*, 713. l) Nenu, C. N.; Weckhuysen, B. M. *Chem. Commun.* **2005**, 1865. m) Mahomed, H. A.; Bollmann, A.; Dixon, J. T.; Gokul, V.; Griesel, L.; Grove, J. J. C.; Hess, F.; Maumela, H.; Pepler, L. *Appl. Catal. A* **2003**, *255*, 355. n) Grove, J. J. C.; Mahome, H. A.; Griesel L. (Sasol Technology), WO 03/004158, **2002.** o) Jabri, A.; Mason, C. B.; Sim, Y.; Gambarotta, S.; Burchell, T. J.; Duchateau, R. *Angew. Chem.* **2008,** *120*, 9863; *Angew. Chem. Int. Ed*. **2008**, *47*, 9717. p) Zhang, J.; Braunstein, P.; Hor, T. S. A. *Organometallics* **2008**, *27*, 4277. q) Zhang, J.; Li, A.; Hor, T. S. A. *Organometallics* **2009**, *28*, 2935.

2. a) McDermott, X.; White, J. F.; Whitesides, G. M. *J. Am. Chem. Soc.* **1976**, *98*, 6521. b)

Manyik, R. M.; Walker, W. E.; Wilson, T. P. *J. Catal*. **1977**, *47*, 197. c) McDaniel, M. P. *Adv. Catal.* **1985**, *33*, 47. d) Briggs, J. R. (Union Carbide Corporation), US 4,668,838, **1987**. e) Briggs, J. R. *J. Chem. Soc. Chem. Commun*. **1989**, 674. f) Meijboom, N.; Schaverien, C. J.; Orpen, A. G. *Organometallics* **1990**, *9*, 774. g) Emrich, R.; Heinemann, O.; Jolly, P. W.; Kr_ger, C.; Verhovnik, G. P. J. *Organometallics* **1997**, *16*, 1511. h) Tomov, A. K.; Chirinos, J. J.; Jones, D. J.; Long, R. J.; Gibson, V. C. *J. Am. Chem. Soc*. **2005**, *127*, 10166.

3. a) Agapie, T.; Labinger, J. A.; Bercaw, J. E. *J. Am. Chem. Soc*. **2007**, *129*, 14281, and references therein. b) Temple, C.; Jabri, A.; Crewdson, P.; Gambarotta, S.; Korobkov, I.; Duchateau, R. *Angew. Chem.* **2006**, *118*, 7208; *Angew. Chem. Int. Ed*. **2006**, *45*, 7050. c) Jabri, A.; Temple, C.; Crewdson, P.; Gambarotta, S.; Korobkov, I.; Duchateau, R. *J. Am. Chem. Soc.* **2006**, *128*, 9238. d) McGuinness, D. S.; Suttil,J. A.; Gardiner, M. G.; Davies, N.W. *Organometallics* **2008**, *27*, 4238.
4. a) Kuhlmann, S.; Blann, K.; Bollmann, A.; Dixon, J. T.; Killian, E.; Maumela, M. C.; Maumela, H.; Morgan, D. H.; Prtorius, M.; Taccardi, N.; Wasserscheid, P. *J. Catal.* **2006**, *245*, 279, and references therein. b) Han, T. K. M.; Ok, A.; Chae, S. S.; Kang, S. O. (SK Energy Corporation), WO 2008/088178, **2008**.
5. Berry, J. F.; Cotton, F. A.; Lu, T.; Murillo, C. A.; Roberts, B. K.; Wang, X. *J. Am. Chem. Soc*. **2004**, *126*, 7082.
6. a) Edema, J. J. H.; Gambarotta, S. *Comments Inorg. Chem.* **1991**, *4*, 195. b) Hao, S.; Gambarotta, S.; Bensimon, C.; Edema, J. *Inorg.Chim. Acta* **1993**, *213*, 65. c) Noor, A.; Wagner, F. R.; Kempe, R. *Angew. Chem*. **2008**, *120*, 7356; *Angew. Chem. Int. Ed*. **2008**, *47*, 7246. d) Dyker. G.; Muth. O. *Eur. J. Org. Chem*. **2004**, 4319.

7. Kuhlmann, S.; Dixon, J. T.; Haumann, M.; Morgan,D. H.; Ofili, J.; Spuhl, O.; Taccardi, N.; Wasserscheid, P. *Adv. Synth. Catal*. **2006**, *348*, 1200.

8. a) McGuinness, D. S.; Overett, M.; Tooze, R. P.; Blann, K.; Dixon, J. T.; Slawin, A. M. Z. *Organometallics* **2007**, *26*, 1108. b) Jiang, T.; Liu, X.; Ning, Y.; Chen, H.; Luo, M.; Wang, L.; Huang, Z. *Catal. Commun.* **2007**, *8*, 1145. c) Jiang, T.; Ning, Y.; Zhang, B.; Li, J.; Wang, G.; Yi, J.; Huang, Q. *J. Mol. Catal. A* **2006**, 259, 161.

9. a) Killian, E.; Blann, K.; Bollmann, A.; Dixon, J. T.; Kuhlmann, S.; Maumela, M. C.; Maumela, H.; Morgan, D. H.; Nongodlwana, P.; Overett, M. J.; Pretorius, M.; H_fener, K.; Wasserscheid, P. *J. Mol. Catal. A* **2007**, *270*, 214. b) Weng, Z.; Teo, S.; Hor, T. S. A. *Dalton Trans.* **2007**, 3493. c) Jiang, T.; Zhang, S.; Jiang, X.; Yang, C.; Niu, B.; Ning, Y. *J. Mol. Catal. A* **2008**, *279*, 90.

10. Peitz, S.; Aluri, B. R.; Peulecke, N.; Mller, B. H.; Whl, A.; Mller, W.; Al-Hazmi, M. H.; Mosa, F. M.; Rosenthal, U. *Chem. Eur. J*. **2010**, *16*, 7670.

11. CCDC 777160, 777161, 777162, 777163, 777164 (1c, 1e, 1g, 2c, and 3b) contain the supplementary crystallographic data for this work. These data can be obtained free of charge from The Cambridge Crystallographic Data Centre via www.ccdc.cam.ac. Uk/data_request/cif.

Publication:

1) **Thapa, I.;** Gambarotta, S.; Korobkov, I. *Organometallics* (Submitted).

Strategy for Introducing Selectivity in the Ethylene Oligomerization Cycle: Isolation of a Self-Activating Chromium Amido-Aluminate Complex.

5.1 Introduction

Non-selective ethylene oligomerization is an industrially relevant catalytic process continually receiving attention for the challenges posed by its understanding.[1-5] The mixtures of linear alpha olefins (LAO) produced by this process provide a large market of valuable commodity chemicals for a range of industrial and household applications (detergents, surfactants, cosmetics, etc.).[6]

A possible way to look at non-selective oligomerization is to regard it as a regular chain growth polymerization randomly truncated at its early stages (Cossee-Arlman mechanism).[7] During such a catalytic cycle the metal oxidation state remains unchanged. Occasionally, some non-selective system[8] may also proceed by the same redox metallacycle mechanism proposed for selective tri- and tetramerization.[9] This is possible only when there is

comparable activation barrier between the two processes such as further ring-expansion and reductive elimination.[10] Hence, identification and discriminating between the two processes will lead the catalytic behavior to switch from general statistical oligomerization to a selective process.

The majority of the catalytic systems including selective,[11] and non-selective ethylene oligomerization,[12] as well as polymerization catalysts[13] practically use trivalent chromium as catalyst precursors. Specifically, the trivalent state is normally providing inert complexes which are conveniently used to supply the metal into the catalytic cycle. Ready reduction of the metal center to either the di- or monovalent state often occurs during the activation process (alkylation) with each of these states having its own characteristic catalytic behavior.[14] The redox dynamism of the organochromium derivatives in addition to the large number of oxidation states available is likely to be responsible for the versatility of this element.[14] Most importantly, the original trivalent state may also be regenerated during the catalytic cycles via repetitive sequences of disproportionation and reductions.[11o-15] Catalyst deactivation may occur with further reduction to the zero valent state with eventual separation of metallic chromium or formation of inert complexes. The co-existence and easy interconversion of the three catalytically active oxidation states such as (+I, +II, +III) reasonably explains the presence of polymeric material during the production of LAO and/or the enrichment of the statistical distribution of α-olefins in 1-hexene and/or 1-octene.[11o-15]

The judicious selection of the ligand system, of the reducing power of the activator and of the reaction conditions, is central to the possibility of controlling the chromium redox dynamism and introducing selectivity in the catalytic cycle. In other words, being able of stabilizing a particular chromium oxidation state will enable to control the catalytic behavior

of the metal center. While the effect of the activator and of the temperature on the reduction towards the lower valent state can be easily assessed via rapid experimentation including HT, understanding the influence of the ligand features is a time consuming task implying the screening of libraries of ligands. A possible and alternative strategy to bypass this problem is to understand the interaction of the chromium catalyst precursor with the aluminate activator *vis-à-vis* the preparation of self-activating catalysts. Previous work on an anionic and neutral ligand systems based on the NPN framework of tri- and pentavalent phosphorus has clearly indicated that this ligand frame is versatile for catalytic purposes, having allowed isolation of rare species, self activating and switchable catalytic systems.[16] During the activation process of its chromium derivatives, the ligand-P atom was always attacked by the alkylating agent used for catalyst activation.[16] The alkylation at the P atom in turn caused retention of alkyl aluminum residues, in the end enabling the formation of single-component and switchable ethylene oligomerization and polymerization catalysts. It was argued that eliminating the possibility of alkylation at the phosphorus atom might afford a different catalytic behavior.

As a part of systematic exploration on ligand systems, we have now examined the chemistry of trivalent chromium amides and isolated an aluminate adduct that acts as self-activating non-selective catalyst. Herein we describe our findings.

5.2 Experimental Section

All reactions were carried out under dry nitrogen atmosphere. Solvents were dried using an aluminum oxide solvent purification system. The liquid reaction mixtures of catalytic runs were analyzed by using a CP 9000 gas chromatograph (GC) equipped with a 30 mL × 0.32 mm id, capillary CP-Volamine column and a FID detector. All single-point experiments

were performed in duplicate. The yields were determined by ^{1}H NMR spectroscopy (Bruker Avance 300 MHz spectrometer). Samples for magnetic susceptibility were pre-weighed inside a VAC dry box equipped with an analytical balance and measured on a Johnson Matthey Magnetic Susceptibility balance. Elemental analyses were carried out with a Perkin-Elmer 2400 CHN analyzer. Data for X-ray crystal structure determination were obtained with a Bruker diffractometer equipped with a 1K Smart CCD area detector. Methylaluminoxane (MAO, 10% in toluene) was purchased from Aldrich. MMAO was purchased from Akzo-Nobel and used as received.

5.2.1 Preparation of $Cr(Cy_2N)_3$ (5.1)

Distilled dicyclohexyl amine (18 g, 99 mmol) was dissolved in dry hexane (200 mL) under nitrogen and treated with a solution of *n*-BuLi (44 mL, 2.5 M in hexane, 109 mmol,) at room temperature. Stirring was continued at room temperature for 3 hours. A white precipitate of lithium salt of dicyclohexylamine was then filtered and used without further purification. $CrCl_3(thf)_3$ (4.79 g, 13 mmol) was added to a solution of Cy_2NLi (7.4 g, 39 mmol) in THF (80 mL) and stirring at room temperature and the mixture allowed to stir for additional 48 hours under nitrogen. The solvent was evaporated and the brown residue was redissolved in toluene (30 mL), centrifuged to separate the LiCl salt from the mother liquor, concentrated to 15 mL and cooled to -35 ^oC to afford brown crystals of $Cr(NCy_2)_3$ (4.31 g, 11 mmol, 90% yield). Elemental Analysis Calcd. (Found) for C_{36} H_{66} Cr N_3: C 72.92 (72.86), H 11.22 (11.18), N 7.09 (7.01).

5.2.2 Preparation of [(μ-Cy_2N)(μ-Me)$AlMe_2$]$_2$Cr 0.5 (toluene) (5.2)

A solution of $Cr(NCy_2)_3$ (1.0 g, 1.7 mmol) in toluene (10 mL) was cooled to -35 ^oC for 10 minutes. The cold solution was then treated with neat trimethylaluminum (0.364 g, 5.1 mmol) and stirred at room temperature for 10 minutes. Upon overnight standing at -35 °C, purple, paramagnetic and air-sensitive crystals of **5.2** separated and which were collected, filtered, washed with cold hexane and dried in *vacuo* (0.4 g, 0.7 mmol, 41%).

Elemental Analysis Calcd. (Found) for $C_{33.50}H_{66}Al_2CrN_2$: C 66.74 (66.68), H 11.04 (10.96), N 4.65 (4.57). [μ_{eff} = 4.89 μ_B].

5.2.3 Preparation of [(μ-Cy_2N)(μ-Cl)$AlEt_2$]$_2$Cr (5.3)

A solution of $Cr(NCy_2)_3$ (1.0 g, 1.7 mmol) in toluene (10 mL) was cooled to -35 ^oC for 10 minutes. The cold solution was then treated with neat diethylaluminiumchloride (0.6 g, 5.1 mmol) and stirred at room temperature for 10 minutes. Upon overnight standing at -35 °C, blue paramagnetic crystals of **5.3** were collected, filtered, washed with cold hexane and dried in *vacuo* (0.9 g, 1.3 mmol, 76%).

Elemental Analysis Calcd. (Found) for $C_{32}H_{64}Al_2Cl_2CrN_2$: C 58.79 (58.72), H 9.87 (9.83), N 4.29 (4.22). [μ_{eff} = 4.87 μ_B].

5.3 X-ray Data

Table 5.1. Crystal Data and Structure Analysis Results of Complexes **5.2 and 5.3**.

	5.2	**5.3**
Formula	$C_{33.50}H_{66}Al_2CrN_2$	$C_{32}H_{64}Al_2Cl_2CrN_2$
FW	602.84	653.71
Space group	Monoclinic, C2/c	Triclinic, P-1
a (Å)	40.1023(6)	10.1416(2)
b (Å)	8.46310(10)	10.2413(2)
c (Å)	21.5401(3)	10.7747(2)
α (deg)	90	62.5290(10)
β (deg)	98.9680(10)	82.4380(10)
γ (deg)	90	64.3860(10)
V (Å^3)	7221.12(17)	892.11(3)
Z	8	1
radiation (Kα, Å)	0.71073	0.71073
T (K)	200(2)	200(2)
D_{calcd} (g cm^{-3})	1.109	1.217
μ_{calcd} (mm^{-1})	0.388	0.543
F_{000}	2648	354
R, R_w [2 a]	0.0634,0.1754	0.0286,0.0847
GoF	1.020	1.036

[a] $R = \Sigma||Fo| - |Fc||/\Sigma|F|$. $Rw = [\Sigma(|Fo| - |Fc|)^2/\Sigma wFo^2]^{1/2}$.

5.4 Results and Discussion

The anion of bis-cyclohexylamine was selected for this work due to its excellent solubility properties in hydrocarbon solvent. The *triangulo* $[Cy_2N]_3Cr$ (**5.1**)[17] was easily prepared via reaction of $CrCl_3(THF)_3$ with three equivalents of the Cy_2NLi salts in THF followed by isolation and crystallization from hexane. Complex **5.1** reacts readily with either Me_3Al or Et_2AlCl in toluene (Scheme 5.1) affording the corresponding divalent $[(\mu\text{-}Cy_2N)(\mu\text{-}X)AlR_2]_2Cr$ [R = Me, X = Me (**5.2**); R = Et, X = Cl (**5.3**)]. Both species were isolated as extremely air-sensitive crystalline material. Both complexes are paramagnetic with values of the magnetic moments [μ_{eff} = 4.89 μ_B (**5.2**) and 4.87 μ_B (**5.3**)] as expected for divalent

chromium in square planar ligand fields. The structures were elucidated by X-ray diffraction methods.

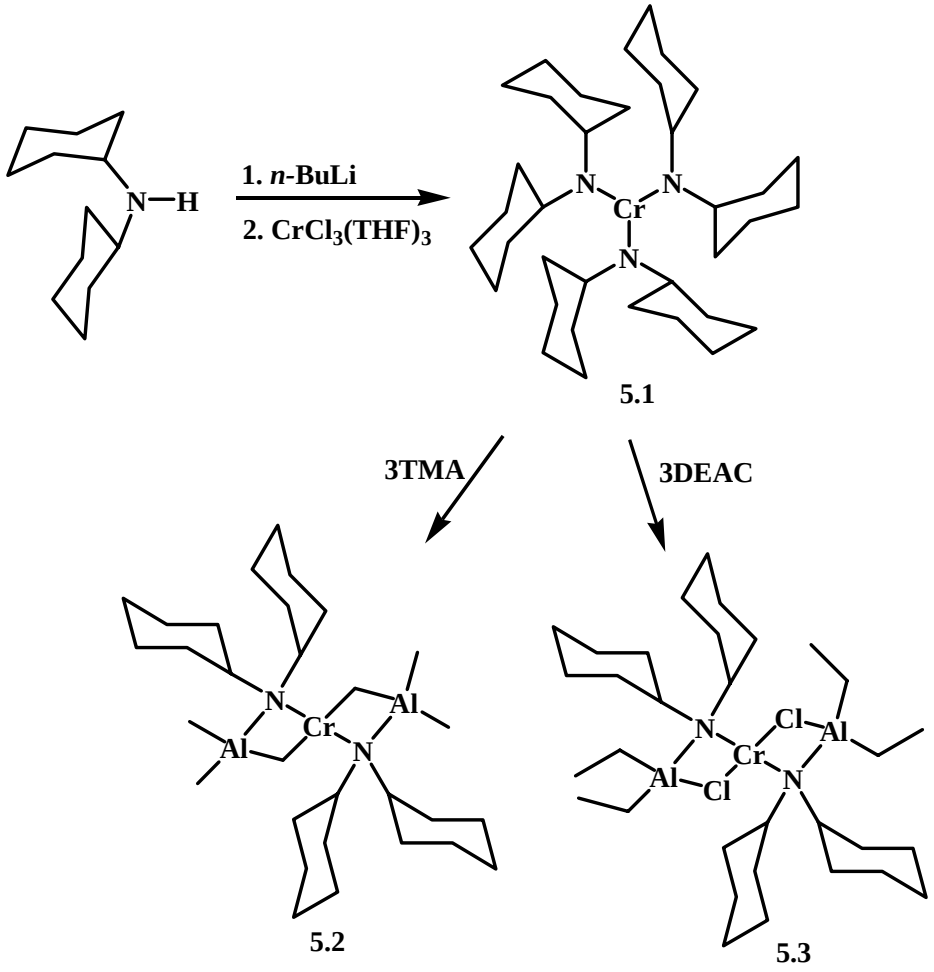

Scheme 5.1: Synthesis of Cr(II)-aluminate complexes (5.2) and (5.3).

The metal center adopted in each structure the square-planar coordination geometry expected for the d^4 electronic configuration of divalent chromium (Figure 5.1). The coordination environment around chromium in **5.2** is defined by the two nitrogen atoms of two *trans*-located bridging amide groups [Cr1-N1 = 2.130(3)Å, Cr1-N2 = 2.132(3)Å, N1-Cr1-N2= 169.95(11)^o] and two bridging methyl groups [Cr1-C25 = 2.304(3)Å, Cr1-C28 = 2.309(3)Å] also placed in *trans* to each other [C28-Cr1-C25 = 166.68(11)^o]. In turn each pair

of amide and methyl groups bridge one Me_2Al residue forming an overall trimetallic structure with a linear Al-Cr-Al array.

Complex **5.3** also adopts a very similar arrangement the only difference being the presence of bridging chlorides instead of the Me groups, and two Et_2Al residues [N1-Cr1-Cl1 = 85.26(3)^o, N1-Cr1-Cl1a = 94.74(3)^o, N1a-Cr1-Cl1 = 94.74(3)^o, N1a-Cr1-Cl1a = 85.26(3)^o, N1-Cr1-N1a = 180.0^o, Cl1-Cr1-Cl1a = 180.0^o, Cr1-N1 = 2.1529(9)Å, Cr1-N1a = 2.1528(9)Å, Cr1-Cl1 = 2.3959(3)Å, Cr1-Cl1a = 2.3959(3)Å].

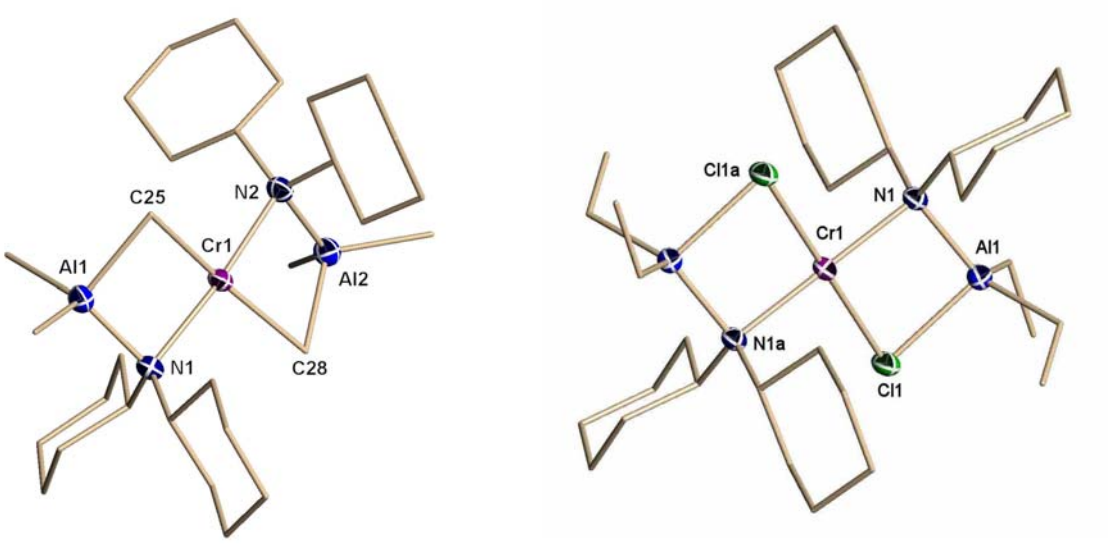

5.2 **5.3**

Figure 5.1. Partial thermal ellipsoids drawing of complex 5.2 & 5.3 (50 % probability level).

Both complexes have been tested for catalytic oligomerization activity in both toluene and MeCy as solvent and with/without activators (Table 5.2). Upon heating under ethylene pressure and in the absence of activator, complex **5.2** showed an intriguing self activating behavior, producing polymer and a mixture of 1-hexene and 1-octene. Interstingly not even traces of the heavier oligomers were present in the reaction mixtures. When a low loading of

MAO was used, only a substantial increase in the amount of polymer was observed. Larger loading of MAO in toluene instead greatly increased the activity and switched the behavior to a rather flat S-F distribution of oligomers characterized though by an intriguing excess of 1-octene. By using TMA-depleted MAO (DMAO), it gave exclusively polymer with good activity and no trace of oligomers. Addtion of TEAl to DMAO decreased the amount of polymer in favor of the formation of the same mixture of 1-hexene/1-octene. Activation with stoichiometric amount of TEAl gave no polymer and 1-hexene with high purity, the only contaminant being 1-octene. MAO/Et_2Zn mixtures activated the complex towards a S-F distribution with only little polymer formation. MMAO gave the highest purity 1-hexene but unfortunately with substantial amount of polymer.

As anticipated **5.3** was not a self activating catalyst, most likely due to the fact that the alkyl groups are not bonded to the Cr center. Its activation with large amount of MAO gave very high activity for S-F distribution, while similar to the case of **5.2**, DMAO gave exclusively polymer oligomer free.

The self-activating behavior of **5.2** is interesting and while comparing with the lack of activity of **5.3** indicates that there is not mobility within the complex in terms of alkyl interchange with the aluminate moiety coordinates at the periphery of the molecule. Nonetheless, the fact that only a mixture of 1-hexene and 1-octene free of heavier oligomers has been obtained in the case of **5.2**, indicates that some reduction to the monovalent state indeed occurred. The contamination of 1-hexene with 1-octene has to be ascribed to the ring expansion mechansim where the elimination of 1-hexene and ring further expansion have comparable activation barriers. The presence of polymer instead is probabaly due to the

original divalen state of a fraction of catalyst that is not thermally reduced to Cr(I) or perhaps disproportionate back towards higher oxidations states.

Table 5.2. Catalytic behavior of **5.2** and **5.3.**

Cat. (μmol)	Co-cat. (eq)	Activity g/mmol/ Cat/h	PE (g)	Olig. (mL)	Mol %						
					C6	C8	C10	C12	C14	C16	C18
5.2(50)	-	160	2	2	60	40	-	-	-	-	-
5.2(50)	MAO(10)	360	7	2	40	60	-	-	-	-	-
5.2(50) *	MAO(50)	1,560	2	37	19.2	26.5	18.8	14.0	9.3	6.9	5.2
5.2(20)	DMAO(50)	1,400	14	0	-	-	-	-	-	-	-
5.2(20)	DMAO(50)/TEAL(20)	720	5.2	2	69.3	13.7	5.5	4.5	3.9	1.7	1.5
5.2(20)	DMAO(400)/TEAL(20)	500	2	3	62	38	trace	trace	trace	trace	trace
5.2(20)	TEAL (5)	100	0	1	90	10	-	-	-	-	-
5.2(20) *	MAO(500)/Et_2Zn(100)	4,300	1	42	33.0	24.4	15.7	10.4	7.9	5.	3.1
5.2(20)	MAO(10)/Et_2Zn(10)	100	1	traces	-	-	-	-	-	-	-
5.2(20)	MMAO(500)	600	2.4	3	95	5	-	-	-	-	-
5.3(50)	-	-	-	-							
5.3(20)	MAO(1000)	6,300	3	63	18.3	19.9	18.5	14.9	11.5	9.2	7.8
5.3(20)	MAO(10)	-	trace	0							
5.3(20)	DMAO(400)	1,000	10	0							
5.3(20)	DMAO(50)	600	3.6	0							

Conditions: 40 bar ethylene, 30 mins reaction time, total volume 100 mL , in methylcyclohexane (toluene), 70 ^oC.*

5.5 Conclusions

In conclusion, the elimination of the P atom from the ligand frame of the PN system and use of a regular amide anion has a remarkable impact on the catalytic behavior of the chromium complex. It is interesting to observe that upon activation with TEAl high selectivity may be obtained without polymer formation. The predominance of 1-octene in one case is also intriguing as well as the absence of higher oligomers in the case when only 1-hexene and 1-octene mixtures have been obtained. This is likely to be ascribed to the ability of the amide ligand to provide sufficient stabilization to the monovalent state of chromium but not the

appropriate steric environment necessary for discriminating between insertion and elimination in the ring expansion mechanism.

In order to further clarify the issue of steric protection around the metal centre and its effect in catalytic behaviors, we have designed various bidentate and tridentate Amidinate (NCN) and Amidate (NCO) ligands which will be presented in the next chapter.

References

1. a) McGuinness, D. S.; Gibson, V. C.; Steed, J. W. *Organometallics* **2004**, *23,* 6288. b) Tenza, K.; Hanton, M. J.; Slawin, A. M. Z. *Organometallics* **2009**, *28*, 4852.
2. Kirillov, E.; Roisnel, T.; Razavi, A.; Carpentier, J. F. *Organometallics* **2009**, *28,* 2401.
3. Junges, F.; Kuhn, M. C. A.; dos Santos, A. H. D. P.; Rabello, C. R. K.; Thomas, C. M.; Carpentier, J. F.; Casagrande, O. L. Jr. *Organometallics* **2007**, *26,* 4010.
4. a) Chen, Y.; Zuo, W.; Hao, P.; Zhang, S.; Gao, K.; Sun, W-H. *J. Organomet. Chem.* **2008**, *693*, 750. b) Gao, R.; Liang, T.; Wanga, F.; Sun, W-H. *J. Organomet. Chem.* **2009**, *694*, 3701.
5. Small, B. L.; Rios, R.; Fernandez, E. R.; Gerlach, D. L.; Halfen, J. A.; Carney, M. J. *Organometallics, ASAP*.
6. Vogt, D. Oligomerization of ethylene to higher linear α-olefins; in *Applied Homogeneous Catalysis with Organometallic Compounds*; Cornils, B., Herrmann, W. A., Eds.; Wiley-VCH: Weinheim, Germany, **2000**; Chapter 2, pp 245.
7. a) Cossee, P. *J. Catal*. **1964**, *3*, 80. b) E. J. Arlman, P. Cossee*, J. Catal*. **1964**, *3*, 99. c) J. Skupinska, *Chem. Rev*. **1991**, *91*, 613.
8. a) Groppo, E.; Lamberti, C.; Bordiga, S.; Spoto, G.; Zecchina, A. *Chem. Rev.* **2005**, *105*, 115. b) Theopold, K. H. *CHEMTECH* **1997**, *27*, 26. c) Tomov, A. K.; Chirinos, J. J.; Jones, D. J.; Long, R. J.; Gibson, V. C. *J. Am. Chem. Soc.* **2005**, *127*, 10166. d) Tomov, A. K.; Chirinos, J. J.; Long, R. J.; Gibson, V. C.; Elsegood, M. R. J. *J. Am. Chem. Soc.* **2006**, *128*, 7704. e) McGuinness, D. S.; Suttil, J. A.; Gardiner, M. G.; Davies, N. W. *Organometallics* **2008**, *27*, 4238. f) McGuinness, D. S. *Organometallics* **2009**, *28,* 244.

9. a) Briggs, J. R. *Chem. Commun.* **1989**, *11*, 674. b) Emrich, R.; Heinemann, O.; Jolly, P. W.; Krüger, C.; Verhovnik, G. P. J. *Organometallics* **1997**, *16*, 1511. c) Agapie, T.; Schofer, S. J.; Labinger, J. A.; Bercaw, J. E. *J. Am. Chem. Soc.* **2004**, *126*, 1304. d) Dixon, J. T.; Green, M. J.; Hess, F. M.; Morgan, D. H. *J. Organomet.Chem.* **2004**, *689*, 3641. e) van Rensburg, W. J.; Grové, C.; Steynberg, J. P.; Stark, K. B.; Huyser, J. J.; Steynberg, P. J. *Organometallics* **2004**, *23*, 1207. f) Overett, M. J.; Blann, K.; Bollmann, A.; Dixon, J. T.; Haasbroek, D.; Killian, E.; Maumela, H.; McGuinness, D. S.; Morgan, D. H. *J. Am. Chem. Soc.* **2005**, *127*, 10723. g) Schofer, S. J.; Day, M. W.; Henling, L. M.; Labinger, J. A.; Bercaw, J. E. *Organometallics* **2006**, *25*, 2743. h) Elowe, P. R.; McCann, C.; Pringle, P. G.; Spitzmesser, S. K.; Bercaw, J. E. *Organometallics* **2006**, *25*, 5255. i) van Rensburg, W. J.; Berg, J. A.; Steynberg, P. J. *Organometallics* **2007**, *26*, 1000. j) Wass, D. F. *Dalton Trans.* **2007**, 816. k) Köhn, R. D. *Angew. Chem. Int. Ed.* **2007**, *46*, 2. l) Arteaga-Müller, R.; Tsurugi, H.; Yanagawa, M.; Oda, S.; Mashima, K. *J. Am. Chem. Soc.* **2009**, *131*, 5370. m) Beweries, T.; Fischer, C.; Peitz, S.; Burlakov, V. V.; Perdita, A.; Baumann, W.; Spannenberg, A.; Heller, D.; Rosenthal, U. *J. Am. Chem. Soc.* **2009**, *131*, 4463. n) Bhaduri, S.; Mukhopadhyay, S.; Kulkarni, S. A. *J. Organomet. Chem.* **2009**, *694*, 1297. o) Peitz, S.; Aluri, B. R.; Peulecke, N.; Müller, B. H.; Wöhl, A.; Müller, W.; Al-Hazmi, M. H.; Mosa, F. M.; Rosenthal, U. *Chem. Eur. J.* **2010**, *16*, 7670. p) McGuinness, D. S. *Chem. Rev.* **2011**, *111*, 2321.

10. Agapie, T.; Labinger, J. A.; Bercaw, J. E. *J. Am. Chem. Soc.* **2007**, *129*, 14281.

11. a) Freeman, J. W.; Buster, J. L.; Knudsen, R. D. (Phillips Petroleum Co.) US 5,856,257, **1999**. b) Köhn, R. D.; Haufe, M.; Kociok-Köhn, G.; Grimm, S.; Wasserscheid, P.; Keim, W. *Angew. Chem. Int. Ed.* **2000**, *39*, 4337. c) Yoshida, T.; Yamamoto, T.; Okada, H.;

Murakita, H. (Tosoh Corporation) US2002/0035029, **2002**. d) Carter, A.; Cohen, S. A.; Cooley, N. A.; Murphy, A.; Scott, J.; Wass, D. F. *Chem. Commun.* **2002**, 858. e) McGuinness, D. S.; Wasserscheid, P.; Keim, W.; Hu, C.; Englert, U.; Dixon, J. T.; Grove, C. *Chem. Commun.* **2003**, 334. f) Mahomed, H. A.; Bollmann, A.; Dixon, J. T.; Gokul, V.; Griesel, L.; Grove, J. J. C.; Hess, F.; Maumela, H.; Pepler, L. *Appl. Catal. A* **2003**, *225*, 355. g) McGuinness, D. S.; Wasserscheid, P.; Keim, W.; Morgan, D. H.; Dixon, J. T.; Bollmann, A.; Maumela, H.; Hess, F. M.; Englert, U. *J. Am. Chem. Soc*. **2003**, *125*, 5272. h) Morgan, D. H.; Schwikkard, S. L.; Dixon, J. T.; Nair, J. J.; Hunter, R. *Adv. Synth. Catal.* **2003**, *345*, 939. i) Dixon, J. T.; Green, M. J.; Hess, F. M.; Morgan, D. H. *J. Organomet. Chem.* **2004**, *689*, 3641. j) McGuinness, D. S.; Wasserscheid, P.; Morgan, D. H.; Dixon, J. T. *Organometallics* **2005**, *24*, 552. k) Blann, K.; Bollmann, A.; Dixon, J. T.; Hess, F. M.; Killian, E.; Maumela, H.; Morgan, D. H.; Neveling, A.; Otto, S.; Overett, M. J. *Chem. Commun.* **2005**, 622. l) Blann, K.; Bollmann, A.; Dixon, J. T.; Hess, F. M.; Killian, E.; Maumela, H.; Morgan, D. H.; Neveling, A.; Otto, S.; Overett, M. J. *Chem. Commun.* **2005**, 620. m) Bluhm, M. E.; Walter, O.; Döring, M. *J. Organomet. Chem.* **2005**, *690*, 713. n) Agapie, T.; Day, M. W.; Henling, L. M.; Labinger, J. A.; Bercaw, J. E. *Organometallics* **2006**, *25*, 2733. o) Zhang, J.; Braunstein, P.; Hor, T. S. A. *Organometallics* **2008**, *27*, 4277. p) Klemps, C.; Payet, E.; Magna, L.; Saussine, L.; Le Goff, X. F.; Le Floch, P. *Chem. Eur. J.* **2009**, *15*, 8259. q) Licciulli, S.; Thapa, I.; Albahily, K.; Korobkov, I.; Gambarotta, S.; Duchateau, R.; Chevalier, R.; Schuhen, K. *Angew. Chem. Int. Ed.* **2010**, *49*, 9225. r) Peitz, S.; Peulecke, N.; Aluri, B. R.; Hansen, S.; Müller, B. H.; Spannenberg, A.; Rosenthal, U.; Al-Hazmi, M. H.; Mosa, F. M.; Wöhl, A.;

Müller, W. *Eur. J. Inorg. Chem.* **2010**, 1167. s) Zhang, W.; Sun, W.-H.; Zhang, S.; Hou, J.; Wedeking, K.; Schultz, S.; Fröhlich, R.; Song, H. *Organometallics* **2010**, *29*, 5805.

12. a) Rüther, T.; Cavell, K. J.; Braussaud, N. C.; Skelton, B. W.; White, A. H. *J. Chem. Soc*., *Dalton Trans*., **2002**, 4684. b) Crewdson, P.; Gambarotta, S.; Djoman, M. C.; Korobkov, I.; Duchateau, R. *Organometallics* **2005,** *24,* 5214. c) Tomov, A. K.; Chirinos, J. J.; Long, R. J.; Gibson, V. C.; Elsegood, M. R. J. *J. Am. Chem. Soc.* **2006**, *128*, 7704. d) Zhang, W.; Sun, W-H.; Zhang, S.; Hou, J.; Wedeking, K.; Schultz, S.; Fröhlich, R.; Song, H. *Organometallics* **2006**, *25,* 1961. e) Zhang, S.; Jie, S.; Shi, Q.; Sun, W. H. *J. Mol. Catal. A: Chem.* **2007**, *276*, 174. f) Greiner, E.; Gubler, R.; Inoguchi, Y. *Linear Alpha Olefins*, CEH Marketing Research Report, Chemical Economics Handbook; SRI International: Menlo Park, CA, May **2004**.
13. a) Hogan, J. P.; Banks, R. L. (Phillips Petroleum Co.) US 2,825,721, **1958**. b) Karapinka, G. L. (Union Carbide Corp.) Ger. Offen. DE 1808388, **1970**. c) Karol, F. J.; Karapinka, G. L.; Wu, C.; Dow, A. W.; Johnson, R. N.; Carrick, W. L. *J. Polym. Sci., Polym. Chem. Ed.***1972**, *10*, 2621. d) Karapinka, G. L. (Union Carbide Corp.) US 3,709,853, **1973**. e) Bhandari, G.; Kim,Y.; McFarland, J. M.; Rheingold, A. L.; Theopold, K. H. *Organometallics* **1995**, *14*, 738. f) White, P. A.; Calabrese, J.; Theopold, K. H. *Organometallics* **1996**, *15,* 5473. g) Theopold, K. H. *Eur. J. Inorg. Chem.* **1998**, 15. h) Gibson, V. C.; Maddox, P. J.; Newton, C.; Redshaw, C.; Solan, G. A.; White, A. J. P.; Williams, D. J. *Chem. Commun.* **1998**, 1651. i) Döhring, A.; Göhre, J.; Jolly, P. W.; Kryger, B.; Rust, J.; Verhovnik, G. P. J. *Organometallics* **2000**, *19*, 388. j) Rogers, J. S.; Bu, X. H.; Bazan, G. C. *Chem. Commun.* **2000**, 1209. k) Gibson, V. C.; Mastroianni, S.; Newton, C.; Redshaw, C.; Solan, G. A.; White, A. J. P.; Williams, D. J. *J. Chem. Soc.,*

Dalton Trans. **2000**, 1969. l) Bazan, G. C.; Rogers, J. S.; Fang, C. C. *Organometallics* **2001**, *20*, 2059. m) Enders, M.; Fernandez, P.; Ludwig, G.; Pritzkow, H. *Organometallics* **2001**, *20*, 5005. n) MacAdams, L. A.; Kim, W. K.; Liable-Sands, L. M.; Guzei, I. A.; Rheingold, A. L.; Theopold, K. H. *Organometallics* **2002**, *21*, 952. o) Esteruelas, M. A.; López, A. M.; Méndez, L.; Oliván, M.; Oñate, E. *Organometallics* **2003**, *22*, 395. p) Carney, M. J.; Robertson, N. J.; Halfen, J. A.; Zakharov, L. N.; Rheingold A. L. *Organometallics* **2004**, *23,* 6184. q) MacAdams, L. A.; Buffone, G. P.; Incarvito, C. D.; Rheingold, A. L.; Theopold, K. H. *J. Am. Chem. Soc.* **2005**, *127*, 1082. r) Vidyaratne, I.; Scott, J.; Gambarotta, S.; Duchateau, R. *Organometallics* **2007**, *26*, 3201. s) McDaniel, M. P. *Advances in Catalysis* **2010**, *53*, 123.

14. a) Jabri, A.; Crewdson, P.; Gambarotta, S.; Korobkov, I.; Duchateau, R. *Organometallics* **2006**, *25,* 715. b) Jabri, A.; Mason, C. B.; Sim, Y.; Gambarotta, S.; Burchell, T. J.; Duchateau, R. *Angew. Chem., Int. Ed.* **2008**, *47*, 9717. c) Vidyaratne, I.; Nikiforov, G. B.; Gorelsky, S. I.; Gambarotta, S.; Duchateau, R.; Korobkov, I.; A*ngew. Chem. Int. Ed.* **2009**, *48*, 6552. d) Zhang, J.; Li, A.; Hor, T. S. A. *Organometallics* **2009**, *28*, 2935.
15. a) Thapa, I.; Gambarotta, S.; Korobkov, I.; Duchateau, R.; Kulangara, S. V.; Chevalier, R. *Organometallics* **2010**, *29*, 4080. b) Blann, K.; Bollmann, A.; Dixon, J. T.; Neveling, A.; Morgan, D. H.; Maumela, H.; Killian, E.; Hess, F. M.; Otto, S.; Pepler, L.; Mahomed, H. A.; Overett, M. J. (Sasol Technology LTD) WO 04/056479, **2004**. c) Han, T. -K.; Ok, M. A.; Chae, S. S.; Kang, S. O.; Jung, J. H. (SK Energy Corporation) WO 08/088178, **2008**.
16. a) Albahily, K.; Koç, E.; Al-Baldawi, D.; Savard, D.; Gambarotta, S.; Burchell, T. J.; Duchateau, R. *Angew. Chem. Int. Ed.* **2008**, *47*, 5816. b) Albahily, K.; Al-Baldawi, D.;

Gambarotta, S.; Koç, E.; Duchateau, R. *Organometallics*, **2008**, *27*, 5708. c) Albahily, K.; Al-Baldawi, D.; Gambarotta, S.; Koç, E.; Duchateau, R. *Organometallics* **2008**, *27*, 5943.

Publication:

1) **Thapa**, **I.**; Peneau,V.; Noel, C. W; Gambarotta, S.; Korobkov, I. *Organometallics* (Submission in process)

Highly Active Ethylene Oligomerization Chromium Amidinate/Amidate Complexes

6.1 Introduction

Linear alpha olefins (LAOs) are valued commodity chemicals for a range of industrial and household applications, detergents, plasticizer alcohols, synthetic lubricants, surfactants, cosmetics and as co-monomer for LLDPE.[1] All the three full range producers of LAOs (Shell, BP Amoco and Chevron Phillips) utilize the route of ethylene oligomerization to produce a Schulz-Flory[2] distribution ranging from C_4-C_{20} (SHOP[3] process), and from which the desired products may be separated through an energy intensive fractionation. Therefore, the possibility of selectively producing the most valuable α-olefins (1-butene, 1-hexene and 1-octene) is not only challenging but also very attractive from the commercial point of view. Thus, the main focus of research in this field has been for developing more selective and active catalysts. Apart from dimerization, the majority of selective tri-[4-13] /tetramerization[14-17] and non-selective oligomerization[18-22] and polymerization[23-30] catalysts are all based on chromium. The versatility in product outcome basically relies on this metal's unique character of adopting a range of oxidation states (+I, +II, +III), each with a distinctive catalytic behavior. For example, the monovalent state of chromium has been linked to selective behaviour[12c, d, 31,32] whereas the

divalent and trivalent states are related to non-selective oligomerization and polymerization each of them following a different mechanistic pathway.[12c,d,33] It is commonly believed that a selective process follows a metallacycle mechanism.[4-17,21,34-45] rather than non-redox chain growth (Cossee-Arlman) mechanism and which results into non-selective product distribution.[46]

The incomplete reduction of the trivalent state to di- or monovalent and their ready interconvertion during the activation process explains the often observed partial selectivity and polymer fouling.[33-37] Therefore, being able to stabilize a particular oxidation state would enable to control the catalytic behavior. From the previous studies we have known that the nature of the ligand plays a critical role in stabilizing a particular oxidation state and consequently determines the catalytic behavior.[12, 20b, 37]

As a part of our systematic exploration on ligands, their ability to stabilize a particular oxidation state and their role in catalytic behaviours, we have now attempted to evaluate the hard donors bi- and tri-dentate amidinates and amidate ligands. We have in particular examined their ability to affect the stability of the chromium divalent state based on denticity, and steric effects.

Herein, we report the results of our findings in relation to the catalytic behavior of these complexes.

6.2 Experimental

All reactions were carried out under a dry nitrogen atmosphere unless otherwise stated. Solvents were dried using an aluminum oxide solvent purification system. $CrCl_2(THF)_2$ and $CrCl_3(THF)_3$ were prepared according to standard procedure. Et_3N was dried over potassium hydroxide pellets and distilled before use. Lithium reagents were purchased from Aldrich and used as it was. Infrared spectra were recorded on an ABB Bomen FTIR instrument from Nujol

mulls prepared in a dry box except in the case of air stable compounds. Samples for magnetic susceptibility were weighed inside a dry box equipped with an analytical balance and sealed into calibrated tubes and measurements were carried out with a Johnson Matthey Magnetic Susceptibility balance at room temperature. NMR data were collected on a Bruker Avance 300 spectrometer. Data for X-ray crystal structure determination were obtained with a Brucker diffractometer equipped with a 1K Smart CCD area detector. Mass spectra were recorded on a Micromass Quattro-LC Electrospray-Triple Quadrupole Mass Spectrometer. Ligand N, N'-Bis(2,6-diisopropylphenyl)benzamidine (**1c**)[47] and N-Phenyl-N'-Pyridine–2-ylmethyl-benzamidine (**3c**)[47d] were prepared following the previously published procedure.

6.2.1 Preparation of 2, 6 – diisopropylphenyl benzamidate (1a)

A solution of benzoyl chloride (20 mL 173 mmol) in dry CH_2Cl_2 (50 mL) was added slowly to a stirred solution of 2,6-Diisopropylaniline (20 mL, 173 mmol,) and triethylamine (47.25 mL, 346.2 mmol) in dry CH_2Cl_2 (200 mL) at 0 ^oC. Stirring was continued for 18 hours at room temperature. The resulting mixture was washed with dilute HCl (2M), saturated brine and then dried over Na_2SO_4. Concentration under reduced pressure afforded an off-white solid. Recrystallization from ethanol afforded pure **1a** (38.97 g, 138 mmol, 80%) as an isolated yield. ^1H-NMR (300 MHz, $CDCl_3$, 25 ^oC) δ: 7.95 (2H, m), 7.52 (3H, m), 7.37(2H, m), 7.34 (2H, m), 3.16 (2H, septet), 1.61(1H, s), 1.87 (12H, d, J = 6.6 Hz). ^{13}C {1H}-NMR (300 MHz, $CDCl_3$, 25 ^oC) δ: 146.7, 135.0, 132.2, 131.5, 129.2, 128.9, 127.5, 123.9, 29.3, 24.0. EI-MS *m/z* = 281.3(M+).

6.2.2 Isolation of O-methoxyphenyl benzamidate (2a)

A solution of benzoyl chloride (20 mL 173 mmol) in dry CH_2Cl_2 (50 mL) was added slowly to a stirred solution of O-Anisidine (19.5 mL, 173 mmol) and triethylamine (48.2 mL, 346 mmol) in dry CH_2Cl_2 (200 mL) at 0 ^oC. Stirring was continued for 18 hours at room temperature. The resulting mixture was washed with dilute HCl (2M), saturated brine and then dried over Na_2SO_4. Concentration under reduced pressure afforded white solid. Recrystallization from ethanol give pure **2a** (34 g, 150 mmol, 87%).

^{1}H-NMR (300 MHz, $CDCl_3$, 25 ^oC) δ: 8.57(1H, br, s), 8.55-8.51(1H, dd, J_1 = 3 Hz, J_2 = 3 Hz), 7.90-7.87(2H, m), 7.56-7.45 (3H, m), 7.11-6.98 (2H, m), 6.92-6.88 (1H, dd, J_1 = 3 Hz, J_2 = 3 Hz) 3.90 (3H, s). ^{13}C{1H}-NMR (300 MHz, $CDCl_3$, 25 ^oC) δ: 165.6, 144.9, 133.0, 130.6, 128.9, 128.9, 125.3, 124.0, 121.4, 120.6, 112.5, 56.6. EI-MS *m/z* = 227.1 (M+).

6.2.3 Preparation of N, N'-Bis(O-methoxyphenyl) benzamidine (2c)

Solid **2a** (30 g, 132 mmol) was dissolved in excess of $SOCl_2$ (50 mL) and reflux for 3 hrs. Excess of $SOCl_2$ was evaporated off under reduced pressure. The crude product was heated with hexane (50 mL) for 1 hr. Filtered off the product as a yellow liquid and concentrated to allow crystallization at room temperature yielding a bright yellow solid (32 g, 131 mmol, 99%). The solid was then dissolved in dry THF (200 mL) under nitrogen at room temperature. Added distilled triethylamine (20 mL, 144 mmol) at 0 ^oC and allowed to stir for further 1 hour. To the reaction mixture slowly added O-Anisidine (14.8 mL, 131 mmol) under nitrogen and continued stirring for 48 hours at room temperature. The title product **2c** was separated from the ammonium salt through filtration. Excess of solvent was removed under reduced pressure to afford an analytically pure yellow solid (34.2 g, 103 mmol, 79%). ^{1}H-NMR (300 MHz, $CDCl_3$,

25 ^{o}C) δ: 8.63 (1H, br), 7.39-7.36 (5H, m), 7.24-7.10 (3H, m), 6.68-6.53 (5H, m), 3.67 (3H, s), 3.59 (3H, s). ^{13}C{1H}-NMR (300 MHz, $CDCl_3$, 25 ^{o}C) δ: 157.1, 156.2, 133.6, 133.0, 132.5, 131.3, 128.5, 128.0, 124.2, 123.5, 121.1, 120.2, 116.5, 115.3, 110.8, 55.9, 55.2. EI-MS *m/z* = 332.1 (M+).

6.2.4 Preparation of {[(C_6H_3-2,6-di-^{i}Pr) NC(C_6H_5)N(C_6H_3-2,6-di-^{i}Pr)]$_2$ Cr } (6.1)

Ligand N,N'-Bis(2,6-diisopropylphenyl)benzamidine (**1c**) (0.88 g, 2 mmol) was dissolved in Et_2O (5 mL). A solution of *n*-Buli (0.84 mL 2.1 mmol, 2.5 M in hexane) was added slowly to the cold solution (-30 ^{o}C) and stirred for 3 hrs. A suspension of $CrCl_2(THF)_2$ (0.27 g, 1 mmol) in THF (5 mL) was added to the lithium salt of ligand and the resulting mixture stirred at room temperature for 18 hrs. Solvent was evaporated under reduced pressure and the residue redissolved in Et_2O (10 mL) and centrifuged. Supernatant was decanted and reduced to 5 mL under reduced pressure. Single crystals of **6.1** were grown upon standing at -35 ^{o}C for 5 days which were isolated by filtration, washed with cold hexane and dried in *vacuo* to yield (0.56 g, 0.6 mmol, 60%). Elemental Analysis Calcd. (Found) for C_{62} H_{78} Cr N_4: C 79.96 (79.87) H 8.44 (8.37) N 6.02 (5.08). [μ_{eff} = 4.86 μ_B].

6.2.5 Preparation of {[(C_6H_5OMe)NC(C_6H_5)N(C_6H_5OMe)]$_2$ Cr_2 (μ-Cl)} (6.2)

N, N'-Bis(O-methoxyphenyl) benzamidine **2c** (0.66 g, 2 mmol) was dissolved in THF (5 mL). A solution of *n*-Buli (0.84 mL, 2.1 mmol, 2.5 M in hexane) was added slowly to the cold solution (-30 ^{o}C) of ligand and allowed to stir for 3 hrs. A suspension of $CrCl_2(THF)_2$ (0.27 g, 1 mmol) in THF (5 mL) was added to the lithium salt of ligand. The resulting brown solution was allowed to stir at room temperature for 24 hrs. Solvent was evaporated under reduced pressure and the residue redissolved in toluene (10 mL), centrifuged and decanted as a clear dark brown

solution. Single brown X-ray quality crystals **6.2** were grown upon standing at -35 ^{o}C for 7 days which were collected by filtration, washing with cold hexane and dried in *vacuo* to yield (0.52 g, 0.39 mmol, 39%). Elemental Analysis Calcd. (Found) for C_{77} H_{73} Cl Cr_2 N_6 O_6: C 70.18(70.12) H 5.58 (5.49) N 6.38 (6.35). [μ_{eff} = 2.69 μ_B].

6.2.6 Preparation of {[$(C_6H_5)NC(C_6H_5)NCH_2(C_5H_4N)]_2$ $Cr_2Cl_2\}_2$ (6.3)

Solid **3c** (0.27 g, 1 mmol) was dissolved in THF (5 mL) and its cold solution (-30 ^{o}C) treated with a solution of *n*-Buli (0.44 mL, 1.1 mmol, 2.5 M in hexane). Stirring was continued for 3 hrs. A suspension of $CrCl_2$ $(THF)_2$ (0.54 g, 2 mmol) in THF (5 mL) was added to the mixture and the resulting brown solution allowed to stir at room temperature for 24 hrs. Solvent was evaporated under reduced pressure and the residue redissolved in toluene (10 mL), centrifuged and the supernatant decanted as clear dark brown solution. Single brown crystals of **6.3** were grown upon standing at -35 ^{o}C for 10 days and which were collected through filtration, washing with cold hexane and dried in *vacuo* to yield (0.35 g, 0.19 mmol, 19%).

Elemental Analysis Calcd. (Found) for C_{104} H_{94} Cl_4 Cr_4 N_{12}: C 67.09 (67.01), H5.09 (5.02) N 9.03(9.01), [μ_{eff} = 8.13 μ_B] *per tetrameric unit*.

6.2.7 Preparation of {[$(C_6H_5)NC(C_6H_5)NCH_2(C_5H_4N)]_2$ Cr_2Cl_4} 0.5(toluene) (6.4)

Ligand **3c** (0.27 g, 1 mmol) was dissolved in THF (5 mL) and treated at -30 ^{o}C with a solution of *n*-Buli (0.44 mL, 1.1 mmol, 2.5 M in hexane). Stirring was continued for 3 hrs, after which, a suspension of $CrCl_3$ $(THF)_3$ (0.38 g, 1 mmol) in THF (5 mL) was added to the mixture. The resulting green solution was allowed to stir at room temperature for 18 hrs. The solvent was evaporated under reduced pressure and the residue redissolved in toluene (10 mL), centrifuged and the supernatant decanted as clear dark green solution. Single green crystals of **6.4** were

grown upon standing at -35 ^{o}C for 8 days which were collected through filtration, washed with cold hexane and dried in *vacuo* to yield (0.39 g, 0.41 mmol, 41%). Elemental Analysis Calcd. (Found) for $C_{48.50}H_{44}Cl_4Cr_2N_6$: C60.89 (60.85) H 4.64 (4.61) N 8.78 (8.74). [μ_{eff} = 3.10 μ_B] .

6.2.8 Preparation of {[(Cy)NC(C_4H_9)N(Cy)] Cr (Cl_2) ($THF)_2$} (6.5)

Dicyclohexylcarbodiimide (0.20 g, 1 mmol) was dissolved in Et_2O (5 mL) and the solution was treated with of *n*-Buli (0.44 mL, 1.1 mmol, 2.5 M in hexane) at -30 ^{o}C. Stirring was continued for 5 hrs. after which a suspension of $CrCl_3(THF)_3$ (0.38 g, 1 mmol) in THF (5 mL) was added. Stirring was continued for further 18 hrs at room temperature. The solvent was evaporated under reduced pressure, the residue was redissolved in THF (10 mL), centrifuged and the supernatant decanted as clear dark purple solution. Purple single crystals of **6.5** were grown upon standing at -35 ^{o}C for 7 days, which were collected by filtration, washed with cold hexane and dried in *vacuo* (0.52 g, 0.86 mmol, 86%). Elemental Analysis Calcd. (Found) for $C_{29}H_{54}Cl_2CrN_2O_3$: C 57.89 (57.86) H9.05 (9.02) N 4.66 (4.58). [μ_{eff} = 3.89 μ_B].

6.2.9 Preparation of {Cr[(Cy)NC(C_4H_9)N(Cy)]$_3$} (6.6)

Dicyclohexylcarbodiimide (0.62 g, 3 mmol) was dissolved in Et_2O (10 mL) and treated with a solution of *n*-Buli (1.3 mL, 3.1 mmol, 2.5 M in hexane) at -30 ^{o}C. After stirring for 5 hrs, a suspension of $CrCl_3(THF)_3$ (0.38 g, 1 mmol) in THF (5 mL) was added to the solution and stirring was continued for further 18 hrs at room temperature. The solvent was evaporated under reduced pressure and the residue redissolved in toluene (10 mL). After centrifugation, the supernatant was decanted as clear dark green solution. Single green crystals of **6.6** were grown upon standing at -35 ^{o}C for 7 days which were collected through filtration, washed with cold hexane and dried in *vacuo* to yield (0.65 g, 0.77 mmol, 77%). Elemental Analysis Calcd. (Found)

for C_{51} H_{93} Cr N_6: C 72.72 (72.68) H11.13 (11.08) N 9.98 (9.95). [μ_{eff} = 3.88 μ_B] .

6.2.10 Preparation of {$Cr_2[(C_6H_5)C(O)N(C_6H_3$-2,6-^{i}Pr)]$_4$} .(thf).(toluene) (6.7)

A solution of *n*-Buli (2.1 mmol, 0.84 mL) was added slowly to a cold solution of 2,6-Diisopropylbenzamidate **1a** (0.56 g, 2 mmol) THF (5 mL). After stirring for 3 hrs, a suspension of $CrCl_2$ $(THF)_2$ (0.26 g, 1 mmol,) in THF (5 mL) was added. Stirring was continued at room temperature for 18 hrs. The solvent was evaporated under reduced pressure and the residue redissolved in toluene (10 mL) and centrifuged. The supernatant was decanted and reduced to 5 mL under reduced pressure. Diamagnetic single crystals of **6.7** were grown upon standing at -35 ^oC for several days which were collected through filtration, washed with cold hexane and dried under reduced pressure(0.6 g, 0.48 mmol, 48%). ^{1}H-NMR (300 MHz, C_6D_6, 25 ^oC) δ: 7.01 (4H, m), 6.13-6.11 (8H, m), 5.61(10H, m), 5.31 (10H, m), 1.34 (8H, septet), -0.67- 0.69 (48H, d, J = 6 Hz), ^{13}C{H}-NMR (300 MHz, C_6D_6, 25 ^oC) δ: 168.8, 144.6, 133.4, 131.0, 128.9, 126.1, 125.5, 120.8, 104.5, 26.7, 21.1. (co-ordinated ligand).

6.2.11 Preparation of Complex, {$Cr[(C_6H_5)C(O)N(C_6H_3$-2,6-di-^{i}Pr)]$_3$} (6.8)

A solution of *n*-Buli (1.24 mL, 3.1 mmol, 2.5 M in hexane) was added slowly to a cold solution 2,6-Diisopropylbenzamidate **1a** (0.84 g, 3 mmol) in THF (5 mL). After stirring for 3 hrs, a suspension of $CrCl_3$ $(THF)_3$ (0.37 g, 1 mmol) in THF (5 mL) was added. The resulting green solution was stirred at room temperature for 24 hrs. The solvent was evaporated under reduced pressure and the residue redissolved in toluene (10 mL) and centrifuged. The supernatant was decanted as clear green solution. Paramagnetic, green, single-crystals of **6.8** were grown upon standing at -30 ^oC for 2 days which were collected by filtration, washed with cold hexane and

dried under reduced pressure (0.8 g, 0.9 mmol, 90%). Elemental Analysis Calcd. (Found) for C_{57} H_{66} Cr N_3 O_3: C 76.65 (76.61), 7.45(7.42), N 4.70(4.72). [μ_{eff} = 3.91 μ_B].

6.3 X-ray Data

Table 6.1: Crystal data and structural analysis Results of Complex **6.1-6.8**.

	6.1	**6.2**	**6.3**
Formula	C_{62} H_{78} Cr N_4	C_{77} H_{73} Cl Cr_2 N_6 O_6	C_{104} H_{94} Cl_4 Cr_4 N_{12}
FW	931.28	1317.86	1861.71
Space group	Monoclinic, C2/c	Triclinic, P-1	Monoclinic, C2/c
a (Å)	23.845(2)	11.689(5)	24.2941(8)
b (Å)	10.4906(9)	14.690(6)	21.1258(7)
c (Å)	25.244(2)	20.232(8)	23.2043(9)
α (deg)	90	79.049(6)	90
β (deg)	115.8510(10)	87.415(6)	90.447(2)
γ (deg)	5682.6(9)	85.482(6)	90
V (Å^3)	5682.6(9)	3399(2)	11908.8(7)
Z	4	2	4
radiation (Kα, Å)	0.71073	0.71073	0.71073
T (K)	203(2) K	200(2)	200(2)
D_{calcd} (g cm^{-3})	1.089	1.288	1.038
μ_{calcd} (mm^{-1})	1.089	0.417	0.488
F_{000}	2008	1380	3864
R, R_w [2 a]	0.0549, 0.1731	0.0674, 0.1242	0.0842, 0.2106
GoF	1.074	1.035	1.043

	6.4	**6.5**	**6.6**
Formula	$C_{48.50}$ H_{44} Cl_4 Cr_2 N_6	C_{29} H_{54} Cl_2 Cr N_2 O_3	C_{51} H_{93} Cr_1 N_6
FW	956.70	601.64	842.315
Space group	Triclinic, P-1	Monoclinic, P2(1)/c	Monoclinic, P2(1)/c
a (Å)	11.7872(8)	23.03(2)	22.892(10)
b (Å)	14.1780(12)	12.524(10)	20.196(8)
c (Å)	16.2814(13)	30.712(19)	23.271(10)
α(deg)	105.769(4)	90	90
β(deg)	100.732(4)	131.55(4)	109.985(7)
γ(deg)	104.489(3)	90	90
V (Å^3)	2439.1(3)	6629(9)	10111(7)
Z	2	8	4
radiation (Kα, Å)	0.71073	0.71073	0.71073
T (K)	200(2)	200(2)	203(2)
D_{calcd} (g cm^{-3})	1.303	1.206	1.107
μ_{calcd} (mm^{-1})	0.703	0.536	0.264
F_{000}	986	2592	3720
R, R_w [2 a]	0.0537, 0.1527	0.1043, 0.2699	0.0714, 0.1861
GoF	1.021	1.044	1.039

[a] $R = \Sigma||Fo| - |Fc||/\Sigma|F|$. $Rw = [\Sigma(|Fo| - |Fc|)^2/\Sigma wFo^2]^{1/2}$

	6.7	6.8
Formula	$C_{87}H_{105}Cr_2N_4O_5$	$C_{57}H_{66}CrN_3O_3$
FW	1390.75	893.13
Space group	Monoclinic, P2(1)/n	Monoclinic, P2(1)/n
a (Å)	20.030(3) Å	17.439(2)
b (Å)	17.780(2) Å	18.066(2)
c (Å)	24.544(3) Å	17.456(2)
α (deg)	90	90
β (deg)	113.917(2)	93.541(2)
γ (deg)	90	90
V (Å^3)	7990.4(17)	5488.8(12)
Z	4	4
radiation (Kα, Å)	0.71073	0.71073
T (K)	202(2)	200(2)
D_{calcd} (g cm^{-3})	1.156	1.081
μ_{calcd} (mm^{-1})	0.324	0.250
F_{000}	2972	1908
R, R_w [2 a]	0.0773, 0.1910	0.0769, 0.2093
GoF	1.059	1.050

6.4 Results and Discussion

Amidinate family of ligands provide an excellent example to stabilize transition metal complexes by offering steric and electronic flexibility.[48] The steric bulk of the substituents may adjust the ligand bite and nuclearity of the complexes that would impact on the over all geometric arrangements of the chromium structures.

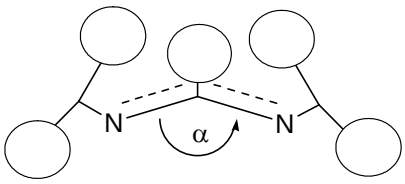

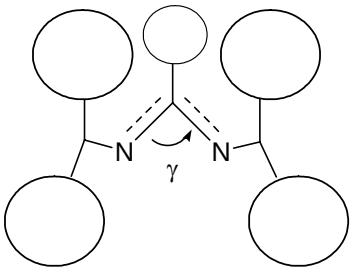

Synthesis of ligands were carried out following the published procedures highlighted in Scheme 6.1.

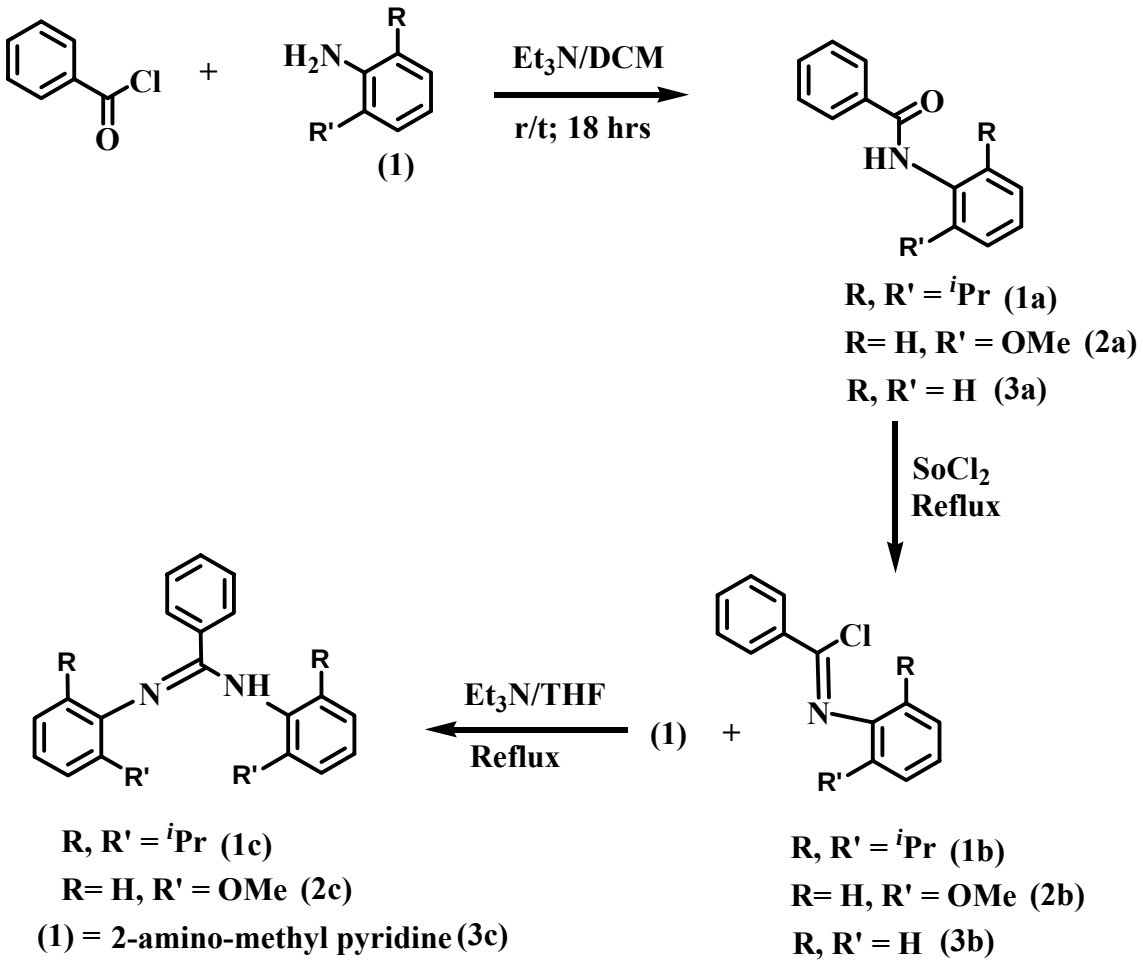

Scheme 6.1: Synthesis of ligands

The reaction of two equivalents of lithium salt of the 2,6-bis-diisopropylbenzamidinate ligand with one equivalent of $CrCl_2(THF)_2$ in THF yielded the mononuclear bis-amidinate complex $\{[(C_6H_3\text{-}2,6\text{-di-}^i\text{Pr})NC(C_6H_5)N(C_6H_3\text{-}2,6\text{-di-}^i\text{Pr})]_2Cr\}$ (**6.1**) (Scheme 6.2).

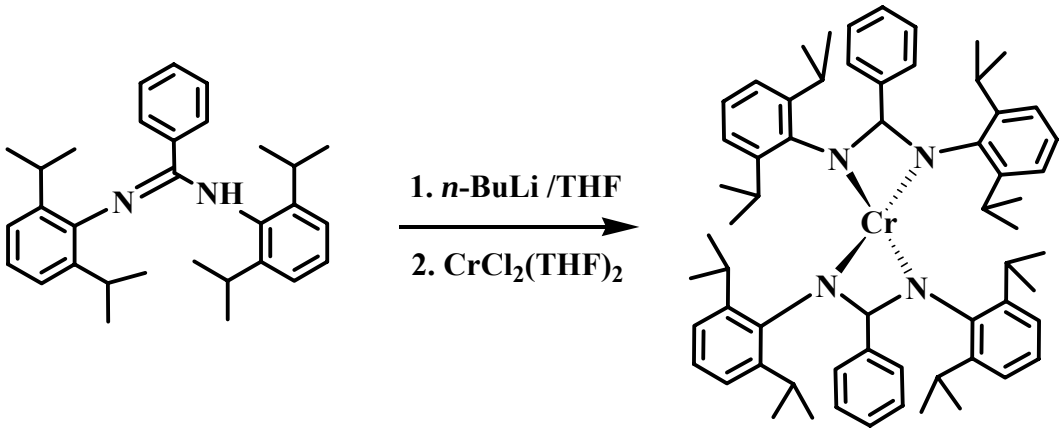

6.1

Scheme 6.2: Synthesis of complex 6.1

The crystal structure (Figure 6.1) showed a mononuclear complex. The coordination geometry around chromium is severely distorted [N1A-Cr-N2A = 64.63(10)^{o}, N1-Cr-N2A = 115.55(10)^{o}, N1A-Cr-N2 = 115.55(10)^{o}, N1-Cr-N2 = 64.62(10)^{o}, N1A-Cr-N1 = 174.32(14)^{o}, N2A-Cr-N2 = 176.88(14)^{o}, Cr-N1 = 2.054(2)Å, Cr-N2 = 2.062(2)Å] due to the narrow bite angle of the amidinate anion [N1-C-N2 = 111.0(3)Å].

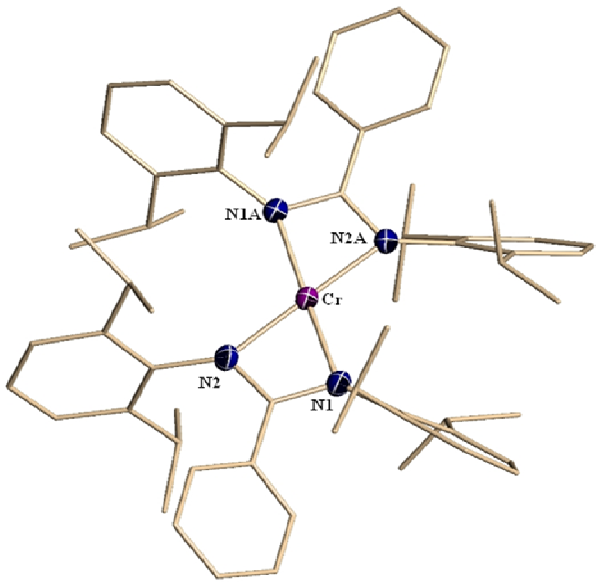

Figure 6.1: Crystal structure of Complex 6.1 with thermal ellipsoids drawn at the 50% probability level.

Previous work on the mono- and dinuclear amidinates has shown that the steric interactions among the substituents in the amidinate backbone determines the nuclearity of the complex.[48] Since this may have an impact on the catalytic behavior, we have replaced the bulky diisopropyl groups with a methoxy group and which may provide further coordination ability via its hard oxygen donor (Scheme 6.1).

The complex $\{[(C_6H_4OMe)NC(C_6H_4)N(C_6H_4OMe)]_2Cr_2(\mu\text{-}Cl)\}$ **(6.2)** was obtained by treating one equivalent of $CrCl_2(THF)_2$ with two equivalents of lithium salt of N, N'- Bis(O-methoxyphenyl) benzamidine ligand in toluene (Scheme 6.3).

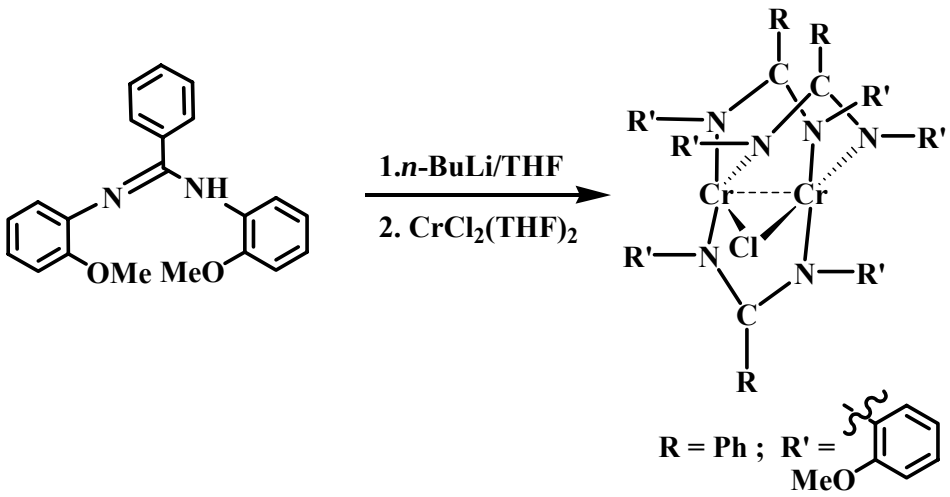

6. 2

Scheme 6.3: Synthesis of dinuclear Cr(II) complex 6.2

The chemical connectivity was yielded by a crystal structure (Figure 6.2). The complex is dinuclear with the two divalent Cr centres bridged by three amidinates adopting the typical three centre chelating geometry. One bridging chlorine atoms completes the structure. The geometry around each metal centre is distorted square planar [Cr2-Cr1-N3 = 94.63(10)°, Cr2-Cr1-N5 = 90.98(10)°, N3-Cr1-N5 = 93.53(11)°, Cr2-Cr1-N1 = 97.85(9)°, N3-Cr1-N1 = 92.55(11)°, N5-

Cr1-N1 = 168.83(13)°, Cr2-Cr1-Cl = 66.00(4)°]. The short Cr…Cr contact falls in the range normally regarded as diagnostic for the presence of a Cr-Cr quadruple bond in the supershort range [Cr1-Cr2 = 1.9168(10) Å].

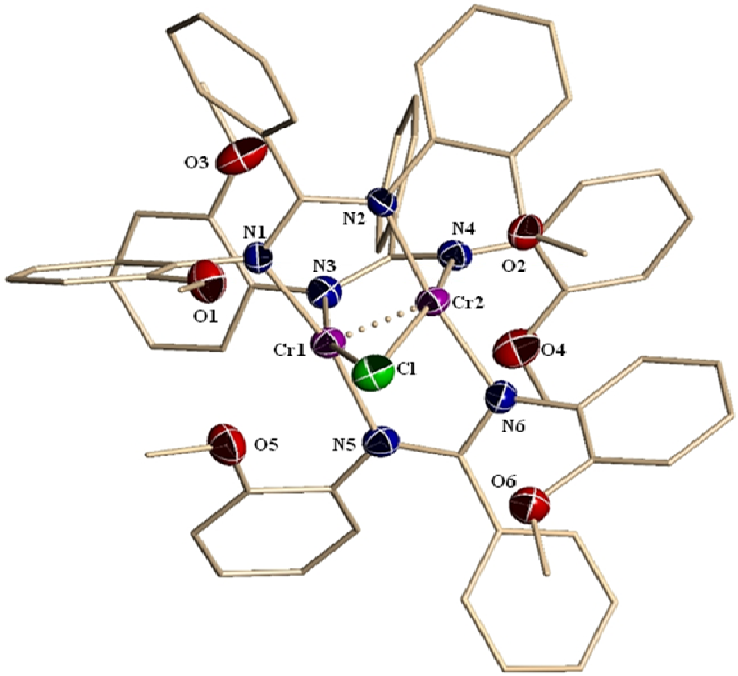

Figure 6.2: Crystal structure of 6.2 with thermal ellipsoids drawn at the 50% probability level.

Given the ability of pyridine rings to embark on electron transfer reaction with consequent stabilization of low-valent synthons, the next modification on "NCN" core was to add pyridine pendent to create a tridentate [PhNC(Ph)N(H)CH_2(Pyridine)] ligand (Scheme 6.1). Complexation of the ligand lithium salt, with $CrCl_2(THF)_2$ and $CrCl_3(THF)_3$ afforded the tetrameric and the dimeric clusters $\{[(C_6H_5)NC(C_6H_5)NCH_2(C_5H_4N)]_2Cr_2Cl_2\}_2$ **(6.3)** and $\{[(C_6H_5)NC(C_6H_5)NCH_2(C_5H_4N)]_2\ Cr_2Cl_4\}$ **(6.4)** respectively (Scheme 6.4). The tetrameric **6.3** was obtained while using a stoichiometric ratio ligand:Cr of 2:1. An unanticipated feature of this complex was the oxidative coupling of two ligands through the former -CH_2 carbon of CH_2-

pyridine sidearm and formation of a C-C single bond [C2-C2a = 1.523(14)Å]. The transformation implies the formal loss of one molecule of H_2. Radical type of coupling of imines, including those directly bonded to pyridine rings, have been observed before and always imply the intervention of the transition metal in what seemingly is a redox transformation.[49] In the present case however, the reaction has no explanation given that the metal has retained the original divalent state and no hydride formation seem to be involved in the overall reaction. Any attempt to isolate reaction byproducts was unsuccessful.

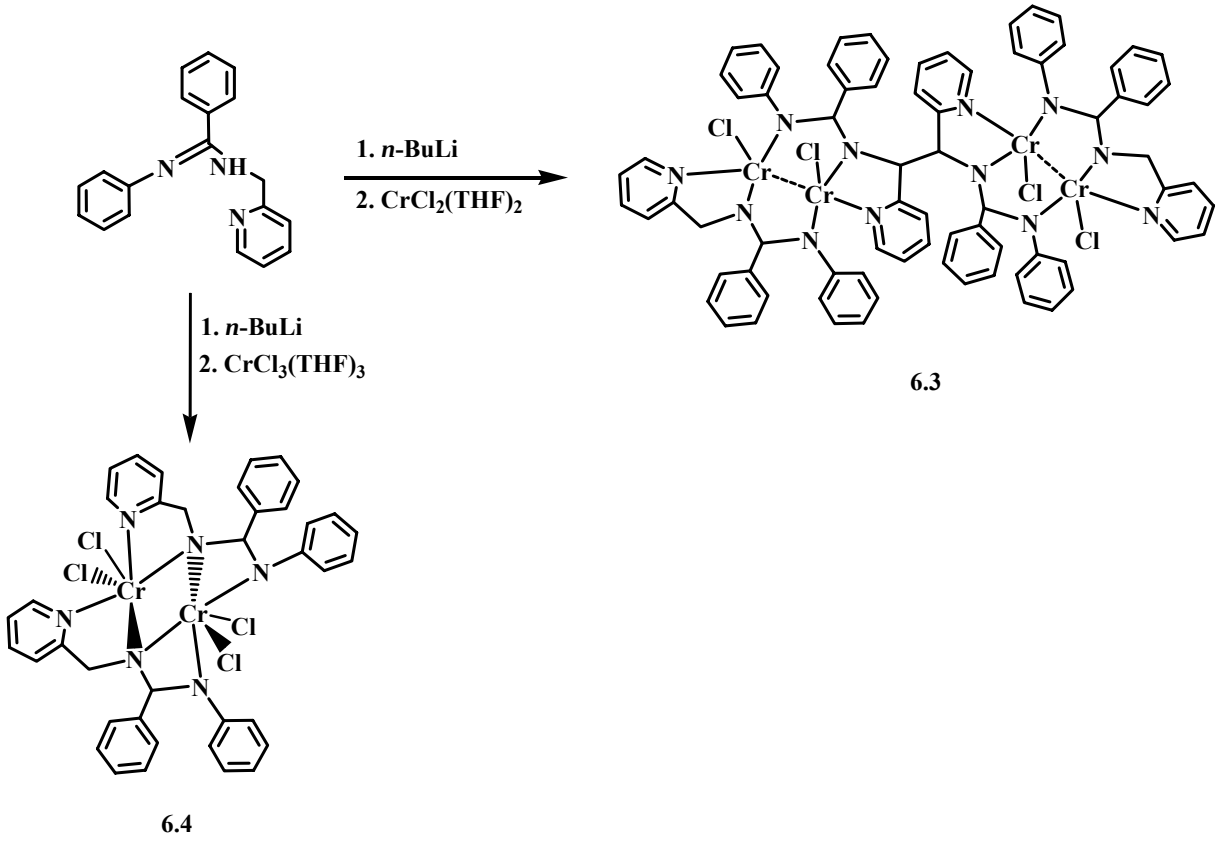

Scheme 6.4: Synthesis of complex 6.3 and 6.4

The structure consists of two identical dimeric subunits with the two metals in a distorted square planar geometry (Figure 6.3). One terminally bonded chlorine atom [Cr1-Cl1 =

2.304(2)Å] is present on each chromium, while one intact ligand is adopting the usual bridging three-centre chelating geometry [Cr1-N5 = 2.003(6)Å, Cr1-N1 = 2.041(6)Å, N5-Cr1-N1 = 90.6(2)^o, N5-Cr1-N6 = 78.0(2)^o, N1-Cr1-N6 = 160.6(3)^o, N5-Cr1-Cl1 = 167.89(19)^o, N1-Cr1-Cl1 = 97.07(18)^o, N6-Cr1-Cl1 = 91.98(19)^o] with the N-atom of the pyridine pendant coordinating the Cr atom at the periphery of the cluster [Cr1-N6 = 2.093(6)Å]. The coupled ligand [C2-C2a = 1.523(14)Å] also adopts the same bridging mode on each of the two dimetallic units. In turn the two pyridine rings coordinate each one chromium atom on each dimetallic subunit. The Cr…Cr distance within each dimetallic subunit is intriguingly long and at the edge of it is considered the bonding range [2.5148(18) Å].

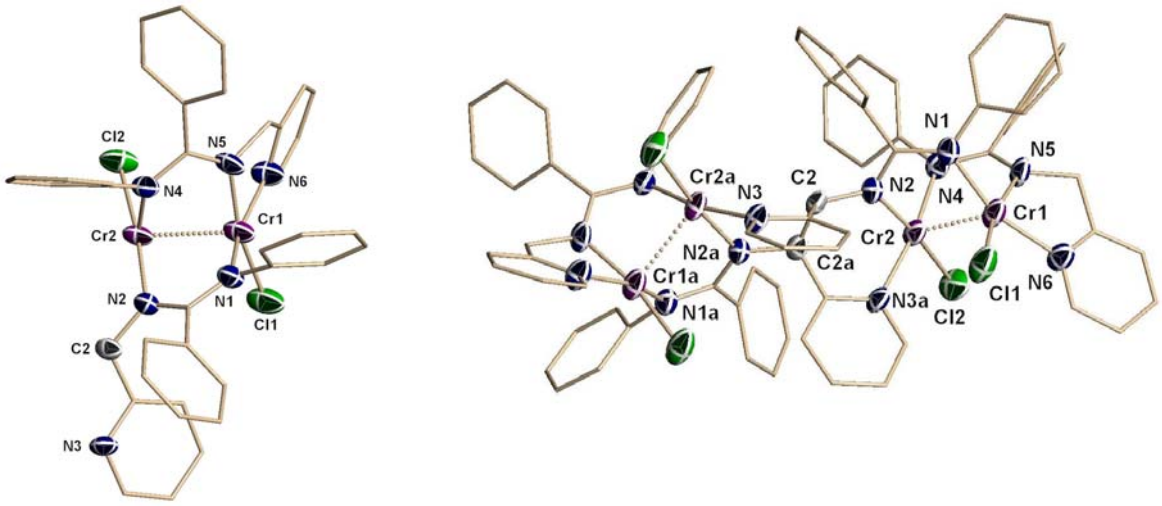

Figure 6.3: Crystal structure of Complex 6.3 with thermal ellipsoids drawn at the 50% probability level. Drawing on the left show one of the two dimetallic subunits.

The complex obtained via treatment of one equivalent of the lithium salt of N-Phenyl-N'-Pyridine-2-ylmethyl-benzamidine ligand with one equivalent of $CrCl_3(THF)_3$ has resulted in a dinuclear trivalent Cr(III) complex **6.4** (Scheme 6.4). Given the tendency of Cr(III) to achieve

the octahedral coordination geometry, the bonding mode of the ligand appeared to be completely different with the two metal in dissimilar ligand environment (Figure 6.4). The asymmetry of the dimeric unit arises from the fact that the two amidinate ligands have oriented the pyridine rings towards the same metal center. As a result, the first Cr atom has its octahedral geometry defined by two terminally bonded chlorine [Cr1-Cl1 = 2.2999(7)Å, Cr1-Cl2 = 2.3016(8)Å] in *cis* positions, and two pyridine ring N atoms [Cr1-N6 = 2.060(2)Å, Cr1-N3 = 2.067(2)Å] in *trans*. The second chromium has also similar arrangement except the axial positions, which are now occupied by the amidinate nitrogens [Cr(2)-N(1) = 2.034(2)Å , Cr(2)-N(4) = 2.064(2)Å] of two ligands placed at the edge of the ligand backbone. The edge-sharing bioctahedral structure is completed in both cases by the two centrally located bridging nitrogen [Cr1-N2 = 2.097(2)Å, Cr1-N5 = 2.115(2)Å] of two amidinate ligands.

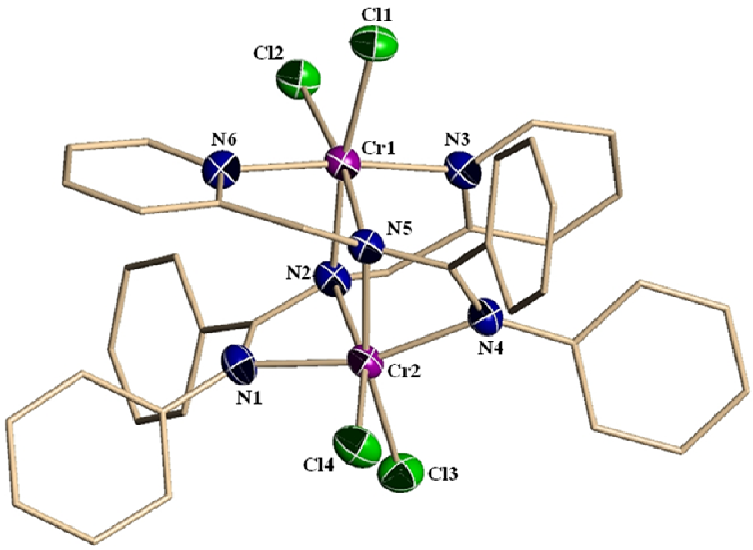

Figure 6.4: Crystal structure of Complex 6.4 with thermal ellipsoids drawn at the 50% probability level.

To bypass the systematic problem arising from the poor solubility of these complexes, we have also prepared a simple dicyclohexylcarbodiimide ligand with a butyl substituent on the central carbon atom. Treatment of lithium salt of the ligand with one equivalent of $CrCl_3(THF)_3$ afforded the monomeric and trivalent $\{[(Cy)NC(C_4H_9)N(Cy)]Cr(Cl_2)(THF)_2\}$ **(6.5)** (Scheme 6.5).

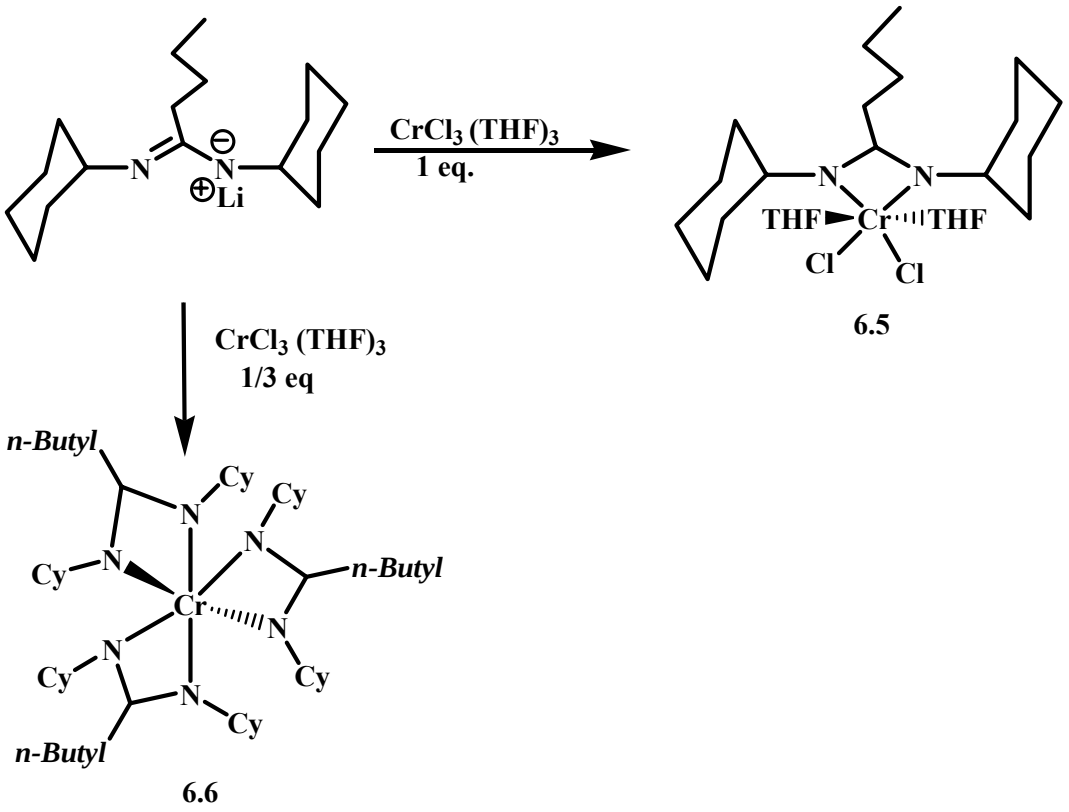

Scheme 6.5: Synthesis of complexes 6.5 and 6.6

The metal centre is surrounded by two nitrogen donor atoms from the ligand [Cr1-N1 = 2.035(10)Å, Cr1-N2 = 2.044(10)Å] two *trans*-located chlorine atoms [Cr1-Cl1 = 2.333(4)Å, Cr1-Cl2 = 2.349(4)Å; Cl1-Cr1-Cl2 = 95.11(16)^o] and two THF molecules [Cr1-O2 = 2.039(8)Å, Cr1-O1 = 2.039(8)Å, O2-Cr1-O1 = 178.6(4)^o] completing the octahedral ligand field [N1-Cr1-N2 = 64.5(4)^o, N2-Cr1-Cl1 = 164.4(3)^o, N1-Cr1-Cl2 = 164.4(3)^o, N1-Cr1-O1 = 88.6(3)^o].

Use of larger amount of ligand afforded the expected homoleptic as a monomeric trivalent complex $\{Cr[(Cy)NC(C_4H_9)N(Cy)]_3\}$ **(6.6)** (Scheme 6.5). The structure was elucidated by X-ray crystallography (Figure 6.5). The monomeric chromium centre is hexa coordinated with six nitrogen atoms of three ligands [Cr1-N2 = 2.058(4)Å, Cr1-N3 = 2.062(4)Å, Cr1-N4 = 2.073(4)Å, Cr1-N5 = 2.074(4)Å, Cr1-N1 = 2.076(4)Å, Cr1-N6 = 2.078(3)Å] in an octahedral environment [N4-Cr1-N1 = 161.24(15)^o, N2-Cr1-N5 = 160.85(15)^o, N3-Cr1-N6 = 161.18(15)^o, N2-Cr1-N1 = 63.88(14)^o, N3-Cr1-N4 = 64.25(14)^o].

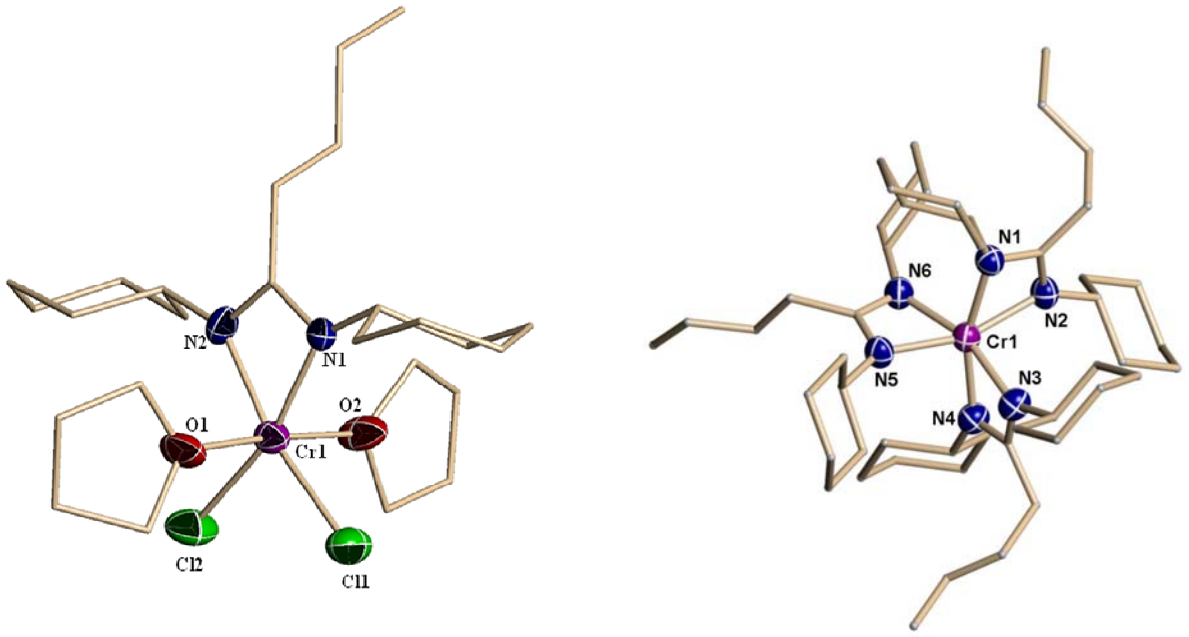

6.5 **6.6**

Figure 6.5: Crystal structure of complex 6.5 and 6.6 with thermal ellipsoids drawn at the 50% probability level.

To enable a complete survey on the catalytic behavior of chromium complexes of this family of ligands, we have also examined the possibility of introducing hard donor atom in the ligand system, such as the replacement in the NCN-backbone with an oxygen atom to form an amidate anion.

The diamagnetic complex $\{Cr_2[(C_6H_5)C(O)N(C_6H_3\text{-}2,6\text{-}^{i}Pr)]_4\}$ **(6.7)** was obtained by treating one equivalent of $CrCl_2(THF)_2$ with two equivalents of deprotonated form of 2,6-diisopropylbenzamidate ligand. The crystallization was commenced in toluene by cooling a brown solution at -35 ^{o}C for several days. Single X-ray quality crystals were obtained in 49 % isolated yield (Scheme 6.6).

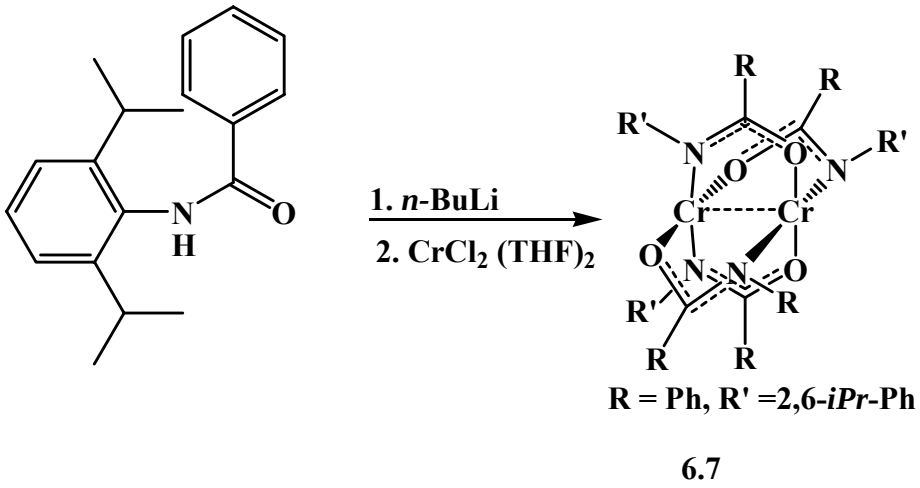

6.7

Scheme 6.6: Synthesis of complex 6.7

The structure was elucidated by X-ray analysis (Figure 6.6). Complex **6.7** has the expected dinuclear lantern-type structure with four ligands bridging two Cr(II) centres [Cr1-N1 = 2.055(8)Å, Cr2-O1 = 1.994(7)Å] in square-planar ligand field [Cr(2)-Cr(1)-O(4) = 92.61(19)^{o}, Cr(2)-Cr(1)-O(2) = 92.54(19) ^{o}, O(4)-Cr(1)-O(2) = 174.8(3)^{o}, Cr(2)-Cr(1)-N(3) = 97.1(2)^{o}, O(4)-Cr(1)-N(3) = 91.7(3)^{o}, O(2)-Cr(1)-N(3) = 87.2(3)^{o}, Cr(2)-Cr(1)-N(1) = 97.6(2)^{o}, O(4)-Cr(1)-N(1) = 87.4(3)^{o}, O(2)-Cr(1)-N(1) = 92.4(3)^{o}, N(3)-Cr(1)-N(1) = 165.3(3)^{o}, Cr(1)-Cr(2)-O(1) = 92.39(19)^{o}, Cr(1)-Cr(2)-O(3) = 92.77(19)^{o}, O(1)-Cr(2)-O(3) = 174.6(3)^{o}, Cr(1)-Cr(2)-N(2) = 97.5(2)^{o}, O(1)-Cr(2)-N(2) = 87.8(3)^{o}, O(3)-Cr(2)-N(2) = 93.0(3)^{o}, Cr(1)-Cr(2)-N(4) = 97.1(2)^{o}, O(1)-Cr(2)-N(4) = 91.4(3)^{o}]. The a Cr…Cr contact [Cr1-Cr2 = 1.9013(19)Å] is very short and in what is commonly regarded as supershort quadruple bond range.

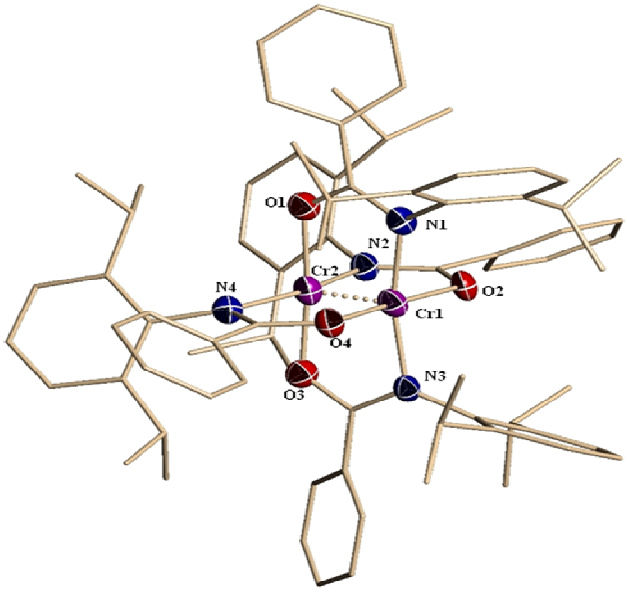

Figure 6.6: Crystal structure of complex 6.7 with thermal ellipsoids drawn at the 50% probability level.

Similarly, complex $\{Cr[(C_6H_5)C(O)N(C_6H_3\text{-}2,6\text{-}di\text{-}^{i}Pr)]_3\}$ **(6.8)** was obtained by salt metathesis between the three equivalents of benzamidate ligand with one equivalent of $CrCl_3(THF)_3$ (Scheme 6.7). The complex **6.8** was isolated as a monomeric chromium with ligands adopting a propeller-type of arrangement.

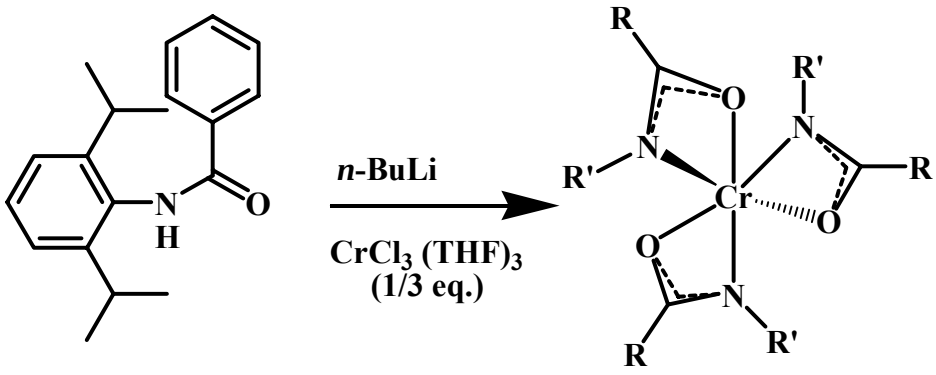

6.8 R = Ph, R' =2,6-*iPr*-Ph

Scheme 6.7: Synthesis of Cr(III)-amidate complex 6.8.

The structure was elucidated by X-ray analysis (Figure 6.7). The central metal is surrounded by the three bi-dentate ligands occupying the six octahedral sites [Cr1-O3 = 1.991(3)Å, Cr1-O2 = 1.999(3)Å, Cr1-O1 = 2.001(3)Å, Cr1-N1 = 2.065(4)Å, Cr1-N2 = 2.079(4)Å, Cr1-N3 = 2.081(4)Å] completing the octahedral geometry around the trivalent metal centre [O3-Cr1-O2 = 96.88(13)^{o}, O3-Cr1-O1 = 95.12(13)^{o}, O2-Cr1-O1 = 97.74(13)^{o}, O3-Cr1-N1 = 92.02(14)^{o}, O2-Cr1-N1 = 161.48(14)^{o}, O1-Cr1-N1 = 65.19(14)^{o}, O3-Cr1-N2 = 161.10(14)^{o}, O2-Cr1-N2 = 65.16(14)^{o}, O1-Cr1-N2 = 93.23(14)^{o}, N1-Cr1-N2 = 106.87(15)^{o}, O3-Cr1-N3 = 64.93(13)^{o}, O2-Cr1-N3 = 93.51(14)^{o}, O1-Cr1-N3 = 158.21(14)^{o}, N1-Cr1-N3 = 104.98(15)^{o}, N2-Cr1-N3 = 108.44(15)^{o}].

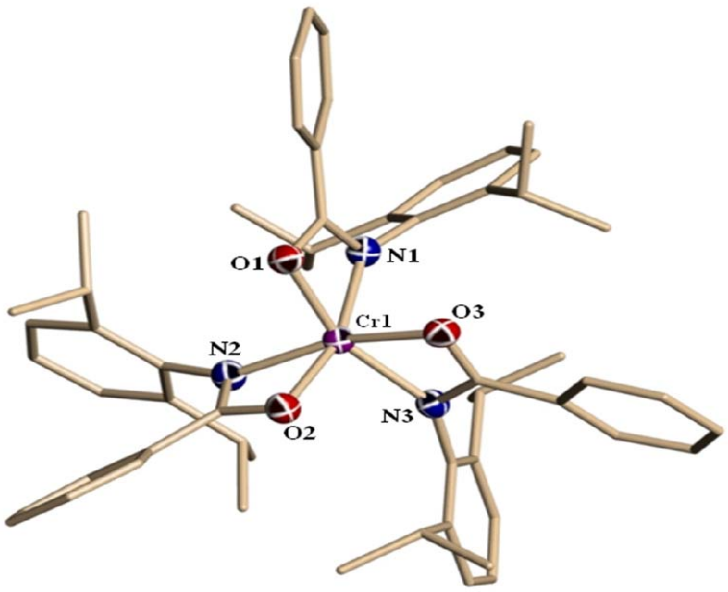

Figure 6.7: Crystal Structure of Complex 6.8 with thermal ellipsoids drawn at the 50% probability level.

Catalytic Activity

All the six isolated amidinate complexes described above have been tested for ethylene oligomerization under standard Ziegler-Natta conditions (Table 6.2). Among the other activators

MAO seems to be the only effective activator in all cases driving the reactivity towards statistical distributions of oligomers. The activities were in general quite high for all the divalent and trivalent complexes **6.1** to **6.6** when tested in toluene. Increasing the Al:Cr ratio resulted in an increased catalytic activity with either formation of negligible amount or even complete absence of waxes or polymers. Complex **6.2** showed the highest activity of S-F distribution of oligomers. The formation of S-F distributions of oligomers with high activity and negligible amount of solids (higher α-olefins) in the case of the trivalent **6.5** and **6.6** suggests the reduction of trivalent state to more stable divalent oxidation state but no further reduction. Accordingly, the rather similar catalytic behaviours of **6.3** and **6.4** under same reaction conditions, suggest the formation of the same catalytically active species during the catalytic cycle. Production of S-F distribution of oligomers accompanied by some waxes also suggests the co-existence of two different oxidation states at the same time in the reaction mixture.

Table 6.2: Catalytic activity of complexes **6.1-6.6**[a]

Cat. (μmol)	Co-cat. (eq)	Solvent	Activity g/mmol, Cat.h	PE (g)	Oligo. (mL)	Mol %						
						C6	C8	C10	C12	C14	C16	C18
6.1(20)	MAO (400)	Tol	2,700	3	24	39.2	28.1	17.1	9.8	3.6	1.5	0.5
6.1(20)	MAO (1000)	Tol	5,600	1 (wax)	55	26.7	17.7	16.8	13.2	10.8	8.3	6.2
6.1(10)	MAO (2000)	Tol	8,800	1 (wax)	43	30.8	17.7	20.6	14.6	8.6	4.7	2.7
6.1(10)	DMAO (1000)	Tol	4,540	0.7	22	28.4	26.8	18.5	12.3	7.7	4.4	2.2
6.1(10)	DMAO (1000)	MeCy	1,200	4	2	44	55	-	-	-	-	-
6.2(20)	MAO (400)	Tol	2,480	3.8	21	20.2	30	20.3	14.3	9.4	5.9	3.8
6.2(20)	MAO (2000)	Tol	6,100	0	61	24.8	31	18.0	11.4	7.2	4.5	3.2
6.2(20)	MMAO (400)	MeCyl	170	0.7	1	99	-	-	-	-	-	-
6.2(20)	DMAO (400)	MeCyl	250	1.5	1	99	-	-	-	-	-	-
6.2(20)	DMAO (1000)	Tol	4,300	1	42	30.7	24.4	19.2	12.1	7.3	4.1	2.3
6.3(10)	MAO (2000)	Tol	12,200	6 (wax)	55	16.6	19.0	16.4	14.5	13.0	12.0	9.0
6.4(10)	MAO (2000)	Tol	10,800	6 (wax)	48	31.5	30.0	20.2	9.6	5.0	2.5	1.4
6.4(10)	DMAO (1000)	MeCy	500	1	1.5	29	71	-	-	-	-	-
6.5(10)	MAO (2000)	Tol	10,600	1 (wax)	52	15.0	19.3	20.1	15.4	11.8	10.3	8.2
6.6(10)	MAO (2000)	Tol	11,560	0.8 wax	57	23.5	13.7	22.5	15.7	11.8	7.7	5.0

Conditions: 60 °C, 30 minutes reaction time, 600 psi ethylene pressure, 100 mL toluene/methylcyclohexane reaction solvent.C4 fraction is not reported due to volatility. Waxes- are higher molecular weight α-olefins.

Activation of **6.1** with TMA-depleted MAO (DMAO) in toluene did not modify catalytic behavior. However, when the reaction solvent was replaced for methylcyclohexane, the formation of only 1-hexene and 1-octene was observed in the oligomeric mixture along with some polymers and the usual lowering of activity. Similar results were observed with the trivalent **6.4** but with a remarkable excess of 1-octene over 1-hexene. Complex **6.2** is instead a selective trimerization catalyst forming 1-hexene upon activation with DMAO and MMAO in methylcyclohexane. Nonetheless, the fact that only a mixture of 1-hexene and 1-octene was obtained in the case of **6.1** and **6.4** indicates that some reduction to the monovalent state has occurred. The presence of polymer again suggests that the original trivalent state of a fraction of catalyst that was not thermally reduced to Cr(I) or perhaps disproportionation of divalent state back towards higher oxidations states. The exclusive formation of 1-hexene in the case of **6.2** when activated with MMAO explains that *i*-Bu_3Al present in MMAO is sufficiently strong to further reduce divalent to monovalent state.

Complexes **6.7** and **6.8** were tested for ethylene oligomerization in standard conditions for above mentioned amidinate complexes (Table 6.3). The trivalent complex **6.8** showed activity and selectivity comparable to the amidinate complex **6.2** possibly indicating that the trivalent state was reduced to divalent state but no further reduction. The divalent **6.7** on the other hand formed S-F distribution of oligomers enriched in 1-hexene with some hard polymer. This result indicates that some disproportionation to monovalent state and higher states occurred. The formation of only polymer with high activity upon activation with TiBAO suggests the reoxidation of the original divalent state to trivalent state. However, strongly reducing TiBA is indeed able to form some monovalent species as it is suggested by the selective formation of 1-hexene. Complex **6.7** behaves as a selective trimerization catalyst upon activation with a mixture

of TEAl/DEAC. This result instead indicats the complete reduction of divalent state to monovalent state. This result instead indicaets the complete reduction of divalent state to monovalent state. Interestingly, upon activation with DEAC, an exclusive formation of polymer was obtained indicating oxidation of the divalent state or stabilization of higher valent state.

Table 6.3: Catalytic activity of complexes **6.7** and **6.8.**

Cat. (μmol)	Co-Cat. (eq)	Solvent	Activity g/mmol, Cat.h	PE (g)	Oligo. (mL)	Mol %						
						C6	C8	C10	C12	C14	C16	C18
6.7(10)	MAO (1000)	Tol	11,000	8	47	47	27	13	7	3	2	1
6.7(10)	MAO (500)	Tol	7,600	14	24	46.5	26.8	12.9	6.8	4	1.8	1
6.7(10)	TiBAO(500)	Tol	3,000	15	0							
6.7(10)	TiBA (100)	Tol	600	2	1	99.9						
6.7(10)*	TEAL(50)	MeCy	200		1	30	20	traces	-	-	-	-
6.7(10)	TEAL/DEAC (20/10)	MeCy	400	0	2	99	1	-	-	-	-	-
6.7(10)	DEAC (20)	MeCyl	400	2	0							
6.8(20)	MAO (1000)	Tol	5,600	0.2	56	27.7	23.9	15.9	11.7	7.3	5.2	8.1

Conditions : traces of saturated C8, C10 and C12 have also been seen in case of activator TEAL(50) and 40 mol % C4, 50 ^{o}C, 600 psi ethylene pressure, 300 mL parr reactor, total volume 100 mL.*

6.5 Conclusions

In conclusion, we have reported here some divalent and trivalent chromium catalyst precursors that are producing non-selective α-olefins. High activity and lack of PE formation in case of complexes **6.2** and **6.8** makes these complexes attractive for commercial applications. The rather systematic lack of selectivity of the complexes reported above, despite having probed diversified ligand arrangements, suggest that the catalytically active species in all cases may contain divalent state of chromium.

In the following chapters, we are exploring some nickel complexes of established ligands with the hope of isolating low valent complexes and to evaluate ethylene oligomerization activity.

References

1. a) Vogt, D. Oligomerization of ethylene to higher linear α-olefins; in *Applied Homogeneous Catalysis with Organometallic Compounds*; Cornils, B., Herrmann, W. A., Eds.; Wiley-VCH: Weinheim, Germany, **2000**; Chapter 2, pp 245. b) Lappin, G. R.; Sauer, J. D. in *Alpha Olefins Application Handbook.* Vol 37, Marcel Dekkers, INC: New York, **1989**. p. 1. (c) *Alpha Olefins* (**02/03-4**), PERP Report, Nexant Chem Systems.
2. Flory, P. J. *J. Am. Chem. Soc*. **1940**, *62*, 1561. b) Schulz. G. V. Z. *Phys. Chem. Abt. B*. **1939**, *43*, 25. c) Schulz, G. V. Z. *Phys. Chem. Abt. B*. **1935**, *30*, 379.
3. Thomas, J. M.; Thomas, W. J. *Principals and Practice of Heterogeneous Catalysis* VCH: Weindheim, **1997**.
4. a) Reagan, W. K. (Phillips Petroleum Company)EP 0417477, **1991**. b) Tanaka, E.; Urata, H.; Oshiki, T.; Aoshima, T.; Kawashima, R.; Iwade, S.; Nakamura, H.; Katsuki, S.; Okanu, T. (Mitsubishi Chemical Corporation) EP 0611743, **1994**. c) Wu, F. J. (Amoco Corporation) US 5811618, **1998**. d) Yoshida, T.; Yamamoto, T.; Okada, H.; Murakita, H. (Tosoh Corporation) US2002/0035029, **2002.** e) Grove, J. J. C.; Mahome, H. A.; Griesel, L. (Sasol Technology) WO 03/004158, **2002.**
5. a) K€ohn, R. D.; Haufe, M.; Kociok-K€ohn, G.; Grimm, S.; Wasserscheid, P.; Keim, W. *Angew. Chem., Int. Ed*. **2000**, *39*, 4337. b) K€ohn, R. D.; Smith, D.; Mahon, M. F.; Prinz, M.; Mihan, S.; Kociok-K€ohn, G. *J. Organomet. Chem*. **2003**, *683*, 200.
7. Carter, A.; Cohen, S. A.; Cooley, N. A.; Murphy, A.; Scutt, J.; Wass, D. F. *Chem. Commun*. **2002**, 858.
8. a) McGuinness, D. S.; Wasserscheid, P.; Keim, W.; Hu, C.; Englert, U.; Dixon, J. T.; Grove, C. *Chem. Commun*. **2003**, 334. b) McGuinness, D. S.; Wasserscheid, P.; Keim,W.;

Morgan, D. H.; Dixon, J. T.; Bollmann, A.; Maumela, H.; Hess, F. M.; Englert, U. *J. Am. Chem. Soc.* **2003**, *125*, 5272. c) McGuinness, D. S.; Wasserscheid, P.; Morgan, D. H.; Dixon, J. T. *Organometallics* **2005**, *24*, 552.

9. a) Morgan, D. H.; Schwikkard, S. L.; Dixon, J. T.; Nair, J. J.; Hunter, R. Adv. *Synth. Catal*. **2003**, *345*, 939. b) Mahomed, H. A.; Bollmann, A.; Dixon, J. T.; Gokul, V.; Griesel, L.; Grove, J. J. C.; Hess, F.; Maumela, H.; Pepler, L. *Appl. Catal., A* **2003**, *225*, 355.
10. Bluhm, M. E.; Walter, O.; D€oring, M. *J. Organomet. Chem*. **2005**, *690*, 713.
11. Nenu, C. N.; Weckhuysen, B. M. *Chem. Commun*. **2005**, 1865.
12. a) Temple, C.; Jabri, A.; Crewdson, P.; Gambarotta, S.; Korobkov, I.; Duchateau, R. *Angew. Chem., Int. Ed.* **2006,** *45*, 7050. b) Albahily, K.; Koc, E.; Al-Baldawi, D.; Savard, D.; Gambarotta, S.; Burchell, T. J.; Duchateau, R. *Angew. Chem., Int. Ed.* **2008,** *47,* 5816. c) Jabri, A.; Mason,C.B.; Sim,Y.; Gambarotta, S.; Burchell, T. J.; Duchateau, R. *Angew. Chem.,Int. Ed.* **2008**, *47*, 9717. d) Vidyaratna, I.; Nikiforov, G. B.; Gorelsky, S. I.; Gambarotta, S.; Duchateau, R.; Korobkov, I. *Angew. Chem., Int. Ed*. **2009**, *48*, 6552.
13. a) Zhang, J.; Braunstein, P.; Hor, T. S. A. *Organometallics* **2008**, *27*, 4277. b) Zhang, J.; Li, A.; Hor, T. S. A. *Organometallics* **2009**, *28*, 2935.
14. Klemps, C.; Payet, E.; Magna, L.; Saussine, L.; Le Goff, X. F.; Le Floch, P. *Chem.Eur. J.* **2009**, *15*, 8259.
15. a) Bollmann, A.; Blann, K.; Dixon, J. T.; Hess, F. M.; Killian, E.; Maumela, H.; McGuinness, D. S.; Morgan, D. M.; Neveling, A.; Otto, S.; Overett, M.; Slawin, A. M. Z.; Wasserscheid, P.; Kuhlman, S. *J. Am. Chem. Soc*. **2004**, *126*, 14712. b) Blann, K.; Bolmann, A.; Dixon, J. T.; Hess, F.; Kilian, E.; Maumela, H.; Morgan, D. H.; Neveling, A.; Otto, S.; Overett, M. *Chem. Commun*. **2005**, 620. c) Blann, K.; Bollmann, A.; Dixon,

J. T.; Hess, F. M.; Killian, E.; Maumela, H.; Morgan, D. H.; Neveling, A.; Otto, S.; Overett, M. *J. Chem. Commun*. **2005**, 622. d) Overett, M. J.; Blann, K.; Bollmann, A.; Dixon, J. T.; Haasbroek, D.; Killian, E.; Maumela, H.; McGuinness, D. S.; Morgan, D. H. *J. Am. Chem. Soc.* **2005**, *127*, 10723. e) Kuhlmann, S.; Blann, K.; Bollmann, A.; Dixon, J. T.; Killian, E.; Maumela, M. C.; Maumela, H.; Morgan, D. H.; Pr_etorius, M.; Taccardi, N.; Wasserscheid, P. *J. Catal.* **2006**, *245*, 279. f) Walsh, R.; Morgan, D. H.; Bollmann, A.; Dixon, J. T. *Appl. Catal. A*: Gen. **2006**, *306*, 184. g) Kuhlmann, S.; Dixon, J.; Haumann, T.; Morgan, D. H.; Ofili, J.; Spuhl, O.; Taccardi, N.; Wasserscheid, P. *Adv. Synth. Catal.***2006**, *348*, 1200. h) Kuhlmann, S.; Blann, K.; Bollmann, A.; Dixon, J. T.; Killian, E.; Maumela, M. C.; Maumela, H.; Morgan, D. H.; Pretorius, M.; Taccardi, N.; Wasserscheid, P. *J. Catal*. **2007**, *245*, 279. i) Killian, E.; Blann, K.; Bollmann, A.; Dixon, J. T.; Kuhlmann, S.; Maumela, M. C.; Maumela, H.; Morgan, D. H.; Nongodlwana, P.; Overett, M. J.; Pr_etorius, M.; H€ofener, K.; Wasserscheid, P. J. *Mol. Catal. A: Chem*. **2007**, *270*, 214. j) McGuinness, D. S.; Overett, M.; Tooze, R. P.; Blann, K.; Dixon, J. T.; Slawin, A. M. Z. *Organometallics* **2007**, *26*, 1108.

16. Jabri, A.; Crewdson, P.; Gambarotta, S.; Korobkov, I.; Duchateau, R. *Organometallics* **2006**, *25*, 715.
17. Han, T.K.; Ok, M. A.; Chae, S. S.; Kang, S. O. (SK Energy Corporation) WO 2008/088178, **2008**.
18. Greiner, E.; Gubler, R.; Inoguchi, Y. Linear Alpha Olefins, CEH Marketing Research Report, *Chemical Economics Handbook*; *SRI International: Menlo Park,* CA, May **2004**.
19. a) Tomov, A. K.; Chirinos, J. J.; Long, R. J.; Gibson, V. C.; Elsegood, M. R. J. *J. Am. Chem. Soc.* **2006**, *128*, 7704.

20. a) Crewdson, P.; Gambarotta, S.; Djoman, M.C.; Korobkov, I.; Duchateau, R. Organometallics **2005**, *24*, 5214. b) Albahily, K.; Koc, E.; Al-Baldawi, D.; Savard, D.; Gambarotta, S.; Burchell, T. J.; Duchateau, R. *Angew. Chem., Int. Ed.* **2008**, *47*, 5816.
21. McGuinness, D. S.; Suttil, J. A.; Gardiner,M. G.; Davies, N. W. *Organometallics* **2008**, *27*, 4238.
22. Kirillov, E.; Roisnel, T.; Razavi, A.; Carpentier, J.F. *Organometallics* **2009**, *28*, 2401.
23. a) Hogan, J. P.; Banks, R. L. (Phillips Petroleum Co.) U.S. Patent 2,825,721, **1958**. b) Karapinka, G. L. (Union Carbide Corp.) Ger. Offen. DE 1,808,388, **1970**. c) Karol, F. J.; Karapinka, G. L.; Wu, C.; Dow, A. W.; Johnson, R. N.; Carrick, W. L. *J. Polym. Sci*. *Polym. Chem. Ed*. **1972**, *10*, 2621. d) Karapinka, G. L. (Union Carbide Corp.) U.S. Patent 3,709,853, **1973**.
24. a) MacAdams, L. A.; Buffone, G. P.; Incarvito, C. D.; Rheingold, A. L.; Theopold, K. H. *J. Am. Chem. Soc*. **2005**, *127*, 1082. b) Theopold, K. H. *Eur. J. Inorg. Chem*. **1998**, *15*. c) Bhandari, G.; Kim,Y.; McFarland, J. M.; Rheingold, A. L.; Theopold, K. H. *Organometallics* **1995**,*14*, 738. d) MacAdams, L. A.; Kim,W. K.; Liable-Sands, L. M.; Guzei, I. A.; Rheingold, A. L.; Theopold, K. H. *Organometallics* **2002**, *21*, 952.
25. D€ohring, A.; Gohre, J.; Jolly, P. W.; Kryger, B.; Rust, J.; Verhovnik, G. P. J. *Organometallics* **2000**, *19*, 388.
26. a) Rogers, J. S.; Bu, X. H.; Bazan, G. C. *Chem. Commun*. **2000**, 1209. b) Bazan, G. C.; Rogers, J. S.; Fang, C. C. *Organometallics* **2001**, *20*, 2059.
27. Enders, M.; Fernandez, P.; Ludwig, G.; Pritzkow, H. *Organometallics* **2001**, *20*, 5005.
28. a) Gibson, V. C.; Maddox, P. J.; Newton, C.; Redshaw, C.; Solan, G. A.; White, A. J. P.; Williams, D. J. *Chem. Commun*. **1998**, 1651. b) Gibson, V. C.; Mastroianni, S.; Newton,

C.; Redshaw, C.; Solan, G. A.; White, A. J. P.; Williams, D. J. *Dalton Trans*. **2000**,1969.

29. Esteruelas, M. A.; Lopoez, A. M.; Mendez, L.; Olivan, M.; Onate, E. *Organometallics* **2003**, *22*, 395.
30. Vidyaratne, I.; Scott, J.; Gambarotta, S.; Duchateau, R. *Organometallics* **2007**, *26*, 3201.
31. See for example: a) Licciulli, S.; Thapa, I; Albahily, K.; Korobkov, I.; Gambarotta, S.; Duchateau, R.; Chevalier, R.; Schuhen, K. *Angew. Chem. Int. Ed.* **2010**, *49*, 9225. b) Skobelev, I. Y.; Panchenko, V. N.; Lyakin, O. Y.; Bryliakov, K. P. V.; Zakharov, A.; Talsi, E. P. *Organometallics* **2010**, *29*, 2943.
32. a) Bowen, L. E.; Haddow, M. F.; Orpen, A. G.; Wass, D. *Dalton Trans* **2007**, 1160. b) Dulai, A.; de Bod, H.; Hanton, M. J.; Smith, D. M.; Downing, S.; Mansell, S. M.; Wass, D. F. *Organometallics* **2009**, *28*, 4613.
33. a) Klemps, C.; Payet, E.; Magna, L.; Saussine, L.; Le Goff, X. F.; Le Floch, P. *Chem. Eur. J.* **2009**, *15*, 8259. b) Peitz, S.; Peulecke, N.; Aluri, B. R.; Hansen, S.; Müller, B. H.; Spannenberg, A.; Rosenthal, U.; Al-Hazmi, M. H.; Mosa, F. M.; Wöhl, A.; Müller, W. *Eur. J. Inorg. Chem.* **2010**, 1167. c) Zhang, W.; Sun, W. H.; Zhang, S.; Hou, J.; Wedeking, K.; Schultz, S.; Fröhlich, R.; Song, H. *Organometallics* **2010**, *29*, 5805.
34. a) Rüther, T.; Cavell, K. J.; Braussaud, N. C.; Skelton, B. W.; White, A. H. J. *Chem. Soc., Dalton Trans.* **2002**, 4684. b) Zhang, W.; Sun, W.H.; Zhang, S.; Hou, J.; Wedeking, K.; Schultz, S.; Fröhlich, R.; Song, H. *Organometallics* **2006**, *25*, 1961. c) Zhang, S.; Jie, S.; Shi, Q.; Sun, W-H. *J. Mol. Catal. A: Chem*. **2007**, *276*, 174.
35. a) White, P. A.; Calabrese, J.; Theopold, K. H. *Organometallics* **1996**, *15*, 5473. b) Gibson, V. C.; Maddox, P. J.; Newton, C.; Redshaw, C.; Solan, G. A.; White, A. J. P.; Williams, D. *J.* Chem. Commun. **1998**, 1651. c) Döhring, A.; Göhre, J.; Jolly, P. W.; Kryger, B.; Rust, J.;

Verhovnik, G. P. J. *Organometallics* **2000**, *19*, 388. d) Carney, M. J.; Robertson, N. J.; Halfen, J. A.; Zakharov, L. N.; Rheingold A. L. *Organometallics* **2004**, *23*, 6184. e) McDaniel, M. P. *Advances in Catalysis* **2010**, *53*, 123.

36. a) Vidyaratne, I.; Nikiforov, G. B.; Gorelsky, S. I.; Gambarotta, S.; Duchateau, R.; Korobkov, I.; *Angew. Chem. Int. Ed*. **2009**, *48*, 6552. b) Zhang, J.; Li, A.; Hor, T. S. A. *Organometallics* **2009**, *28*, 2935.
37. a) Thapa, I.; Gambarotta, S.; Korobkov, I.; Duchateau, R.; Kulangara, S. V.; Chevalier, R. *Organometallics* **2010**, *29*, 4080. b) Blann, K.; Bollmann, A.; Dixon, J. T.; Neveling, A.; Morgan, D. H.; Maumela, H.; Killian, E.; Hess, F. M.; Otto, S.; Pepler, L.; Mahomed, H. A.; Overett, M. J. (Sasol Technology LTD) WO 04/056479, **2004**.
38. a) McDermott, J. X.; White, J. F.; Whitesides, G. M. *J. Am. Chem. Soc*. **1973,** *95*, 4451. b) McDermott, X.; White, J. F.; Whitesides, G. M. *J. Am. Chem. Soc*. **1976**, *98*, 6521.
39. Manyik, R. M.; Walker, W. E.; Wilson, T. P. *J. Catal*. **1977**, *47*, 97.
40. Briggs, J. R. *Chem. Commun*. **1989**, *11*, 674.
41. Meijboom, N.; Schaverien, C. J.; Orpen, A. G. *Organometallics* **1990**, *9*, 774.
42. Emrich, R.; Heinemann, O.; Jolly, P. W.; Kr€uger, C.; Verhovnik, G. P. J. *Organometallics* **1997**, *16*, 544.
43. a) Blok, A. N. J.; Budzelaar, P. H. M.; Gal, A. W. *Organometallics* **2003**, *22*, 2564. b) Tobisch, S.; Ziegler, T. *Organometallics* **2003**, *22*, 5392. c) Tobisch, S.; Ziegler, T. *J. Am. Chem. Soc*. **2004,** *126*, 9059. d) Van Rensburg,W. J.; Grove, C.; Seynberg, J. P.; Stark, K. B.; Huyser, J. J.; Steynberg, P. J. *Organometallics* **2004**, *23*, 1207.
44. a) Agapie, T.; Schofer, S. J.; Labinger, J. A.; Bercaw, J. E. *J. Am.Chem. Soc*. **2004**, *126*, 1304. b) Agapie, T.; Day, M. W.; Henling, L. M.; Labinger, J. A.; Bercaw, J. E.

Organometallics **2006**, *25*, 2733. c) Agapie, T.; Labinger, J. A.; Bercaw, J. E. *J. Am. Chem. Soc.* **2007**, *129*, 14281. d) Schofer, S. J.; Day, M.W.; Henling, L. M.; Labinger, J. A.; Bercaw, J. E. *Organometallics* **2006**, *25*, 2743.

45. Tomov, A. K.; Chirinos, J. J.; Jones, D. J.; Long, R. J.; Gibson, V. C. *J. Am. Chem. Soc*. **2005**, *127*, 10166.
46. a) Cossee, P. *J. Catal*. **1964**, *3*, 80. b) Arlman, E. J.; Cossee, P. *J. Catal*. **1964**, *3*, 99. c) Skupinska, *J. Chem. Rev*. **1991**, *91*, 613.
47. a) Bambirra, S.; Leusen, van D.; Meetsma, A.; Teuben, J. H.*Chem. Commun.* **2003**, 522. b) Nijhuis, C. A.; Jellema, E.; Sciarone, T. J. J.; Meetsma, A.; Budzellar, P. H.; Hessen,B.; *Eur. J. Inorg. Chem.* **2005**, 2089. c) Richeson, D. S.; Zhou, Y. *J. Am. Chem. Soc*. **1996** *118*, 10850.
48. For example: a) Hao, S.; Gambarotta, S.; Bensimon, C.; Edema, J. J. H. *Inorganic Chemica Acta.* **1993**, *213*, 65. b) Harder, S.; Boersma, J.; brandsma, L. *Organometallics.* **1990**, *9*, 515. c) Jiabi, C.; Guixin, L.; Weihua, X.; xianglin, J.; Meicheng, S.; Youqi, T.; *J. Organomet. Chem.* **1980**, *15*, 241. d) Pornet, J.; Miginiac, L. *Bull. Soc. Chimi. Fra*. **1974**, *5-6*, 997. e) Patai, S.; Rappoport, Z. *The Chemistry of Amidines and Imidinates*, Vol. 2, Wiley, new York, **1991** (Chapter 10). f) Sadique, A. R.; Heeg, M. J.; Winter, C. H. *J. Am. Chem. Soc.* **2003**, *125*, 7774.
49. Zhu, D.; Thapa, I.; Korobkov, I.; Gambarotta, S.; Budzelaar, H.M. P. *Inorg .Chem.* **2011**, *50*(20), 9879.

Part II

Nickel Catalysts

Publications:

1) Zhu, D.; **Thapa, I**.; Korobkov, I.; Gambarotta, S.; Budzelaar, P. H. M. *Inorg. Chem.* **2011,** *50*(20), 9879-9887.
2) **Thapa, I**.; Gambarotta, S.; Korobkov, I. *Inorg. Chem.* (submission in process)

Nickel Bis(imino)pyridine Chemistry

Since the breakthrough discovery of Brookhart and Gibson concerning the polymerization of ethylene by the Fe and Co systems of 2,6-bis(imino)pyridine ligand, other transition metals incorporating this ligand have become much of academic and industrial interest. Nonetheless, all the ethylene polymerization catalysts with this ligand are limited to Fe(II) and Co(II) systems and very little is known about the catalytic performances of this ligand with nickel. In order to extend our understanding with nickel bis(imino)pyridine systems, we have herein synthesized nickel complexes in different oxidation states (0, +I, +II). During our study, we have encountered interesting chemical transformations. Thus, we have studied the unique properties of this fascinating ligand with respect to nickel.

This chapter is divided into two sections; 1) Section A: describes the properties of bis(imino)pyridine ligand, isolation of novel dinitrogen, alkyl complexes and related reactions. 2) Section B: describes the isolation of a novel Nickel hydride complex and ethylene oligomerization activity of Nickel dinitrogen and Nickel hydride complexes.

A. Redox−Active Ligands and Organic Radical Chemistry

7.1 Introduction

Conjugated carbon-nitrogen ligands like α-diimines, imine-pyridines, bipyridines, terpyridines and in particular 2,6-diiminepyridines (DIMPY)[1,] (Scheme 7.1) have long been recognized as "non-innocent". Their π-systems can easily accept one or more electrons, leading to formation of stable complexes where the metal has a deceptively low *formal* oxidation state, while the actual electronic structure is best viewed as containing a higher-valent metal bound to a negatively charged ligand ("electronic non-innocence"). [2-11] The same ligands (at least the imine-containing DIM, IMPY and DIMPY) also have a tendency to become involved in chemical reactions ("chemical non-innocence"), the most important one being alkylation at various positions of the ligand skeleton (DIM[3,11-19]; IMPY[3,17, 20, 21]; DIMPY[22-29]). It seems reasonable to assume that these two properties are somehow connected,[30] although limited evidence for this has been provided so far for DIMPY ligands.[31]

In this section, we will summarize what is known about bonding and electronic structure of DIMPY complexes of Fe, Co and Ni halides, alkyls and dinitrogen complexes, then discuss some of the reactivity of these complexes, and finally try to link electronic and chemical non-innocence with each other and with reactivity of the complexes.

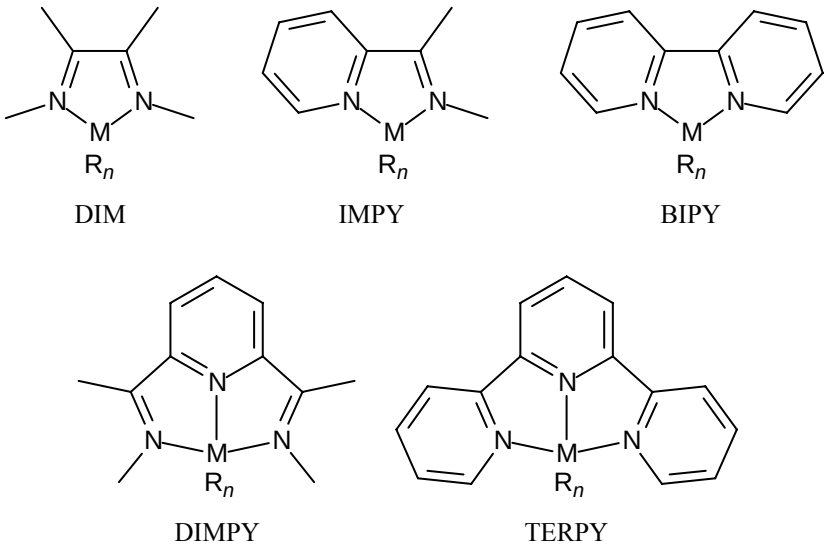

Scheme 7.1. Some common π-acceptor ligands.

The "standard" DIMPY ligand (L^1, Scheme 7.2) has methyl groups at the imine carbons, and 2,6-di*iso*propylphenyl groups at the imine nitrogens. In addition, we will in this chapter regularly refer to the somewhat less bulky ligand L^2 with 2,6-dimethylphenyl groups at N. Other ligands will be denoted more explicitly as L(R, Ar) where necessary; the symbol L indicates a generic diiminepyridine ligand.

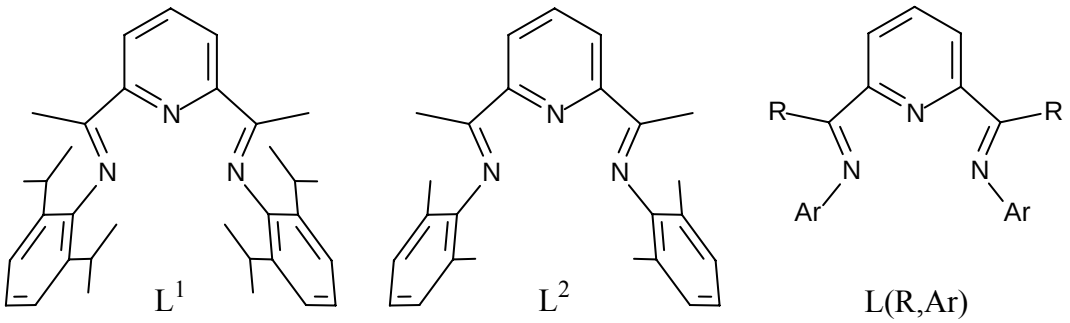

Scheme 7.2. Notation used here for DIMPY ligands.

7.2 Experimental

All experiments were performed under an argon atmosphere using standard Schlenk techniques, or in a nitrogen-filled dry-box. Pentane, toluene, diethyl ether, tetrahydrofuran, benzene, THF-d_8 and benzene-d_6 were distilled from sodium/benzophenone. 4-$CF_3C_6H_4Cl$ was purchased from Aldrich, degassed and dried over 4 Å molecular sieves before use. Sodium hydride was purchased from Aldrich and washed with hexane under nitrogen to remove the oil. $NiBr_2$(DME) was obtained from Strem Chemicals. The ligand L^1,[32] complex $L^1Co(N_2)$,[33,34] mixtures of L^2CoAr and L^2CoCl,[34] and pure L^2CoAr[34] were prepared according to published procedures.

Infrared spectra were recorded on an ABB Bomen FTIR instrument from Nujol mulls prepared in a dry box except in the case of air stable compounds. Samples for magnetic susceptibility were weighed inside a dry box equipped with an analytical balance and sealed into calibrated tubes and measurements were carried out with a Johnson Matthey Magnetic Susceptibility balance at room temperature. Magnetic moments were calculated following standard methods and corrections for the diamagnetisms were applied to the data. Data for X-ray crystal structure determination were obtained with a Bruker diffractometer equipped with a 1K Smart CCD area detector.

^{1}H-NMR, ^{13}C{H}-NMR, ^{29}Si{H}-NMR and ^{19}F-NMR spectra were recorded on Bruker Avance 300 MHz and 500 MHz spectrometers. All ^{1}H and ^{13}C-NMR shifts (δ, ppm) were referenced to the solvent (benzene-d_6, ^{1}H-NMR: C_6D_5H δ 7.16 ppm; ^{13}C-NMR: C_6D_6 δ 128.0 ppm; $CDCl_3$, ^{1}H-NMR: $CHCl_3$ δ 7.26 ppm; ^{13}C-NMR: $CDCl_3$ δ 77.0 ppm). ^{19}F{H}-NMR spectra were referenced to internal benzotrifluoride in benzene-d_6 (δ -62.4 ppm). Data were collected at room temperature unless otherwise noted. GC/MS instrument: Varian 3800 gas-chromatograph

with a 30 meter VF-5ms column coupled to a Varian 320-MS operated in single quadrupole mode.

7.2.1 Reaction between $L^1Co(N_2)$ and 4-$CF_3C_6H_4Cl$.

In a N_2-filled dry-box, $L^1Co(N_2)$ (11.8 mg, 20 μmol) was weighed and dissolved in about 0.4 mL dry benzene-*d*6, and 4-$CF_3C_6H_4Cl$ (2.45μL, 19.6 μmol) was added. The mixture turned gray-blue. The immediately recorded ^{1}H NMR spectrum showed that the reaction was not complete (still $L^1Co(N_2)$ visible) and three diamagnetic cobalt(I) complexes could be clearly observed: L^1CoH : L^1CoAr : L^1CoCl = 0.11 : 0.14 :1.00. After 4 h, the ^{1}H-NMR spectrum showed that there was no $L^1Co(N_2)$ left and the reaction was complete, with product ratio L^1CoH : L^1CoAr : L^1CoCl = 0.045: 0.14: 1.00. Assignments for L^1CoH and L^1CoCl are based on literature values[35]and for L^1CoAr on analogy with previously reported L^2CoAr.[34]

Tentative, partial assignments for L^1CoAr: ^{1}H-NMR (300 MHz, benzene-d_6, 25°C) δ: 10.27 (1H, t, *J* = 7.6 Hz, Py *H*4), 5.14 (2H, d, *J* = 7.1 Hz, CoAr *H*2), -0.65 (6H, s, CH_3C=N). ^{19}F-NMR (282 MHz, benzene-d_6, 25°C) δ: -61.2.

7.2.2 Reaction of $L^2CoCH_2SiMe_3$ with CH_3I.

In a dry-box, $L^2CoCH_2SiMe_3$ (37.5 mg, 72 μmol) was dissolved in benzene-*d*6, followed by injecting 8 μL CH_3I (130 μmol, 1.8 eq.). The mixture immediately turned pink. ^{1}H NMR showed only broad peaks. After 30 mins, a lot of solid had precipitated. In dry-box, this sample was filtered over glass wool and the filtrate was analyzed by ^{1}H NMR, but the peaks were still too broad for useful interpretation. Around 0.5 mL air was injected into the NMR tube to quench any paramagnetic Co complexes and after shaking the sample was quickly filtered over glass

wool in air. The ^{1}H-NMR obtained this way (Figure S1-supporting info) had reasonable line widths and showed a new quartet at δ 0.45 ppm (J = 8.0 Hz). GC/MS analysis of this NMR sample clearly showed that $EtSiMe_3$ was the main compound and the ^{1}H-^{29}Si COSY (found in supporting information of reference 34b) also confirmed that the ethyl group and methyl groups were attached to the same silicon atom.

7.2.3 C-C coupling reactions.

A mixture of LCoAr and LCoX was generated as described previously,[34] by treating 27 μmol $L^2CoCH_2SiMe_3$ in 0.4 mL benzene-d_6 with H_2/N_2 and then adding 27 μmol ArX. To this mixture was added with a syringe 0.5 eq. (relative to ArX) of the alkyl halide. For benzyl bromide and methyl iodide, the reaction is instantaneous; for benzyl chloride and allyl chloride, it takes hours to complete. The mixture turned to green and deposited black solids. After the sample had turned to grey, 0.5 mL water was added. The organic layer was filtered over glass wool and analyzed by GC/MS. This procedure was followed for all entries except entry 8 in Table 7.2.

7.2.4 $L^1Ni(\eta^1\text{-}N_2)$.

Solid $NiBr_2$(DME) (0.154 g, 0.5 mmol) and ligand L^1 (0.241 g, 0.5 mmol) were mixed together in THF (15 mL) and allowed to stir for two days at room temperature resulting in a brown suspension. Solid NaH (0.025 g, 1.05 mmol) was added to the suspension and stirring was continued at room temperature for four days. During this time the suspension became dark purple. The suspension was then dried under vacuum, the residue suspended in hexane, and centrifuged to remove undissolved materials and excess NaH. The resulting dark purple

supernatant was concentrated to 5 mL and left undisturbed at -35 °C for 4 days. Dark purple diamagnetic crystals of X-ray quality were formed (0.200 g, 0.35 mmol, 70%).

IR (Nujol mull, cm^{-1}): 2922, 2854 (Nujol), 2156 (N_2), 1580w, s, 1457w, 1377s, 1283w, s, 125m, 1120, 1053, 960, 807, 760, 665. ^{1}H-NMR (300 MHz, C_6D_6, 25 ^{o}C) δ: 7.50 (2H, d, *J* = 7.5 Hz, Py H3), 7.23 (6H, s, Ar), 6.90 (1H, t, *J* = 7.5 Hz, Py H4), 3.41 (4H, sept, CHMe2), 1.57 (6H, s, MeCdN), 1.49 (12H, d, *J* = 6.9 Hz,$CHMe_2$), 1.13 (12H, d, *J* = 6.9 Hz, $CHMe_2$). ^{13}C{1H}- NMR (300 MHz, C_6D_6, 25 ^{o}C) δ: 149.6, 146.9, 140.2, 139.5, 126.3, 124.4, 123.2, 111.4, 27.9 ($CHMe_2$), 24.5 (MeCdN), 24.0 ($CHMe_2$), 16.7 ($CHMe_2$).

7.2.5 L^1NiMe.

Dark purple crystals of $L^1Ni(N_2)$ (0.100 g, 0.175 mmol) were dissolved in toluene (5 mL). Me_3Al (0.0126 g, 0.175 mmol) was added to the stirred solution and stirring was continued at room temperature for another 30 minutes. The solution was then layered with an equal volume of hexane and left undisturbed at -35 °C for 7 days, yielding dark-brown, X-ray quality and paramagnetic crystals (0.06 g, 0.11 mmol, 62%).

IR (Nujol mull, cm^{-1}): 2955, 2924.7, 2854.1(Nujol), 1588w, 1457.3w, 1377.4s, 1321.2s, 1236.6, 1177.5w, 1078.7w, 935.7w, 862.0w, s, 789.8, 721.4, 698.6, 665.5s.

7.2.6 (L^1-L^1)Ni_2

Method A

Solid $NiBr_2$(DME) (0.154 g, 0.5 mmol) and ligand L^1 (0.241 g, 0.5 mmol) were mixed together in THF (15 mL) and allowed to stir for two days at room temperature, affording a brown suspension. Solid NaH (0.039 g, 1.65 mmol) was added to the stirred suspension and

stirring was continued for four days. The resulting dark-purple suspension was dried under vacuum and the residue suspended in hexane, and centrifuged to remove undissolved materials and excess of NaH. The dark purple solution was concentrated to 5 mL and left undisturbed at -35 °C for 4 days, during which, dark brown X-ray quality crystals of $(L^1\text{-}L^1)Ni_2$ were formed (0.220 g, 0.152 mmol, 30%).

IR (Nujol mull, cm^{-1}): 2956.5, 2924.1, 2854.2, 1644.3s, 1576.4s, 1461.6w, 1377.6s, 1366.6, 1325.8, 1325.8, 1254.8, 1192.7, 1124.3, 1105.3, 1055.9, 991.3w, 828.38, 768.22, 665.48s. [μ_{eff} = 1.38 μ_B].

Method B

Dark purple crystals of $L^1Ni(N_2)$ (0.100 g, 0.175 mmol) were dissolved in toluene (10 mL). Ethylene gas (1 atmosphere) was passed through the stirred solution and stirring was continued at room temperature for 24 hours, during which time the solution became darker. The solution was then dried under vacuum and dissolved in hexane, and centrifuged to remove small amount of undissolved solid. The dark supernatant was concentrated to 5 mL and left undisturbed at -35 °C for few days, affording dark brown crystals of $(L^1\text{-}L^1)Ni_2$ (0.061 g, 0.042 mmol, 24%).

Method C

Dark purple crystals of $L^1Ni(N_2)$ (0.100 g, 0.175 mmol) were dissolved in toluene (10 mL). Solid diphenylacetylene (0.3115 g, 0.175 mmol) was added to the stirred solution and stirring was continued at room temperature for 24 hours. The solution became darker and was dried under vacuum. The residue was dissolved in hexane, and the suspension centrifuged to remove small amount of undissolved residue. The dark supernatant was concentrated to 5 mL

and left undisturbed at -35 °C for few days to afford dark-brown crystals of $(L^1\text{-}L^1)Ni_2$ (0.079 g, 0.054 mmol, 31%).

7.3 X-ray Data

Crystal structure determinations

Single crystals of complex $L^1Ni(N_2)$, L^1NiMe and $(L^1\text{-}L^1)Ni_2$ suitable for X-ray diffraction, were selected under an inert atmosphere and mounted on a glass fiber. Unit cell measurements and intensity data collections were performed on a Bruker-AXS SMART 1K CCD diffractometer using graphite monochromatized Mo K_α radiation (λ = 0.71073 Å). The data reduction included a correction for Lorentz and polarization effects, with an applied multi-scan absorption correction (SADABS[36]). The crystal structures were solved and refined using the SHELXTL program suite.[37] Direct methods yielded all non-hydrogen atoms which were refined with anisotropic thermal parameters. All hydrogen atom positions were calculated geometrically and were riding on their respective atoms. The crystal data and refinement parameters for the complexes are listed in Table 7.1. Interatomic distances and angles are given in found in supporting information of reference 34b).

Table 7.1. Details of X-ray structure determinations

	$L^1Ni(N_2)$	L^1NiMe	$(L^1\text{-}L^1)Ni_2\cdot C_6H_{14}$
Formula	$C_{33}\ H_{43}\ N_5\ Ni$	$C_{34}\ H_{46}\ N_3\ Ni$	$C_{86}\ H_{126}\ N_6\ Ni_2\ O_5$
M_w	568.43	555.45	1441.35
T(K)	200(2)	202(2)	202(2) K
Wavelength (Å)	0.71073	0.71073	0.71073 Å
Crystal sys	Orthorhombic	Monoclinic	Monoclinic
Space group	$P2_12_12_1$	$P2_1/c$	C2/c
a (Å)	8.5334(11)	15.268(8)	26.340(3)
b (Å)	17.997(2)	14.920(8)	13.5083(14)
c (Å)	20.322(3)	14.715(8)	24.279(3)
α (deg)	90	90	90
β (deg)	90	112.557(7)	109.447(2)
γ (deg)	90	90	90
***V* (Å^3)**	3120.9(7)	3096(3)	8145.6(15)
Z	4	4	4
D_{calcd} (Mg/m^3)	1.210	1.192	1.175
Abs coeff mm^{-1}	0.650	0.652	0.515
F(000)	1216	1196	3120
R, Rw2	0.055, 0.1243	0.0561, 0.1328	0.0635, 0.1539
GOF	0.991	1.040	1.051

7.4 Results and Discussion

7.4.1 Electronic structure of metal halides and metal alkyls

Complexes LMX_2 (M = Fe, Co, Ni; X = halide) are all high-spin and contain a neutral ("innocent") ligand $L^{(0)}$ and a truly divalent metal centre.[28] Reduction of high-spin (*S* = 2) $LFeX_2$ to LFeX is ligand-centered, and the resulting complexes have a ligand radical anion L^- (*S* = ½) antiferromagnetically coupled to high-spin Fe^{II} (*S* = 2), leading to a final *S* = ³⁄₂ ground state.[38] The C_{py}-C_{im} and C_{im}-N_{im} bond lengths in DIMPY complexes usually provide an indication of the extent of metal-to-ligand electron transfer,[5,2,38] although sometimes disorder and/or (partial)

ligand deprotonation makes interpretation of the observed bond lengths difficult; for LFeX complexes, they support the assignment as $L^{-}Fe^{II}X$.[39] For halide complexes, ligand reduction does not appear to affect the metal spin state, which remains high-spin Fe^{II}.[5] Also, iron alkyl derivatives $LFeR_2$ and LFeR have the same spin state and electronic structure as the analogous halides.[28,38]

For cobalt, the situation is slightly different. While the dihalides are high-spin (S = ⅗),[32] the spin state of the monohalides LCoX depends on details of the ligand structure. With *aryl* groups at N, the monohalides are diamagnetic[40,41] (S = 0) and are best viewed as having a ligand radical anion (S = ½) antiferromagnetically coupled to a *low-spin* Co^{II} (S = ½) centre.[8] With *alkyl* groups at N, the same electronic structure is observed at low temperature, but at higher temperatures crossover to a paramagnetic state (S = 1) occurs, which was interpreted as having high-spin Co^{II} (S = ⅗) antiferromagnetically coupled to the ligand radical anion.[42] Dialkyl complexes $LCoR_2$ have not been observed so far and are probably unstable.[43,44] The corresponding monoalkyl complexes LCoR seem to be diamagnetic regardless of the ligand substitution pattern,[40-42] and are again best viewed as having a ligand radical anion antiferromagnetically coupled to low-spin Co^{II}. Though diamagnetic, these singlet-biradical-like complexes show some peculiar ^{1}H NMR chemical shifts (pyridine H4 around 10 ppm; imine methyl signals at 0 to -2 ppm). These unusual shifts were originally attributed to thermal population of a low-lying triplet state,[8] and the direct observation of such thermal population for N-alkyl Co(I) halide complexes[42] supports this interpretation. However, the even more extreme shifts found for $LFe(N_2)_2$ complexes have been attributed to residual temperature-independent paramagnetism (TIP) caused by spin-orbit coupling[38,45,46] rather than thermally populated triplet states, and if that explanation is correct a contribution from TIP for LCoR and LCoX complexes

seems likely as well. More studies are probably needed to resolve the TIP vs thermal population issue.

Apart from the unexceptional $LNiX_2$ complexes,[47] much less is known about the chemistry of Ni complexes of DIMPY ligands. One well-characterized monohalide (L^1NiCl) has been reported so far,[48] and bond lengths support a description with a low-spin Ni^{II} center and a ligand radical anion. We here report on the first mono-alkyl complex, L^1NiMe, prepared via the somewhat unconventional route of treating $LNi(N_2)$ (*vide infra*) with trimethylaluminum (we will discuss the mechanism of this reaction later in this section). The complex (Figure 7.1) shows the Ni atom in a standard square-planar environment. In view of the discussion above, this complex most likely contains low-spin Ni^{II} bound to a ligand radical anion; bond lengths in the X-ray structure are consistent with the transfer of 1-2 electrons from metal to ligand.

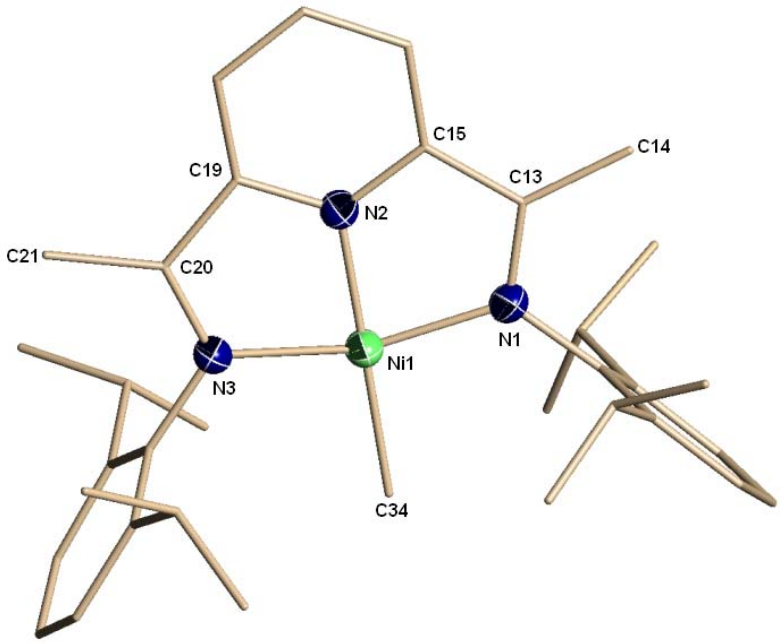

Figure 7.1: Partial thermal ellipsoid plot of L^1NiMe (7.1), drawn at 50 % probability level.

7.4.2 Electronic structures of dinitrogen complexes

Both for Fe and Co, a number of dinitrogen complexes have been reported; in the present work, we add the new complex $L^1Ni(N_2)$ to the collection. Dinitrogen complexes are interesting by themselves, but also as sources of reactive LM fragments, as will be discussed below. The group of Chirik has prepared mononuclear $LFe(N_2)_2$ complexes (bearing 2,6-^{i}Pr$_2$C$_6$H$_3$ groups at N[46,49]) as well as several binuclear $[LFe(N_2)]_2(\mu\text{-}N_2)$ complexes (bearing less bulky 2,6-Et$_2$C$_6$H$_3$ and 2,6-Me$_2$C$_6$H$_3$ groups at N).[45,46] In all cases, the complexes are diamagnetic, containing intermediate-spin (S = 1) Fe^{II} antiferromagnetically coupled to a triplet ligand diradical dianion (S = 1). Interestingly, the anion $LFe(N_2)(CH_2CMe_3)^-$ was proposed to contain *low-spin* Fe^{II} (S = 0) and a closed-shell (S = 0) ligand dianion;[50] the reason for the apparently different electronic structures of the two types of complexes is not clear. In any case, reduction from $LFeX_2$ to LFeX and then $LFe(N_2)_2$ seems to occur exclusively at the ligand, but the stronger ligand field of the reduced ligand induces a flip of one [in $LFe(N_2)_2$ [45]] or two [in $LFe(N_2)(CH_2CMe_3)^-$ [50]] electrons at the metal. Several anionic N_2 complexes have also been prepared, and these still appear to contain Fe^{II}: apparently a third electron can be accepted by the ligand, but calculations indicate that on addition of a fourth electron the metal would finally get reduced.[51]

Again, the situation is markedly different for cobalt. The diamagnetic cationic complex $LCo(N_2)^+$, unlike neutral LCoX/LCoR, seems to contain true low-spin Co^I (S = 0) and a neutral, innocent DIMPY ligand. Interestingly, the unusual ^{1}H NMR shifts observed for the "non-innocent" LCoX/LCoR complexes (vide supra) are not found for the "innocent" $LCo(N_2)^+$ complex or for the analogous ethene complex.[33]

One-electron reduction to neutral $LCo(N_2)$ occurs at the ligand, and a further one-electron reduction yields diamagnetic $LCo(N_2)^-$ still containing low-spin Co^I but now bound to a closed-shell ligand dianion.[35] Thus, compared to Fe, Co seems to be more easily reduced to the

univalent state. The different bonding interactions in LCoX ($L^{-}Co^{II}_{LS}$) and $LCo(N_2)^{+}$ ($L^{0}Co^{I}_{LS}$) reflect the weaker donating power of N_2 compared to halide or alkyl, resulting in a lowered stability of Co^{II} vs Co^{I}. At the same time, it is clear that metal-centred and ligand-centred reduction do not differ much in energy for the LCo^{II} fragment.

Only a handful of nickel-dinitrogen complexes have been reported to date.[52-55] The new complex $L^1Ni(N_2)$ was prepared by stirring a yellowish-brown suspension of L^1NiBr_2 in THF for four days at room temperature with two equivalents of NaH. A bright burgundy solution was formed which after work-up gave the crystalline and diamagnetic dinitrogen complex; the X-ray structure (Figure 7.2) shows an approximately square-planar nickel metal center surrounded by the terdentate ligand and one terminally bonded dinitrogen unit. The dinitrogen N≡N bond distance [N(4)-N(5) = 0.92 Å] is extremely short, indicative of the absence of any significant N_2 activation. The fact that the N-N distance is even shorter than in free dinitrogen is probably a crystallographic artifact due to nitrogen atom thermal motions or some minor disorder that could not be modeled. In agreement with the minimal extent of reduction of the N≡N bond, the IR stretching was found at a high frequency (2160 cm^{-1}).

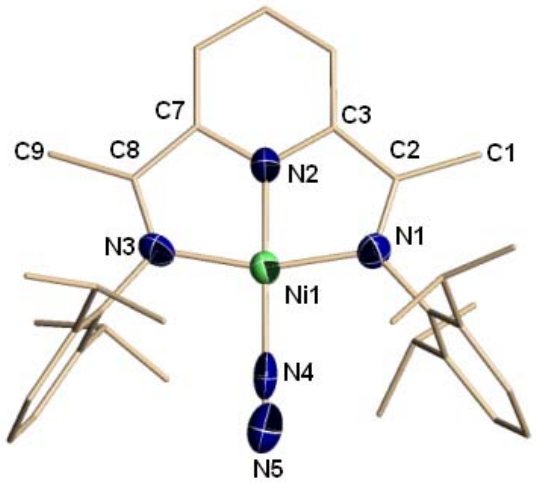

Figure 7.2: Partial thermal ellipsoid plot of $L^1Ni(N_2)$ (7.2), drawn at the 50% probability level.

It is not immediately obvious how the bonding in $L^1Ni(N_2)$ should be interpreted. Possibilities are (a) $Ni^{(0)}$ and a neutral (innocent) ligand, (b) low-spin Ni^{II} and a closed-shell dianionic ligand,[56] or (c) the intermediate situation: Ni^{I} antiferromagnetically coupled to a ligand radical anion. All well-characterized $Ni(N_2)$ complexes reported to date contain $Ni^{(0)}$, which would argue for option (a). On the other hand, the N_2 appears to be very weakly bound in this complex. Also, $Ni^{(0)}$ prefers a tetrahedral environment; the approximately square-planar one found for our complex is more typical for Ni^{II}, which would support option (b). Ni^{I} is not a very common oxidation state, and its geometric preferences are probably less pronounced. The C_{py} - C_{im} and C_{im}-N_{im} bond lengths in the X-ray structure are very similar to those found for L^1NiMe and would be consistent with a transfer of 1-2 electrons to the ligand, arguing in favor of option (c). The complex is iso-electronic with $LCo(N_2)^-$ and for simplicity we assume here an analogous electronic structure, i.e. low-spin Ni^{II} and a closed-shell ligand dianion. It should be noted here that none of the Fe, Co and Ni dinitrogen complexes to date show evidence of strong activation of the N_2 ligand.

7.4.3 Reactivity of N_2 complexes

Regardless of whether the N_2 complexes contain a reduced metal or a reduced ligand (or both), one would expect them to be strong reductants, strong enough perhaps to break C-X bonds. Indeed, Chirik has reported that the formally $Fe^{(0)}$ complex $LFe(N_2)_2$ is able to break the activated C-O bonds of esters and allyl ethers.[57] The mechanism proposed for this reaction involves a "classical" oxidative addition of R-OR' to one iron center, followed by loss of an R radical which is then captured by a second $Fe^{(0)}$ complex, yielding ultimately a mixture of LFeOR' and LFeR. Supporting this mechanism is the isolation of $LFe(OAc)(\eta^1\text{-}C_2H_3)$, where apparently loss of vinyl radical does not occur. Alkyl halides RX also react with $LFe(N_2)_2$ to give mixtures of LFeX and LFeR.[39]

The group of Budzealaar recently investigated the reaction of $LCo(N_2)$ with both alkyl and aryl halides.[58] Aryl halides are in general more difficult to activate than alkyl halides, and chlorides are usually less reactive than bromides. Gratifyingly, it was found that even aryl chlorides react with $LCo(N_2)$ to give a mixture of LCoAr and LCoCl, though generally in a ratio smaller than 1:1. The choice of DIMPY ligand proves to be crucial: with L^1 the reaction produces only small amounts of L^1CoAr (about 15% relative to L^1CoCl for 4-trifluorochlorobenzene; for details, see supporting information of reference 34b)), whereas the less hindered ligand L^2 gives much better ratios (> 0.7:1 for most aryl chlorides).[58] The mechanism proposed for this reaction, and supported by calculations, is direct halide abstraction from ArCl by an LCo fragment, leading to LCoCl and a free Ar radical which then mostly finds its way to a second Co centre. Interestingly, more reactive substrates (aryl bromides and iodides), though reacting more quickly, give poorer yields of LCoAr products, possibly due to the higher free radical concentration during the reaction.

The potential of L^2CoAr complexes for C-C coupling reactions was also investigated. A mixture of L^2CoAr and L^2CoCl was generated by treating $L^2CoCH_2SiMe_3$ first with H_2/N_2 and then with 0.5 equiv of ArCl as described earlier,[58] and to this mixture was then added a second organic halide in excess. Results are summarized in Table 7.2. L^2CoAr reacts only with activated alkyl halides like benzyl bromide, benzyl chloride or allyl chloride, giving a mixture of products, e.g. for L^2CoPh + BzCl (entry 7): Bz-Bz : Bz-Ph : Ph-Ph ≈ 1 : 3.5 : 0.03, consistent with a radical-type mechanism. As mentioned above, $L^2Co(N_2)$ is a strong enough reductant to abstract a halide from ArCl. In contrast, L^2CoAr is a much weaker reductant and can only abstract a halogen atom from activated halides like BzBr. Also, L^2CoAr complexes with electron-poor aryls should be poorer reductants and indeed require more highly activated halides to react: compare entries 7, 10 and 11. We propose that, after abstraction of bromide by L^2CoAr, the intermediate $L^2Co(Ar)(Br)$ quickly loses the aryl group as a radical, which mostly combines with the previously generated benzyl radical. This mechanism, based on the instability of $LCo(Ar)(Br)$, is consistent with the previously reported easy loss of an alkyl radical from $LCoR_2$.[43,59] Alkyl-alkyl couplings are also possible, as illustrated by the formation of Me_3SiEt from $LCoCH_2SiMe_3$ and MeI (entry 8).

Table 7.2: C-C coupling reactions with L^2CoAr.[a]

Entry	Ar	RX	Products[b]
1	C_6H_4-4-CF_3	allylCl	allyl-Ar (M), Ar-Ar (m)
2	C_6H_5	allylCl	allyl-Ar (M), Ar-Ar (m)
3	C_6H_4-4-OMe	allylCl	allyl-Ar (M), Ar-Ar (m)
4	C_6H_4-4-Cl	BzCl	Bz-Ar (M), Bz-Bz (M)
5	C_6H_5	*n*-$C_6H_{13}Br$	N.R.
6	C_6H_4-4-CF_3	BzBr	Bz-Ar (m), Bz-Bz (M)
7	C_6H_5	BzCl	Bz-Ar (3.5), Bz-Bz (1.0), Ar-Ar (0.03)
8	CH_2SiMe_3 [d]	MeI	$EtSiMe_3$
9	C_6H_5 [c]	PhI	N.R.
10	2-C_5H_3N-6-Cl	BzCl	N.R.
11	2-C_5H_3N-6-Cl	BzBr[e]	Bz-Ar (m), Bz-Bz (M)

[a] Mixture of L^2CoAr and L^2CoCl generated from $L^2Co(N_2)$ as described in ref 34, then RX added (0.5 equiv relative to original ArCl used). [b] Detected by GC/MS. For entry 7, amounts calibrated against authentic samples; other entries: M = major, m = minor product. [c] Using separately prepared pure L^2CoPh instead of the mixture with LCoCl. [d] Using separately prepared pure $L^2CoCH_2SiMe_3$ and 1.8 equiv of CH_3I; product identified by NMR. [e] Using 2.0 equiv of BzBr relative to $L^2Co(N_2)$.

The reactivity and C-C coupling potential of $LNi(N_2)$ and LNiR complexes is yet to be explored. However, (terpy)NiR complexes are active in C-C coupling reactions, most likely involving a radical mechanism,[60,61] so, DIMPY complexes might well show similar reactivity.[62]

7.4.4 Ligand non-innocence and radical chemistry

Ligand alkylation and loss of alkyl groups is a recurring theme in the chemistry of metal-alkyl complexes of DIMPY ligands. Alkylation can even be reversible.[23-25, 27-29] We believe that much of this chemistry can be interpreted in terms of radical formation induced by the electronic

non-innocence of the DIMPY ligand. In effect, the neutral DIMPY ligand, terdentate coordinated to the metal, is a strong oxidant, even capable of abstracting an electron from a metal-carbon bonding orbital, thus leading to easy loss of an organic radical. Where that radical then ends up depends on details of the system like size and stability of the alkyl, steric hindrance of the DIMPY ligand, nature of the central metal atom, and distribution of unpaired electron density over the ligand. The binuclear oxidative addition of ArCl to $L^2Co(N_2)$ can be explained this way (Scheme 7.3); the C-C coupling reactions mentioned earlier can be rationalized in a similar manner (Scheme 7.4): $L^{\cdot-}Co^{II}Ar$ abstracts a halide from BzBr to form $L^0Co^{II}(Ar)(Br)$, in which L^0 oxidizes the Co-Ar bond to give $L^{\cdot-}Co^{II}Br$ and $Ar^{\cdot}$. Thus, C-C coupling would be another illustration of the "ennobling" character of redox-active ligands in combination with first-row transition metals.[63]

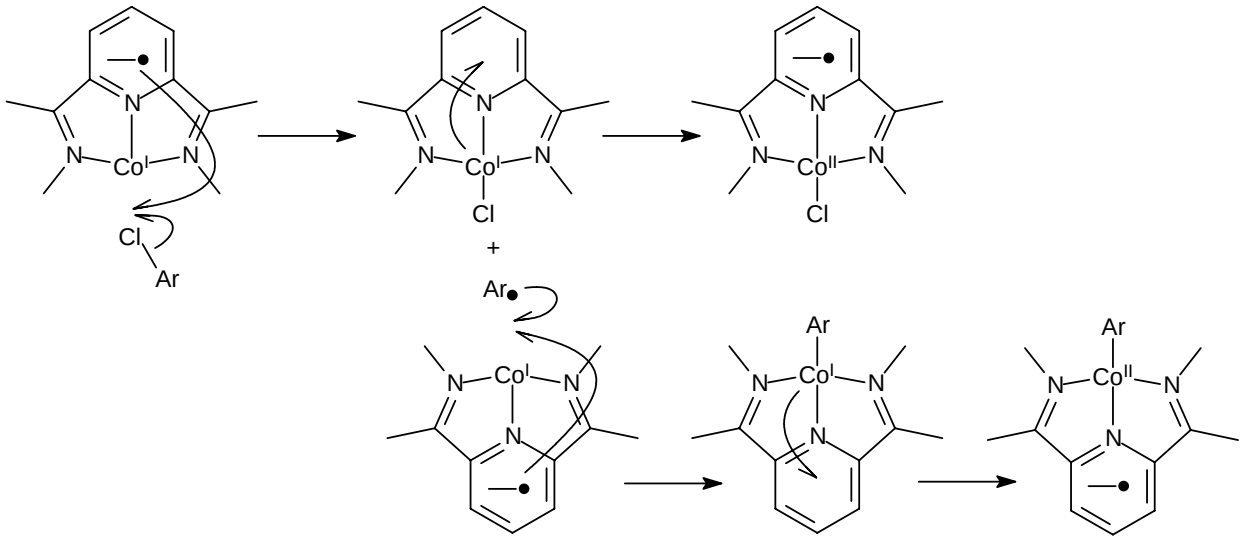

Scheme 7.3. Radical- type oxidative addition at LCo fragments.[64]

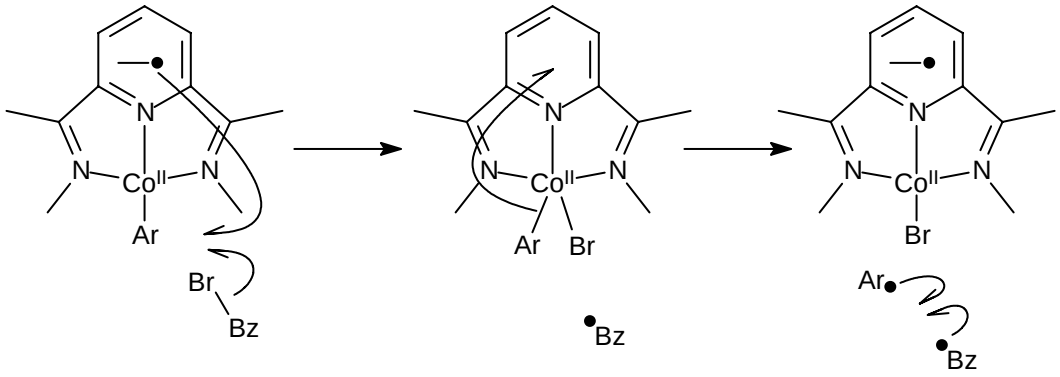

***Scheme 7.4. C-C coupling using LCoAr.*[64]**

This idea can also explain why alkylation at various positions of the ligand happens with comparable ease for main-group metals (Li, Mg, Zn, Al) and transition metals (V, Cr, Fe).[2]

Preliminary calculations on simple Al model systems (Table 7.3) support the extreme stabilization of low oxidation states by the DIMPY ligand, and hence the facilitation of loss of alkyl radical. This stabilization is nearly enough to make ejection of even the highly reactive Me radical thermoneutral, and explains the easy release of R radicals from $LCoR_2$ mentioned earlier.

Table 7.3. Reaction energies (kcal/mol)[a] for loss of Me radical from $AlMe_3$ complexes.

	$LAlMe_3 \rightarrow LAlMe_2 + Me\cdot$			
	Me at N		**2,6-$Me_2C_6H_3$ at N**	
Ligand[b]	**E_{rxn}**	**E_{act}**	**E_{rxn}**	**E_{act}**
(none)	81.0		-	
TMEDA	82.7		-	
DIM	8.3	15.1	7.0	21.4
IMPY	16.5	23.9	15.1	22.3
BIPY	19.7	25.9	-	-
DIMPY	6.5	22.3	15.3	

[a] Electronic energies only, ub3-lyp/SV(P), not corrected for ZPE, thermal effects, or solvent effects. [b] For ligand abbreviations, see Scheme 7.1.

Returning now to the mechanism of L^1NiMe formation from $L^1Ni(N_2)$ and $AlMe_3$, this can be rationalized by similar radical chemistry. The first step would likely be expulsion of Ni from its complex by Al. This would initially form L^1AlMe_3 which would eject a methyl radical, giving L^1AlMe_2 (such a species was isolated and fully characterized from a similar reaction of the Fe congener[10]). The released Me radical would then find its way to a second $L^1Ni(N_2)$ molecule and bind to the Ni atom (Scheme 7.5) similar to the formation of L^2CoAr from $L^2Co(N_2)$ and Ar in Scheme 7.1.

.

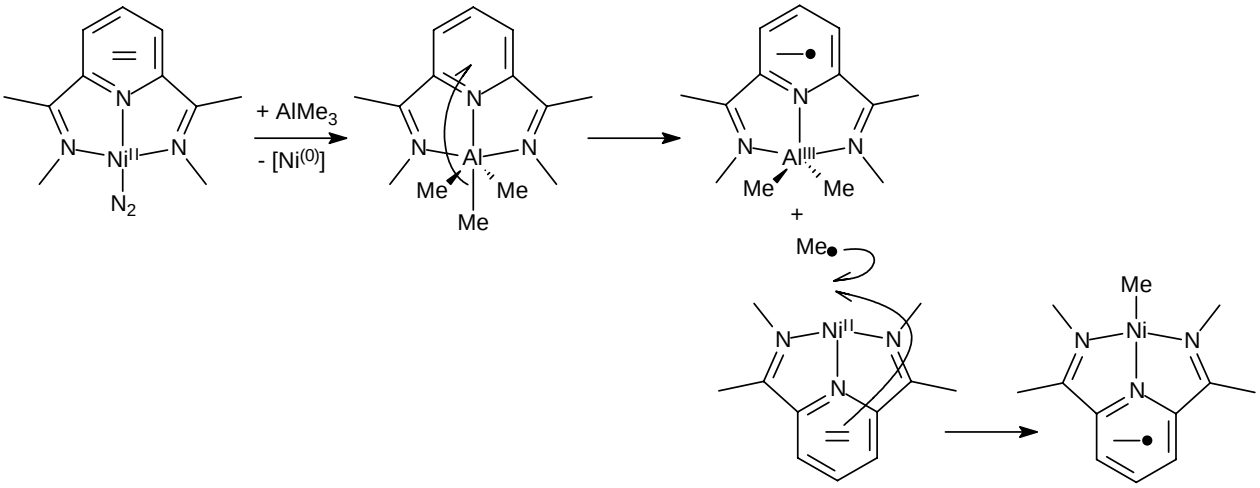

Scheme 7.5. Possible mechanism for formation of L^1NiMe from $L^1Ni(N_2)$ and $AlMe_3$.[64]

7.4.5 Unusual coordination modes

The DIMPY ligand is usually assumed to coordinate in a terdentate fashion. However, we here report an example from Ni chemistry that illustrates a surprisingly different coordination mode. If the synthesis of $L^1Ni(N_2)$ is attempted by combining *in situ* $NiBr_2(DME)$, L^1 and 3 equiv of NaH, a different complex was obtained. The same new complex is obtained if

previously isolated $L^1Ni(N_2)$ is treated with ethylene or tolane to attempt replacement of the labile dinitrogen ligand (Scheme 7.6).

A single-crystal X-ray diffraction study revealed the complex to contain a dimerized ligand, here indicated as L^1-L^1, wrapped around two nickel atoms which have no other ligands bound to them (Figure 7.3). It is a symmetry generated dimer consisting of two ligand systems and two Ni centers. The two ligands are linked by a C-C bond between the two former imine Me groups that in the process have lost one hydrogen each. Each ligand half chelates one nickel atom with an imine-pyridine fragment [Ni(1)-N(1) = 1.961(3)Å, Ni(1)-N(2) = 1.909(3)Å], and uses its second imine function (at which it has dimerized) to η^2-coordinate to the other nickel atom [Ni(1)–N(3) = 1.902(3)Å, Ni(1)–C(21) = 1.916(4)Å]. This second imine group is visibly elongated [N(3)–C(21) = 1.398(5)Å] relative to the first one [N(1)–C(13) = 1.291(5)Å], indicating extensive backdonation from the formally $Ni^{(0)}$ metal center.[65] The remaining imine methyl group appears to be intact, with a C-Me distance as expected for a single bond [C(13)–C(14) = 1.513(6)Å]. The tetracoordinate geometry around each nickel center is severely distorted, with angles of N(1)-Ni(1)-N(2) = 83.24(14)°, N(2)-Ni(1)–N(3) = 148.74(14)°, N(1)–Ni(1)–N(3) = 124.55(14)°, N(2)-Ni(1)-C(21) = 106.30(15)°.

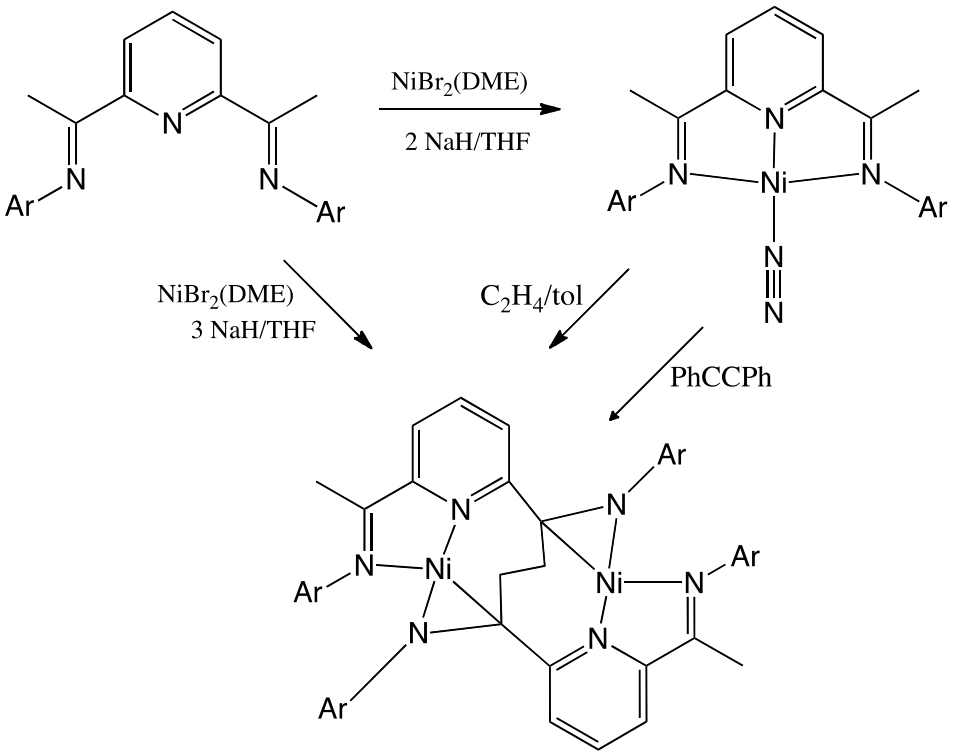

Scheme 7.6: Different routes towards (L^1-L^1)Ni_2.

The ligand dimerization has precedents in Mn[6] and Co[66] chemistry and arises from the deprotonation of one of the two methyl imino groups and coupling of the resulting CH_2 unit with an identical one from a second unit. This transformation clearly arises from the one electron transfer to the imine functionality. The release of a hydrogen atom - possibly as a radical H transfer to some acceptor - results in formation of the CH_2 radical of sufficiently long life time to enable dimerization. The way in which the dimerized ligand of (L^1-L^1)Ni_2 is bound to both Ni atoms is unprecedented; the Mn and Co examples mentioned above show the much less surprising κ^3:κ^3 coordination mode.

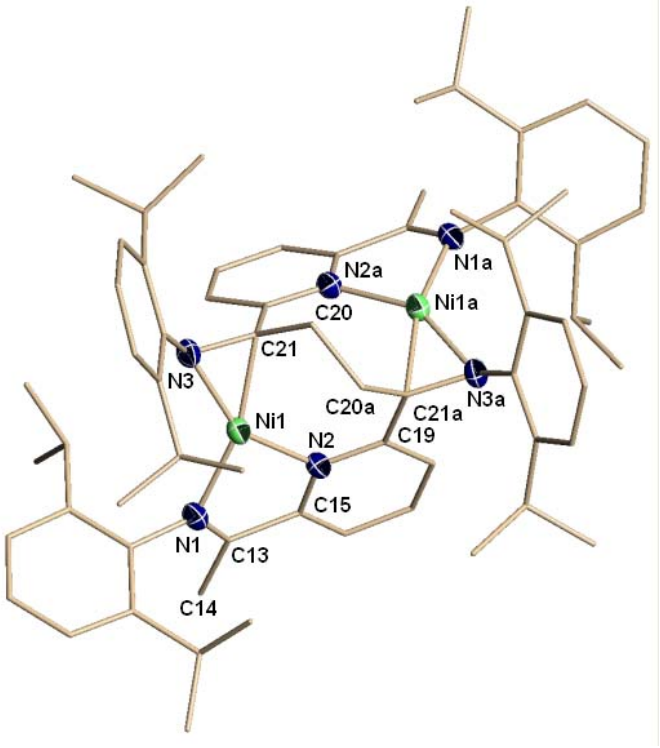

Figure 7.3: Partial thermal ellipsoid plot of (L^1-L^1)Ni_2 (7.3), drawn at the 50 % probability level. Hydrogen atoms are omitted for clarity.

Sometimes, unusual coordination modes of ligands like DIMPY might be obtained because a metal salt and L are combined *in situ* and maybe never arrive at the standard terdentate coordination mode; that might apply to the synthesis of (L^1-L^1)Ni_2 from L^1, $NiBr_2$(DME) and NaH in Scheme 7.6. But in the ethylene and tolane reactions also reported here, the ligand starts out terdentate and opens up at some point, showing that terdentate coordination should not be identified with rigid, fixed and unbreakable coordination. Flexible coordination modes are obviously important during initial complexation of the ligand to a metal. In addition, temporary (or permanent) opening of the terdentate chelation may well be relevant in many reactions of DIMPY complexes.[67]

7.5 Conclusions and outlook

The DIMPY ligand is capable of promoting an unprecedented diversity of chemical reactions, both at the metal and at the ligand itself. While the original application of the ligand in polymerization catalysis[32,68] is probably not directly connected to its non-innocent character,[69] many other aspects of its chemistry are likely to be intimately connected to metal-to-ligand electron transfer.[70] In particular, we propose that ligand non-innocence and alkyl/aryl radical chemistry are two sides of the same coin. One of the more exciting aspects of the C-C coupling reaction described here is that, although it superficially resembles the one catalyzed by noble metals, the mechanism is clearly different, which may well lead to different selectivities, functional-group tolerance and areas of application. Versatility of coordination modes, not available to other "staple" ligands like cyclopentadienyls, might also be relevant in reactions of DIMPY complexes. It seems obvious this ligand has more surprises in store.

7.6 Computational Methods

All geometries were optimized with Turbomole[71,72] using the SV(P) basis set,[73] the b3-lyp functional[74-77]and the unrestricted DFT formalism in combination with an external optimizer (PQS OPTIMIZE).[78,79] Transition states for Me dissociation were calculated using a broken-symmetry $S_z = 0$ solution. Vibrational analyses were carried out to confirm the nature of all stationary points.

B. 7.7 Nickel Hydride Catalyst for Ethylene Oligomerization.

As mentioned in section A, the unique ability of bis(imino)pyridine ligand to host electrons and supply spin density "in demand" leads to various transformations with the direct participation of the ligand in the chemistry of metal centre. Yet, no nickel hydride complex have been reported with this ligand. On the other hand, due to its reactive nature only a handful of structurally characterized nickel hydrides have been described in the literature. This is in spite of a continuous search for this function, given its involvement in homogenous catalysis, coordination chemistry as well as in enzymatic reaction mechanisms.[80] It is reported that ethylene dimerization/polymerization by nickel catalyst also proceeds via metal hydride intermediate.[81] Hence, characterizing these derivatives is important for understanding mechanistic details of chemical transformations. In this section, we are describing the synthesis of nickel hydride complex via an unconventional route of nickel dinitrogen complex. Its catalytic behaviour towards ethylene oligomerizations has been also studied.

7.7.1 Preparation of [{2,6-[(*i*-pr)$_2$PhN = C(CH$_2$)]$_2$(C$_5$H$_3$N)}Ni(μ^1- H)Na(thf)$_2$] (7.4)

Method A

Dark purple crystals of complex **7.2** (0.1 g, 0.17 mmol) were dissolved in THF (5 mL). To the stirred solution NaH (0.018 g, 0.77 mmol) was added and the mixture further stirred at room temperature for 7 days. The dark brown solution was then dried in vacuum and dissolved in hexane, centrifuged to remove undissolved materials and excess of NaH. The dark purple supernatant was concentrated to 5 mL and left undisturbed at -35 ^{o}C for 7 days to form dark purple crystals of **7.4** (0.05 g, 0.07 mmol, 40 %).

IR (Nujol mull, cm^{-1}): 2955, 2924, 2854 (Nujol), 2279w, 1644w, 1570, 1459w, 1377s, 1324s, 1267s, 1226s, 1166s, 1087w, 1051w, 973m, 892, 808, 722, 665.

^{1}H- NMR (300 MHz, C_6D_6, 25^{o}C) δ: Singlet at (-21.03 ppm, Ni-H), 1.22 (8H, m), 1.45 (12H, d, *J* = 6.9 Hz), 1.52 (12H, d, *J* = 6.9 Hz), 3.04 (8H, m), 3.26 (1H, s), 3.33 (1H,s), 4.16 (1H, s), 4.27 (1H, s), 4.42 (4H, sept), 6.73 (1H, m), 6.91 (2H, m), 7.04 (6H, m).

^{13}C{1H}-NMR (300 MHz,C_6D_6, 25 ^{o}C) δ: 24.0, 24.4, 24.5, 24.8, 25.0, 27.8, 28.0, 67.4, 75.0, 75.3, 115.9, 116.3, 122.5, 122.7, 122.9, 123.4, 133.4, 133.6, 145.9, 147.3, 148.1, 154.4, 156.5, 157.4, 157.7, 158.7.

Method B

Solid $NiBr_2$(DME) (0.154 g, 0.5 mmol) and ligand 2,6-{(*i*-pr)$_2$PhN= C(CH_3)}$_2$(C_5H_3N) (0.241 g, 0.5 mmol) were mixed together in THF (15 mL) and allowed to stir for two days at room temperature affording a brown suspension. To the stirred suspension solid NaH (0.079 g, 3.3 mmol) was added under continuous stirring at room temperature for 4 days. The dark purple solution was then dried under vacuum and dissolved in hexane, centrifuged to remove undissolved materials and excess of NaH. The dark purple solution was concentrated to 5 mL and left undisturbed at -35 ^{o}C for 4 days to form dark purple crystals **7.4** (0.20 g, 0.35 mmol, 70%).

7.8 X-ray Data

Table 7.4. Crystal data and structural analysis results of complex $L^1Ni(H)$ **7.4**

	$L^1Ni(H)$ **7.4**
Formula	$C_{41}\ H_{58}\ N_3\ Na\ Ni\ O_2$
FW	706.60
Space group	Monoclinic, P2(1)/n
a (Å)	12.262(3)
b (Å)	22.524(6)
c (Å)	14.878(4)
α (deg)	90
β (deg)	101.953(4)
γ (deg)	90
V ($Å^3$)	4019.8(19)
Z	4
radiation (Kα, Å)	0.71073
T (K)	202(2)
D_{calcd} ($g\ cm^{-3}$)	1.168
μ_{calcd} (mm^{-1})	0.529
F_{000}	1520
R, R_w [2 a]	0.0648, 0.1578
GoF	1.025

[a] $R = \Sigma||Fo| - |Fc||/\Sigma|F|$. $Rw = [\Sigma(|Fo| - |Fc|)^2/\Sigma wFo^2]^{1/2}$.

7.9 Results and Discussion

The lability of coordinating dinitrogen, as highlighted in section A, prompted us to investigate the behavior of $L^1Ni(N_2)$ (**7.2)** towards hydride sources (Scheme 7.7). Treatment of a solution of **7.2** with 4 equivalents of NaH in THF afforded a diamagnetic complex $L^1Ni(H)$ (**7.4)**. Complex **7.4** could alternatively be obtained via an *in situ* reaction of ligand with $NiBr_2$(DME) followed by direct treatment of 6 equivalents of NaH in THF. It implies that two equivalents of NaH are necessary for the reduction of nickel and formation of dinitrogen complex (which is likely to be an intermediate species in this case). Two additional equivalents of NaH are

probably needed for the complex to undergo double deprotonation although there was reoxidation of the metal centre to the formal divalent state. It is tempting to speculate that the reoxidation might have occurred at the expenses of the dinitrogen molecule possibly forming hydrazine.

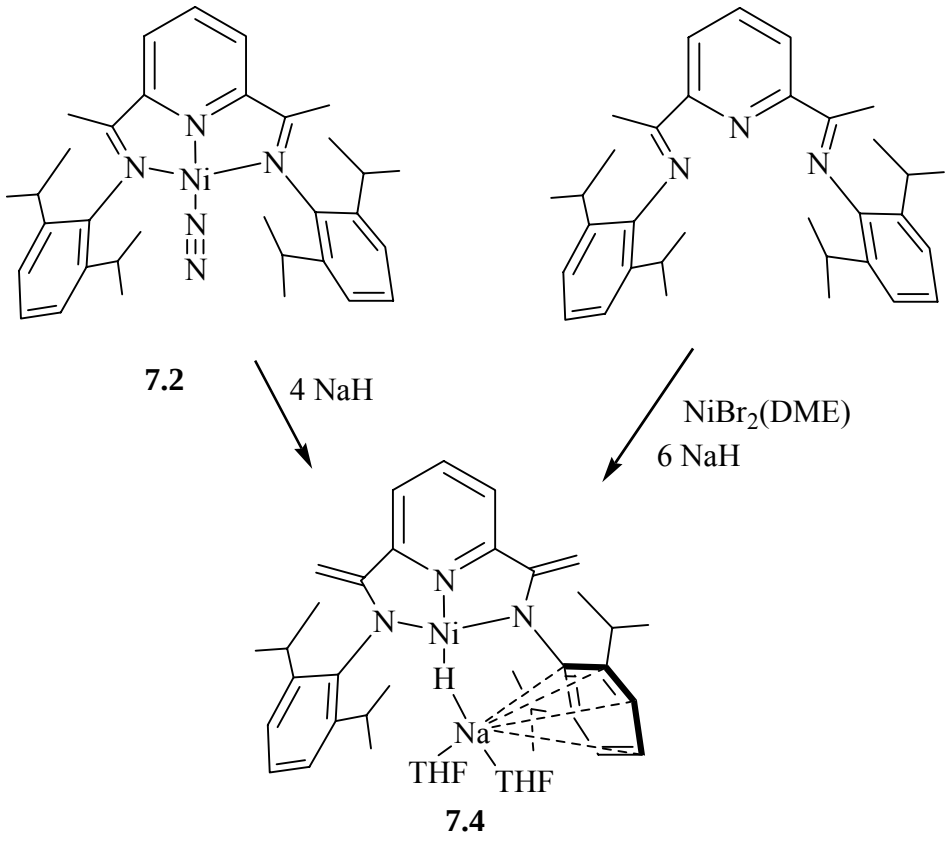

Scheme 7.7: Different routes towards 7.4

The formulation was yielded by X-ray crystal structure **7.4** (Figure 7.4), showing the distorted square planar nickel [N1 – Ni1 – N2 = 82.6(2)^o , N1 – Ni1 – N3 = 83.62^o, N1 – Ni1 – H1 = 177.61(2)^o , N3 – Ni1 – H1 = 96.31(1)^o , N2 – Ni1 – H1 = 97.57(2)^o] surrounded by the ligand three donor atoms [Ni1 –N1 = 1.841(5)Å, Ni1 – N2 = 1.902(5)Å, Ni1 – N3 = 1.878(5)Å].

The hydride bridges nickel [Ni1–H1 = 1.759(0)Å] to a sodium atom [H1– Na1 = 2.006(3)Å, Ni1-H1 – Na1 = 134.61(2)^{o}] which in turn is η^5 – bonded to one of the two ligand aryl rings [Na1- C15 = 2.941(7)Å, Na1 – C10 = 2.851(6)Å, Na1 – C11 = 2.959(7)Å] and also bonded to two molecules of THF [Na1 – O40 = 2.298(12)Å, Na1 – O50 = 2.333(15)Å]. The bond distances between C_{imine}- C_{methyl} [C6–C7 = 1.359(10)Å, C8–C9 = 1.354(9)Å] clearly indicate double bond character thereby making the ligand dianionic. Consequently, the imino functions have been lengthened [N2-C6 = 1.375(8)Å, N3-C8 = 1.386(7)Å].

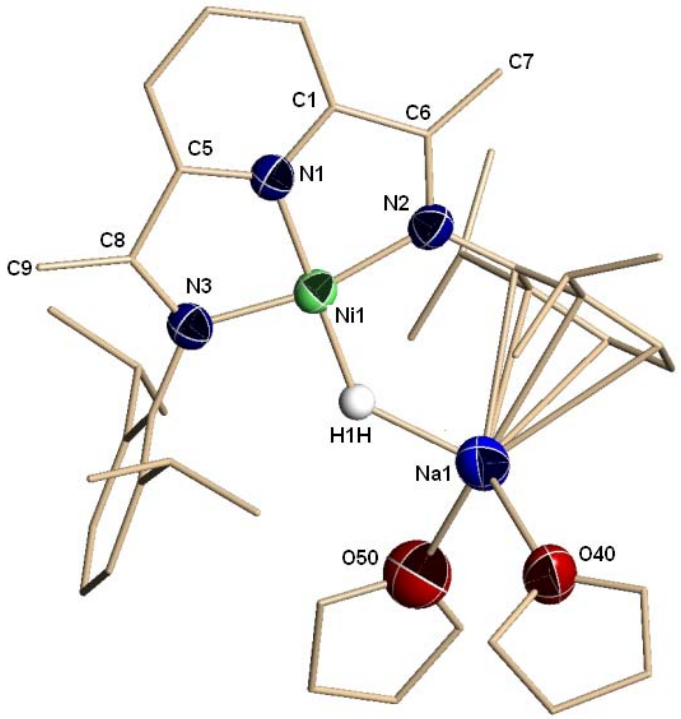

Figure 7.4: Partial thermal ellipsoid plot of complex L^1Ni(H) 7.4 drawn at the 50% probability level.

Solution NMR of **7.4** provided a clear evidence for the presence of hydride as highlighted by the upfield proton chemical shift value at -21 ppm in ^{1}H-NMR (Figure 7.5).

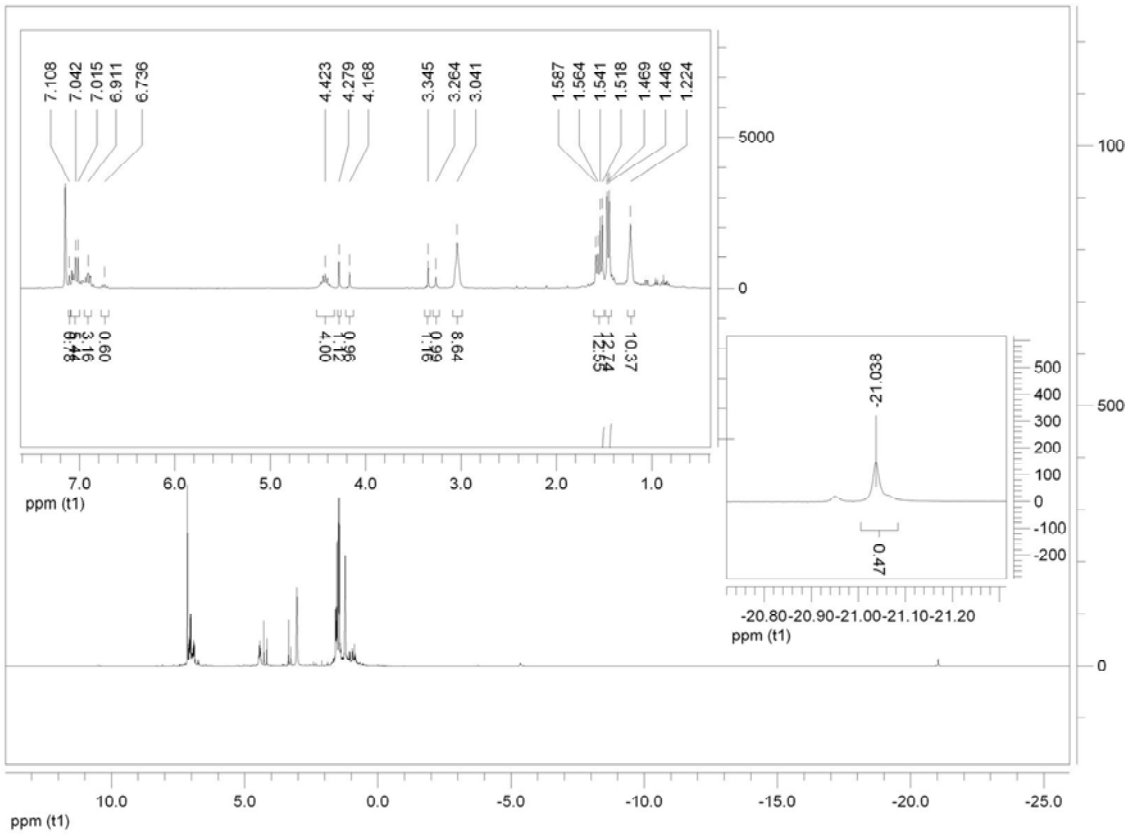

Figure 7.5: ^{1}H-NMR spectrum for complex 7.4 showing the existence of hydride at -21 ppm.

Interestingly, along with the hydride resonance at -21 ppm, another small peak at -5 ppm was also observed. To conclusively identify the Ni-H resonance, we exposed the solution of **7.4** in NMR-tube to deuterium gas. The experiment showed that the peak at -21 ppm, rapidly exchange with deuterium decreasing its intensity (Figure 7.6). Simultaneously, additional peaks of H/D started to appear, while the pick at -5 ppm remained unchanged (Figure 7.6).

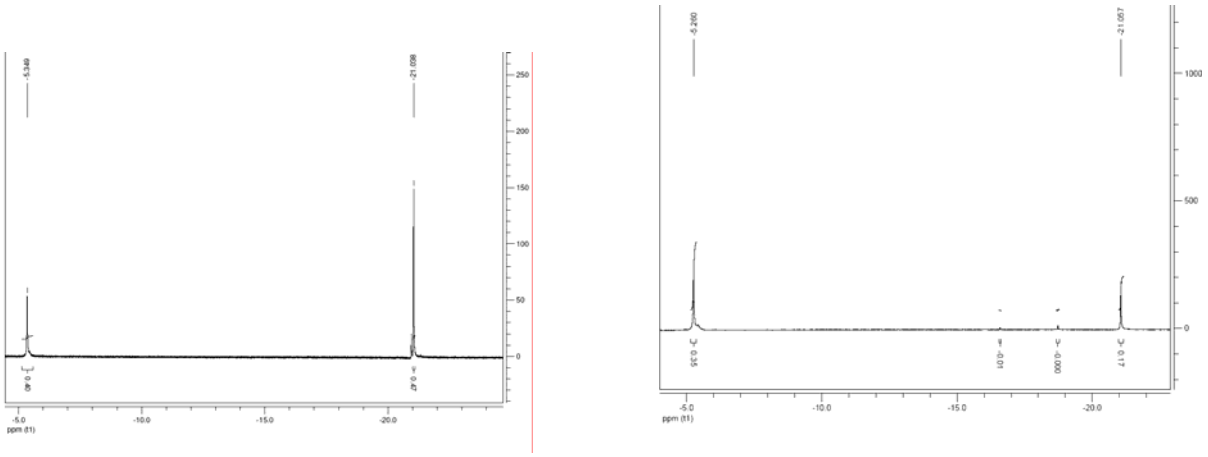

A ***B***

Figure 7.6:Comparative intensities: (A) ^{1}H Spectrum of complex 7.4 before D_2 experiment; (B)) ^{1}H Spectrum of complex 7.4 after D_2 experiment showing the hydrogen deuterium exchange at -21 ppm and gradual appearance of new Picks for the formation of H-D.

In order to rule out any possibility of contamination from any other hydride, we performed DOSY experiment. The data analysis (Figure 7.7) has clearly shown that there were only three diffusions from the complex **7.4** corresponding to 1) two THF molecules, 2) the hydride and 3) the rest of the molecules.

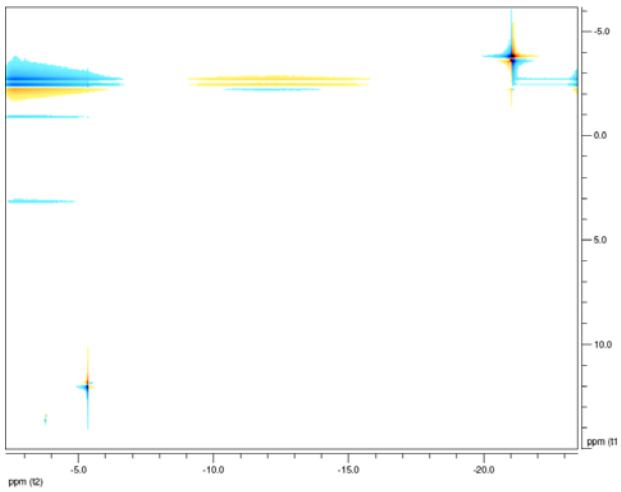

Figure 7.7: DOSY experiment showing three diffusions 1) THF, 2) hydride , 3) The rest of the complex.

Therefore, the peak at -5 ppm might be attributed to a long distance interaction of the metal with one *ipso* hydrogen of one of the isopropyl groups (Ni…H distance 2.963Å) which is oriented towards the Ni metal centre.

Catalytic Activity

Catalytic activity for complexes **7.2** & **7.4** is summarized in Table 7.5. It can be observed that the reaction temperature has a pronounced effect on both activity and selectivity. Firstly it should be noted that both complexes produced oligomerization as opposed to the highly active polymerization behavior shown by the Fe(II) and Co(II) analogues.[32]

Table 7.5: Ethylene oligomerization activity of complexes **7.2** and **7.4**.

Cat. (*μ*mol**)**	Temp (^{o}C)	Alkenes (mL)	Activity g/mmol, cat.h	Mol% 1-C4	2-C4	C6	PE (g)
7.2(30)	20	9	600	99	1	-	-
7.2(10)	50	32	6,400	63	37	-	-
7.2(30)	90	66	4,400	40	30	30	-
7.2(30)	110	61	4,066	25	20	55	-
7.2(30)*	50	1.5	100	99.9	-	-	-
7.4(30)	50	3	200	70	30	--	-
7.4(30)$^{\$}$	50	-	-				-
Blank	$NiBr_2$(DME)	-	-	-	-	-	-

*Conditions : 600 Psi (C_2H_4), 30 mins, 100 mL toluene, MAO co-catalyst, 1000 equivalents, *TIBAO 250, $^{\$}$tested as single component.*

Upon activation with MAO, **7.2** is highly active ethylene oligomerization catalyst. However, the selectivity is also affected by the reaction temperature, the lower the temperature, the higher the selectivity for 1-butene. For example, at room temperature **7.2** produced exclusively (99%) 1-butene. Interestingly, the complex showed selective behavior (99.9%) even upon activation with TiBAO. Under similar reaction conditions **7.4** showed similar selectivity.

7.10 Conclusions

In summary, we have shown that chemistry of nickel supported by the DIMPY ligand is indeed rich. The labile nature of dinitrogen allowed us to isolate a rare hydride complex although the replacement involved a redox transformation that has not been clarified. It is also interesting to observe that the formally low valent Ni(0) dinitrogen complex is highly active oligomerization catalyst. On the other hand, the divalent Ni(II) hydride complex showed similar trend in selectivity as with its dinitrogen congener albeit low activity possibly indicating that the two complexes form upon activation the same catalytically active species.

The next chapter will describe our continuous effort of isolating mono valent nickel complexes by employing dianionic pyrrolide ligand to further probe the catalytic behavior of nickel complexes.

References

1. General review of DIMPY and related ligands: Gibson, V.C.; Redshaw, C.; Solan, G. *Chem. Rev.* **2007**, *107*, 1745.

2. Review focusing on ligand non-innocence: Knijnenburg, Q.; Gambarotta, S.; Budzelaar, P.H.M. *Dalton Trans.* **2006**, 5442.

3. Wissing, E.; Van der Linden, S.; Rijnberg, E.; Boersma, J.; Smeets, W.J.J.; Spek, A.L.; Van Koten, G. *Organometallics* **1994**, *13*, 2602.

4. De Bruin, B.; Bill, E.; Bothe, E.; Weyhermüller, T.; Wieghardt, K. *Inorg. Chem.* **2000**, *39*, 2936.

5. Budzelaar, P.H.M.; De Bruin, B.; Gal, A.W.; Wieghardt, K.; Lenthe, J. H. *Inorg. Chem.* **2001**, *40*, 4649.

6. Reardon, D.; Aharonian, G.; Gambarotta, S.; Yap, G.P.A. *Organometallics* **2002**, *21*, 786.

7. Sugiyama, H.; Aharonian, G.; Gambarotta, S.; Yap, G.P.A.; Budzelaar, P.H.M. *J. Am. Chem. Soc.* **2002**, *124*, 12268.

8. Knijnenburg, Q.; Hetterscheid, D.G.H.; Kooistra, T.M.; Budzelaar, P.H.M. *Eur. J. Inorg. Chem.* **2004**, 1204.

9. Sugiyama, H.; Korobkov, I.; Gambarotta, S.; Möller, A.; Budzelaar, P.H.M. *Inorg. Chem.* **2004**, *43*, 5771.

10. Scott, J.; Gambarotta, S.; Korobkov, I.; Knijnenburg, Q.; De Bruin, B.; Budzelaar, P.H.M. *J. Am. Chem. Soc.* **2005**, *127*, 17204.

11. Bailey, P. J.; Dick, C. M.; Fabre, S.; Parsons, S.; Yellowlees, L. J. *Dalton Trans.* **2006**, 1602.

12. Van Koten, G.; Jastrzebski, T. B. H.; Vrieze, K. *J. Organomet. Chem.* **1983**, *250*, 49.

13. Kaupp, M.; Stoll, H.; Preuss, H.; Kaim, W.; Stahl, T.; Van Koten, G.; Wissing, E.; Smeets, W.J.J.; Spek, A.L. *J. Am. Chem. Soc.* **1991**, *113*, 5606.

14. Wissing, E.; Van Gorp, K.; Boersma, J.; Van Koten, G. *Inorg. Chim. Acta* **1994**, *220*, 55.

15. Wissing, E.; Rijnberg, E.; Van der Schaaf, A.; Van Gorp, K.; Boersma, J.; Van Koten, G. *Organometallics* **1994**, *13*, 2609.

16. Wissing, E.; Kaupp, M.; Boersma, J.; Spek, A.L.; Van Koten, G. *Organometallics* **1994**, *13*, 2349.

17. Gibson, V. C.; Redshaw, C.; White, A. J. P.; Williams, D.J. *J. Organomet. Chem.* **1998**, *550*, 453.

18. Riollet, V.; Copéret, C.; Basset, J.M.; Rousset, L.; Bouchu, D.; Grosvalet, L.; Perrin, M. *Angew. Chem. IE* **2002**, *41*, 3025.

19. Fedushkin, I. L.; Tishkina, A. N.; Fukin, G. K.; Hummert, M.; Schumann, H. *Eur. J. Inorg. Chem.* **2008**, 483.

20. Spek, A. L.; Jastrzebski, T. B. H.; Van Koten, G. *Acta Cryst. C* **1987**, *43*, 2006.

21. Nienkemper, K.; Kehr, G.; Kehr, S.; Fröhlich, R.; Erke, G. *J. Organomet. Chem.* **2008**, *693*, 1572.

22. Bruce, M.; Gibson, V.C.; Redshaw, C.; Solan, G.A.; White, A.J.P.; Williams, D.J. *Chem. Commun.* **1998**, 2523.

23. Reardon, D.; Conan, F.; Gambarotta, S.; Yap, G.P.A.; Wang, Q. *J. Am. Chem. Soc.* **1999**, *121*, 9318.

24. Clentsmith, G. K. B.; Gibson, V.C.; Hitchcock, P.B.; Kimberley, Brian, S.; Rees, C.W. *Chem. Commun.* **2002**, 1498.

25. Khorobkov, I.; Gambarotta, S.; Yap, G.P.A. *Organometallics* **2002**, *21*, 3088.

26. Cameron, T. M.; Gordon, J. C.; Michalczyk, R.; Scott, B. L. *Chem. Commun.* **2003**, 2282.

27. Blackmore, I. J.; Gibson, V. C.; Hitchcock, P. B.; Rees, C. W.; Williams, D. J.; White, A. J. P. *J. Am. Chem. Soc.* **2005**, *127*, 6012.

28. Scott, J.; Gambarotta, S.; Korobkov, I.; Budzelaar, P. H. M. *J. Am. Chem. Soc.* **2005**, *127*, 13019.

29. Kijnenburg, Q.; Smits, J. M. M.; Budzelaar, P. H. M. *Organometallics* **2006**, *25*, 1036.

30. The involvement of radicals in alkylation of DIM and IMPY ligands is well-established, see refs 15, 3, 11, 16,12,13.

31. Radicals have been observed associated with the N-alkylation of DIMPY ligands, see ref 27.

32. Small, B. L.; Brookhart, M.; Bennett, A. M. A. *J. Am. Chem. Soc.* **1998**, *120*, 4049.

33. Bowman, A. C.; Milsmann, C.; Atienza, C. C. H.; Lobkovsky, E.; Wieghardt, K.; Chirik, P. J. *J. Am. Chem. Soc.* **2010**, *132*, 1676.

34. a) *Zhu, D.; Budzelaar, P. H. M. Organometallics **2010**, 29,* 5759. b) Zhu, D.; Thapa, I.; Korobkov, I.; Gambarotta, S.; Budzelaar, P. H. M. *Inorg.Chem.* **2011,** *50*(20), 9879.

35. Humphries, M. J.; Tellmann, K. P.; Gibson, V. C.; White. A. J. P.; Williams, D. J. *Organometallics* **2005**, *24*, 2039.

36. Blessing, R. *Acta Crystallogr*. **1995**, *A51*, 33.

37. Sheldrick, G. M. *Acta Crystallogr*. **2008**, *A64*, 112.

38. Bart, S. C.; Chłopek, K.; Bill, E.; Bouwkamp, M. W.; Lobkovsky, E.; Neese, F.; Wieghardt, K.; Chirik, P. J. *J. Am. Chem. Soc.* **2006**, *128*, 13901.

39. Trovitch, R. J.; Lobkovsky, E.; Chirik, P. J. *J. Am. Chem. Soc.* **2008**, *130*, 11631.

40. Gibson, V. C.; Humphries, M. J.; Tellmann, K. P.; Wass, D. F.; White, A. J. P.; Williams, D. J. *Chem. Commun.* **2001**, 2252.

41. Kooistra, T. M.; Knijnenburg, Q.; Smits, J. M. M.; Horton, A. D.; Budzelaar, P. H. M.; Gal, A.W. *Angew. Chem. IE* **2001**, *40*, 4719.

42. Bowman, A. C.; Milsmann, C.; Bill, E.; Lobkovsky, E.; Weyhermüller, T.; Wieghardt, K.; Chirik, P.J. *Inorg. Chem.* **2010**, *49*, 6110.

43. Zhu, D.; Janssen, F. F. B. J.; Budzelaar, P. H. M. *Organometallics* **2010,** *29*, 1897.

44. Treatment of $(Py)_2Co(CH_2SiMe_3)_2$ with L^2 cleanly produces $L^2CoCH_2SiMe_3$ without any detectable intermediates. However, the same reaction with a PyBOX ligand initially forms paramagnetic $(PyBOX)Co(CH_2SiMe_3)_2$, detected by ^1H NMR.[43]

45. Russell, S. K.; Darmon, J. M.; Lobkovsky, E.; Chirik, P. J. *Inorg. Chem.* **2010**, *49*, 2782.

46. Bart, S. C.; Lobkovsky, E.; Chirik, P.J. *J. Am. Chem. Soc.* **2004**, *126*, 13794.

47. Su, B.; Feng, G. *Polym. Int.* **2010**, *59*, 1058 and reference cited there.

48. Manuel, T. D.; Rohde, J. U. *J. Am. Chem. Soc.* **2009**, *131*, 15582.

49. Krcher, A. M.; Bouwkamp, M. W.; Cortez, M. P.; Lobkovsky, E.; Chirik, P. J. *Organometallics* **2006**, *25*, 4269.

50. Tondreau, A. M.; Milsmann, C.; Patric, A. D.; Hoyt, H. M.; Lobkovsky, E.; Wieghardt, K.; Chirik, P. J. *J. Am. Chem. Soc.* **2010**, *132*, 15046.

51. Scott, J.; Vidyaratne, I.; Korobkov, I.; Gambarotta, S.; Budzelaar, P. H. M. *Inorg. Chem.* **2008**, *47*, 896.

52. Kruger, C.; Tsay, Y.H. *Angew. Chem.* **1973**, *85*, 1051.

53. Jolly, P.W.; Jonas, K.; Kruger, C.; Tsay, Y.H. *J. Organomet. Chem.* **1971**, *33*, 109.

54. Waterman, R.; Hillhouse, G.L. *Can. J. Chem.* **2005**, *83*, 328.

55. Pfirrmann, S.; Limberg, C.; Herwig, C.; Stosser, R.; Ziemer, B. *Angew. Chem. IE* **2009**, *48*, 3357.

56. One could also think of high-spin Ni^{II} antiferromagnetically coupled to a triplet ligand dianion. However, for square-planar high-spin Ni^{II} there would be one electron in the d_{x2-y2}, orbital which has the wrong symmetry to couple with a ligand π* orbital. Therefore, we believe we can safely rule out this variation.

57. Trovitch, R. J.; Lobkovsky, E.; Bouwkamp, M. W.; Chirik, P. J. *Organometallics* **2008**, *27*, 6264.

58. Zhu, D.; Budzelaar, P. H. M. *Organometallics* **2010**, *29*, 5759.

59. Like in the previously studied reaction of LCo(N2) with organic halides,[58] we cannot Exclude the fact that the actual mechanism of oxidative addition is substrate-dependent. In The absence of experimental evidence pointing either way, we here assume for simplicity a Single common mechanism.

60. Anderson, T. J.; Jones, G. D.; Vicic, D. A. *J. Am. Chem. Soc.* **2004**, *126*, 8100.

61. Jones, G. D.; Martin, J. L.; McFarland, C.; Allen, O. R.; Hall, R. E.; Haley, A. D.; Brandon, R. J.; Konovalova, T.; Desrochers, P. J.; Pulay, P.; Vicic, D. A. *J. Am. Chem. Soc*. **2006,** *128*, 13175.

62. For examples of radical-mediated C-C coupling at nickel, see: (a) Csok, Z.; Vechorkin, O.; Harkins, S. B.; Scopelliti, R.; Hu, X. *J. Am. Chem. Soc.* **2008,** *130*, 8156. (b) Vechorkin, O.; Proust, V.; Hu, X. *J. Am. Chem. Soc.* **2009,** *131*, 9756. (c) Terao, J.; Watanabe, H.; Ikumi, A.; Kuniyasu, H.; Kambe, N. *J. Am. Chem. Soc*. **2002,** *124*, 4222. (d) Powell, D. A.; Fu, G. C. *J. Am. Chem. Soc.* **2004**, *126*, 7788.

63. Chirik, P. J.; Wieghardt, K. *Science* **2010**, *327*, 794.

64. The half arrows in these schemes are not intended to indicate outer-sphere electron transfer but rather the flow of electrons accompanying atom abstraction reactions.

65. A C-N bond length of 1.415(4) Å has been reported for an iminepyridine ligand side-on coordinated to a formally rhodium(I) complex: Tejel, C.; Ciriano, M. A.; Del Río, M. P.; Van den Bruele, F.; Hetterscheid, D. G. H.; Tsichlis i Spithas, N.; De Bruin, B. *J. Am. Chem. Soc*. **2008,** *130*, 5844.

66. Scott, J.; Gambarotta, S.; Korobkov, I. *Can. J. Chem*. **2005,** *83*, 279.

67. Campora, J.; Cartes, M. A.; Rodríguez-Delgado, A.; Naz, A. M.; Palma, P.; Perez, C. M. *Inorg. Chem*. **2009,** *48*, 3679.

68. Britovsek, G. J. P.; Gibson, V. C.; Kimberley, B. S.; Maddox, P. J.; McTavish, S. J.; Solan, G. A.; White, A. J. P.; Williams, D. J. *Chem. Commun.* **1998**, 849.

69. Activation of the LCoCl2 catalyst precursor involves "noninnocent" cobalt(I) complexes,[40,41] but the actual active species in polymerization is likely to contain cobalt(II) or cobalt(III) and an innocent DIMPY ligand.

70. Ligand oxidation may also be connected to electron transfer. See, e.g., ref [48] and the following: (a) Tejel, C.; Ciriano, M. A.; Del Río, M. P.; Hetterscheid, D. G. H.; Tsichlis i Spithas, N.; Smits, J. M. M.; De Bruin, B. *Chem. Eur. J*. **2008**, *14*, 10932. (b) Tejel, C.; Del Río, M. P.; Ciriano, M. A.; Reijerse, E. J.; Hartl, F.; Z_ali_s, S.; Hetterscheid, D. G. H.; Tsichlis i Spithas, N.; De Bruin, B. *Chem. Eur. J.* **2009**, *15*, 11878.

71. Ahlrichs, R.; Bär, M.; Baron, H.-P.; Bauernschmitt, R.; Böcker, S.; Ehrig, M.; Eichkorn, K.; Elliott, S.; Furche, F.; Haase, F.; Häser, M.; Hättig, C.; Horn, H.; Huber, C.; Huniar, U.;

Kattannek, M.; Köhn, A.; Kölmel, C.; Kollwitz, M.; May, K.; Ochsenfeld, C.; Ohm, H.; Schäfer, A.; Schneider, U.; Treutler, O.; Tsereteli, K.; Unterreiner, B.; Von Arnim, M.; Weigend, F.; Weis, P.; Weiss, H. *Turbomole* Version 5; *Theoretical Chemistry Group, University of Karlsruhe*, **2002**.

72. Treutler, O.; Ahlrichs, R. *J. Chem. Phys.* **1995**, *102*, 346.

73. Schäfer, A.; Horn, H.; Ahlrichs, R. *J. Chem. Phys.* **1992**, *97*, 2571.

74. All Turbomole calculations were performed with the functional "b3-lyp" of that package, which is similar to (but not identical with) the Gaussian "B3LYP" functional.

75. Lee, C.; Yang, W.; Parr, R. G. *Phys. Rev. B* **1988**, *37*, 785.

76. Becke, A. D. *J. Chem. Phys*. **1993**, *98*, 1372.

77. Becke, A. D. *J. Chem. Phys*. **1993**, *98*, 5648.

78. *PQS*, version 2.4; Parallel Quantum Solutions: Fayetteville, AR, **2001** (the Baker optimizeris available separately from Parallel Quantum Solutions upon request).

79. Baker, J. *J. Comput. Chem*. **1986,** *7*, 385.

80. a) Boro, B. J.; Deusler, E. N.; Goldberg, K. I.; Kemp, R. A. *Inorg. Chem. Commun*. **2008**, *11*, 1426. b) Ozerov, O. V.; Guo, C.; Fan, L.; Foxman, B. M. *Organometallics* **2004**, *23*, 5573. c) Liang, L. C.; Chien, P. S.; Huang, Y. L. *J. Am. Chem. Soc*. **2006,** *128*, 15562. d) Adhikari, D.; Mossin, S.; Basuli, F.; Dible, M. C.; Fan, H.; Huffman, J. C.; Meyer, K.; Mindiola, D. J. *Inorg. Chem.* **2008**, *47*, 10479. e) Liang, L. C.; Chien, P. S.; Lee, P.-Y. *Organometallics* **2008**, *27*, 3082. f) Moulton, C. J.; Shaw, B. L. *J. Chem. Soc*., *Dalton Trans*. **1976**, *11*, 1020. f) Hue, X.; Scopelliti, R.; Breitenfeld, J. *Organometallics* **2012**, *31*, 2128. g) Tolman, C. A. *J. Am. Chem. SOC.* **1970,** *92,* 6777. h) Crabtree, R. H. *Inorg. Chim. Acta* **1986,** *125,* L7 and references therein.

81. a) Muller, U.; Keim, W.; Kruger, C.; Betz, P. *Angew. Chem., Int. Ed. Engl.* **1989**, *28*, 1011.

b) Polymerization of ethylene: 1) Hicks, F.A.; Jenkins, J. C.; Brookhart, M. *Organometallics* **2003**, *22*, 3533. 2) Jenkins, J. C.; Brookhart, M. *J. Am. Chem. Soc*. **2004**, *126*, 5827.

Publication:

1) **Thapa, I**.; Gambarotta, S.; Korobkov, I. *Inorg. Chem*. (Submission in process)

Isolation of a Dimetallic Ni(I) Pyrrolide Complex

8.1 Introduction

One of the most remarkable characteristics of low valent nickel consists of its ability to promote formation of a variety of chemical bonds.[1] The versatility of nickel in engaging in both reductive elimination and oxidative addition is at the very basis of its remarkable catalytic behavior.[2] This wealth of chemical reactivity is mainly governed by the Ni(0)/(II) redox couple since the other oxidation states (namely +III and +I) remain rare due to their exceedingly high reactivity.[3] In particular, Ni(I) is a versatile one-electron reductant, its reactivity being well rationalized in terms of radical type of behavior.[4] Monovalent nickel, even in situ generated, is capable of promoting a large variety of highly desirable organic reactions, it may also form rare superoxide species which in turn have successfully been used for controlled oxidation of organic compounds.[5] Last but not least, monovalent nickel seems to be the active species in the hydrogenase enzyme.[6]

The stabilization of Ni(I) is normally achieved by using combinations of phosphines, cyclopentadienyl and CO ligands.[7] Monovalent derivatives of other anionic ligands are exceedingly rare and confined to a handful of complexes.[8] Our previous studies in low-valent lanthanides have emphasized the ability of pyrrolide anion-based ligand systems to stabilize low-

valent states and to promote very high reactivity including cooperative reduction of dinitrogen.[9] Aiming at the preparation of novel Ni(I) complexes, hopefully capable of displaying self activating behavior towards ethylene oligomerization/polymerization, we have used a dipyrrolide dianion with an additional alkylated pyrrole spacer. This what in the ultimate view of relating the metal oxidation states to the type of catalytic performances. We were particularly interested in using a tridentate σ-, π-donor with a dianionic charge capable of providing hemilabile coordination on demand. This simple strategy proven versatile in transition metal, lanthanide and actinide chemistry, having allowed the preparation of highly reactive low-valent synthons and supported dinitrogen cleavage.[9] Given the unquestionable ability of mono-alkylated tripyrrole to stabilize highly reactive oxidation states, we have now attempted the preparation of monovalent heterobimetallic nickel species.

This chapter will describe its preparation, isolation, characterization and catalytic behavior of divalent and monovalent complexes.

8.2 Experimental Section

All reactions were carried out under a dry nitrogen atmosphere unless otherwise stated. Solvents were dried using an aluminum oxide solvent purification system. $NiBr_2$(DME) was prepared according to published procedure.[10] Ligand {2,2'-[$CPh_2(C_4H_3N(H)]_2[C_4H_2N(Me)]$} was prepared according to published procedure (see 8.2.1 and 8.2.2). Reagent grade pyrrole was purchased from Aldrich and used after distillation under reduced pressure. Infrared spectra were recorded on an ABB Bomen FTIR instrument from Nujol mulls prepared in a drybox except in the case of air stable compounds. Samples for magnetic susceptibility were weighed inside a dry box equipped with an analytical balance and sealed into calibrated tubes and measurements were

carried out with a Johnson Matthey Magnetic Susceptibility balance at room temperature. NMR data were collected on a Bruker Avance 300 spectrometer. Data for X-ray crystal structure determination were obtained with a Brucker diffractometer equipped with a 1K Smart CCD area detector.

8.2.1 Preparation of 2,5-[$(C_6H_5)_2C(OH)_2$(N-Me-pyrrole)]

A solution of N-Methylpyrrole (10 mL, 110 mmol) in hexane (150 mL) was treated with neat TMEDA (51 mL, 330 mmol) and then cooled to 0 ^oC in an ice bath. A solution of *n*-Buli in hexane (330 mmol) was added drop wise while stirring. The reaction mixture was allowed to warm up to room temperature and refluxed for four hours. The resulting off-white suspension was filtered and the solid portion was washed with hexane (3 x 50 mL) yielding a white product. The solid was dried under vacuum, redissolved in THF (100 mL) and the resulting solution cooled to -20 ^oC. To this solution, a cold (0 ^oC) solution of benzophenone (41.2 g, 220 mmol) in THF (100 mL) was added. The resulting deep blue solution was stirred for 12 hours, after which time the solvent was removed under vacuum. Hexane (200 mL) was then added along with 4 equivalents of water (8 mL, 452 mmol) resulting an off-white suspension. The suspension was then filtered and the solid was washed with hexanes (4 x 40 mL). The product was extracted with CH_2CL_2 (5 x 40mL) and dried under vacuum affording the final product an off-white solid. Yield : (30 g, 67 mmol, 61%). EI-MS Calcd. for $C_{31}H_{27}O_2N$: *m/z* = 445(M^+), Found 445. ^{1}H-NMR (300 MHz, $CDCl_3$, 25 ^oC) δ: 2.86 (2H, br, O*H*), 3.13 (3H, s, N-C*H*$_3$), 5.29 (2H, s, central pyrrole) 7.27 (20H, m, phenyl). $^{13}C\{H\}$-NMR (300 MHz, $CDCl_3$, 25 ^oC) δ: 35.0 (N-*C*H_3), 78.7 (*C*-OH), 110.0 (pyrrole), 126.9 (phenyl), 127.1 (phenyl), 127.7 (phenyl), 145.5 (ipso-phenyl). IR (KBr pellet, cm^{-1}) ν: 3484s, br (OH), 3084, 3058, 3025, 2946 s, 1597m, 1490, 1447

s, 1411w, 1329, 1293s, 1234w, 1204m, 1153s, 1061w, 1018, 1001s, 924, 899m, 867m, 792w, 755, 721, 701s, 670s, 628, 612 m, 559w.

8.2.2 Preparation of {2,2'-[$CPh_2(C_4H_3N(H))]_2[C_4H_2N(Me)]$}

Neat 2,5-[$(C_6H_5)_2C(OH)_2$(N-Me-pyrrole) (15 g, 30 mmol) was dissolved in excess of pyrrole (60 mL) by slow heating and treated with 5 drops of Methanesulfonic acid. The resulted dark-red suspension was stirred at room temperature for 72 hours. The solid was then filtered and washed with cold methanol (3 x 30 mL) affording the title compound as a white solid in quantitative yield (15 g, 27 mmol, 92%). The product was dried under vacuum and characterized as follows:

EI-MS Calcd. for $C_{39}H_{33}N_3$: *m/z* = 543 (M^+), Found 543.

^{1}H-NMR (300 MHz, $CDCl_3$, 25 ^{o}C) δ: 2.14 (3H, s, N–C*H3*), 5.46 (2H, s, central pyrrole), 5.98 (2H, m, pyrrole), 6.05 (2H, m, pyrrole), 6.68 (2H, m, pyrrole), 7.07 (8H, m, pheny), 7.13 (4H, m, phenyl), 7.18 (8H, m, phenyl), 7.69 (2H, br s, N-*H*). ^{13}C{H}-NMR (300 MHz, $CDCl_3$, 25 ^{o}C) δ: 34.8 (N–*C*H3), 56.1 (quarternary), 108.1 (pyrrole), 109.3 (pyrrole), 110.3 (pyrrole), 117.2 (phenyl), 126.7 (phenyl), 127.9 (phenyl), 129.6 (*ipso*-pyrrole), 139.06 (*ipso*-central pyrrole), 145.5 (*ipso*-phenyl).

IR (Nujol, cm^{-1}): 3426m, 3085, 3065, 3026, 2954m, 1955, 1899, 1816w; 1595, 1550m, 1490, 1443 s, 1410, 1394m, 1233, 1299, 1267, 1231, 1183m, 1115, 1093, 1042, 1031m, 1002w, 962, 930w, 903, 885, 847m, 799, 761, 747, 722, 704s, 622w, 568, 548s.

8.2.3 {2,2'-[$CPh_2(C_4H_3N(H))]_2[C_4H_2N(Me)]$)Ni(THF)} (8.1)

A suspension of KH (0.084 g, 2.1 mmol) in THF (5 mL) was added to a solution of {2,2'-[$CPh_2(C_4H_3N(H))]_2[C_4H_2N(Me)]$} (0.635 g, 1 mmol) in THF (20 mL). The mixture was stirred overnight at room temperature to ensure complete deprotonation of the ligand. $NiBr_2$(DME) (0.308 g, 1 mmol) was added to the solution resulting a dark-green solution. After stirring overnight the solution was dried under vacuum, washed with toluene then redissolved in THF and centrifuged to remove a small amount of insoluble material and KBr. The solution was concentrated to 5 mL and allowed to stand at room temperature. After 2 days a dark-green X-ray quality crystals of **8.1** were formed (0.50 g, 0.74 mmol, 74%).

Elemental Analysis Calcd. (Found) for C_{46} H_{43} N_3 Ni O: C 77.54 (77.45), H 6.08 (5.92), N 5.90 (5.82). IR (Nujol mull, cm^{-1}): 1595, 1488, 1459, 1424, 1376, 1233, 1187, 1160, 1084, 1053, 1023, 865, 785, 763, 746, 720, 702, 665, 626. [$\mu_{eff} = 2.89\ \mu_B$].

8.2.4 {2,2'-[$CPh_2(C_4H_3N(H))]_2$ $[C_4H_2N(Me)]$)AlEt}(8.2)

Dark-green crystalline **8.1** (0.333 g, 0.50 mmol) was suspended in toluene (10 mL). To the stirred suspension triethylaluminum (0.171 g, 3 mmol) was added dropwise at -35 ^oC. Immediate colour changed into dark-brown solution along with the evolution of gas was observed. The resulting dark-brown solution was centrifuged and allowed to stand for 4 days at -35 ^oC to form pale yellow X-ray quality crystals of **8.2** (0.130g, 0.2 mmol, 40%).

^1H–NMR (300 MHz, C_6D_6, 25 ^oC) δ: 0.11 (2H, q, J_1 = 8.1 Hz, J_2 = 8.4 Hz, J_3 = 8.1 Hz, Al-CH_2), 1.22 (3H, *t*, J_1 = 8.4 Hz, J_2 = 8.1 Hz, $AlCH_2$-CH_3), 2.41 (3H, s), 5.95 (2H, m) 6.58 (2H, m), 6.76 (2H, m), 7.14 (20H, m), 7.52 (2H, m). $^{13}C\{1H\}$-NMR (300 MHz, C_6D_6, 25^oC) δ: 8.7,40.7, 57.7, 112.3, 112.5, 118.9, 122.5, 127.0, 127.1, 129.6,129.8, 138.5, 143.0, 146. 4, 148.8.

8.2.5 Preparation of {2,2'-[$CPh_2(C_4H_3N(H))]_2[C_4H_2N(Me)]$ Al(*i*-Bu)} (8.3)

A dark-green crystalline powder **8.1** (0.17 g, 0.25 mmol) was suspended in toluene (10 mL). To the stirred solution tetraisobutyldialuminoxane (3.7 g, 1.25 mmol, 10% w/w in toluene) was added dropwise at -35 ^{o}C. The solution was allowed to warm up to room temperature and stirred for overnight. The resulting greenish-brown solution was centrifuged. After 4 days at -35 ^{o}C, the solution afforded pale yellow X-ray quality crystals of **8. 3** (0.08 g, 0.11 mmol, 44%).

^{1}H-NMR (300 MHz, C_6D_6, 25 ^{o}C) δ: 0.04 (2H, d, J = 6.9 Hz, Al-CH_2), 1.19 (6H, d, J = 6.6 Hz, -CHMe_2), 1.95 (1H, m, -C*H*-), 2.36 (3H, s), 6.00 (2H, m) 6.49 (2H, m), 6.50 (2H, m), 7.14 (20H, m), 7.51 (4H, m). ^{13}C{H}-NMR (300 MHz, C_6D_6, 25 ^{o}C) δ: 9.3, 35.0, 45.7, 56.4, 108.3, 109.5, 110.5, 117.4, 118.3, 122.4, 126.9, 128.1, 129.8, 135.0, 139.2, 145.7, 149.2.

8.2.6 Preparation of {2,2'-[$CPh_2(C_4H_3N(H))]_2[C_4H_2N(Me)]$)Ni($PMe_3)_2$} 1.25 (THF) (8.4)

A solution of trimethylphosphine (0.025 mL, 0.25 mmol) in toluene was added dropwise to a suspension in toluene(10 mL) at -35 ^{o}C of dark-green **8.1** (0.167 g, 0.25 mmol). The solution was allowed to warm up to room temperature while stirring continued overnight. The resulting cherry red solution afforded X-ray quality crystals of **8.4** after standing 7 days at -35 ^{o}C (0.13 g, 0.15 mmol, 60%).

^{1}H–NMR (300 MHz, C_6D_6, 25 ^{o}C) δ : 7.88 (3H, br), 7.20-7.04 (20H, m), 6.77 (3H, br), 6.27-6.23 (1H, br d, J = 12 Hz), 5.22 (1H, br), 3.23 (3H, br), 1.40 (9H, br), 0.67-0.63(3H, br), 0.22 (6H, br). ^{13}C {1H}–NMR (300 MHz, C_6D_6, 25^{o}C) δ: 154.4, 146.4, 138.8, 134.0,

134.0, 130.6, 126.7, 126.3, 125.7, 117.3, 110.7, 108.1, 107.8, 33.6, 25.4, 11.3. $^{31}P\{H\}$-NMR (300 MHz, C_6D_6, 25 ^oC) δ: 32.93.

8.2.7 Preparation of {[μ,η^5,η^5,η^5-({2,2'-[$CPh_2(C_4H_3N(H))]_2$ [$C_4H_2N(Me)$])K]Ni}$_2$ (8.5)

A dark-green crystalline powder of **8.1** (0.712 g, 1 mmol) was dissolved in toluene (10 mL). To the stirred solution KC_8 (0.135 g, 1 mmol) was added at room temperature. The mixture was allowed to stir at room temperature for 4 hours, after which time the green solution turned yellow. A yellow solid was separated from the residual graphite via solubilized in THF, followed by centrifugation. The supernatant was left undisturbed at -30 ^oC for overnight. Yellow paramagnetic crystals of X-ray quality of **8.5** were isolated, washed with cold hexane, dried in *vacuo* (0.613 g, 0.39 mmol, 39%). Elemental Analysis Calcd. (Found) for C_{94} H_{92} K_2 N_6 Ni_2 O_4: C 72.12 (71.97), H 5.92 (5.80), N 5.37(5.39). [μ_{eff} = 2.61 μ_B] per dimer.

8.3 X-ray Data

Table 8.1. Crystal data and structural analysis Results of Complex **8.1**, **8.2**, **8.4** & **8.5**

	8.1	**8.2**	**8.4**	**8.5**
Formula	C_{46} H_{43} N_3 Ni O	C_{89} H_{80} Al_2 N_6	C_{50} H_{59} N_3 Ni $O_{1.25}P_2$	C_{50} H_{53} K N_3 Ni $O_{2.75}$
FW	712.58	1287.55	842.65	1565.36
Space group	Triclinic, P-1	Monoclinic, P2(1)/c	Monoclinic, P2(1)/c	Triclinic, P-1
a (Å)	11.665(3)	30.334(5)	12.5903(2)	12.341(3)
b (Å)	13.363(3)	8.9440(13)	13.6283(2)	13.245(4)
c (Å)	13.633(4)	28.352(4)	29.0143(5)	13.269(4)
α(deg)	93.072(3)	90	90	108.713(4)
β(deg)	92.391(3)	117.028(2)	92.0700(10)	94.503(4)
γ(deg)	113.356(3)	90	90	107.665(4).
V (Å^3)	1943.55	6852.0(17)	4975.15(14)	1919.8(9)
Z	2	4	4	1
radiation (Kα, Å)	0.71073	0.71073	0.71073	0.71073
T (K)	200(2) K	344(2)	200(2)	202(2)
D_{calcd} (g cm^{-3})	1.228	1.248	1.125	1.354
μ_{calcd} (mm^{-1})	0.537	0.096	0.491	0.658
F_{000}	758	2728	1792	*824*
R, R_w [2 a]	0.0506, 0.1263	0.0780, 0.1727	0.0616, 0.1656	0.0931, 0.2163
GoF	1.043	1.003	1.040	

[a] $R = \Sigma||Fo| - |Fc||/\Sigma|F|$. $Rw = [\Sigma(|Fo| - |Fc|)^2/\Sigma wFo^2]^{1/2}$

8.4 Results and Discussions

The tripyrrole ligand {2,2'-[$CPh_2(C_4H_3N(H))]_2[C_4H_2N(Me)]$} was prepared according to published procedures and its deprotonation was conveniently carried out with KH. The reaction of the corresponding potassium salt with $NiBr_2$(DME) in THF formed dark-green crystals of {2,2'-[$CPh_2(C_4H_3N(H))]_2[C_4H_2N(Me)]$)Ni(THF)} **(8.1)** in good yield (Scheme 8.1).

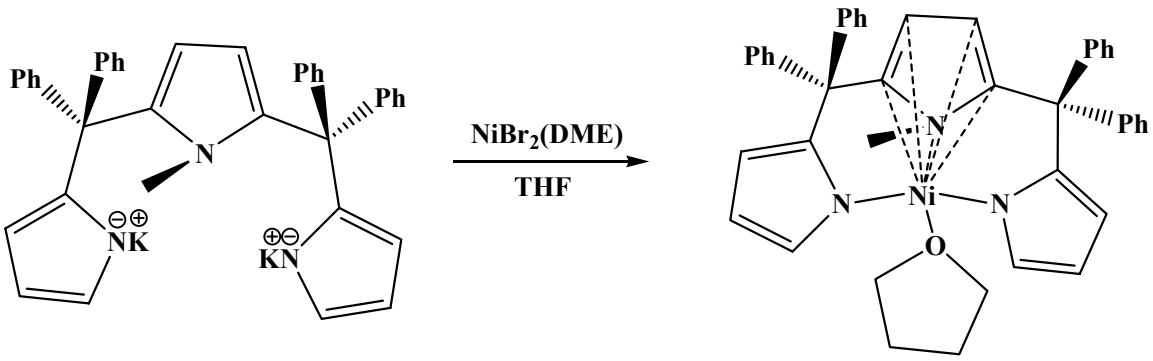

8.1

Scheme 8.1: Synthesis of complex 8.1

The formulation of **8.1** was yielded by X-ray crystal structure (Figure 8.1) consisting of a nickel atom in a distorted tetrahedral environment [N1-Ni1-N3 = 119.97(8)^o, N1-Ni1-O = 102.53(9)^o, N3-Ni1-O = 102.42(8)^o, N1-Ni1-N2 = 89.93(8)^o, N2-Ni1-N3 = 88.93(7)^o, N2-Ni-O = 155.54(9)^o]. The coordination geometry is defined by the centroid of the central N-methylated ring which adopts a regular η^5 -bonding mode [Ni1-N2 = 2.261(2)Å, Ni1-C21 = 2.487(2)Å, Ni1-C18 = 2.507(2)Å]. The two lateral deprotonated rings are instead σ-bonded [Ni1-N1= 1.933(2)Å, and N3-Ni1 = 1.932(2)Å]. One oxygen donor atom of a coordinated THF [Ni1-O1 = 2.024(2)Å], complete the coordination of the metal center.

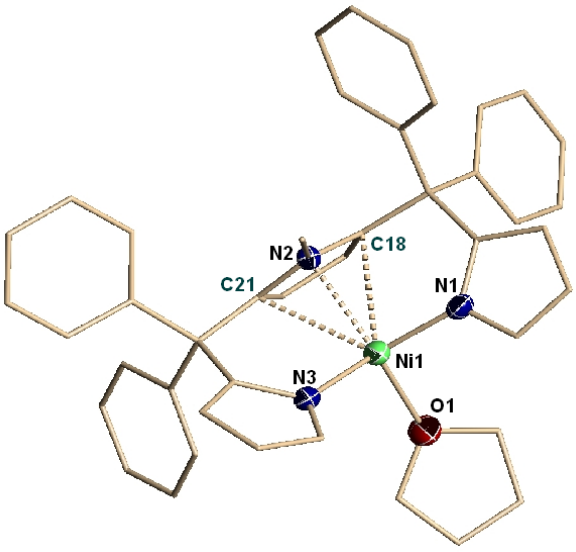

Figure 8.1: Crystal structure of Complex 8.1 with thermal ellipsoids drawn at the 50% probability level.

The complex is paramagnetic with the magnetic moment as expected for the d^8 electronic configuration if Ni(II) in a tetrahedral field [μ_{eff} = 2.89 μ_B]. The NMR spectra only show broad lines. Attempts to extract THF from the coordination sphere of **8.1** and to assemble polymetallic structures were carried out with alkyl aluminum and phosphine reagents (Scheme 8.2). Unexpectedly, reaction with either TIBAO or TEAL led to ligand extraction and formation of the diamagnetic {2,2'-[$CPh_2(C_4H_3N(H))]_2$ [$C_4H_2N(Me)$])AlEt} (**8.2**) and {2,2'-[$CPh_2(C_4H_3N(H))]_2[C_4H_2N(Me)]$Al(*i*-Bu)} (**8.3**). Both complexes were isolated and fully characterized and provided the expected NMR spectra.

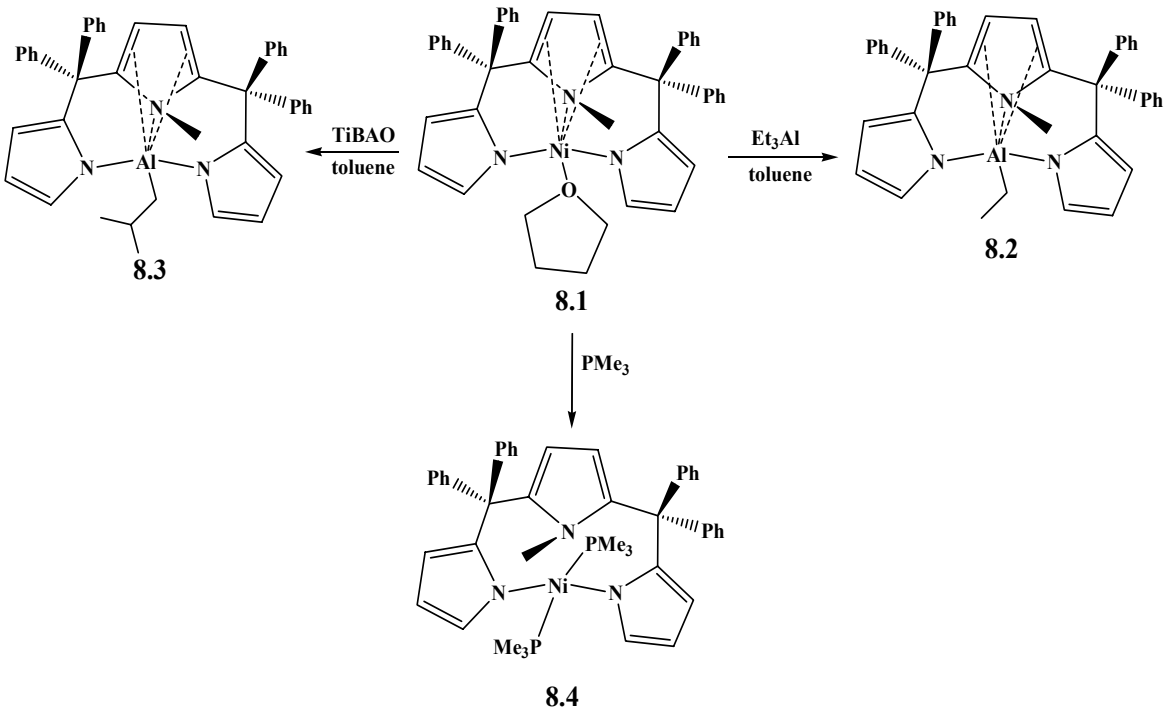

Scheme 8.2: Various attempts to extract THF molecules

The structure of **8.2** (Figure 8.2) did not show any particular figure other than the ligand assuming the same arrangement of **8.1** and imposing a tetrahedral geometry to the Al-R unit. The ^{1}H-NMR spectrum showed the ethyl group resonances at 0.11 ppm (2H, q, J = 8.1Hz; J = 8.4 Hz; J = 8.1Hz) and 0.12 ppm (3H, t, J = 8.4 Hz, J = 8.1 Hz) corresponding to 8.7 and 40.7 ppm of the ^{13}C-NMR spectrum.

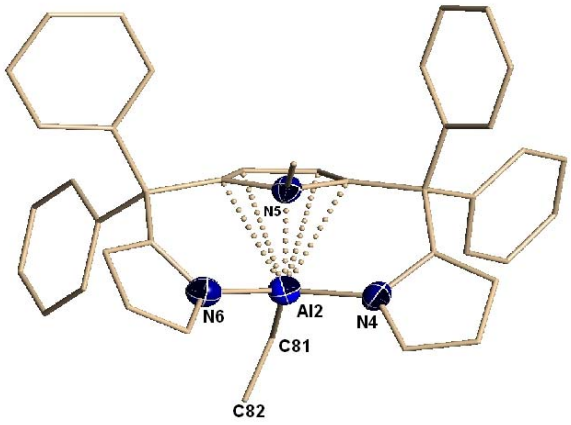

Figure 8.2: Partial thermal ellipsoid plot of 8.2 with thermal ellipsoids drawn at the 50% probability level.

The structure of **8.3** was inferred from NMR spectra showing the *i*-Bu resonances at 0.04 (2H, d, J = 6.9), 1.19 (6H, d, J = 6.6) and 1.95 (1H, m) with the corresponding lines at 9.3, 35.0 and 45.7 ppm of the ^{13}C-NMR spectrum.

Simple treatment of **8.1** with Me_3P afforded THF replacement and coordination of an additional molecule of phosphine with formation of the square pyramidal {2,2'-$[CPh_2(C_4H_3N(H))]_2[C_4H_2N(Me)]$)Ni$(PMe_3)_2$} (**8.4**), Scheme 8.2. The pentacoordination of Ni is however questionable since the fifth coordination site, supposedly occupied by the centroid of the alkylated central pyrrole ring, show a rather long distance outside what is normally considered as a bonding range (Figure 8.3). Therefore, a distorted square planar geometry is perhaps a better description of this molecule [N3-Ni1-N1 = 177.69(9)^o, N3-Ni1-P1 = 90.20(7)^o, N1-Ni1-P1 = 91.64(7)^o, N3-Ni1-P2 = 89.297^o, N1-Ni1-P2 = 90.00(7)^o, P1-Ni1-P2 = 144.95(3)^o] and the bond distances are [Ni1-N3 = 1.907(2)Å, Ni1-N1 = 1.911(2)Å, Ni1-P1 = 2.2259(8)Å, Ni1-P2 = 2.2675(8)Å]. The NMR shows the expected ^{31}P and ^{1}H resonances.

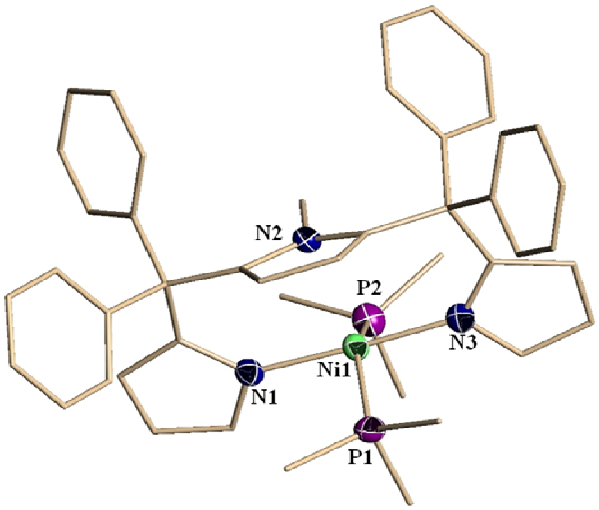

Figure 8.3: Partial thermal ellipsoid plot of 8.4 with thermal ellipsoids drawn at the 50% probability level.

Reduction of **8.1** with one equivalent of potassium graphite in toluene resulted in the formation of the dimeric Ni complex $\{[\mu,\eta^5,\eta^5,\eta^5\text{-}\{2,2'\text{-}[CPh_2(C_4H_3N(H))]_2[C_4H_2N(Me)]\}K]Ni\}_2$ (**8.5**) formed by two monovalent nickel centers and two potassium cations as a part of a hetero- tetrametallic structure (Scheme 8.3).

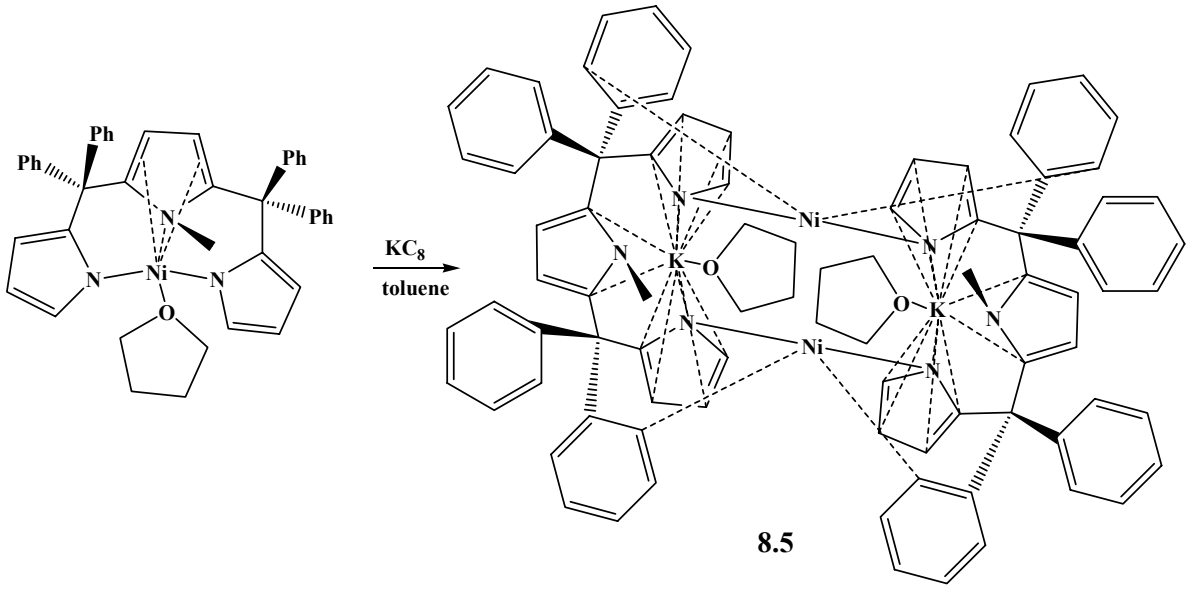

Scheme 8.3: Reduction of Ni(II) to Ni(I) 8.5

The structure consists of two ligands each surrounding a potassium cation π-bonded to all the three pyrrole rings [K1-N1 = 2.913(3)Å, K1-N3 = 2.910(3)Å, K1-N2 = 2.993(3)Å] (Figure 8.4). One molecule of THF completes the coordination sphere of each potassium [K1-O1 = 2.703(3)Å]. Each deprotonated pyrrole ring uses the N donor atom to σ-bond one Ni atom [Ni1-N1 = 1.925(3)Å] which in turn is also equally bonded to the N atom of a second identical unit [Ni1-N3A = 1.927(3)Å] while assembling the dimetallic structure. Interestingly, the two nitrogen donors form with nickel an almost linear array [N1-Ni1-N3A = 170.35(13)^{o}]. The seemingly di-coordinated Ni(I) shows an additional weak π-coordination to one phenyl ring of each of the two ligands.

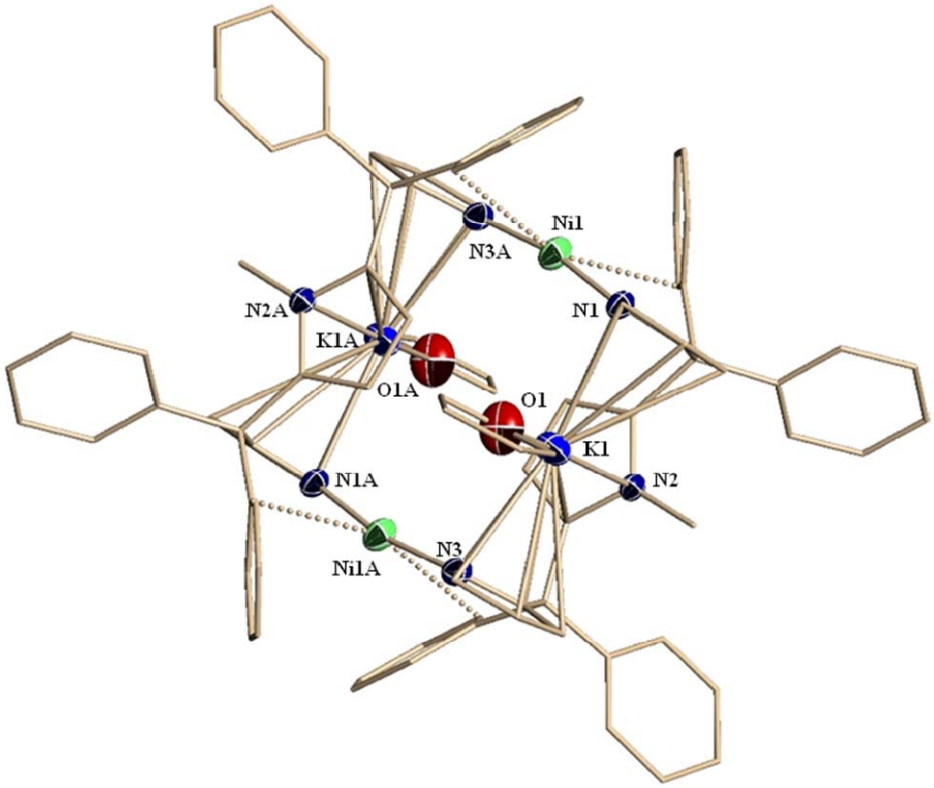

Figure 8.4: Partial thermal ellipsoid plot of 8.5 with thermal ellipsoids drawn at the 50% probability level.

Catalytic Activity:

Preliminary screening of the complex **8.1** at varying temperatures, pressures and co-catalyst loadings (MAO) are summarizes in Table 8.2. The co-catalyst loading has a pronounced effect on activity. With 100 equivalents, the catalytic activity is 10 times less than with 1000 equiv at the same temperature and ethylene pressures (600psi). At 200 psi ethylene pressure, the activity was further reduced. On the other hand, the increase in reaction temperature from 50 to 75 ^{o}C increased the catalytic activity. The higher the temperature, pressure and co-catalyst loadings, increased the activity at the expenses of selectivity.

Table 8.2. Catalytic activity for **8.1**, **8.4** and **8.5**[a]

Cat.	Temp (^{o}C)	Press (Psi)	Alkenes (mL)	Activity g/mmol, cat.h	Mol % 1-C4	2-C_4	C_6	$>C_8$	PE (g)
8.1	75	600	20	1,333	50	45	5	-	-
8.1	50	600	18	1,200	72	22	5	-	-
8.1*	50	600	2	133	75	25	-	-	-
8.1	50	200	1	67	75	25	-	-	-
8.4	50	600	8	533	75	25	-	-	-
8.5	50	600	2	133	50	50	-	-	-
Blank	$NiBr_2$ (DME)		-	-	-	-	-	-	-

[a] *Conditions: 30 µmol catalyst; 30 minutes reaction time, total volume 100 mL in toluene, traces <0.1g;1000 MAO (co-catalyst) * 100 MAO.*

At optimized temperature, pressure and co-catalyst loadings, the activity of complex **8.1** for ethylene oligomerization was moderate with no polyethylene formation (Table 8.2). The moderate activity could be ascribed to the nature of the complex prone to transmetallation with alkyl aluminum activators as emphasized by the isolation of **8.2** and **8.3** and which might be regarded as a possible deactivation pathway. Small amount of 1-hexene (~5%) were formed alongside the dimerization products. Along with α-olefins, internal olefins were also detected from NMR. This is due to fast β-hydrogen elimination and chain immigration step occurring during oligomerization process.[11] Complex **8.4** showed exclusive selectivity for C_4 fraction that

might be due to the effect of PMe_3.[12] Complex **8.5** on the other hand, did not show the anticipated self activating behavior. However, upon activation with MAO it showed oligomerization activity at the lower range.

8.5 Conclusions

In conclusion, we have isolated a rare example of heterobimetallic Ni(I) species. This ligand indeed has ability to stabilize a low valent metal centre. However, due to its encumbered structure a single component catalytic behavior was not observed. Nonetheless, both monovalent and divalent oxidation states of isolated complexes were active for dimerization of ethylene upon activation with co-catalyst.

In the next chapter we are using sterically less encumbered and commercially amenable 2,5-dimethy pyrrole ligand in order to further investigate the nickel catalysts.

References

1. a) Arévalo, A.; García, J. J. *Eur. J. Inorg. Chem.* **2010**, 4063. b) Murai, S. *Topics in Organometallic Chemistry: Activation of Unreactive Bonds and Organic Synthesis*, Springer-Verlag, **1999**, Berlin, Germany, pp. 1. c) Wilting, J.; Müller, C.; Hewat, A. C.; Ellis, D. D.; Tooke, D. M.; Spek, A. L.; Vogt, D. *Organometallics* **2005**, *24*, 13. d) Keen, A. L.; Doster, M.; Johnson, S. A. *J. Am. Chem. Soc.***2007**, *129*, 810. e) Jones, G. D.; Martin, J. L.; McFarland, C.; Allen, O. R.; Hall, R. E.; Haley, A. D.; Brando, R. J.; Konovalova, T.; Descrochers, P.; Pulay, P.; Vicic, D. *J. Am. Chem. Soc*.**2006,** *128*, 13175.
2. a) Zargarian, D. *Coord. Chem. Rev.* **2002**, *233*, 157. b) Ogoshi, S.; Tonomori, K-I.; Oka, M-A.; Kurosawa, H.; *J. Am. Chem. Soc*. **2006**, *128*, 7077. c) Guihaume, J.; Halbert, S.; Eisenstein, O.; Perutz, R.. N. *Organometallics* **2012**, *31*, 1300. d) Hosseini, F. N.; Ariafand, A.; Rashidi, M.; Azimi, G.; Nabavizadeh, S.M. *J. Orgmet. Chem*. **2011**, *696*, 3351.
3. a) Bouffard, J.; Itami, K. *Organic Letters* **2009**, *11*, 4410. b) Diederich, F., Stang, P. J. *Metal-Catalyzed Cross-Coupling Reactions*; Wiley-VCH: Weinheim, Germany; **1998**. c) de Meijere, A.; Diederich, F. *Metal-Catalyzed Cross-Coupling Reactions,* 2nd ed.; Wiley-VCH: Weinheim, Germany; **2004**. d) Beller, M.; Bolm, C. *Transition Metals for Organic Synthesis,* 2nd ed.; Wiley-VCH:Weinheim, **2004**.
4. a) Pfirrmann, S.; Limberg, C.; Herwig, C.; St€oßer, R.; Ziemer, R. *Angew. Chem., Int. Ed.***2009**, *48*, 3357. b) Anderson,T. J.; Jones,G. D.; Vicic, D. A. *J. Am. Chem. Soc*. **2004**, *126*, 8100. c) Bakac, A.; Espenson, J. H.*J. Am. Chem. Soc*. **1986**, *108*, 719. d) Morrell, D. G.; Kochi, J. K. *J. Am. Chem. Soc*. **1975**, *97*, 7262.

5. a) Kieber-Emmons, M. T.; Riordan, C. G. *Acc. Chem. Res*.**2007,** *40*, 618. b) Yao, S.; Bill, E.; Milsmann, C.; Wieghardt, K.; Driess, M. A. *Angew. Chem., Int. Ed*. **2008,** *47*, 7110. c) Hikichi, S.; Yoshizawa, M.; Sasakura, Y.; Akita, M.; Moro-oka, Y. *J. Am. Chem. Soc.* **1998**, *120*, 10567. d) Shiren, K.; Ogo, S.; Fujinami, S.; Hayashi, H.; Suzuki, M.; Uehara, A.; Watanabe, Y.; Moro-oka, Y. *J. Am. Chem. Soc*.**2000**, *122*, 254. e) Cho, J.; Furutachi, H.; Fujinami, S.; Suzuki, M. A. *Angew. Chem., Int. Ed*.**2004**, *43*, 3300. f) Brown, E. J.; Duhme-Klair, E. R.. K.; Elliott, M. I.; Thomas-Oates, J. E.; Timmins, P. L.; Walton, P. H. *Angew. Chem., Int. Ed*.**2005**, *44*, 1392. g) Cho, J.; Sarangi, R.; Annaraj, J.; Kim, S. Y; Kubo, M.; Ogura, T.; Solomon, E. I.; Nam, W. *Nat. Chem.***2009**, *1*, 568. h) Kieber- Emmons, M. T.; Annaraj, J.; Seo, M. S.; Van Heuvelen, K. M.; Tosha, T.; Kitagawa, T.; Brunold, T. C.; Nam, W.; Riordan, C. G. *J. Am. Chem. Soc*.**2006**, *128*, 14230. i) Otsuka, S.; Nakamura, A.; Tatsuno, Y. *J. Am. Chem. Soc*. **1969**, *91*, 6994. j) Matsumoto,M.; Nakatsu, K. *Acta Crystallogr*.**1975**, *B31*, 2711.

6. a) Schilter, D.; Nilges, M. J.; Chakrabarti, M.; Lindahl, P. A.; Rauchfuss, T.B.; Stein, M. *Inorg. Chem*. **2012**, *51*, 2338. b) Tard, C.; Pickett, C. J. *Chem. Rev*.**2009**, *109*, 2245.

7. a) Eckert, N. A.; Dinescu, A.; Cundari,T. R.; Holland, P. L. *Inorg. Chem.* **2005**, *44*, 7702. b) Bradley, D. C.; Hursthouse, M. B.; Smallwood, R. J.; Welch, A. J. *J. Chem. Soc., Chem. Commun*. **1972**, 872. c) Nilges, M. J.; Barefield, E. K.; Belford, R. L.; Davis, P. H. *J. Am. Chem. Soc*. **1977**, *99*, 755. d) Ellis, D. D.; Spek, A. L. *Acta Crystallogr*. **2000**, C56, 1067. e) Eaborn, C.; Hill, .S.; Hitchcock, P.B.; Smith, J. D. *Chem. Commun*. **2000**, 691. f) Mindiola, D. J.; Hillhouse, G. L. *J. Am. Chem. Soc*. **2001**, *123*, 4623. g) Melenkivitz, R.; Mindiola, D. J.; Hillhouse, G. L. *J. Am. Chem. Soc*. **2002**, *124*, 3846. h) Kitiachvili, K. D.; Mindiola, D. J.; Hillhouse, G. L. J. Am. Chem. Soc. **2004**, *126*, 0554.

i) Kogut, E.; Wiencko, H. L.; Zhang, L.; Cordeau, D. E.; Warren, T. H. *J. Am. Chem. Soc.* **2005**, *127*, 11248. Structural review: j) Drennan, C. L.; Doukov, T. I.; Ragsdale, S. W.J. *Biol. Inorg. Chem.* **2004**, *9*, 511. Mechanisticreview: k) Hegg, E. L. *Acc. Chem. Res*. **2004**, *37*, 775. Calculations: l) Schenker, R. P.; Brunold, T. C. *J. Am.Chem. Soc*. **2003**, *125*, 13962. m) Webster, C. E.; Darensbourg, M. Y.; Lindahl, P. A.;Hall, M. B. *J. Am. Chem. Soc*. **2004**, *126*, 3410. n) Amara, P.; Volbeda, A.; Fontecilla-Camps, J. C.; Field, M. J. *J. Am. Chem. Soc.* **2005**, *127*, 2776. o) George, S. J.; Seravalli, J.; Ragsdale, S.W.*J. Am. Chem. Soc.* **2005**, *127*,13500. p) Jones, R. A.; Atwood, J. L.; Stuart, A. L.; Hunter, W. E.; Rogers, R. D. *Organometallics* **1982**, *1*, 1721. q) Hanko, R. *Angew. Chem.* **1985**, *97*, 707; *Angew. Chem. Int. Ed. Engl*. **1985,** *24*, 704. r) Tenorio, M. J.; Puerta, M. C.; Valerga, P. *J. Chem. Soc. Dalton Trans*. **1996**, 1305. s) Fryzuk, M. D.; Clentsmith, G. K. B.; Leznoff, D. B.; Rettig, S. J.; Geiib, S. J.; *Inorg. Chim. Acta* **1997**, *265*, 169. t) Kriley, C. E.; Woolley, C. J.; Krepps, M. K.; Popa, E. M.; Fanwick,P. E.; Rothwell,I. P. *Inorg. Chim. Acta* **2000**, *300–302*, 200.

8. a) Shenglai, y.; Matthias, D. *Acc. Chem. Res.* **2012**, *45*, 276. b) Chen, Y.; Sui-Seng, C.; Zargarian, D. *Angew. Chem. Int. Ed*. **2005**, *44*, 7721.

9. a) Lalonde, M. P.G.; Gambarotta, S.; Yap, G.P.A. *Organometallics* **2001**, *20*, 2443. b) Zanotti-Gerosa, A.; Solari, E.; Giannini, E.; Floriani, C.; Chiesi-Villa, A.; Rizzoli, C. *J. Am. Chem. Soc.* **1998**, *120*, 437. c) Tayebani, M.; Gambarotta, S.; Yap, G. P. A. *Angew. Chem. Int. Ed. Engl.* **1998**, *37*, 3002; *Angew. Chem.* **1998**, *110*, 3222. d) Tayebani, M.; Gambarotta, S.; Yap, G. P. A. *Organometallics,* **1998**, *17*, 3639. e) Tayebani, M.; Feghali, K.; Gambarotta, S.; Bensimon, C. *Organometallics* **1997**, *16*, 5084.

10. *Inorg. Syhth.* **1972**, *13*, 154.

11. Jolly, P. W. *Comprehensive Organometallic Chemistry* (Eds.: G. Wilkinsion, F.G.A. Stone, E. W. Abel), Pergamon Press, Oxford, U. K., **1982**, *8*, 384.

12. Heinicke, J.; Peulecke, N.; Köhler, M.; He, M.; Keim, W. *J. Orgmet. Chem*. **2005**, *690*, 2449.

Publication:

1) **Thapa, I**.; Gambarotta, S.; Korobkov, I. *Inorg Chem.* (Submission in process)

Participation of the DMP anion (DMP = dimethylpyrrolide) in the Redox Chemistry of Nickel via C-C Bond Formation and Cleavage.

9.1 Introduction

Carbon-carbon bond forming reactions between sp^3 or sp^2 atoms, as promoted by nickel catalysts, are one of the active fields of research actively pursued today for a variety of valued organic transformations.[1] One of the important characteristics of nickel catalysts is their versatility for the formation and cleavage of carbon-carbon bonds.[2] The pioneering work of Eisch[1a-c] and Hoberg [1d-g] in this field has open the road to researchers for the use of nickel complexes in metal-promoted organic synthesis as an inexpensive alternative to the 2nd and 3rd row analogues. The most common oxidation states of the nickel precursors used in catalytic transformation involves Ni(0)/Ni(II)[3a-c] redox couples. However, mechanistic studies also suggest that Ni(I) could be involved in the carbon-carbon bond forming catalytically active intermediate,[3d] due to its versatility as one-electron radical-type reductant.[4] Because of its exceedingly high reactivity only a few related dinuclear Ni(I) complexes[1b,5] are known. In addition, C-C bonds are normally either formed or cleaved.[6] In only a few instances such a process can be reversed.[7] The "reversible" C-C bond formation and usage of C-C bonds as electron storage has been observed in the chemistry of metal complexes of Schiff bases.[8]

Pyrrolide anions are well known ligands to support a variety of catalysts. What makes these ligand interesting is the close similarity with the cyclopentadienyl anions, an increase ring tendency towards slippage being the main behavioral difference. In turn, this decreases the stability of the complexes and, by increasing the molecular dynamism, makes possible catalytic transformations. The chemistry of chromium and vanadium pyrrolides is a good example of this. While both chromocene and vanadocene are unreactive towards ethylene, the pyrrolide analogues are the best trimerization catalysts, providing highly active and selective commercial systems.[9]

Our recent mechanistic work on the Mitsubishi and Phillips catalysts (pyrrole-based)[10] has also highlighted the ability of these anions to give accessibility to unusual oxidation states, such as Cr(I), most likely responsible for the selectivity of the catalytic cycle. In spite of the remarkable dynamism of these species and the variety of transformation and complexes isolated and characterized, in no instance the pyrrolide anion gave any sign of non-innocent behavior. We have therefore analyzed in this work the behavior of the Ni analogues given the well-established catalytic behavior of this element for selective dimerization or non-selective oligomerization.

During this work we have serendipitously discovered the dimerization of 2,5-dimethyl pyrrolide anion in the presence of nickel salt via C-C bond formation between the two pyrrolide α-positions. The oxidative coupling of the two anionic rings occurred in spite of the consequent considerable increment of steric crowd and with the formation of zerovalent nickel being the most likely driving force of the reaction.

Herein we describe our results.

9.2 Experimental:

All reactions were carried out under a dry nitrogen atmosphere unless otherwise stated. Solvents were dried using an aluminum oxide solvent purification system. $NiBr_2$(DME) was prepared according to published procedure. Reagent grade pyrrole was purchased from Aldrich and used after distillation under reduced pressure. Infrared spectra were recorded on an ABB Bomen FTIR instrument from Nujol mulls prepared in a dry box except in the case of air stable compounds. Samples for magnetic susceptibility were weighed inside a dry box equipped with an analytical balance and sealed into calibrated tubes and measurements were carried out with a Johnson Matthey Magnetic Susceptibility balance at room temperature. NMR data were collected on a Bruker Avance 300 spectrometer. Data for X-ray crystal structure determination were obtained with a Brucker diffractometer equipped with a 1K Smart CCD area detector.

9.2.1 Preparation of [α-(α,α'-$Me_2C_4H_2N$)(α,α'-$Me_2C_4H_2N$)]$NiBr_2$ (9.1)

A solution of dimethyl pyrrole (0.095 g, 1 mmol) was dissolved in THF (10 mL) and a suspension of KH (0.044 g, 1.1 mmol) was added to the stirred solution. After stirring overnight at room temperature, the addition of a suspension of $NiBr_2$(DME) (0.308 g, 1 mmol) in THF (5 mL) turned the color brown. After further overnight stirring, the brown solution was dried under reduced pressure, the residue washed with hexane, redissolved in THF and centrifuged to remove insoluble materials. The solution was concentrated to 5 mL and kept undisturbed at -35 ^oC for 2 days to afford brown block crystals of **9.1** (0.16 g, 0.39 mmol, 39%). Elemental Analysis Calcd. (Found) for $C_{12}H_{16}Br_2N_2Ni$: C 35.43(35.31), H 3.96(3.85), N 6.89 (6.81).

IR (Nujol mull, cm^{-1}): 1615w, 1522s, 1460w, 1378, 1352, 1285, 1192, 1151, 1076, 1023, 966, 939, 917, 882, 812, 766, 727, 662. [$\mu_{eff} = 2.90\ \mu_B$].

9.2.2 Preparation of [α-(α,α'-$Me_2C_4H_2N$)(α,α'-$Me_2C_4H_2N$)]Ni(α,α'-$Me_2C_4H_2N$)$_2$ (9.2)

A solution of dimethyl pyrrole (0.19 g, 2 mmol) was dissolved in THF (10 mL) and added with a suspension of KH (0.088 g, 2.1 mmol). The resulting pale yellow suspension was stirred overnight and then treated with a suspension of $NiBr_2$(DME) (0.308 g, 1 mmol) in THF (5 mL). The resulting brown solution was further stirred overnight, and subsequently dried under reduced pressure. The residue was washed with hexane, re-dissolved in THF and centrifuged to remove insoluble materials. The solution was concentrated to 5 mL and kept undisturbed at -35 ^oC for 7 days to afford brown block crystals of **9.2** (0.070 g, 0.73 mmol, 36.8%). Elemental Analysis Calcd. (Found) for $(C_6H_8)_2N_4Ni(C_6H_8)_2$: C 66.23 (66.11), H 7.41 (7.35), N 12.87 (12.81). ^{1}H-NMR (300 MHz, $CDCl_3$, 25^oC) δ: 7.23 (2H, d, *J* = 5.1 Hz), 6.34 (2H, d, *J* = 6.3 Hz), 5.54 (4H, d, *J* = 3.6 Hz), 2.72 (6H, s), 2.11 (6H, s), 1.49 (6H, s), 1.18 (6H, s). ^{13}C{1H}-NMR (300 MHz, $CDCl_3$, 25^oC) δ: 182.2, 155.2, 135.4, 134.4, 105.6, 85.4, 22.6, 18.9, 17.8, 16.1, 14.8. IR (Nujol mull, cm^{-1}): 1615w, 1522s, 1460w, 1378, 1352, 1285, 1192, 1151, 1076, 1023, 966, 939, 917, 882, 812, 766, 727, 662.

9.2.3 Preparation of (α,α'-$Me_2C_4H_2N$)$_2$Ni(PMe_3)$_2$ (9.4)

A green solution of potassium-napthalene 1:1 in THF (0.038 g, 0.98 mmol of potassium) was added drop wise to a stirred solution of **9.1** (0.200 g, 0.49 mmol) in THF (10 mL). An immediate colour change to dark brown was observed within 5 minutes. To this mixture added neat PMe_3 (0.49 mmol) and continued further stirring at room temperature for 2 hours, the solvent was removed under reduced pressure from the brown solution, and the residue redissolved in THF and centrifuged to remove the insoluble materials. The solution was concentrated to 5 mL and kept undisturbed at -35 ^oC for 2 days to furnish brown block crystals of

9.4 (0.107 g, 0.27 mmol, 55%). Elemental Analysis Calcd. (Found) for C_{18} H_{34} N_2 Ni P_2: C 54.17(54.01), H 8.59(8.47), N 7.02(6.98).

^{1}H-NMR (300 MHz, C_6D_6, 25 ^{o}C) δ: 7.62 (2H, s), 6.31 (1H, s), 6.00 (1H, s), 2.86 (4H, s), 2.09 (4H, s), 1.30 (4H, s), 0.83-0.79 (12H, d), 0.41 (6H, s). ^{13}C{1H}- NMR (300 MHz, C_6D_6, 25^{o}C) δ: 164.4, 125.6, 109.1, 105.9, 100.1, 18.02, 17.6, 17.1, 12.8, 11.9, 11.8, 11.6. ^{31}P{1H}-NMR(300 MHz, C_6D_6, 25^{o}C): 28.03.

9.3 X-ray data

Table 9.1: Crystal data and structural analysis Results of Complex **9.1, 9.2 and 9.4**

	9.1	**9.2**	**9.4**
Formula	$C_{12}H_{16}Br_2N_2Ni$	$C_{24}H_{32}N_4Ni$	C_{18} H_{34} N_2 Ni P_2
FW	406.80	435.25	399.12
Space group	Monoclinic, C 2/c	Monoclinic, P2(1)/c	Monoclinic, P2(1)/n
a (Å)	15.4154(4)	7.810(3	9.1866(2)
b (Å)	7.9004(16)	16.777(5)	9.5006(2)
c (Å)	13.969(3)	18.553(6)	12.4664(3)
α(deg)	90.00	90	90
β(deg)	118.3115	114.337	101.5520(10)
γ(deg)	90.00	90	90
V (Å^3)	1497.76	2214.92	1066.00(4)
Z	4	4	2
radiation (Kα, Å)	0.71073	0.893	0.71073
T (K)	202.2	100(2)	200(2)
D_{calcd} (g cm^{-3})	1.804	1.305	1.243
μ_{calcd} (mm^{-1})	6.613	0.893	1.061
F_{000}	800	928	428
R, R_w [2 a]	0.0300, 0.0723	0.0567, 0.1257	0.0374, 0.0944
GoF	1.090	0.942	1.041

[a] $R = \Sigma||Fo| - |Fc||/\Sigma|F|$. $Rw = [\Sigma(|Fo| - |Fc|)^2/\Sigma wFo^2]^{1/2}$.

9.4 Results and Discussion

The reaction of $NiBr_2$(DME) with one equivalent of the potassium salt of 2,5-dimethyl pyrrole in THF (Scheme 9.1) afforded a surprising species formulated as [α-(α,α'-Me_2-C_4H_2N)(α,α'-$Me_2C_4H_2N$)]$NiBr_2$ (**9.1**) and isolated in moderate yield (39%) as dark brown, X-ray quality crystals. The formulation of this paramagnetic compound was yielded by its crystal structure showing an unprecedented coupling of two DMP molecules, giving rise to a neutral bidentate ligand that remained coordinated to the metal center.

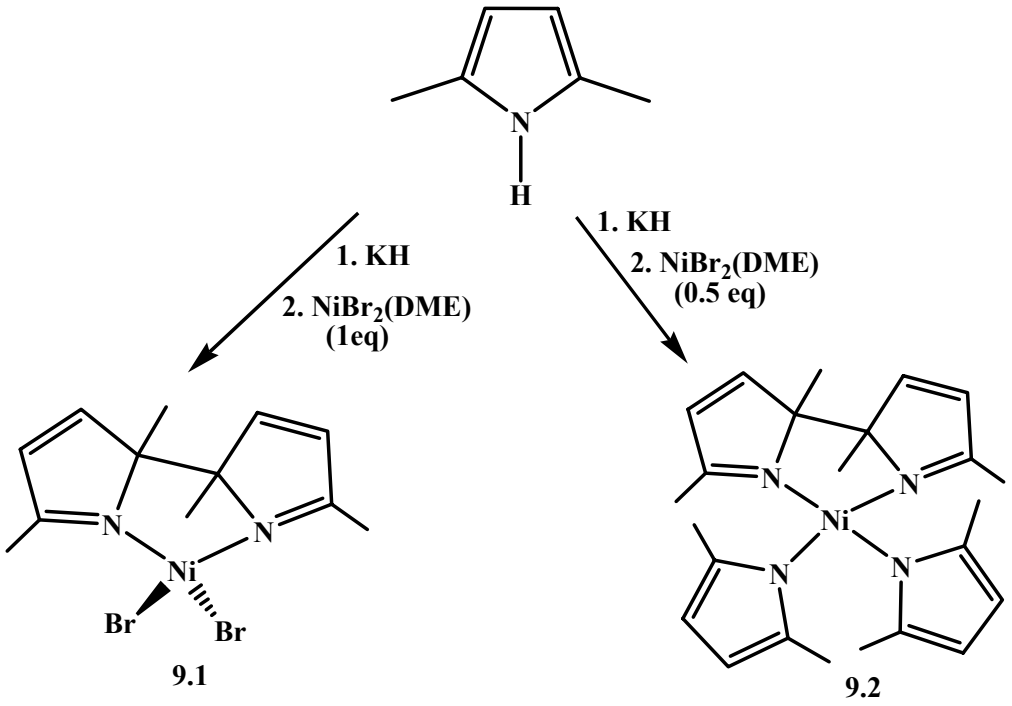

Scheme 9.1: Synthesis of complexes 9.1 and 9.2

The geometry of the metal centre of **9.1** is distorted tetrahedral and defined by two bromine atoms and two coupled former pyrrolide rings [N1-Ni1-Br1 = 108.09(9)^o, Br1A-Ni1-N1A = 108.09(9)^o, N1-Ni1-N1A = 82.61(18)^o, N1A-Ni1-Br1 = 112.22(9)^o, Br1-Ni1-Br1A =

125.43(4)^{o}] (Figure 9.1). The bond linking the two carbons at the α-positions is only slightly longer than expected for a single bond [C4-C4A 1.550(8)Å]. The ring C-C and C-N bond distances show some delocalization of double and single bond character [C2-C3 =1.323(7)Å; N1-C1 = 1.284(5)Å; C1-C2 = 1.464(6)Å].

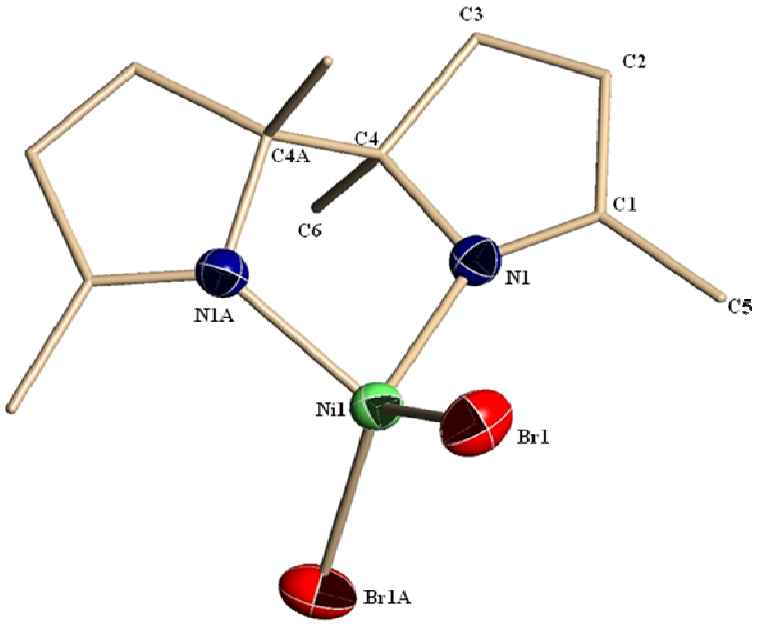

Figure 9.1: Crystal structure of Complex 9.1 with thermal ellipsoids drawn at the 50% probability level.

The formation of **9.1** does not have a straightforward explanation since the coupling between two anionic rings (Scheme 9.2) necessarily requires loss of two electrons. In turn this can only be explained with the reduction of one nickel atom to the zerovalent state. Unfortunately, any attempt to isolate other species did not yield a new compound. Yet, we observed that the insoluble residue of mainly KBr, eliminated during the work-up, also contained another black-colored material probably metallic Ni that could be isolated by washing with water. Accordingly, (Scheme 9.2) summarizes a possible rationalization.

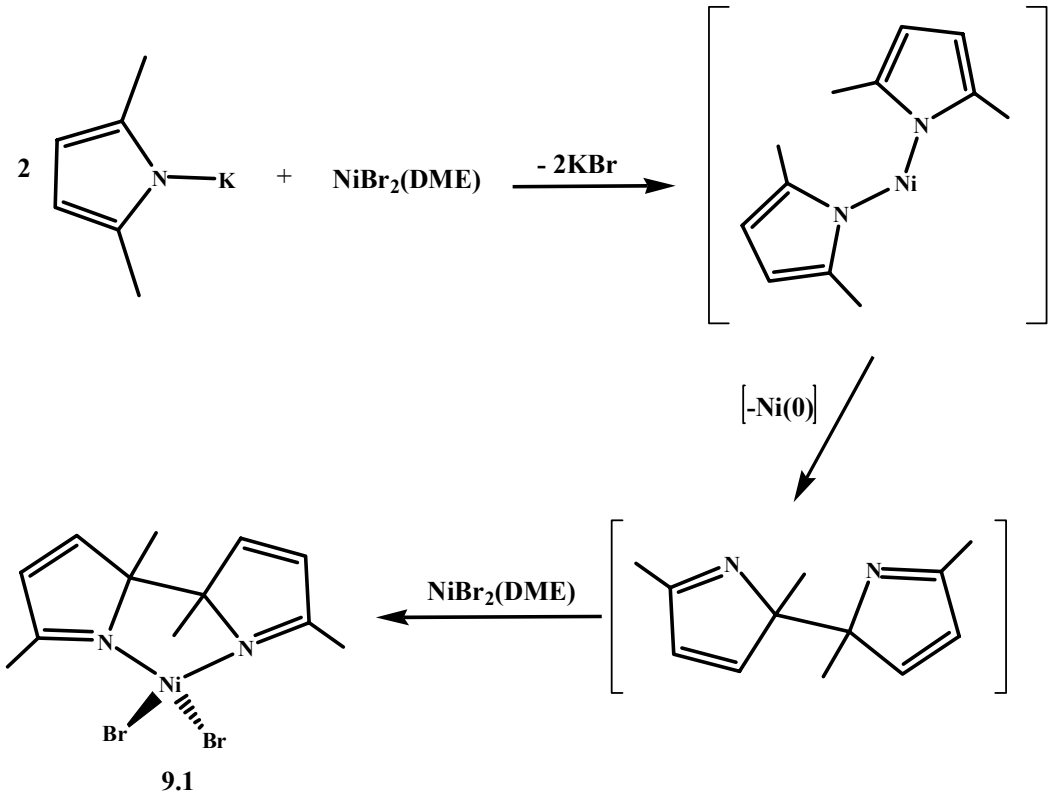

Scheme 9.2: Postulated route for the formation of complex 9.1

The transformation may be envisioned as proceeding via initial formation of an intermediate dipyrrolide species, nickelocene-type.[11] These derivatives are well known to posses a very enhanced reducing power. In this case, we assume that the reducing power targets the metal center by reducing it to the zerovalent state with simultaneous oxidative coupling of the two rings. The unstable zerovalent complex separates metallic nickel and frees the ligand for coordination to the second equivalent of nickel salt.

Interestingly the two bromine atoms of **9.1** can indeed be easily replaced by pyrrolide anions resulting in the new compound formulated as [α-(α,α'-$Me_2C_4H_2N$)(α,α'-$Me_2C_4H_2N$)]Ni(α,α'-$Me_2C_4H_2N$)$_2$ (**9.2**). The reaction can also be conveniently carried out in one step via reaction of $NiBr_2$(DME) with two equivalents of 2,5-dimethyl pyrrole (Scheme 9.1). The

diamagnetism is indicative of a d^8 divalent nickel in a square-planar environment with the NMR spectra showing the ligand expected features.

The crystal structure of **9.2** shows (Figure 9.2) the nickel atom in a square-planar field [N1-Ni1-N4 = 93.09(15)^o, N1-Ni1-N2 = 91.51(15)^o, N2-Ni1-N3 = 93.26(16)^o, N3-Ni-N4 = 82.54(15)^o] defined by the two nitrogen donor atoms of the chelating ligand containing the two coupled rings, and two regular pyrrolide anions. The bond distance and angles of the chelating

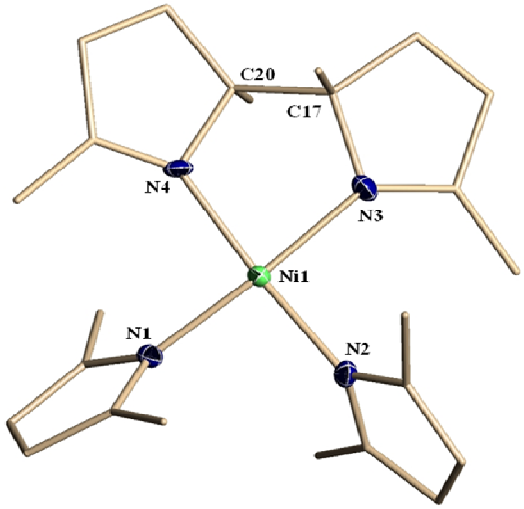

Figure 9.2: Crystal structure of Complex 9.2 with thermal ellipsoids drawn at the 50% probability level.

ligand compare well with those of complex **9.1** with the linking C-C single bond in the expected range [C17-C20 = 1.534(7)Å] and substantial localization of single and double bonds within the two rings [C20-C19 = 1.533(6)Å, N3-C14 = 1.312(5)Å, C14-C15 = 1.462(6)Å, C15-C16 = 1.342(7)Å, C16-C17 = 1.499(6)Å and C17- N3 = 1.471(6)Å]. The two regular pyrrolide anions did not show anything unexpected.

The formation of the C-C bond between the two pyrrolide rings requires two electrons being removed ultimately by the nickel metal center. We became therefore interested to investigate whether such C-C bond formation could be reversed via further reduction. The ligand in its neutral form may be readily replaced by stronger ligands such as Me_3P affording a known compound formulated as $(PMe_3)_3NiBr_2$ (**9.3)** on the basis of its crystallographic cell parameters (Figure 9.4). Instead, reductions carried out with K(naphthalene) in THF and also in the presence of Me_3P as a trapping agent (Scheme 9.3), afforded C-C bond cleavage with formation of (α,α'-$Me_2C_4H_2N)_2Ni(PMe_3)_2$ (**9.4**).

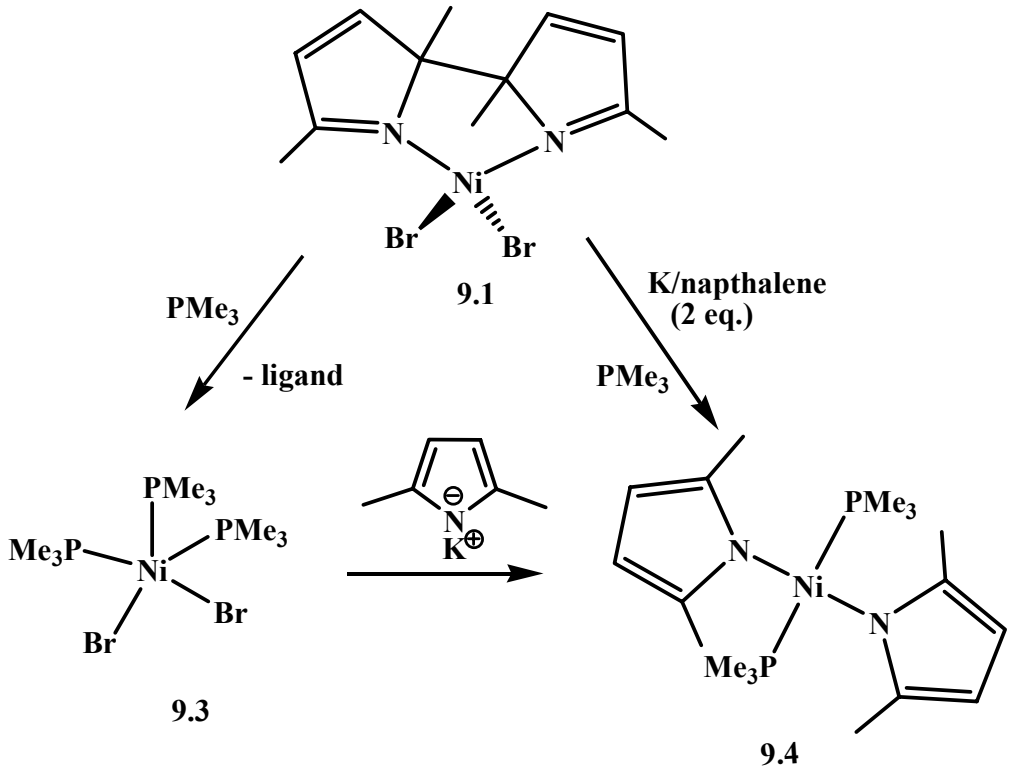

Scheme 9.3: Synthesis of complex 9.4

Complex **9.4** was characterized crystallographically (Figure 9.3). The geometry around the metal centre is square-planar [N1-Ni1-N1a = 180.0°, N1-Ni1-P1 = 90.92(5)°, N1a-Ni1-P1 =

89.08(5)°, N1-Ni1-P1a = 89.08(5)°, N1a-Ni1-P1a = 90.92(5)°, P1-Ni1-P1a = 180.0°] and defined by the two nitrogen pyrrolide rings and the P atom of two phosphine distances [Ni1-N1 = 1.8970(15)Å, Ni1-P1 = 2.2118(5)Å, Ni1-P1a = 2.2118(5)Å].

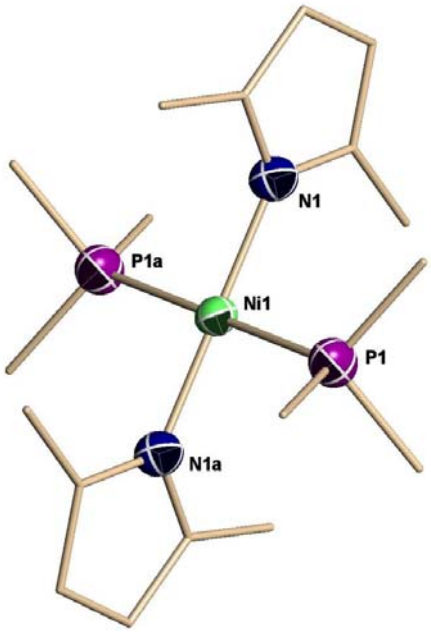

Figure 9.3: Crystal structure of Complex 9.4 with thermal ellipsoids drawn at the 50% probability level.

The penta-coordinated geometry of **9.3** is precedence in the literature (Figure 9.4).[12]

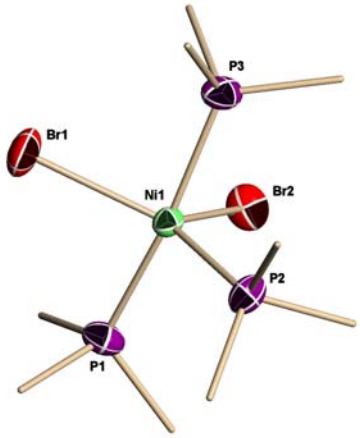

Figure 9.4: Crystal structure of Complex 9.3 with thermal ellipsoids drawn at the 50% probability level.

Catalytic Activity:

The catalytic activity of all these species was probed for ethylene dimerization. Upon activation with MAO, complex **9.1** showed moderate activity towards dimerization to 1-butene. However, the selectivity was rather disappointing (79%), since substantial amount of 2-butene (20%) was also present in the mixture. In turn, this suggests that a Cossee-type insertion mechanism is operating where equilibrium also exists between the species resulting 1-butene and 2-butene isomers. This is rather typical for nickel catalysts. In contrast, complex **9.2** is a highly selective catalyst forming pure 1-butene (99.9 %) once activated with MAO and under identical reaction conditions (Table 9.2). Unfortunately, the high selectivity came at the expenses of the activity, which dropped rather substantially. Nonetheless, the fact that halogen replacement causes the appearance of such a high selectivity is an interesting observation.

Table 9.2. Catalyst Testing for Ethylene Oligomerization.[a]

Cat.	Alkenes (mL)	Activity g/mmol, cat.h	Mol %				PE (g)
			1-C4	2-C4	C6	other	
9.1	14	933	79	20	traces	-	-
9.2	4	267	99.9	-	-	-	-
9.4	10	666	85	15	-	-	-
Blank-$NiBr_2$ (DME)	-	-	-	-	-	-	-

[a] *Conditions: 30 μmol catalyst; 1000 MAO, 600 psi; 50°C; 30 minutes reaction time, total volume 100 mL in toluene.*

Since the β-hydrogen elimination is favorable for late transition metal, it is tempting at this stage to speculate that the high selectivity may be caused by a different mechanism, possibly involving a nickelacyclopentane intermediate[13] as it could be generated by the oxidative coupling of two ethylene molecules. That in turn would imply that the initiating complex carry zero-valent Ni as possibly generated by another oxidative coupling of the two intact pyrrolide anions. The complex

9.4 which was strongly stabilized by PMe_3 molecules and pyrrolide anions did show some improvement in selectivity towards dimerization products as compared to **9.1** albeit lower activity.

9.5 Conclusions

In summary, we have shown an unexpected behavior of the DMP anion as non-innocent ligand capable of assisting the reduction of nickel to the zero-valent state. As a part of the redox behavior of Ni, the formation of the unprecedented, neutral 2,2',5,5'-tetramethyl-3,4-dihydro-2H,2'H-2,2'-bipyrrole ligand, via oxidative coupling of two pyrrolide anions is not only terribly surprising albeit unprecedented in this particular case. However, the possibility of reversing its formation via reduction and the clear switch of catalytic behavior from the dibromo and dipyrrolide Ni derivatives points out to the fact that the pyrrolide anions may be directly involved into the redox chemistry of the metal center by forming and cleaving on demand a C-C bond. Given the fact that the DMP anion is the same ligand system of both the Mitsubishi and Phillips trimerization catalyst, the chemistry of the chromium analogues should be revisited *vis-à-vis* the present findings.

References

1. a) Eisch, J. J.; Galle, J. E. *J. Organomet. Chem.* **1975**, *96*, C23. b) Eisch, J. J.; Piotrowski, A. M.; Han, K. I.; Kruger, C.; Tsay, Y. H. *Organometallics* **1985**, *4*, 224. c) Eisch, J. J.; Galle, J. E.; Aradi, A. A.; Boleslawski, M. P. *J. Organomet. Chem.* **1986**, *312*, 399. d) Hoberg, H.; Herrera, A. *Angew. Chem.* **1980**, *92*, 951. e) Hoberg, H.; Richter, W. *J. Organomet. Chem.* **1980**, *195*, 355. f) Herrera, A.; Hoberg, H.; Mynott, R. *J. Organomet. Chem*. **1981**, *222*, 331. g) Hoberg, H.; Schaefer, D. *J.Organomet.Chem*.**1982**,*238*, 383.

2. a) Anderson, T. J.; Jones, G. D.; Vicic, D. A. *J. Am. Chem.* **2004**. *126*, 8100. b) Campora, J.; Palma, P.; Carmona, E. *Coord. Chem. Rev*. **1999**, *195*, 207. c) Bennett, M. A.; Kopp, M. R.; Wenger, E.; Willis, A. C. J. *Organomet. Chem*. **2003**, *667*, 8. d) Campora, J.; Lopez, J. A.; Maya, C.; Palma, P.; Carmona, E.; Valerga, P. J. *Organomet. Chem*. **2002**, *643,* 331. e) Perthuisot, C.; Edelbach, B. L.; Zubris, D. L.; Simhai, N.; Iverson, C. N.; Muller, C.; Satoh, T.; Jones, W. D. *J. Mol. Catal. A* **2002**, *189*, 157. f) Muller, C.; Lachicotte, R. J.; Jones,W. D. *Organometallics* **2002**, *21*, 1975. g) Koo, K.; Hillhouse, G. L. *Organometallics* **1998**, *17*, 2924.

3. a) Diederich, F., Stang, P. J. *Metal-Catalyzed Cross-Coupling Reactions*; Wiley-VCH: Weinheim, Germany; **1998**. b) de Meijere, A.; Diederich, F. *Metal-Catalyzed Cross-Coupling Reactions,* 2nd ed.; Wiley-VCH: Weinheim, Germany; **2004**. c) Beller, M.; Bolm, C. *Transition Metals for Organic Synthesis,* 2nd ed.; Wiley-VCH:Weinheim, **2004**. d) Keen, A. L.; Doster, M.; Johnson. S. A. *J. Am. Chem. Soc*. **2007**, *129*, 810.

4. a) Pfirrmann, S.; Limberg, C.; Herwig, C.; St€oßer, R.; Ziemer, R. *Angew. Chem., Int. Ed* .**2009**, *48*, 3357. b) Bai, G.; Wei, P.; Stephan, D. W. *Organometallics* **2005**, *24*, 5901.

5. Diercks, R.; Stamp, L.; Kopf, J.; Heindirk, T. D. *Angew. Chem*. **1984**, *96*, 891.

6. For reviews of C-C bond activation by organometallic complexes, see: a) Murakami, M.; Ito, Y. In *Topics in Organometallic Chemistry*; Murai, S., Ed.; Springer-Verlag: New York, **1999**, P 97-129. b) Rybtchinski, B.; Milstein, M. *Angew.Chem., Int. Ed*. **1999**, *38*, 870. c) Perthuisot, C.; Edelbach, B. L.; Zubris, D. L.; Simhai, N.; Iverson, C. N.; Mu¨ller, C.; Satoh, T.; Jones, W. D. *J. Mol. Catal. A* **2002**, *189*, 157. d) McKinney, R. J. *In Homogeneous Catalysis*; Parshall, G. W.; Ed.; Wiley: New York, **1992**, P 42-50.

7. a) Ramakrishna, T. V. V.; Sharp, P. R. *Organometallics* **2004**, *23*, 3079. b) Beck, R.; Johnson, S. A. *Chem. Commun.,* **2011***, 47*, 9233. c) Brunkan, N. M.; Brestensky, D. M.; Jones, W. D. *J. Am. Chem. Soc.* **2004**, *126*, 3627.

8. a) Reardon, D.; Aharonian, G.; Gambarotta, S.; Yap, G.P.A. *Organometallics* **2002**, *21*, 786. b) Scott, J.; Gambarotta, S.; Korobkov, I. *Can. J. Chem*. **2005,** *83*, 279. c) Manuel, T. D.; Rohde, J. U. *J. Am. Chem. Soc.* **2009**, *131*, 15582. d) Zhu, D.; Thapa, I.; Korobkov, I.; Gambarotta, S.; Budzelaar, H.M. P. *Inorg. Chem.* **2011**, *50*(20), 9879.

9. Reagan, W. K. (Phillips Petroleum Company)EP 0417477, **1991**.

10. a) Jabri, A.; Korobkov, I.; Gambarotta, S.; Duchateau, R. *Angew. Chem. Int*. **2007**, *46(32)*, 6119. b) Jabri, A.; Mason, C. B.; Gambarotta, S.; Bruchella, T. J; Duchateau, R. *Angew. Chem. Int*. **2008**, *47(50)*, 9717. c) Vidyaratna, I.; Nikiforov, G. B.; Gorelsky, S. I.; Gambarotta, S.; Duchateau, R.; Korobkov, I. *Angew. Chem., Int. Ed*. **2009**, *48*, 6552.

11. Stubenrauch, S.; Kreutzberg, J.; Henkel, G.; Kuhn, N. *J. Organomet. Chem*. **1993**, *456*, 97.

12. Dawson, J. W.; McLennan, T. J.; Robinson, W.; Merle, A.; Dartiguenave, M.; Dartiguenave, Y.; Gray, H. B. *J. Am. Chem. Soc*. **1974**, *14*, 4428.

13. Saussine, L.; Braustein, P.; Speiser, F. *Acc. Chem. Res.* **2005,** *38*, 784.

Claims to Original Research

1) Clear evidence of the role of metal-oxidation state in the selectivity of ethylene oligomerization was observed. An unprecedented single component self-activating divalent Cr(II) catalyst for Schulz-Flory distribution was isolated. A class-II mixed valence Cr(I)/Cr(II) single component catalyst was isolated. A very rare example of dimerization activity of this complex was also explored. A catalytically active single component monovalent Cr(I) butadiene-butadienyl species for ethylene trimerization was conclusively identified. A remarkable switch in selectivity between 1-butene to 1-hexene and UHMWPE was observed depending on the nature of co-catalyst and solvent used.

2) A highly selective tetramerization catalyst with selectivity for 1-octene > 90 % was achieved with simple R_2NPPh_2 – Cr(III) systems.

3) The very first example of unprecedented selectivity for 1-octene (> 99 %) was discovered with neutral amino bispyridine ligand-Cr(III) system.

4) A hetero-bimetallic chromium-aluminate complex of dicyclohexyl amido with single component catalytic activity for selective 1-octene and 1-hexene was uncovered in a homogeneous system.

5) Novel nickel dinitrogen, hydride and alkyl complexes with well established bisiminopyridine ligand were isolated and their unprecedented oligomerization activity was determined.

6) A rare example of heterobimetallic Ni(I) species was isolated and assessed for its catalytic activity along with its related complexes.

7) The formation and cleavage of C-C bond initiated by dimethyl pyrrole nickel catalyst was uncovered as well as selective dimerization of ethylene to 1-butene was assessed with one of the nickel-pyrrolide complex.

Note: I would like to acknowledge professor Peter Budzelaar for DFT calculations.

Conclusions and Recommendations for future works

Concrete evidence regarding the active species, metal oxidation states and their role in selectivity for the oligomerization processes have been revealed by this thesis work. Data generated by this thesis will be helpful in guiding the future research direction towards designing custom tailored catalysts for commercial use.

Discovery of a solely selective (>99%) tetramerization catalyst challenges the ring expansion mechanism on one hand, and open up the door for the academic community to exercise new ideas and even support the possibility of a " bimetallic mechanism" recently proposed in the literature. Since the information from this thesis clearly shows that a tetramerization catalyst can only be obtained with a "neutral ligand" framework, it is recommended to design a neutral bridging ligand that would be sufficiently stable enough to bind the two monovalent chromium centres with a distance that internal reductive elimination has occurred to selectively release 1-octene. Conclusive evidence could only be obtained when a well-defined catalytically active single component tetramerization species have been isolated, so great efforts need to be put in this direction. It is also evident from this work that the isolation of a well defined catalytically active species including a monovalent chromium oxidation state is also feasible by the judicious choice of ligand. The ability of ligand to stabilize the chromium in different oxidation states is the key to custom design of catalysts for different purposes.

Various novel nickel complexes like dinitrogen, hydride and a rare example of monovalent Ni(I) species were isolated in their stable form at room temperature. Further exploration of these novel nickel complexes in various organic transformations beyond their ethylene oligomerization activity should be continued.

General Oligomerization procedure

A 300 mL Parr reactor was dried in an oven at 115 °C overnight prior to each run and then placed under vacuum for 1 h at 120 °C. The reactor was then cooled to the desired temperature and charged with the solvent and co-catalyst with stirring. After 10 min the catalyst was injected into the reactor under a stream of N_2 and then the reactor was immediately pressurized with ethylene (600 psi). The reaction was allowed to run for 30 min or 1 h while the temperature remained stable. The temperature was then rapidly reduced to 5 °C with an ice bath; the reactor was slowly depressurized and a mixture of MeOH/HCl conc. (45ml/5ml) was injected to quench the reaction. The organic phase was separated from the aqueous phase and analysis and yield of oligomers were obtained respectively by GC, by using calibrated standard solutions, and by ^{1}H-NMR. Precautions were taken to maintain the temperature as low as possible during the workup to minimize loss of volatiles.

APPENDIX A

X-ray crystallography

Suitable crystals were selected, mounted on a thin, glass fiber with paraffin oil, and cooled to the data collection temperature. Data were collected on a Bruker AXS SMART 1 k CCD diffractometer. Data collection was performed with three batch runs at phi = 0.00 deg (600 frames), at phi = 120.00 deg (600 frames), and at phi = 240.00 deg (600 frames). Initial unit-cell parameters were determined from 60 data frames collected at different sections of the Ewald sphere. Semi-empirical absorption corrections based on equivalent reflections were applied. The systematic absences and unit-cell parameters were consistent for the reported space groups. The structures were solved by direct methods, completed with difference Fourier syntheses, and refined with full-matrix least-squares procedures based on *F*2. All non-hydrogen atoms were refined with anisotropic displacement parameters. When it was no possible to locate them, the hydrogen atoms were treated as idealized contributions.

Magnetic Susceptibility Calculation

Spin only formula for $\mu_{eff} = \{n(n+2)\}^{1/2}$

Diamagnetic corrections were done by using Pascal's constant table.

Minor Results:

A few Ni-Complexes Explored for Ethylene Oligomerization

Following few Ni(II) complexes were synthesized, characterized and tested for ethylene oligomerization behaviour. Summary of the results are presented here.

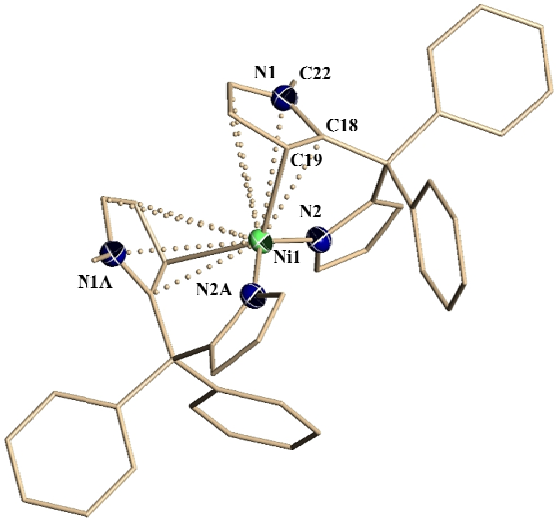

Complex **1**

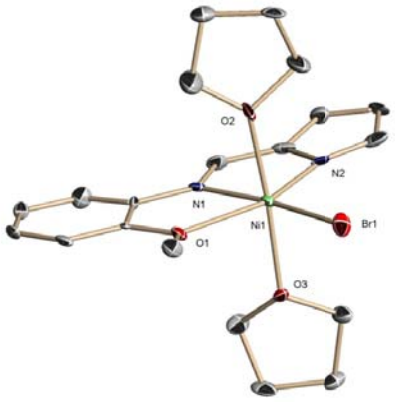

Complex **2**

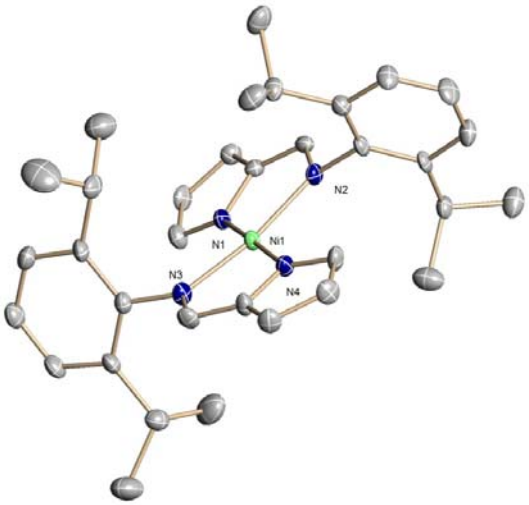

Complex 3

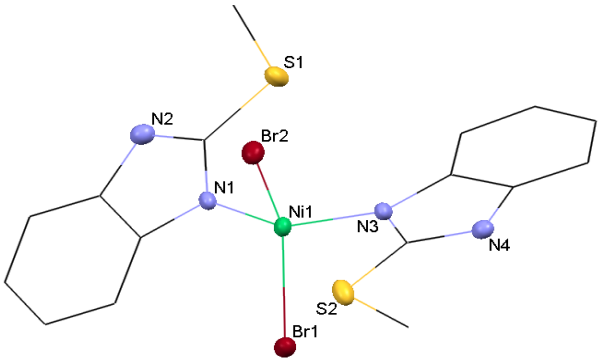

Complex 4

Table 1. catalytic activity for Complex **1, 2, 3 and 4**

catalyst	Alkene (mL)	PE (g)	Activity g/mmol, cat.h	Mol % 1-C4	2-C4	C6	other
1	28.01	-	1,251.11	82	13	5	-
2	4	-	267	80	19	2	-
3	**4**	-	267	80	20	-	-
4	**2**	1	133	90	10	-	-

[a] *Conditions: 30 µmol catalyst; 1000 MAO, 600 psi; 50°C; 30 minutes reaction time, total volume 100 mL in toluene.*

The result showed that among the other complexes, the Ni(II)-dipyrrole, complex **1** was found to be more active for ethylene dimerization producing 82 % 1-butene and 13 % 2-butene. Further exploration of this complex with different co-catalysts and reaction conditions is recommended.